

©2014

Lin Chen

ALL RIGHTS RESERVED

**DESIGN AND SYNTHESIS OF NOVEL SMALL MOLECULE MODULATORS  
OF KEAP1-NRF2-ARE PATHWAY**

by

LIN CHEN

A dissertation submitted to the  
Graduate School-New Brunswick  
Rutgers, The State University of New Jersey

In partial fulfillment of the requirements

For the degree of

Doctor of Philosophy

Graduate Program in Medicinal Chemistry

Written under the direction of

Professor Longqin Hu

And approved by

\_\_\_\_\_  
\_\_\_\_\_  
\_\_\_\_\_  
\_\_\_\_\_

New Brunswick, New Jersey

JANUARY, 2014

## **ABSTRACT OF THE DISSERTATION**

### **DESIGN AND SYNTHESIS OF NOVEL SMALL MOLECULE MODULATORS OF KEAP1-NRF2-ARE PATHWAY**

By LIN CHEN

Dissertation Director: Professor Longqin Hu

Keap1-Nrf2-ARE system represents a key signaling pathway in the regulation of cellular defense mechanisms against oxidative stress and inflammation. Activation of Keap1-Nrf2-ARE system can induce the expression of a number of antioxidant defense enzymes and proteins critical for preventing oxidative damage, inflammation and tumorigenesis.

Curcumin exhibits antioxidant, anti-inflammatory and anti-carcinogenic properties and is demonstrated as an indirect inhibitor of Keap1-Nrf2 protein-protein interaction. Novel classes of iminothiazinylbutadienols and divinylpyrimidinethiones were designed and synthesized as analogs of curcumin with its  $\beta$ -diketone moiety masked as a heterocyclic adduct with thiourea. The chemical stability of these novel heterocyclic compounds was improved as compared to curcumin. The biological activity evaluations revealed that some of these new curcumin analogs are more effective ARE activators than curcumin and isothiocyanates.

Most available modulators of Keap1-Nrf2-ARE pathway modify the cysteine sulfhydryl groups of Keap1 for ARE activation. There are safety concerns about these thiol-reactive compounds. A high-throughput screen (HTS) of the MLPCN library identified the first-in-class inhibitor specifically for the direct inhibition of the Keap1-Nrf2 protein-protein interaction. The HTS hit has three chiral centers and the active stereoisomer was designated as LH601A and its stereochemistry was confirmed by X-ray crystallography and stereospecific synthesis. Various analogs of LH601A were designed and synthesized to improve the binding affinity. The obtained structure activity relationships (SAR) provided guidance for further structural optimization. Several analogs showed to be more potent than LH601A. These direct Keap1-Nrf2 inhibitors can mimic the actions of electrophiles in the induction of cytoprotective enzymes but are more selective and specific. Therefore, these direct inhibitors of Keap1-Nrf2 protein-protein interaction have great potential to be developed into innovative therapeutic agents for many diseases and conditions involving oxidative stress.

## ACKNOWLEDGEMENTS

I would like to express my appreciation to a number of people for their help with this doctoral dissertation.

First of all, I would like to express my sincere gratitude to my advisor, Dr. Longqin Hu, for his support, instruction, guidance and encouragement throughout my graduate studies and researches. It is my fortune to find an advisor who is always providing stimulating research ideas, equipping the laboratory with many modern instruments that not only make my work more efficient but also helped me be familiarized with the latest technology in pharmaceutical industry. Dr. Hu is also an encouraging example who lead me to overcome all kinds of difficulties and gain not only the traditional medicinal chemistry knowledge but also the skills to solve encountered problems during research. His fruitful discussions and constructive comments were essential to the completion of this dissertation, and he has taught me innumerable lessons and insights on the workings of research and how to be successful in career and life.

I'm also indebted to Dr. Edmond J. LaVoie, Dr. Joseph E. Rice and Dr. Spencer Knapp, who serve on my thesis committee for their valuable advice, support and time. I would like to thank Dr. Edmond J. LaVoie and Dr. Joseph E. Rice for giving me opportunity to join in the Ph. D. program in Medicinal Chemistry at Rutgers and awarding me a teaching assistantship during my graduate study. I would like to thank Dr. Spencer Knapp for reading my dissertation draft and attending my independent proposal and defense.

It is my pleasure to acknowledge all my past and present colleagues, Yu Chen, Daigo Inoyama, Yanhui Yang, Sadagopan Magesh, Herve Aloysius, Jing Zhen, Dhulfiqar Ali Abed, for their helpful discussions and suggestions and invaluable help and collaborations on my work.

Finally, I would like to thank mom, dad and my parents in law for taking care of our two kids and their endless support for me throughout my academic journey. I would like to give my exceptional thanks to my wife for her love, support and the two great kids she gave to me. I love my wife, Chen Li, and my two kids, Brian and Terrence in my heart.

## **DEDICATION**

*To my parents, my wife and my kids*

## TABLE OF CONTENTS

<b>ABSTRACT OF THE DISSERTATION.....</b>	<b>ii</b>
<b>ACKNOWLEDGEMENTS .....</b>	<b>iv</b>
<b>DEDICATION.....</b>	<b>vi</b>
<b>TABLE OF CONTENTS .....</b>	<b>vii</b>
<b>LIST OF FIGURES.....</b>	<b>ix</b>
<b>LIST OF TABLES.....</b>	<b>xii</b>
<b>LIST OF SCHEMES .....</b>	<b>xii</b>
<b>ABBREVIATIONS.....</b>	<b>xiv</b>
<b>CHAPTER ONE .....</b>	<b>1</b>
<b>INTRODUCTION.....</b>	<b>1</b>
I. Oxidative Stress and Enzyme Induction.....	1
II. Keap1-Nrf2-ARE Signaling Pathway.....	3
A. Structural Components and Functions of Keap1-Nrf2-ARE Pathway.....	5
B. Mechanisms of Regulation of Keap1-Nrf2-ARE Pathway.....	9
C. Diseases Involving Keap1-Nrf2-ARE Pathway.....	11
III. Novel Small Molecule Modulators of Keap1-Nrf2-ARE Pathway.....	16
IV. Summary.....	18
<b>CHAPTER TWO.....</b>	<b>21</b>
<b>DESIGN AND SYNTHESIS OF NOVEL HETEROCYCLIC CURCUMIN ANALOGS AS ARE INDUCERS.....</b>	<b>21</b>
I. Introduction.....	21
A. Curcumin.....	21

B. Curcumin Relieves Keap1 Inhibition of Nrf2.....	22
C. Biological Properties of Curcumin Involving Keap1-Nrf2-ARE Pathway....	24
D. Limitations of Curcumin.....	26
II. Design and Synthesis of Novel Heterocyclic Curcumin Analogs.....	29
A. Design Principle.....	29
B. Synthesis of Novel Heterocyclic Curcumin Analogs.....	32
III. Results and Discussion.....	35
A. Stability of Novel Iminothiazinylbutadienols and Divinylpyrimidinethiones.....	35
B. Cytotoxicity and ARE Induction Activity of Novel Heterocyclic Curcumin Analog.....	36
IV. Summary.....	39
<b>CHAPTER THREE.....</b>	<b>41</b>
<b>DISCOVERY, DESIGN AND SYNTHESIS OF DIRECT INHIBITORS OF KEAP1-NRF2 PROTEIN-PROTEIN INTERACTION.....</b>	<b>41</b>
I. Introduction.....	41
A. Direct of Keap-Nrf2 Protein-Protein Interaction.....	41
B. Molecular Interactions between Keap1 and Nrf2.....	44
II. Discovery of Direct Small Molecule Inhibitor of Keap1-Nrf2 Protein-Protein Interaction.....	46
A. Hit Discovery by HTS.....	46
B. Resynthesis of Hit 1 for Activity Confirmation and Stereochemistry Assignment.....	50

III. Design of LH601 Analogs.....	56
A. Design Principle.....	56
B. Modification of the Cyclohexane Carboxylic Acid Moiety.....	58
C. Modification of Tetrahydroisoquinoline.....	60
D. Modification of Phthalimido Group.....	63
E. Modification on both Phthalimide and Tetrahydroisoquinoline.....	66
IV. Results and Discussion.....	68
A. Synthesis of LH601 Analogs.....	68
B. Inhibitory Activity Evaluation of the Synthesized Small Molecule Inhibitors.....	79
C. Preliminary Structure Activity Relationship (SAR) .....	93
D. ARE Induction and Nrf2 Nuclear Translocation Assays.....	94
V. Summary.....	96
<b>CHAPTER FOUR.....</b>	<b>98</b>
<b>EXPERIMENTAL SECTION.....</b>	<b>98</b>
I. Novel Heterocyclic Curcumin Analogs.....	99
II. Direct Small Molecule Inhibitors of Keap1-Nrf2 Protein-Protein Interaction.....	111
<b>REFERENCES.....</b>	<b>172</b>
<b>LIST OF FIGURES</b>	
Figure 1. Keap1-Nrf2-ARE Pathway for the Induction of Cytoprotective Enzymes .....	5
Figure 2. Structures and Functions of Keap1.....	7
Figure 3. Structures and Functions of Nrf2 .....	8
Figure 4. Chemical Structure of Curcumin.....	22

Figure 5. Curcumin Relieves Keap1 Mediated Inhibition of Nrf2 .....	24
Figure 6. Degradation of Curcumin under Basic Condition .....	27
Figure 7. Metabolism of Curcumin in vivo .....	28
Figure 8. Tautomeric Structures of Curcumin .....	31
Figure 9. Design of Novel Iminothiazinylbutadienols and Divinylpyrimidinethiones as Conjugates of Curcumin and Thiourea. ....	32
Figure 10. Stability Study of Curcumin and Representative Analogs. ....	35
Figure 11. ARE-Inducing Activity of Novel Heterocyclic Curcumin Analogs.....	38
Figure 12. Chemical Structures of Some Known Reactive Chemical ARE Inducers .....	42
Figure 13. Proposed Model of Nrf2 Activation by Direct Small Molecule Inhibitors of Keap1-Nrf2 Protein-Protein Interaction. ....	46
Figure 14. HTS Screening Flow Chart. ....	48
Figure 15. Chemical Structure of the Hit 1 .....	49
Figure 16. Inhibitory Activity Evaluation of Hit 1 for Keap-Nrf2 Protein-Protein Interaction .....	50
Figure 17. HPLC Chromatograms of LH601 (Mixture of Four Isomers) as Compared to Purified Stereoisomers. ....	53
Figure 18. Comparison of $K_d$ of Different Stereoisomers of LH601 to Hit 1 .....	54
Figure 19. X-ray Crystal Structures and Stereospecific Synthesis. ....	55
Figure 20. Simplification of Lead LH601A.....	57
Figure 21. The Possible Modification Sites in LH601A.....	58
Figure 22. Structures of Analogs with Modification of Carboxylic Acid. ....	59
Figure 23. Structures of Analogs with Replacement of Cyclohexane Ring. ....	60

Figure 24. Structure of an Analog with Dissected Tetrahydroisoquinoline. ....	60
Figure 25. Structure of an Analog with Modification of Tetrahydroisoquinoline.....	61
Figure 26. Structures of Analogs with Substitutions on Tetrahydroisoquinoline.....	62
Figure 27. Structures of Analogs with Substitution on Ethyl of Tetrahydroisoquinoline.	63
Figure 28. Structures of Analogs with Opened Phthalimido Ring. ....	64
Figure 29. Structures of Analogs with Replacement of Phthalimido Group. ....	65
Figure 30. Structure of an Analog with Replacement of Phthalimido Group .....	65
Figure 31. Structure of an Analog with Extended Linker between Phthalimide and Tetrahydroisoquinoline .....	66
Figure 32. Structures of Analogs with Modification on both Phthalimide and Tetrahydroisoquinoline .....	67
Figure 33. Inhibitory Activities of Synthesized Analogs with Modification on Cyclohexane Carboxylic Acid Moiety.....	82
Figure 34. Inhibitory Activities of Synthesized Analogs with Modification on Tetrahydroisoquinoline (THIQ).....	87
Figure 35. Inhibitory Activities of Synthesized Analogs with Modification on Phthalimido Group.....	91
Figure 36. Inhibitory Activities of Synthesized Analogs with Modification on both Phthalimide and Tetrahydroisoquinoline.....	92
Figure 37. Preliminary Structure-Activity Relationships. ....	93
Figure 38. ARE-Inducing Activity of LH601A in CellSensor-Lactamase Reporter Assay .....	95

Figure 39. Nrf2 Nuclear Translocation Effect of LH601A in the PathHunter U2OS

Keap1-Nrf2 Functional Assay. .... 95

## LIST OF TABLES

Table 1. The Cytotoxicity of Novel Curcumin Analogs in the NCI60 Screening ..... 37

Table 2. Inhibitory Activities of Synthesized Analogs with Modification on Cyclohexane Carboxylic Acid Moiety ..... 80

Table 3. Inhibitory Activities of Synthesized Analogs with Modification on Tetrahydroisoquinoline (THIQ)..... 85

Table 4. Inhibitory Activities of Synthesized Analogs with Modification on Phthalimido Group ..... 89

Table 5. Inhibitory Activities of Synthesized Analogs with Modification on both Phthalimide and Tetrahydroisoquinoline ..... 92

## LIST OF SCHEMES

Scheme 1. Synthesis of Novel Iminothiazinylbutadienols from Curcumin and Isothiocyanates..... 33

Scheme 2. Synthesis of Novel Divinylpyrimidinethiones from Iminothiazinylbutadienols. .... 34

Scheme 3. Synthesis of LH601 ..... 51

Scheme 4. Separation of LH601 Stereoisomers ..... 52

Scheme 5. Synthesis of Analogs with Modification of Carboxylic Acid ..... 68

Scheme 6. Synthesis of Analogs with Replacement of Cyclohexane..... 69

Scheme 7. Synthesis of a Dissected Tetrahydroisoquinoline Analog.....	70
Scheme 8. Synthesis of an Analog with Replacement of Tetrahydroisoquinoline.....	71
Scheme 9. Synthesis of Analogs with Substitutions on Tetrahydroisoquinoline .....	72
Scheme 10. Synthesis of Analogs with Substitutions on Ethyl of Tetrahydroisoquinoline .....	73
Scheme 11. Synthesis of Analogs with Opened Phthalimido Ring.....	74
Scheme 12. Synthesis of Analogs with Replacement of Phthalimido Group.....	75
Scheme 13. Synthesis of an Analog with Replacement of Phthalimido Group.....	76
Scheme 14. Synthesis of an Analog with Extended Linker between Phthalimide and Tetrahydroisoquinoline .....	77
Scheme 15. Synthesis of Analogs with Modification on both Phthalimide and Tetrahydroisoquinoline .....	78

## ABBREVIATIONS

Ac	Acetyl
ACE	Angiotensin Converting Enzyme
ACN	Acetonitrile
AcOH	Acetic Acid
AD	Alzheimer's Disease
AGEs	Advanced Glycationend-Products
Ala	Alanine
AIM	Antioxidant Inflammation Modulator
ALI	Acute Lung Injury
Asn	Asparagine
ARDS	Acute Respiratory Distress Syndrome
ARE	Antioxidant Response Elements
Arg	Arginine
Bn	Benzyl
Boc	t-Butoxycarbonyl
BPD	Bronchopulmonary Dysplasia
BTB	Tamtrack and Bric a Brac
Bu	t-Butyl
bZip	Basic Region-Leucine Zipper
Cbz	Benzoxycarbonyl
CKD	Chronic Kidney Disease
CO <sub>2</sub>	Carbon Dioxide

COPD	Chronic Obstructive Pulmonary Disease
CP450	Cytochrome P450
CREB	c-AMP Response Element Binding Protein
CTR	c-Terminal Region
CVD	Cardiovascular Disease
Cul3	Cullin 3
Cys	Cysteine
DCC	Dicyclohexylcarbodiimide
DCM	Dichloromethane
DBTA	Dibenzoyl L-Tartaric Acid
DEA	Diethylamine
DGR	Double Glycine Repeat
DIAD	Diisopropyl Azodicarboxylate
DIEA	Diisopropylethylamine
DLG	Aspartic Acid-Leucine-Glycine
DMAP	4-Dimethylaminopyridine
DMEM	Dulbecco's Modified Eagle's Medium
DMF	N, N-Dimethylformamide
DMSO	Dimethyl Sulfoxide
DNA	Deoxyribonucleic Acid
DTP	Developmental Therapeutics Program
EC <sub>50</sub>	Half Maximal Effective Concentration
EDA	Ethylenediamine

EDC	1-Ethyl-3-(3-dimethylaminopropyl)carbodiimide
e.e.	Enantiomeric Excess
EPA	Eicosapentaenoic Acid
EpRE	Electrophile Response Elements
ETGE	Glutamic Acid-Threonine-Glycine-Glutamic Acid
EtOAc	Ethyl Acetate
FBS	Fetal Bovine Serum
FCC	Flash Column Chromatography
FP	Fluorescence Polarization
FITC	Fluorescein Isothiocyanate
GCL	Glutamate-Cysteine Ligase
Gly	Glycine
GSH	Glutathione
GSTs	Glutathione Transferases
H <sub>2</sub> O <sub>2</sub>	Hydrogen Peroxide
HBTU	2-(1H-benzotriazole-1-yl)-1,1,3,3-tetramethyluronium
HCl	Hydrogen Chloride
HEPES	Hydroxyethyl Piperazineethanesulfonic Acid
His	Histidine
HMOX1	Hemeoxygenase 1
HO-1	Heme Oxygenase-1
HOBt	1-Hydroxybenzotriazole
HPLC	High Performance Liquid Chromatography

HTS High	Throughput Screen
IAB	N-Iodoacetyl-N-Biotinylhexylenedi Amine
ITC	Isocyanates
IC <sub>50</sub>	Half Maximal Inhibitory Concentration
IPF	Idiopathic Pulmonary Fibrosis
IVR	Intervening Region
Kd	Dissociation Constant
Keap1	Kelch-Like ECH-Associated Protein 1
Kg	Kilogram
KOH	Potassium Hydroxide
LC-MS	Liquid Chromatography Mass Spectrometry
Maf	Muscleaponeurotic Fibrosarcoma
mL	milliliter
min	minute
MLPCN	Molecular Libraries Probe Production Centers Network
MTT	3-(4,5-Dimethylthiazol-2-yl)-2,5-diphenyltetrazolium bromide
NAD(P)H	Nicotinamide Adenine Dinucleotide (phosphate), Reduced Form
NCI	National Cancer Institute
NIH	National Institutes of Health
ng	nanogram
NMP	N-Methylpyrrolidone
NQO1	Quinonereductase
NO	Nitric Oxide

Nrf2	Nuclear Factor Erythroid 2-Related Factor 2
NTR	N-Terminal Region
P <sub>2</sub> O <sub>5</sub>	Phosphorus Pentoxide
PBS	Phosphate Buffered Saline
PD	Parkinson's Diseases
PEITC	Phenethyl Isothiocyanate
Phe	Phenylalanine
POCl <sub>3</sub>	Phosphorus Oxychloride
PPh <sub>3</sub>	Triphenylphosphine
SAR	Structure Activity Relationships
RCS	Reactive Carbonyl Species
γ-GCS	γ-Glutamine Cysteine Synthetase
RNS	Reactive Nitrogen Species
ROS	Reactive Oxygen Species
Ser	Serine
SFN	Sulforaphane
SPR	Surface Plasmon Resonance
Suc	Succinyl
tBHQ	Tertiary Butylhydroquinone
TEA	Triethylaluminium
TFA	Trifluoroacetyl
THF	Tetrahydrofuran
THIQ	Tetrahydroisoquinoline

Ub	Ubiquitin
μg	microgram
UGT	UDP-glucuronosyltransferase
μL	microliter
μM	micromolar
UV	Ultraviolet
WHO	World Health Organization
X-ray	X-radiation

## CHAPTER ONE

### INTRODUCTION

#### I. Oxidative Stress and Enzyme Induction

Cells in our body are constantly exposed to a host of oxidizing substances such as reactive oxygen species (ROS), reactive nitrogen species (RNS), reactive electrophilic metabolites, and other electrophiles generated from both exogenous sources and endogenous sources. These reactive species are all capable of causing damage to cells, lipids, proteins, and DNA and lead to cell death and diseases.<sup>1-8</sup> The term oxidative stress is generally defined as a deleterious processes resulting from an imbalance between oxidants and antioxidants, in favor of an excessive amount of reactive oxygen species (ROS), reactive nitrogen species (RNS) and other oxidants. These reactive species can be the results of aerobic metabolism, UV light, radiation, environmental toxins and activities of cytochrome P450 and NADPH oxidases. A series of by-products can also be generated by metabolism including reactive carbonyl species (RCS) such as glyoxal, methylglyoxal that can contribute to the formation of advanced glycation end-products (AGEs) that is related to aging.<sup>8-10</sup> Oxidative stress is a basic process and the oxidative damage can lead to inflammation which could subsequently result in many disease such as cancer, cardiovascular, and diabetes.<sup>11-16</sup> Research has clearly shown that oxidative stress, inflammation and mutation are linked processes.<sup>17, 18</sup> It is now evident that generation of oxidizing substances and the subsequent oxidative stress response have been implicated in the pathogenesis of a variety of diseases such as cancer, Alzheimer's and Parkinson's diseases, diabetes, and pulmonary disease.<sup>16, 19-24</sup>

Moderate production of some reactive oxygen species (ROS) and reactive nitrogen species (RNS) is essential in maintaining cellular redox homeostasis and keeping normal growth and metabolism. However, large amounts or uncontrolled production of these reactive oxygen and nitrogen species can target DNA, proteins and other cellular component and compromise the cellular activity, leading to cell death and diseases. To protect cells against these harmful substances, our human body has developed a series of enzymatic and non-enzymatic antioxidant defenses mechanisms. Among them, the induction of the expression of antioxidant and cytoprotective enzymes is a major protective mechanism against oxidative stress.<sup>5, 8, 25, 26</sup>

Studies have shown that fruit and vegetables contain relatively high amounts of antioxidants or compounds that can induce the expression of oxidative stress response enzymes. Antioxidants can be divided into endogenous and exogenous or direct antioxidants, indirect antioxidants and bifunctional antioxidants.<sup>16, 25, 27, 28</sup> Many natural products like curcumin, sulforaphane, and epigallocatechin gallate from natural sources such as fruits, vegetables, and tea products have preventive properties against oxidative stress through the induction of the antioxidant and cytoprotective enzymes. It has been demonstrated that the generation of oxidizing substances and subsequent oxidative stress have been implicated in many diseases such as cancer, liver disease, and cardiovascular disease.<sup>16, 19-24</sup> Therefore, induction of antioxidant and cytoprotective enzymes is important in control of various diseases and conditions involving inflammation and oxidative stress.

## **II. Keap1-Nrf2-ARE Signaling Pathway**

Uncontrolled production of reactive oxygen species and other reactive oxidants produced during an inflammatory process can target DNA, proteins, lipids and other cellular component and compromise the cellular activity. A major strategy in the cellular defense against oxidative stress is to induce cytoprotective enzymes intimately involved in the neutralization and detoxification of oxidants and electrophilic agents. To protect cells against these harmful substances we have evolved defensive mechanisms to upregulate a number of oxidative stress response enzymes that are antioxidative and cytoprotective. These enzymes are often referred to as “phase II” enzymes and include glutathione transferases (GSTs), UDP-glucuronosyltransferase (UGT) as well as antioxidant enzymes such as heme oxygenase-1 (HO-1), glutamate cysteine ligase, thioredoxin, catalase, superoxide dismutase, and glutathione reductase.<sup>25, 28</sup> Induction of these enzymes represents an adaptive response that helps to maintain cellular redox homeostasis. This enzyme induction can also provide a potential target for developing therapeutic agents associated with various diseases and conditions involving inflammation and oxidative stress.

The Keap1-Nrf2-ARE pathway is a major regulator of cytoprotective responses to both endogenous and exogenous oxidative stresses caused by reactive oxygen species (ROS), reactive nitrogen species (RNS), and other electrophiles.<sup>29, 30</sup> There are three main cellular components involved in this signaling pathway including Kelch-like ECH-associated protein 1 (Keap1), nuclear factor erythroid 2-related factor 2 (Nrf2), and antioxidant response elements (ARE). The Keap1-Nrf2-ARE is a major signaling

pathway that regulates and induces these cytoprotective enzymes at the transcriptional level.<sup>18, 31-36</sup> The Keap1-Nrf2-ARE signaling pathway induces an adaptive response for oxidative stress which otherwise can lead to many diseases including cancer, Alzheimer's and Parkinson's diseases, and diabetes.<sup>19-24</sup> Thus, targeting the Keap1-Nrf2-ARE signaling pathway is considered as a rational strategy to develop preventive and therapeutic agents for diseases and conditions involving oxidative stress and inflammation.<sup>37-42</sup> The proposed Keap1-Nrf2-ARE pathway for the induction of cytoprotective enzymes is depicted in Fig. 1.<sup>16, 43, 93</sup> Nrf2 is sequestered in the cytoplasm by the protein inhibitor, Keap1, and is transcriptionally inactive. Reactive oxygen species or electrophiles can cause the dissociation of Nrf2 from Keap1 or inhibit the ubiquitination and degradation of Keap1-Nrf2 complex, both of which would allow more Nrf2 to translocate to the nucleus and form a transcriptionally active complex with Maf, leading to the induced expression of Nrf2 itself and oxidative stress response enzymes that deactivate reactive oxygen species and electrophiles. In short, the Keap1-Nrf2-ARE is the main signaling pathway that regulates a series of cytoprotective enzymes at the transcriptional level for various diseases and conditions involving inflammation and oxidative stress.<sup>16, 43</sup>

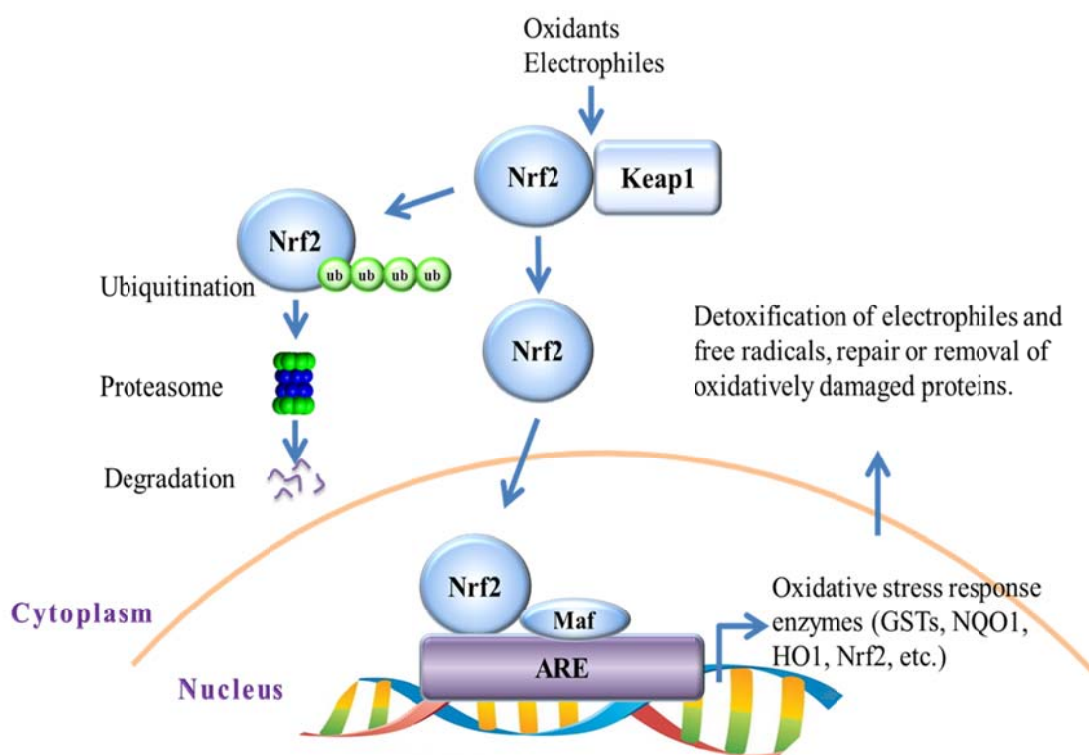


**Figure 1.** Keap1-Nrf2-ARE Pathway for the Induction of Cytoprotective Enzymes

### A. Structural Components and Functions of Keap1-Nrf2-ARE Pathway

Keap1-Nrf2-ARE pathway plays an important role in the maintenance of redox homeostasis and cell survival. Keap1-Nrf2-ARE pathway is a major regulator of antioxidant mechanisms that respond to oxidative and other stress. Under basal conditions, Nrf2 is in an inactive state in the cytoplasm by binding to Keap1. Upon exposure to oxidative or electrophilic stress, Nrf2 is released from Keap1 and translocates to the nucleus. In the nucleus, Nrf2 heterodimerizes with a variety of transcriptional regulatory proteins such as members of the activator protein-1 family and the small Maf family of transcription factors. These protein complexes bind to ARE located in the

upstream promoter region and promotes transcription of a battery of cytoprotective enzymes. There are three main cellular components involved in the Keap1-Nrf2-ARE pathway: they are Kelch-like ECH-associated protein 1 (Keap1), nuclear factor erythroid 2-related factor 2 (Nrf2), and antioxidant response elements (ARE).

### **1. Kelch-Like ECH-Associated Protein 1 (Keap1)**

The amino acid sequences in mouse, rat and human Keap1 proteins are highly conserved. Kelch-like ECH associated protein 1 (Keap1) is a 624-amino acid protein that consists of five domains: the N-terminal region (NTR), a Broad complex, Tamtrack and Bric a brac (BTB) domain, an intervening region or the linker region (IVR), a Kelch/double glycine repeat (Kelch/DGR) and a c-terminal region (CTR). The kelch domain is required to bind Nrf2 and actin, while the BTB and IVR domains are necessary for the modulation and degradation of Nrf2 through binding of Cullin 3 (Cul3), a ubiquitin ligase adaptor protein. The BTB domain is also essential for the dimerization of Keap1. Keap1 is a cysteine-rich protein, containing 25 cysteine residues within the mouse and 27 cysteine residues within the human, most of which can be modified by different oxidants and electrophiles.<sup>29, 44</sup> Several of these cysteine residues such as Cys151, Cys257, Cys273, and Cys288 have been demonstrated to play an important role in altering the conformation of Keap1 leading to nuclear translocation of Nrf2 and subsequent ARE gene expression.<sup>22, 29</sup> Generally, Keap1 containing a number of reactive cysteine residues is an inducer sensor that regulates the level of Nrf2.<sup>16, 45-52</sup>

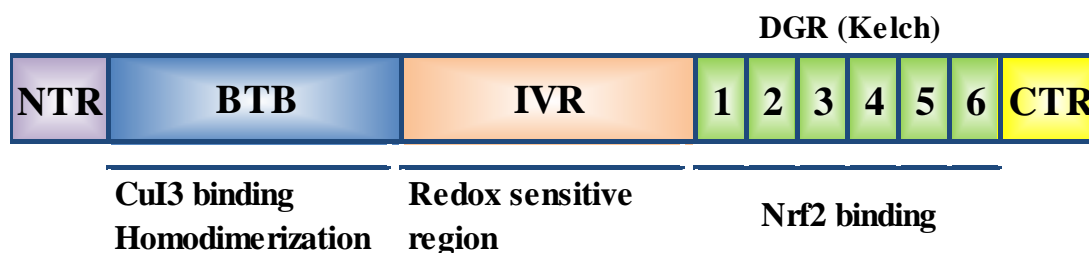


**Figure 2.** Structures and Functions of Keap1

## 2. Nuclear Factor Erythroid 2-Related Factor 2 (Nrf2)

The nuclear factor erythroid 2-related factor 2 (Nrf2) is a 66-kDa basic leucine zipper-type transcription factor that binds to ARE with high affinity as a heterodimer with a small muscle aponeurotic fibrosarcoma (Maf) protein.<sup>53</sup> The Nrf2 protein contains 605 amino acids that form 6 functional domains called Neh1-6 (Nrf2-ECH homology), which are highly conserved across different species.<sup>54-56</sup> Neh1 contains the bZip DNA binding and heterodimerisation domain through which Nrf2 interacts with its transcriptional partners, the small Mafs, and binds to DNA as a heterodimer. Neh2 domain containing the DLG and the ETGE tetrapeptide motif which is the domain binding to Keap1 kelch domain. The Neh3 domain binds to the chromo-ATPase/helicase DNA binding protein family member CHD6, which functions as a transcriptional co-activator to promote transcription of ARE-dependent genes. The Neh4 and Neh5 domains act synergistically to bind another transcriptional co-activator CREB (c-AMP-response element-binding protein)/ATF4 and activate transcription.<sup>55</sup> Finally, the Neh6 domain controls the Keap1-independent regulation of Nrf2. The redox-insensitive Neh6 domain is essential in the degradation of Nrf2 in cells with oxidative stress.<sup>16, 46, 54, 57-64</sup>

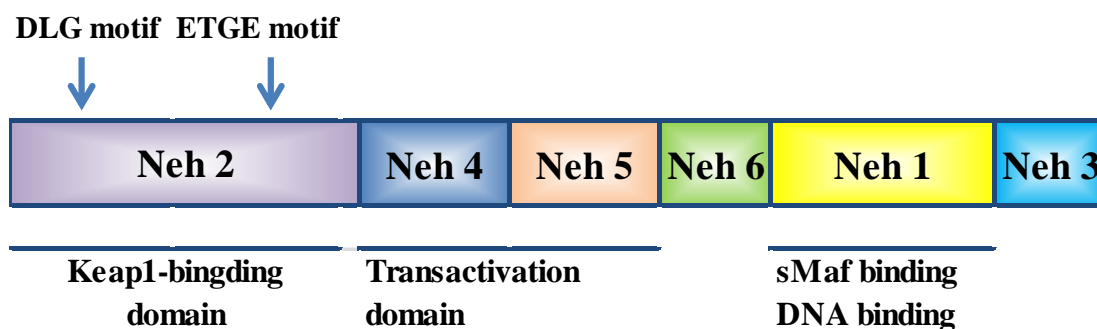


**Figure 3.** Structures and Functions of Nrf2

### 3. Antioxidant Response Elements (ARE)

The upstream regulatory regions of cytoprotective genes to which Nrf2-small Maf heterodimers bind are called antioxidant response elements or electrophile response elements (ARE or EpRE). They were identified by the laboratories of Cecil Pickett and Violet Daniel before the discovery of Nrf2. It is the *cis*-regulatory element containing specific DNA sequences that are present in the upstream regulatory regions of genes encoding the cytoprotective enzymes and proteins. The core sequence was identified as 5'-TGACNNNGC-3' that was shown to be essential for both basal and inducible activity. Bach1 (BTB and CNC homology-1) is one negative regulator of ARE-dependent gene expression which associates with ARE and forms dimers with Maf protein, preventing Nrf2 from binding to DNA under normal physiological conditions. Under oxidative stress conditions, Nrf2 dissociates from Keap1, translocates to the nucleus, forms a heterodimer with Maf, and activates ARE-dependent gene expression.<sup>16, 61, 65-68</sup>

## **B. Mechanisms of Regulation of Keap1-Nrf2-ARE Pathway**

Various studies have shown that Keap1 plays an essential role in the oxidative stress response system. Keap1 is a sensor of oxidative and electrophilic stresses and a major regulator of Nrf2 degradation by proteasome proteolysis.<sup>48, 51, 69, 70</sup> Under basal conditions, Keap1 binds very tightly to Nrf2, anchoring this transcription factor within the cytoplasm, targeting it for ubiquitination and proteasome degradation, thus repressing its ability to induce “phase II” enzymes.<sup>49</sup> Keap1 contributes to Nrf2’s rapid turnover by keeping it within the cytoplasm so that Nrf2 is kept in close proximity to the proteasome system<sup>69</sup> or by promoting the degradation of Nrf2 through recruitment of the E3 ligase and proteasome.<sup>49, 63, 71</sup> In fact, a stable Nrf2 level is maintained by a balance between its rates of synthesis and degradation by the proteasome.<sup>70</sup> Previous studies suggest that the Keap1-Nrf2-ARE pathway may be activated through multiple mechanisms.<sup>51, 72-83</sup> The exact mechanism how Nrf2 is activated by modification of Keap1 is not known, but the key aspect is considered to be post-translational activation of Nrf2 by altering the stability of the protein during ARE induction.

One of the most interesting mechanisms for the regulation of Nrf2 by Keap1 proposed to date is the hinge and latch model.<sup>16, 81, 83, 84</sup> This model indicates that the overall structure of the Keap1 dimer resembles a cherry bob with two globular units connected to the homodimerizing BTB domains. Under basal conditions, Nrf2 binds to a Keap1 dimer. One of the Keap1 monomers binds to Nrf2 through the ETGE motif, while the other monomer binds to the DLG. The DLG motif has relatively low affinity for Keap1 ( $K_d$  about 1000 nmol/L) while the ETGE motif has a higher affinity ( $K_d$  about 5.3 nmol/L).<sup>85</sup>

Binding via the high-affinity ETGE motif and the lower-affinity DLG motif of Nrf2 provides the hinge and latch, which facilitate the optimal positioning of the lysine residues for conjugation with ubiquitin. As a result, Keap1 is able to efficiently target Nrf2 for proteasomal degradation. When inducers enter the cell, they bind to the reactive cysteine residues within Keap1, leading to a conformational change in Keap1 and the release of the weaker interaction with the DLG motif.<sup>63, 86</sup> Under these conditions, the orientation of Nrf2 is not fixed, and it is no longer efficiently targeted for ubiquitination by Keap1.<sup>84</sup> The reduced rate of Nrf2 ubiquitination leads to a reduced rate of Nrf2 degradation. As Nrf2 is still bound to Keap1, any newly translated Nrf2 will not be able to bind Keap1 and can therefore bypass the Keap1 gate, allowing it to accumulate in the cell, translocate to the nucleus, dimerise with small Mafs and activate the transcription of ARE-dependent genes.

An alternative mechanism proposes that Cul3 dissociates from Keap1 upon exposure to the stimuli.<sup>16, 22, 29, 33</sup> Keap1 binds Nrf2 and serves as a substrate adaptor for Cullin 3 (Cul3)-based ubiquitin ligase to target Nrf2 for ubiquitination and proteasomal degradation. In particular, the Keap1-Cul3 interaction seems to be disrupted in the case of modification at Cys151 in BTB domain. Covalent modification of cysteine residue(s) in Cul3 binding BTB domain of Keap1 under induced conditions lead to a steric clash between Keap1 and Cul3.<sup>64</sup> This modification disrupts Keap-Cul3 E3 ligase activity via the dissociation of Keap1-Cul3 interaction without changing the conformation of Keap1.<sup>16, 87</sup> Together, these data suggest that inducers stabilize Nrf2 by dissociating the Keap1-Cul3 complex, leading to the inhibition of Nrf2 ubiquitination and its stabilization.

In both models, the inducer-modified and Nrf2-bound Keap1 is inactivated and, consequently, newly synthesized Nrf2 proteins bypass Keap1 and translocate into the nucleus, bind to the ARE and induce the expression of Nrf2 target genes such as NAD(P)H quinone oxidoreductase 1 (NQO1), heme oxygenase-1 (HO-1), glutamate-cysteine ligase (GCL) and glutathione S transferases (GSTs).<sup>22, 29, 30</sup> In addition to the two models, other alternative mechanisms have also been proposed for Nrf2 stabilization in response to inducers such as nucleocytoplasmic shuttling of Keap1, ubiquitination of Keap1, protein phosphorylation including PKC, MAPK cascade, PI3K and PERK.<sup>16, 26, 88-</sup>

97

### **C. Diseases Involving Keap1-Nrf2-ARE Pathway**

The imbalance between oxidants and antioxidants can be a result of physiological or pathological conditions including aging, and various disease processes. Inflammation has been considered as a contributor to chronic diseases. Inflammation can produce a large amount of ROS, RNS and other electrophiles that can induce oxidative damage to DNA, lipids, proteins and other cellular components.<sup>98</sup> A number of diseases have been identified to involve an oxidative stress and inflammation. Reactive oxidizing substances such ROS and RNS have been identified as potential carcinogens due to their ability to promote mutagenesis and tumor development. In addition to carcinogenesis, elevated level of those reactive oxidizing substances has been shown to alter acute chemical toxicity, asthma and also has been implicated in many diseases such as Alzheimer's and Parkinson's diseases, diabetes, neurodegenerative diseases, and pulmonary disease.<sup>16, 40,</sup>

98-101

Keap1-Nrf2-ARE pathway plays a crucial role in maintaining cellular homeostasis through its ability to regulate the basal and inducible expression of a number of antioxidant proteins and other stress response enzymes.<sup>100</sup> In addition, Keap1-Nrf2-ARE pathway contributes to diverse cellular functions including differentiation, proliferation, inflammation and lipid synthesis. Nrf2 is a transcription factor that is ubiquitously expressed in all human organs. In response to oxidative, electrophilic and environmental stresses, Nrf2 detaches from its cytosolic inhibitor, Keap1, and translocates into the nucleus where it binds to ARE to induce various adaptive defense responses by upregulating a number of “phase II” defense enzymes and antioxidant stress proteins such as HO-1, NQO1, glutathione S-transferases, glutamyl cysteine synthase, and glutathione peroxidase. Increasing attention has been focused on the roles that the Keap1-Nrf2-ARE pathway plays in the protection of our body against many diseases including Alzheimer's and Parkinson's diseases, chronic obstructive pulmonary disease (COPD), osteoarthritis, cardiovascular disease, asthma, and inflammatory bowel disease. Some of Keap1-Nrf2-ARE inducing agents are already in clinical trials as chemopreventive agents for cancer or as therapeutic agents for conditions involving inflammation.<sup>16</sup> Control of the undesirable aspects of the inflammatory process, without compromising its essential role in protection against infection and in tissue repair, is currently the unifying theme for developing new preventive and therapeutic agents.

## **1. Cancer**

Cancer is a group of diseases defined as uncontrolled growth and spread of abnormal cells. Cancer continues to be a growing health problem around the world, particularly

with the steady rise in life expectancy, increasing urbanization and the subsequent changes in environmental conditions. In the United States alone, cancer is the second most common cause of death, accounting for nearly 1 of every 4 deaths. In 2013, it is estimated that approximately 580,350 Americans would die from cancer, almost 1600 people a day. According to the WHO World Cancer Report, cancer causes 7.6 million deaths every year and the number could further increase by 50% to 13 million by 2030. Cancer is still a growing health problem for human.<sup>102</sup>

In addition to the primary prevention strategy of avoiding carcinogenic agents, cancer chemoprevention has emerged as an important means of modulating the process of carcinogenesis. Extensive research has demonstrated the Keap1-Nrf2-ARE system is a key signaling pathway in cancer chemoprevention. The processes of inflammation and oxidative stress are important in the pathogenesis of many diseases. Inflammation can produce a large amount of ROS and other electrophiles that can induce oxidative damage to many cellular components. Our body has evolved a series of defensive mechanisms to up-regulate a number of cytoprotective enzymes to protect our cells from those harmful substances. Keap1-Nrf2-ARE pathway is a common defense mechanism to counteract oxidative stress and protects multiple organs and cells. Activation of Nrf2 upregulates various conjugating enzymes for the detoxification of chemical carcinogens and confers protection against other oxidative stress. Experiments using gene-knockout mouse models have shown that mice with disrupted Nrf2 are more sensitive to toxicological effects of carcinogens, drugs, and inflammatory stresses while mice with disrupted Keap1 exhibited high levels of Nrf2, high constitutive expression of cytoprotective enzymes,

and greater resistance to environmental stresses. Cancer chemopreventive properties of activating Keap1-Nrf2-ARE pathway have been demonstrated in several cancer models including colon cancer, lung cancer, stomach cancer, and liver cancer. Some of the known ARE inducing agents are already in human clinical trials as chemopreventive agents for cancer or as therapeutic agents for conditions involving inflammation. For example, sulforaphane, an isothiocyanate found in cruciferous vegetables and a known ARE inducer, is being tested in clinical trials for the treatment and prevention of prostate cancer and for the treatment of chronic obstructive pulmonary disease (COPD).<sup>20, 42, 103-</sup>

107

## **2. Alzheimer's and Parkinson's diseases**

Parkinson's disease is the second most common neurodegenerative disorder. It is demonstrated that oxidative stress plays a central role in progression of this disease. Brain is sensitive to oxidative stress due to its high lipid content and oxygen consumption. The production of ROS and other electrophiles are implicated in the pathogenesis of Alzheimer's (AD) and Parkinson's (PD) diseases. One way to reduce oxidative stress is through upregulation of the Keap1-Nrf2-ARE pathway to induce the expression of various antioxidant enzymes. The protective role of activating Keap1-Nrf2-ARE pathway against oxidative stress has been demonstrated and it has become a therapeutic target for the treatment of AD and PD disease.<sup>108-112</sup>

## **3. Liver diseases**

The liver is a central organ that performs a wide range of functions such as detoxification and metabolism of xenobiotic. Since it is a metabolically active organ, liver is

particularly susceptible to oxidative stress. It is reported that liver diseases are highly associated with oxidative stress. Keap1-Nrf2-ARE is a major signaling pathway that regulates the expression of antioxidant defense enzymes in the liver. It is activated in response to oxidative stress and electrophiles and induces its target genes by binding to ARE. Keap1-Nrf2-ARE pathway exhibits diverse biological functions against liver disease via target gene expression in several animal models. Therefore, the role of the Keap1-Nrf2-ARE pathway plays an important role in liver pathophysiology and has potential application as a therapeutic target to prevent and treat liver diseases.

#### **4. Chronic obstructive pulmonary disease (COPD)**

Chronic obstructive pulmonary disease (COPD) remains the fourth highest cause of death in United States. COPD is a kind of common disease, which displays incompletely reversible airflow limitation. The imbalance of oxidant and antioxidant is one of the major pathogenesis of COPD. The decline in Nrf2-dependent anti-oxidative enzymes with significant decrease in Nrf2 expression was observed in COPD patient lungs. Activation of Keap1-Nrf2-ARE pathway is a novel therapeutic approach for the treatment of COPD and other airway disorders involving oxidative stress.<sup>113-116</sup>

#### **5. Diabetes**

Diabetes is the major cause of chronic kidney disease. It has been shown recently that Keap1-Nrf2-ARE pathway is involved in the against of development of diabetic nephropathy in mice. Nrf2-mediated expression of endogenous antioxidants has been shown as a critical adaptive defense mechanism against high glucose-induced oxidative damage in diabetes. Those information suggest that activation of Keap1-Nrf2-ARE

pathway could be an effective approach to prevent and treat diabetes and diabetes-related metabolic disorders.<sup>117-121</sup>

### **6. Other disease involving Keap1-Nrf2-ARE pathway**

Other than the diseases mentioned above, the protective roles of activating Keap1-Nrf2-ARE pathway have also been demonstrated in other diseases including cardiovascular disease as well as some associated diseases<sup>122-126</sup>, inflammatory bowel diseases, and autoimmune joint diseases<sup>127-132</sup>.

### **III. Novel Small Molecule Modulators of Keap1-Nrf2-ARE Pathway**

Keap1-Nrf2-ARE pathway represents an attractive target for regulating a series of cytoprotective proteins at the transcriptional level for the control of oxidative stress and inflammation and for the management of many diseases and conditions. Two types of novel small molecule modulators of Keap1-Nrf2-ARE pathway were developed in our lab: 1). heterocyclic curcumin analogs as ARE inducers<sup>133</sup> and 2) direct small molecule inhibitors of Keap1-Nrf2 protein-protein interaction.<sup>43</sup>

Curcumin exhibits antioxidant, anti-inflammatory, chemoprevention, and chemotherapeutic activity. Curcumin was demonstrated as an indirect inhibitor of Keap1-Nrf2 protein-protein interaction. It effectively attenuates oxidative stress and inflammation by modulating Keap1-Nrf2-ARE pathway holding potential for safe treatment of cancer and other diseases involving inflammation and oxidative stress. Unfortunately, the potential clinic utility of curcumin is limited due to its low potency, chemical and metabolic instability, poor bioavailability and selectivity.<sup>133</sup>

Two series of novel heterocyclic curcumin analogues with the diketone moiety masked as a heterocyclic adduct with thiourea while retaining most of the other curcumin structure features were designed and synthesized. These novel analogues were designed to mitigate the chemical reactivity of both curcumin and isothiocyanates, both of which are known to react with biological nucleophiles and be cytotoxic. The chemical stability of these novel heterocyclic compounds has the potential for longer half-lives as compared to curcumin. The biological activity evaluations revealed that some of these new curcumin analogs are more effective ARE activators than curcumin and isothiocyanates.<sup>133</sup>

On the other hand, a high-throughput screen (HTS) of the MLPCN library using a homogenous fluorescence polarization assay developed in our lab identified a small molecule as a first-in-class inhibitor specifically for the direct inhibition of the Keap1-Nrf2 interaction. The HTS hit has three chiral centers. A combination of flash and chiral chromatographic separation demonstrated that Keap1-binding activity resides predominantly in one stereoisomer designated as LH601A, which is at least 100× more potent than the other stereoisomers. The stereochemistry of the four isomers was assigned using X-ray crystallography and confirmed using stereospecific synthesis. LH601A is functionally active in both ARE gene reporter assay and Nrf2 nuclear translocation assay.<sup>43</sup>

Various analogs of LH601A were designed and synthesized to explore the chemical spaces around the various points of the scaffold to improve binding affinity. The preliminary structure activity relationships (SAR) provided more information and

guidance for further structural optimization. All the synthesized analogs were evaluated by FP or SPR assay and several analogs were shown to be more potent direct inhibitors of Keap1-Nrf2 protein-protein interaction. These direct Keap1-Nrf2 inhibitors can mimic the actions of electrophiles like Michael acceptors and isothiocyanates in the induction of cytoprotective enzymes but are more selective and specific against the Keap-Nrf2 interaction at the protein-protein interface without the associated side effects. Therefore, these direct inhibitors of Keap1-Nrf2 protein-protein interaction have great potential to be developed into innovative therapeutic agents for many diseases and conditions involving oxidative stress.<sup>43</sup>

#### **IV. Summary**

The Keap1-Nrf2-ARE pathway is a major regulator of cytoprotective responses to endogenous and exogenous stresses caused by reactive oxygen species (ROS), reactive nitrogen species (RNS), and other electrophiles. There are three main cellular components involved in the pathway including Keap1, Nrf2, and ARE. Activation of Keap1-Nrf2-ARE system by disrupting the Keap1-Nrf2 protein-protein interaction can induce the ARE-dependent expression of various detoxifying and antioxidant defense enzymes and proteins critical for preventing oxidative damage, inflammation and tumorigenesis.

Under basal conditions, Keap1 binds very tightly to Nrf2, anchoring this transcription factor within the cytoplasm, targeting it for ubiquitination and proteasome degradation, thus repressing its ability to induce phase II genes. Upon generation of

oxidative/electrophilic stress, Nrf2 is released from Keap1 and translocates to the nucleus, where Nrf2 heterodimerizes with a variety of transcriptional regulatory proteins, including members of the activator protein-1 family and the small Maf family of transcription factors. These protein complexes bind to ARE located in the upstream promoter region and promotes transcription of a battery of cytoprotective genes.

The protective role of activation of Keap1-Nrf2-ARE pathway has been established in many human disorders including cancer, Alzheimer's and Parkinson's diseases, chronic obstructive pulmonary disease (COPD), asthma, atherosclerosis, diabetes, inflammatory bowel disease, multiple sclerosis, osteoarthritis and rheumatoid arthritis. Some ARE inducing agents are already in clinical trials as chemopreventive agents for cancer or as therapeutic agents for conditions involving inflammation. Keap1-Nrf2-ARE pathway represents a novel molecular target to regulate the cellular Nrf2 level and ARE gene expression for the control of oxidative stress and inflammation. Targeting Keap1-Nrf2 protein-protein interaction provides a new strategy to discover potential antioxidant inflammation modulators for cancer as well as for other diseases and conditions involving oxidative stress and inflammation.

Two series of novel heterocyclic curcumin analogues named as iminothiazinylbutadienols and divinylpyrimidinethiones with its diketone moiety masked as a heterocyclic adduct with thiourea were designed and synthesized. The chemical stability of these novel heterocyclic compounds was improved and some of these new

curcumin analogues are more effective ARE activators than curcumin and isothiocyanates. On the other hand, a direct small molecule inhibitor of the Keap1-Nrf2 interaction was identified by HTS. Various analogs of LH601A were designed and synthesized to improve binding affinity. Several analogs were shown to be more potent direct inhibitors of Keap1-Nrf2 protein-protein interaction than LH601A.

In summary, Keap1-Nrf2-ARE pathway has evolved as a direct molecular target to regulate the cellular Nrf2 level and ARE gene expression for the control of oxidative stress and inflammation. Targeting Keap1-Nrf2 protein-protein interaction opens up a new direction to discover potential antioxidant inflammation modulators for cancer as well as for other diseases and conditions involving oxidative stress and inflammation.

## **CHAPTER 2**

### **DESIGN AND SYNTHESIS OF NOVEL HETEROCYCLIC CURCUMIN ANALOGS AS ARE ACTIVATORS**

#### **I. Introduction**

##### **A. Curcumin**

Dietary fruits and vegetables are rich sources of chemopreventive compounds and are widely investigated due to their low toxicity but significant chemopreventive efficacy. Numerous studies have shown that many natural dietary compounds can potentially modulate the Keap1-Nrf2-ARE pathway, leading to prevention of cancer initiation, promotion and progression. Studies have also shown that these fruit and vegetables contain relatively high amounts of antioxidants or compounds that can activate the Keap1-Nrf2-ARE pathway and induce the expression of anti-oxidative stress cytoprotective enzymes. The ARE-mediated gene expression and therefore the induction of antioxidant enzymes have been linked to important protective mechanisms of cells and tissues against the toxic effects of ROS, RNS and other electrophiles generated from endogenous or exogenous sources. Many natural products like curcumin, phenethylisothiocyanate (PEITC), sulforaphane (SFN), and epigallocatechol gallate obtained from natural sources such as fruits, vegetables, and tea products are known to be Nrf2 activators or ARE inducers.<sup>16, 25, 28, 133</sup>

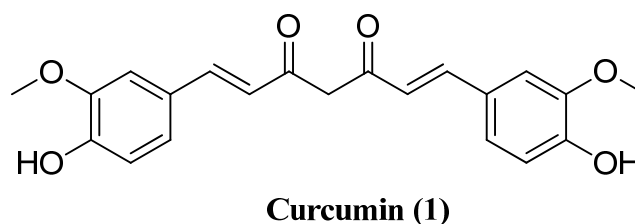


**Figure 4.** Chemical Structure of Curcumin

Curcumin (1,7-bis[4-hydroxy-3-methoxyphenyl]-1,6-heptadiene-3,5-dione, **Fig. 4.**), the yellow principal polyphenol curcuminoid, is the major active component of the popular Indian spice turmeric, originally isolated from the plant *Curcuma longa L.*<sup>106, 134</sup> It has been shown to be able to target Keap1-Nrf2-ARE pathway and activate ARE genes.<sup>133, 135, 136</sup> The activation of ARE genes can lead to the enhanced expression of oxidative stress response enzymes that function as a cytoprotective shield against oxidative stress and inflammation.<sup>16, 135-139</sup> Curcumin has been reported to possess a large number of biological and cellular activities including antioxidative, anti-inflammatory, anticarcinogenic and hypocholesterolemic properties. Curcumin has also been evaluated in many clinical trials for various diseases such as cancer, psoriasis, and Alzheimer's disease.<sup>106, 140</sup>

### **B. Curcumin Relieves Keap1 Mediated Inhibition of Nrf2**

Curcumin has been shown to be an anti-oxidative and anti-inflammatory compound which can activate Keap1-Nrf2-ARE signaling pathway through co-valent modification

of cysteine sulfhydryl groups in Keap1. Under normal conditions, Nrf2 exists in an inactive state and resides in the cytoplasm as part of a complex with Keap1. Nrf2 is ubiquitinated and further degraded by proteasome. After the curcumin treatment, the Keap1-Nrf2 interaction is disrupted and Nrf2 is released from Keap1 and translocated to the nucleus. In the nucleus, Nrf2 binds to ARE and induce the expression of many antioxidant enzymes. These enzymes can act together to deactivate the reactive oxygen species and other electrophiles and restore the redox balance.

An experiment depicted in Figure 5 was reported to examine whether curcumin can modulate the Keap1-Nrf2-ARE pathway. In the assay, expression of Keap1 or co-expression of Keap1 and curcumin only showed basal luciferase activity (lanes b and c). Keap1 almost completely inhibited Nrf2 activation (lane d), but this inhibition of Nrf2 by Keap1 was released by the treatment of curcumin (lane e) and lead to the elevated luciferase activity which proves that curcumin can disrupt the Keap1-Nrf2 interaction and.<sup>136</sup>

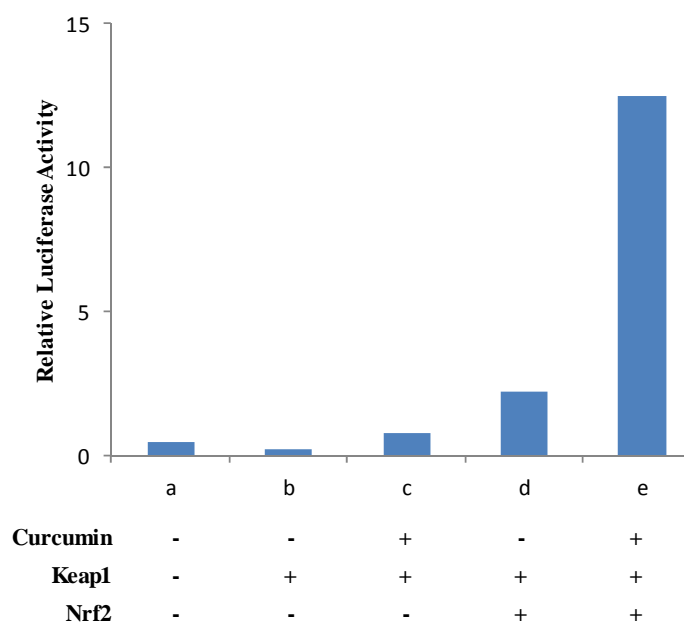


**Figure 5.** Curcumin Relieves Keap1 Mediated Inhibition of Nrf2<sup>136</sup>

### C. Biological Properties of Curcumin Involving Keap1-Nrf2-ARE Pathway

Abundant research has demonstrated the beneficial roles of curcumin in anti-inflammation, anti-oxidation, chemoprevention, and chemotherapeutic activity in both cell culture experiments and animal models.<sup>138, 141-145</sup> It has been shown to protect against many types of cancer and to suppress angiogenesis and metastasis in different animal models. Moreover, the preventive and therapeutic efficacy of curcumin has been demonstrated through its ability to activate the Keap1-Nrf2-ARE pathway and induce the expression of “phase II” detoxifying and antioxidant enzymes.

Curcumin was reported to disrupt the Keap1-Nrf2 protein-protein interaction, leading to increases in the expression and activity of HO-1 in porcine renal epithelial proximal

tubule cells. It was also reported that Nrf2 cytoprotective signaling can be significantly activated by curcumin in astrocytes. Curcumin effectively intercepted and neutralized ROS induced by H<sub>2</sub>O<sub>2</sub>, which was accomplished by activation of Nrf2 signaling. Curcumin also protects human keratinocytes against inorganic arsenite-induced acute cytotoxicity through an Nrf2-dependent mechanism.<sup>136, 146-148</sup>

Curcumin has been evaluated in clinical trials as preventive and therapeutic agents for conditions involving oxidative stress and inflammation such as pancreatic cancer, colon cancer, multiple myeloma, psoriasis, and Alzheimer's disease.<sup>140, 149-155</sup> The chemopreventive ability of curcumin in arresting cancer development and progression is related to its ability to both inhibit cancer initiation, by preventing carcinogen activation, and suppress malignant cell proliferation during promotion and progression stages. Many animal studies suggested health benefits of curcumin. A very recent experimental study showed that short-term curcumin treatment in high-fat diet-fed mice ameliorated muscular oxidative stress by activating Nrf2 function. Topically administered curcumin inhibits TPA-induced mouse ear inflammation and epidermis inflammation. Injected and dietary curcumin alleviates the pathology of Alzheimer transgenic mouse. Curcumin induces a Nrf2 driven response against oxidative and nitrative stress after praziquantel treatment in liver fluke-infected hamsters. Curcumin also enhanced the expression of genes involved in the Keap1-Nrf2-ARE pathway such as glutamate cysteine ligase, manganese superoxide dismutase, and catalase, leading to increased ferric antioxidant capacity in the plasma. Dose-dependent chemotherapeutic effects elicited by curcumin have been established in various animal studies of colon, duodenal, stomach, esophageal,

and oral tumorigenesis. These findings demonstrate that, by modulating Keap1-Nrf2-ARE pathway, the curcumin effectively attenuates oxidative stress and inflammation, which suggest that curcumin hold promising potential for safe treatment of cancer and other diseases involving inflammation and oxidative stress.<sup>140, 149-155</sup>

In short, curcumin exhibits a variety of biological and cellular activities including antioxidant, anti-inflammatory, anti-carcinogenic and hypocholesterolemic properties, anti-angiogenic, anti-malarial, anti-mutagenic, and anti-microbial activities.

#### **D. Limitations of Curcumin**

Generally, there are four major properties of curcumin: anti-oxidation, anti-cancer, anti-inflammatory and anti-microbial activities. Unfortunately, due to its low potency, fast metabolism, poor bioavailability and selectivity, the potential clinical utility of curcumin is limited.<sup>155-159</sup>

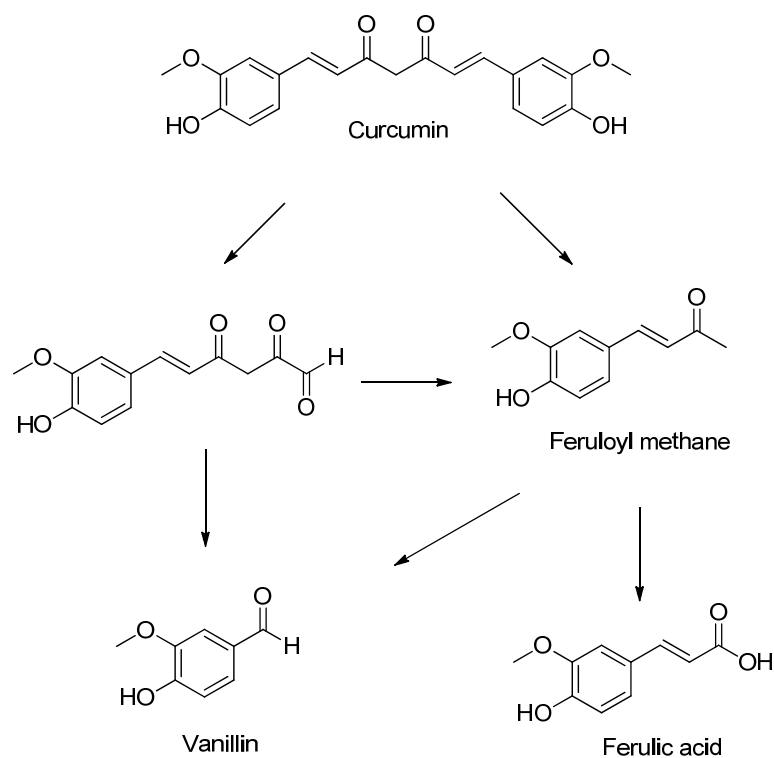


**Figure 6.** Degradation of Curcumin under Basic Condition

The potential utility of curcumin is limited partly due to its chemical and metabolic instability. The presence of the active methylene group and  $\beta$ -diketone moiety contributes to the instability of curcumin under physiological conditions and its fast metabolism *in vivo*.<sup>159-161</sup> The pKa values of the three acidic protons in curcumin have been reported to be 7.8, 8.5 and 9.0, respectively. The low chemical stability of curcumin in buffers from neutral to alkaline pH has been demonstrated in many reports. Curcumin decomposes rapidly under neutral and basic conditions.<sup>159</sup> The main decomposition products have previously been identified as *trans*-6-(4'-hydroxy-3'-methoxyphenyl)-2,4-dioxo-5-hexenal, feruloyl methane, ferulic acid and vanillin and the latter being a secondary degradation product formed by hydrolysis of feruloyl methane.<sup>133</sup>

And *in vivo*, recent studies indicated that the  $\beta$ -diketone moiety in curcumin appears to be a specific substrate of a series of aldo-keto reductases.<sup>161-163</sup> The presence of  $\beta$ -diketone moiety in curcumin probably contribute to its fast metabolism *in vivo*.<sup>161, 164</sup> Curcumin undergoes rapid metabolism after absorption. The major metabolites of curcumin after oral administration are curcumin glucuronide and curcumin sulfate while the major metabolite of curcumin after i.p. injection is tetrahydrocurcumin, which also form glucuronide and sulfate conjugates.<sup>156</sup>

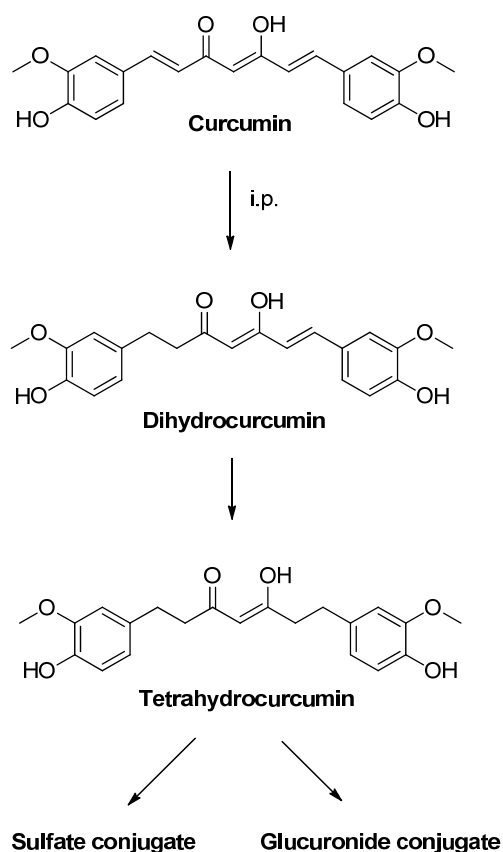


**Figure 7.** Metabolism of Curcumin *in vivo*

Curcumin is soluble in methanol, chloroform and DMSO. It is almost insoluble in water at acidic pH. Its solubility increases at higher pH, however, curcumin undergoes rapid hydrolytic degradation at pH above neutral. Its poor aqueous solubility has also contributed to its low *in vivo* bioavailability. Curcumin is well-known compound with low oral bioavailability. It's reported that most of the unformulated curcumin taken orally is usually found in feces. This is largely due to its low water solubility and slow dissolution in lumen fluid. Another example, the concentration of curcumin is 11.1 nM in plasma and 1.3  $\mu$ M in target tissues with an oral administration of the dose of 3.6 g/day in a phase I clinical trial.<sup>165</sup> From numerous other studies focusing on the pharmacokinetics of curcumin in experiment animals and human, the highest serum concentrations reported are 1.35  $\mu$ g/mL from 2 g/kg curcumin in rat and 51 ng/ml from 12 g/kg curcumin in human.<sup>156</sup>

## **II. Design and Synthesis of Novel Heterocyclic Curcumin Analogs**

### **A. Design Principle**

The use of curcumin is limited due to low chemical stability and fast metabolism and low water solubility under acidic or neutral conditions. A number of synthetic modifications of curcumin have been carried out to enhance its biological activities and to improve its pharmacokinetic properties. From previous reports, the chemical stability and biological activities of curcumin could be enhanced by modifying its  $\beta$ -diketone moiety.<sup>152, 166-168</sup> Some of the curcumin analogs without the  $\beta$ -diketone moiety have been reported to possess enhanced chemical stability and improved pharmacokinetic profiles *in vivo*.<sup>168, 169</sup>

Heterocycles are commonly present in the various molecules and known drugs.<sup>170</sup> Curcumin analogs bearing certain heterocycles also showed improved anticancer and anti-inflammatory activities.<sup>168, 171, 172</sup> Thereby, our strategy is to mask the chemically reactive  $\beta$ -diketone moiety of curcumin with different thioureas and introduce one heterocyclic ring structure to curcumin while retaining most of the other curcumin structure features in order to improve chemical stability and increase ARE induction activity. Furthermore, the basic heterocyclic nitrogen atom in the analogs may provide an opportunity to convert the designed compounds into their salt forms and potentially benefit the aqueous solubility. Finally, the flat shape, lack of flexibility and hydrogen bonding potential of the formed heterocyclic ring might provide some target selectivity for these novel curcumin analogs.<sup>133, 170, 173</sup>

Curcumin has two Michael acceptors when it exists in the keto form. The  $\beta$ -diketone moiety can accept a variety of nucleophiles such as thiols and amines via a Michael addition reaction.<sup>172, 174, 175</sup> However, the tautomeric enol form is energetically more stable. The computational chemistry has predicted that the tautomeric enol form is 6.7 kcal/mol lower in energy than the  $\beta$ -diketone tautomer. Due to the acidic nature of the protons on the methylene carbon, the enol form of curcumin is more stable



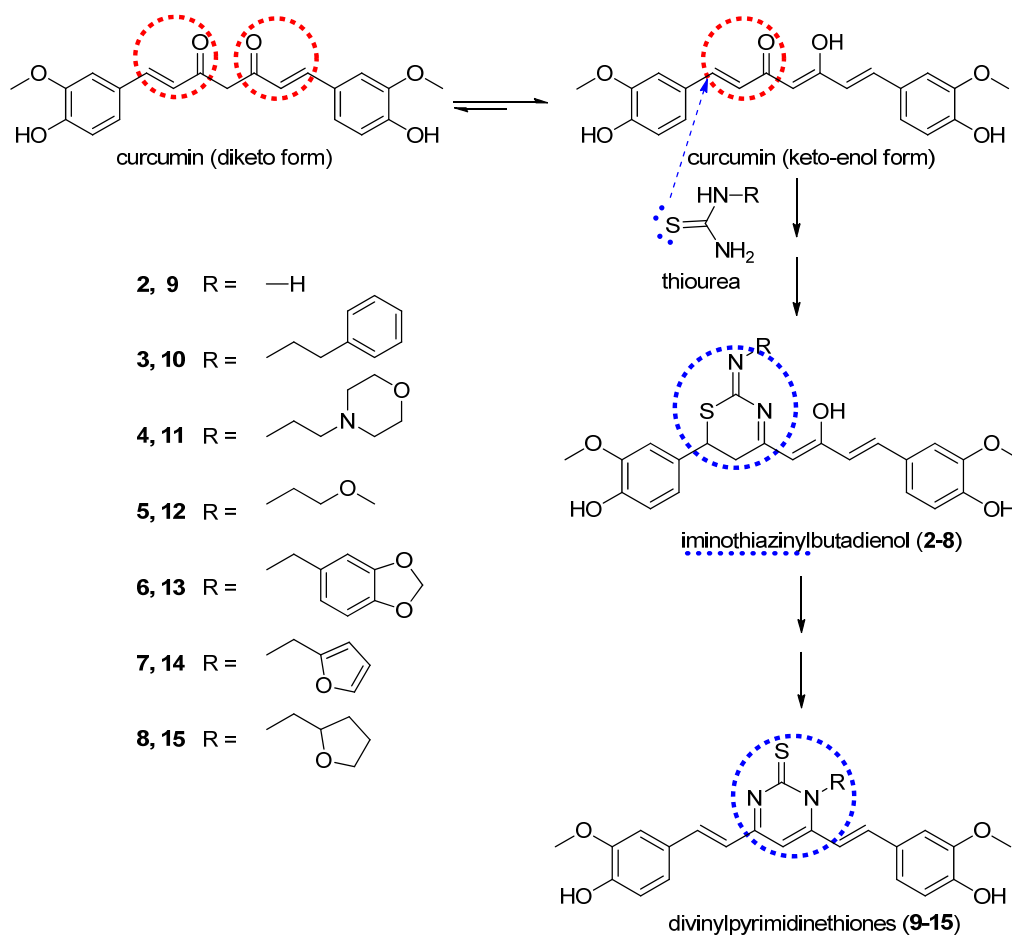
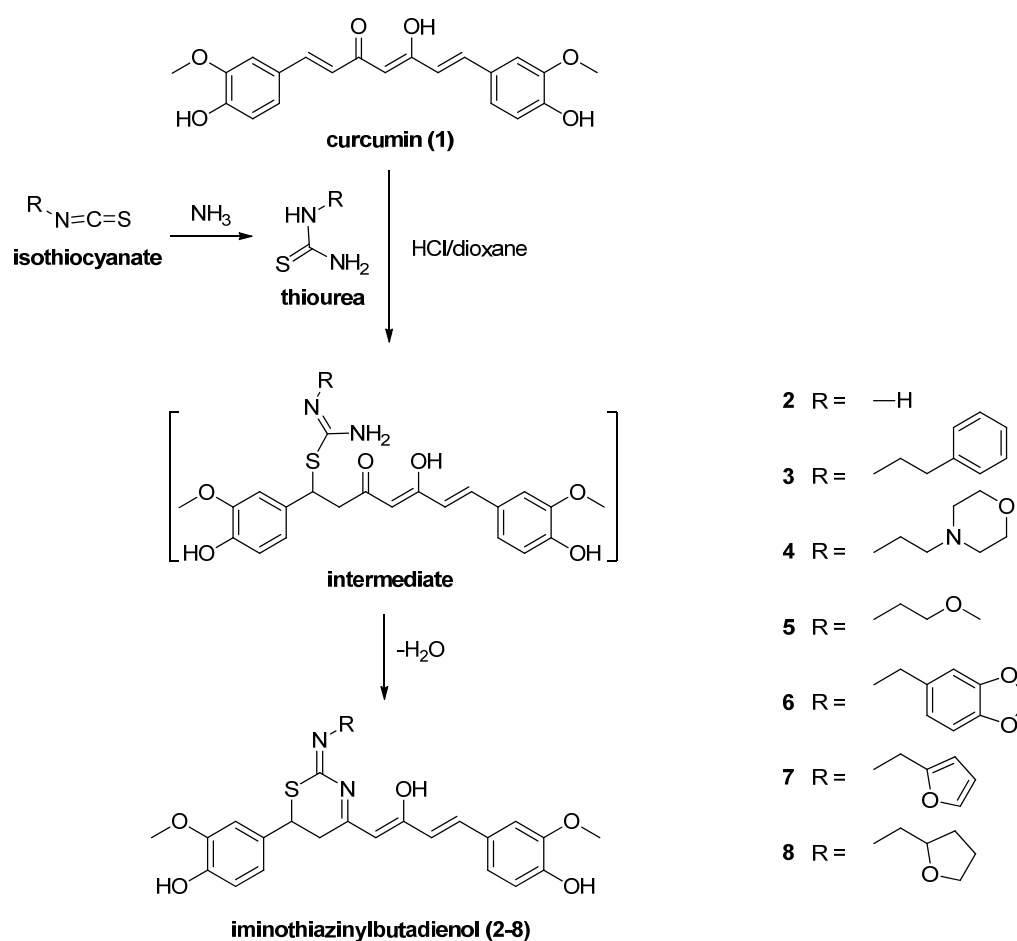


**Figure 9.** Design of Novel Iminothiazinylbutadienols and Divinyldiprimidinethiones as Conjugates of Curcumin and Thiourea.

### B. Synthesis of Novel Heterocyclic Curcumin Analogs

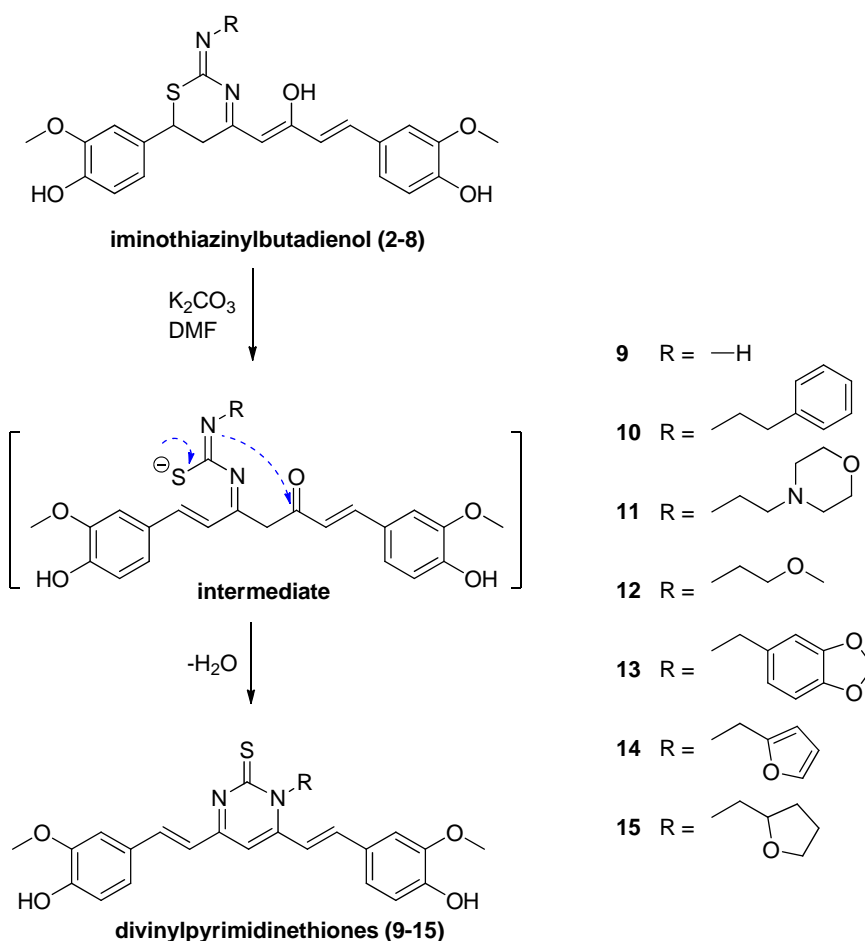
The synthesis of the designed heterocyclic curcumin analogs iminothiazinylbutadienols (2-8) is shown in Scheme 1. Thioureas are either commercially available or readily prepared from the reaction between isothiocyanates and ammonia. The acid-catalyzed addition of thioureas to curcumin is carried out in the presence of 4 N HCl in dioxane.

Nucleophilic attack of the sulfur in thioureas to the  $\beta$ -carbon of the Michael acceptor in enol ketone form of curcumin under the acidic conditions give the Michael adduct intermediates, which then cyclize with the elimination of water to afford the desired iminothiazinylbutadienols **2-8**.<sup>133</sup>



**Scheme 1.** Synthesis of Novel Iminothiazinylbutadienols from Curcumin and Isothiocyanates.

The first class of novel heterocyclic curcumin analogs can be further transformed to form the second class of heterocyclic curcumin analogs under basic conditions. Generally, the thiazine ring of the synthesized iminothiazinylbutadienols (**2-8**) can be opened in the presence of potassium carbonate in DMF to form the intermediate and then cyclize with the elimination of water to afford the second series of desired divinylpyrimidinethiones **9-15**.<sup>133</sup>

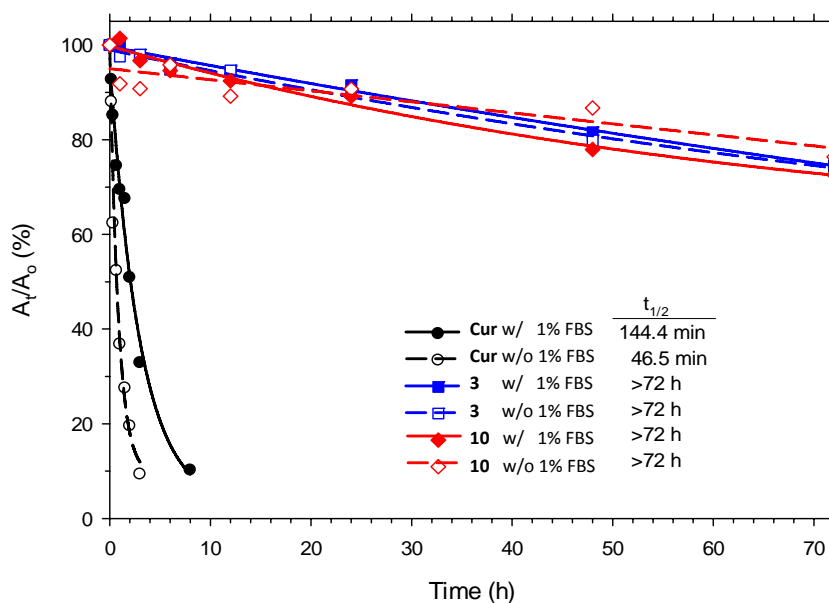


**Scheme 2.** Synthesis of Novel Divinylpyrimidinethiones from Iminothiazinylbutadienols.

### III. Results and Discussions

#### A. Stability of Novel Iminothiazinylbutadienols and Divinylpyrimidinethiones

The chemical reactivity of curcumin is well known as evidenced by the adduct formation when it is incubated with glutathione (GSH).<sup>177</sup> Indeed, when curcumin was incubated with 1 mM GSH in pH 7.4 buffer at 37 °C, it forms 1:2 adduct with GSH as indicated by LC-MS analysis. However, when the selected heterocyclic curcumin analogs 3 and 10 were incubated with GSH under the same conditions, no GSH adducts were detected using LC-MS. Their lack of reactivity towards GSH suggests that we have successfully masked the reactive Michael acceptors of curcumin with iminothiazinylbutadienols and divinylpyrimidinethiones.<sup>133</sup>

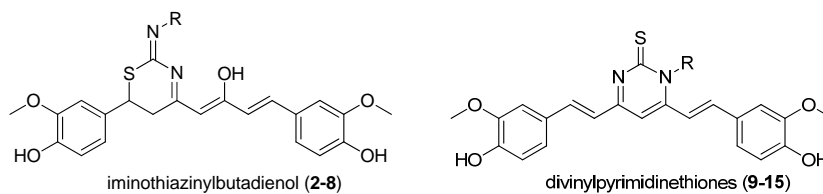


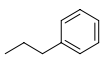
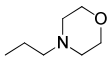
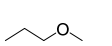
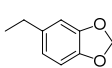
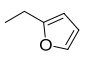
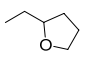
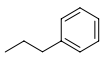
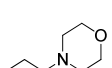
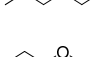
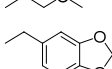
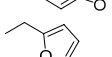
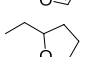
**Figure 10.** Stability Study of Curcumin and Representative Analogs.

To investigate the stability of curcumin analogs under cell culture conditions, curcumin and its analogs were incubated in Dulbecco's Modified Eagle's Medium with pH 7.4 with 5% methanol in the absence or presence of 1% FBS (Fig. 10) and monitored the changes by HPLC. It was found curcumin was not stable under these conditions and degraded very rapidly with a half-life about 46 min in the absence of FBS. In the presence of 1% FBS, the stability of curcumin was also poor, about 50% curcumin degraded only after 2 h. In contrast, the novel heterocyclic curcumin analogs were much more stable. For example, compound **3** and **10** had only about 25% decomposition after 72 h under the same incubation conditions in the presence or absence of FBS, indicating that the novel heterocyclic curcumin analogs were much more stable than curcumin.<sup>133</sup>

### **B. Cytotoxicity and ARE Induction Activities of Novel Curcumin Analogs**

The novel heterocyclic curcumin analogs were submitted to NCI Developmental Therapeutics Program (DTP) for cell growth inhibition evaluation in the NCI-60 human tumor cell lines.<sup>178</sup> The NCI60 screening at NCI is a two-stage process, beginning with the evaluation of all analogs against the 60 cell lines at a single dose of 10  $\mu$ M. Compounds that exhibit significant growth inhibition are evaluated further against the 60 cell panel at five concentrations. As shown in Table 1, four out of the 14 compounds submitted did not show significant cytotoxicity and were not selected for further evaluation and the ten analogs that were evaluated in the five point dose-response assays demonstrated cytotoxicity similar to that of curcumin and isothiocyanates.<sup>133</sup>

**Table 1.** The Cytotoxicity of Novel Curcumin Analogs in the NCI60 Screening

Compd	R	NSC# (Lab ID)	% Mean Cell Growth (% at 10 $\mu$ M) <sup>a</sup>	Average GI <sub>50</sub> <sup>b</sup> ( $\mu$ M)
2	-H	762482 (LH502)	37.84	2.17
3		762483 (LH503)	3.61	2.07
4		762485 (LH505)	70.93	16.5
5		762487 (LH507)	0.50	2.32
6		762489 (LH510)	60.56	54.9
7		762484 (LH504)	101.57	- <sup>c</sup>
8		762520 (LH509)	10.85	2.41
9	-H	762502 (LH525)	93.53	- <sup>c</sup>
10		762503 (LH526)	36.61	6.87
11		762505 (LH528)	85.22	- <sup>c</sup>
12		762507 (LH530)	-18.35	1.67
13		762509 (LH532)	36.95	9.51
14		762504 (LH527)	66.43	- <sup>c</sup>
15		762508 (LH531)	-5.50	2.88
CUR		32982	37.2	8.04
PEITC		87868	52.18	1.09
SFN		749790	87.25	- <sup>d</sup>

<sup>a</sup> Mean Cell Growth (% relative control) in the NCI60 single dose assay at 10  $\mu$ M. <sup>b</sup> Average GI<sub>50</sub> ( $\mu$ M) in the NCI60 5-dose testing. <sup>c</sup> Not selected for 5-dose testing. <sup>d</sup> 5-dose testing data not available in the NCI60 database.

Representative heterocyclic curcumin analogs were then evaluated for their ability to induce ARE gene expression in an ARE luciferase reporter assay in SW480 cell line at 1 and 10  $\mu$ M. Briefly, the SW480 cells were transfected with luciferase reporter gene linked to ARE; the transfected cells cultured and maintained in DMEM supplemented with 5% FBS at 37 °C in a humidified incubator with 5% CO<sub>2</sub>. They are allowed to grow for 24 h to reach 70% confluency before replacing with medium containing the test compounds. At the end of 6-h treatment period, cells are washed twice with ice-cold PBS, pH 7.4 and lysed with the lysis buffer in the Promega luciferase assay kit. After centrifugation at room temperature, supernatant is analyzed for luciferase activity by mixing with assay reagents from the Promega kit and the luminescence counts were read with a microtitre plate reader. Normalization of the luciferase activity is done based on protein concentration. Using this assay, we have evaluated the ARE-inducing activity of six compounds **2-4** and **9-11** as shown in Fig. 11 in comparison to curcumin and sulforaphane (SFN). As expected, curcumin and sulforaphane showed strong ARE-

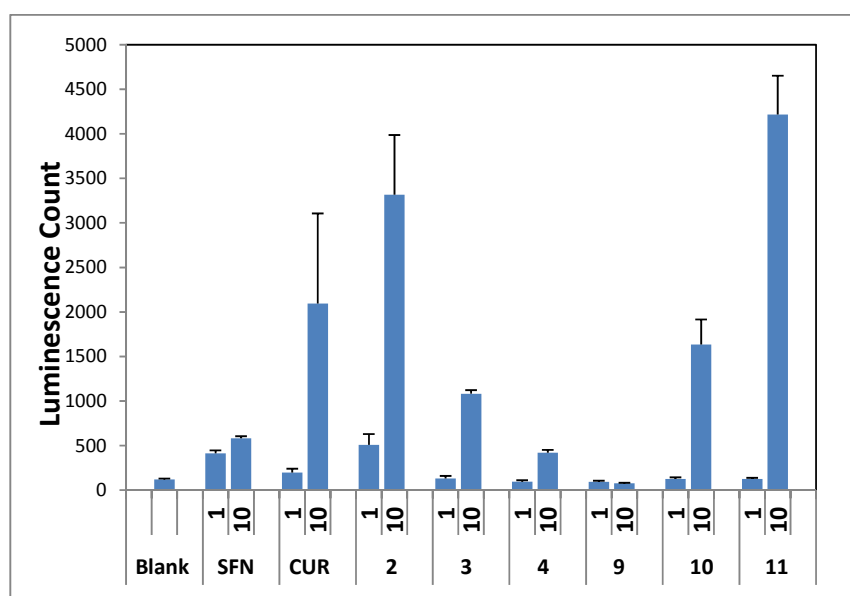


**Figure 11.** ARE-Inducing Activity of Novel Heterocyclic Curcumin Analogs

induction (about 18 and 5 fold increase) at 10  $\mu$ M. Among the novel heterocyclic curcumin analogs tested, novel heterocyclic analogs **3**, **4**, and **10** also showed strong ARE-induction (about 4-15 fold increase) at 10  $\mu$ M. Most importantly, curcumin analogs **2** and **11** exhibited the strongest ARE-induction with 30-35-fold increase in luciferase activity at 10  $\mu$ M. These results are encouraging and the novel heterocyclic curcumin analogs will be further evaluated in additional ARE-induction and antioxidative assays.<sup>133</sup>

#### **IV. Summary**

Curcumin exhibits antioxidant, anti-inflammatory, chemoprevention, and chemotherapeutic activity. Curcumin was demonstrated as an indirect inhibitor of Keap1-Nrf2 protein-protein interaction. It effectively attenuates oxidative stress and inflammation by modulating Keap1-Nrf2-ARE pathway holding potential for safe treatment of cancer and other diseases involving inflammation and oxidative stress. Curcumin has been evaluated in clinical trials as chemopreventive and therapeutic agents for conditions involving inflammation such as pancreatic cancer, colon cancer, multiple myeloma, psoriasis, and Alzheimer's disease. Unfortunately, the potential clinic utility of curcumin is limited due to its low potency, chemical and metabolic instability, poor bioavailability and selectivity.

Two series of novel heterocyclic curcumin analogs named as iminothiazinylbutadienols and divinylpyrimidinethiones with its  $\beta$ -diketone moiety masked as a heterocyclic adduct with thiourea while retaining most of the other curcumin structure features were designed

and synthesized. These novel analogs were designed to mitigate the chemical reactivity of both curcumin and isothiocyanates, both of which are known to react with biological nucleophiles and be cytotoxic. The chemical stability of these novel heterocyclic curcumin analogs was improved with much longer half-lives under physiological conditions as compared to curcumin. The biological activity evaluations revealed that some of these new curcumin analogues are more effective ARE activators than curcumin and isothiocyanates.

## CHAPTER 3

### DISCOVERY, DESIGN AND SYNTHESIS OF DIRECT INHIBITORS OF KEAP1-NRF2 PROTEIN-PROTEIN INTERACTION

#### I. Introduction

##### A. Direct Inhibition of Keap-Nrf2 Protein-Protein Interaction

The Keap1-Nrf2-ARE signaling pathway plays a key role in oxidative stress response and inflammation. Targeting the Keap1-Nrf2-ARE signaling pathway represents an attractive strategy to develop preventive and therapeutic agents for diseases and conditions involving oxidative stress and inflammation. Most research efforts in modulation of oxidative stress and inflammation over the past decade have focused on natural products that are isolated from fruit, vegetables, and tea products, but are indirect inhibitors of Keap1-Nrf2 interaction. Some of the common natural products include sulforaphane, curcumin, and epigallocatechin gallate and some of the synthetic compounds include oltipraz, anetholedithiolethione, bardoxolone methyl. Structurally, these compounds are either chemically reactive or can be metabolized to chemically reactive species that covalently modify Keap1 and activate Nrf2-mediated ARE genes. Quite a few of these reactive chemical inducers have been tested clinically in phase I or phase II trials as chemopreventive agents. Sulforaphane was tested in clinic for the treatment and prevention of prostate cancer and for the treatment of chronic obstructive pulmonary disease (COPD). Bardoxolone methyl was evaluated for the treatment of advanced

chronic kidney disease (CKD) in patients with type 2 diabetes mellitus.<sup>16, 104, 121, 140, 179-183</sup>

However, none of these reactive chemical inducers have been advanced further to market.

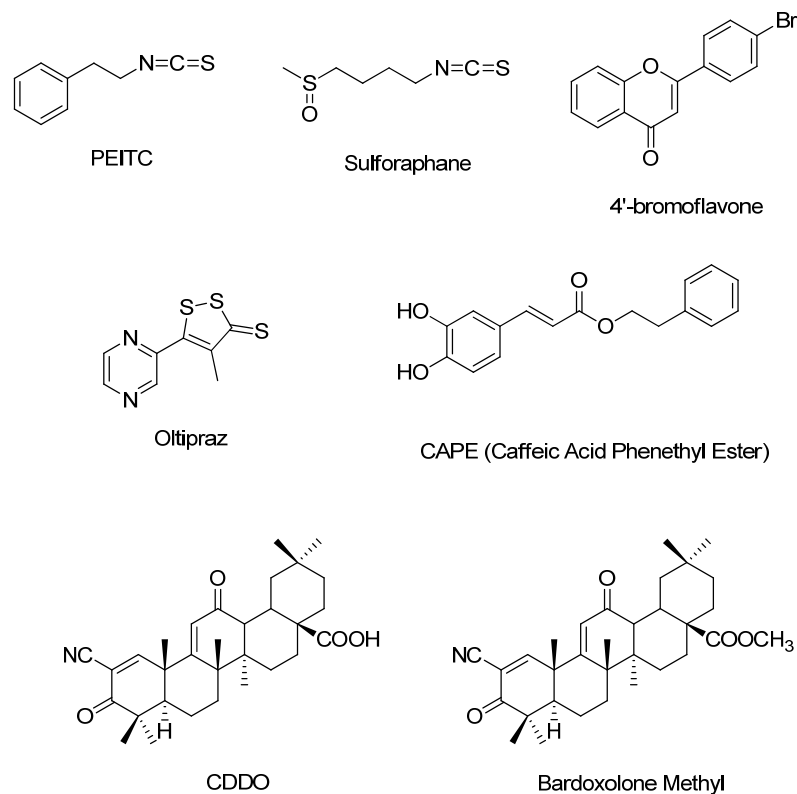


**Figure 12.** Chemical Structures of Some Known Reactive Chemical ARE Inducers

Most of the currently known small molecule inhibitors of Keap1-Nrf2 interaction are believed to be irreversible modifying agents of sensitive cysteine residues found in the redox “sensor” protein Keap1 for causing the translocation of Nrf2 to the nucleus and subsequent upregulation of anti-oxidative stress enzymes. All these compounds are either chemically reactive or can be converted to chemically reactive metabolites that readily oxidize or form covalent adduct with the sulfhydryl group of cysteines in Keap1.<sup>184-186</sup> The reactivity of these compounds raises safety concerns over their long-term use as

chemopreventive and therapeutic agents. Daily consumption of food products containing these reactive inhibitors of Keap1-Nrf2 interaction may not cause any safety concerns due to their low concentrations in food products. However, the previous reports on the SAR of a series of isothiocyanates including sulforaphane in vitro and in vivo indicate that their cellular activities are in the micromolar range and much higher doses appear to be required to produce the Nrf2-activation effect.<sup>187, 188</sup> Thus, the use of these naturally inducers of ARE genes in a purified form for an extended period at higher concentrations may have some safety concerns. Furthermore, risks of off-target toxic effects have also been associated with these indirect inhibitors since they are structurally reactive toward sulfhydryl groups of cysteine in Keap1, they may react with other important signaling proteins that contain cysteine. Finally, these natural and synthetic inducers have multiple targets and their mechanisms of action are complicated. For example, CDDO and its analogs are a series of potent synthetic triterpenoid inducers of ARE genes. They have been evaluated as cancer chemotherapeutic as well as chemopreventive agents and their biological activity involves a complex set of biochemical pathways depending on cell type and context.<sup>189, 190</sup> Therefore, it is not ideal to develop indirect inhibitors of Keap1-Nrf2 protein-protein interaction because of concerns about their off target and long-term toxicity.

Due to the fact that the indirect irreversible inhibitors of Keap1-Nrf2 interaction present safety concerns over extended use at high doses due to their chemical reactivity or formation of reactive metabolites, it provides us a good opportunity to look for potent direct inhibitors of the Keap1-Nrf2 interaction that are chemically stable, reversible, more

potent and specific. However, the only direct inhibitors of Keap1-Nrf2 interaction are the peptides based on the Nrf2 Neh domain that are used in the crystallographic studies or the synthesized peptides for assay development.<sup>191, 192</sup> There are multiple charges present on these peptides and their membrane permeability are poor. These properties prevented their use directly in cellular and in vivo assays. Since studies have demonstrated that inhibition of the Keap1-Nrf2 protein-protein interaction is a good strategy for cancer chemoprevention and for development of therapeutic agents for conditions involving oxidative stress and inflammation. Therefore, it is necessary and important to discover membrane permeable direct inhibitors of Keap1-Nrf2 interaction. New small molecule inhibitors of Keap1-Nrf2 protein-protein interaction that are not chemically reactive to common physiologically important nucleophiles should be much more promising as cancer chemopreventive agents and therapeutic agents for conditions involving inflammation. These inhibitors could potentially be used as chemopreventive agents for a variety of diseases and conditions including cancer, Parkinson's, and Alzheimer's. In addition, they could be used as pharmacological probes for the elucidation of chemoprevention mechanisms involving Keap1-Nrf2-ARE pathway.

### **B. Molecular Interactions between Keap1 and Nrf2**

An evolutionarily conserved amino acid sequence motif ETGE located within the Neh2 domain of Nrf2 is required for its binding to Keap1. The Kelch domain of Keap1 binds specifically the Neh2 domain of Nrf2. X-ray crystal structures of the human and mouse Kelch domain complexes with an Nrf2 peptide bound as well as of the human Keap1 Kelch domain alone were reported. The human and mouse Keap1 are very similar in

sequence with sequence identity of 94% and 97% overall in the Kelch domain. Both cocrystal structures of the human and mouse Keap1 Kelch domain-Nrf2 peptide complexes overlay very well with each other. These data suggested that the Keap1-Nrf2 interaction has a large interface spanning a number of residues involving multiple ionic interactions, H-bond, and hydrophobic interactions. In addition, there is a central channel in the  $\beta$ -propeller structure that can accommodate side chains and various aromatic rings. The Kelch domain folds up into a highly symmetric 6-bladed  $\beta$ -propeller structure. The Nrf2 peptide binds to the top face of the  $\beta$ -propeller with all six blades contributing to the complex formation. Several residues in Keap1 such as Ser363, Asn382, Arg380, Arg415, Arg483, and Ser508 participate in H-bond interactions to the negative carboxylate in the Nrf2 peptide. Several Keap1 residues are also involved in H-bond interactions to the peptide backbone and in van der Waals interactions between the Kelch domain and the Nrf2 peptide. These information suggest that inhibitors that interfere with the Keap1-Nrf2 protein-protein interaction can derive their inhibition by binding Keap1 Kelch domain at the site where Nrf2 peptide binds to.<sup>54, 55, 60, 65, 193-197</sup> The proposed model of Nrf2 activation by direct small molecule inhibitors of Keap1-Nrf2 protein-protein interaction is depicted in Fig. 13. Nrf2 is sequestered in the cytosol by its protein inhibitor, Keap1, and is transcriptionally inactive. A direct inhibitor binds to the Kelch domain of Keap1 and suppresses the ubiquitination of Nrf2, which decreases degradation of Nrf2 and allows more Nrf2 to translocate to the nucleus and form a transcriptionally active complex with Maf, leading to the induced expression of Nrf2 itself and oxidative stress response enzymes that deactivate reactive oxygen species and electrophiles.<sup>43</sup>

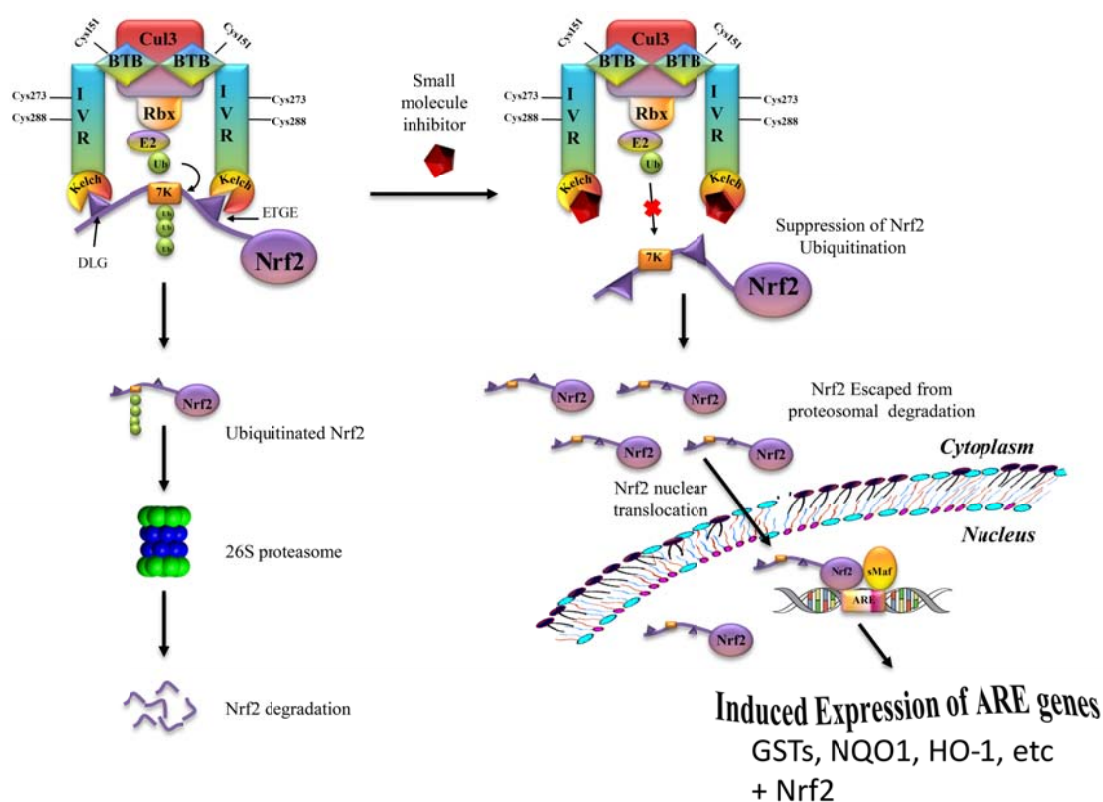


**Figure 13.** Proposed Model of Nrf2 Activation by Direct Small Molecule Inhibitors of Keap1-Nrf2 Protein-Protein Interaction.<sup>43</sup>

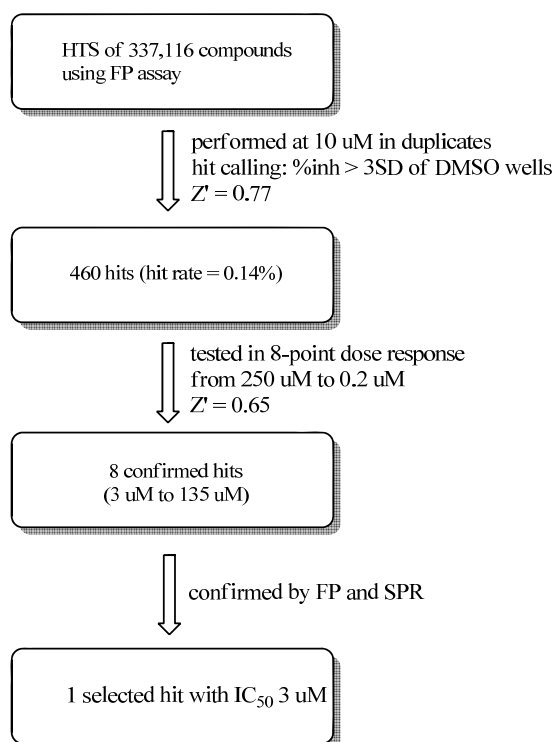
## II. Discovery of a Direct Small Molecule Inhibitor of Keap1-Nrf2 Protein-Protein Interaction

### A. Hit Discovery by HTS

Developing small molecules for protein-protein interaction is very challenging and difficult, however, it represents a more attractive novel strategy to promote translocation of Nrf2 to the nucleus and elevate the expression of ARE enzymes. Keap1-Nrf2 interaction has a large interface spanning a number of residues and it has been challenging to find small molecule inhibitors for similar protein-protein interactions.

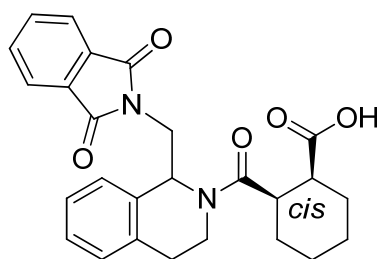
Because there are no known small molecule inhibitors of Keap1-Nrf2 interaction that can be used as leads, our group decided to take the HTS approach. In the absence of known drugs and other compounds with desired activity, a random screen is a valuable approach and all compounds are evaluated in the bioassay without regard to their structures. Currently, this is an important approach to discover lead compounds, especially it is now possible to screen huge numbers of compounds rapidly with HTSs.

Our approach to the discovery of novel direct small molecule inhibitors of Keap1-Nrf2 interaction is through the high throughput screening of the small molecule library to discover novel leads for further optimization into potent direct inhibitors of the protein-protein interaction between Keap1 and Nrf2. To discover novel non-reactive small molecules as direct inhibitors of the protein-protein interaction between Keap1 and Nrf2, a fluorescence polarization (FP) assay was developed with fluorescein-labeled 9mer Nrf2 peptide amide as the fluorescent probe and Keap1 Kelch domain as the target protein. The FP assay was submitted to NIH screening center at Broad Institute and applied successfully to the screening of 337,116 compounds.<sup>43, 191</sup>



**Figure 14.** HTS Screening Flow Chart.

The HTS screening process for hit discovery is shown in Fig. 14. The primary screen at 10  $\mu\text{M}$  generated a list of 489 hits using inhibition  $>3x$  standard deviation of DMSO wells (corresponding to 12% inhibition) for hit calling. After excluding 29 fluorescent compounds, 460 of the initial hits were cherry-picked and retested in the FP assay for 8-point dose-response curves. In the retest, eight compounds were confirmed as hits with  $\text{IC}_{50}$  from 3  $\mu\text{M}$  to 135  $\mu\text{M}$ . Among the eight confirmed hits, based on the chemical structures and inhibitory activity, we selected one molecule named as hit 1 shown in Fig. 15 as our first hit molecule for further modifications.<sup>43</sup>

**Hit 1****Figure 15.** Chemical Structure of the Hit 1

The inhibitory activity of hit 1 for Keap1-Nrf2 protein-protein interaction was evaluated by both a FP assay and a SPR assay. The dose-response curve of the hit 1 in the FP assay was shown in Fig. 16A. The FP dose-response curve demonstrated its 3  $\mu\text{M}$   $\text{IC}_{50}$ . The sensorgrams of the hit 1 in the SPR assay is shown in Fig. 16B. The binding constant ( $K_d$ ) of hit 1 to Keap1 Kelch domain was confirmed to be 1.9  $\mu\text{M}$  using an SPR solution competition assay recently developed in our lab.<sup>43, 191, 192</sup> In order to confirm and distinguish it from previously reported indirect inhibitors of Keap1-Nrf2 interaction, we exposed hit 1 to a high concentration (50  $\mu\text{M}$ ) of glutathione that used to mimic cysteine residues. No thiol addition or decomposition were detected over 48 h, indicating that hit 1 inhibits the Keap1-Nrf2 protein-protein interaction by non-covalent binding. Therefore, a small molecule hit as the first-in-class direct small molecule inhibitor of Keap1-Nrf2 protein-protein interaction was discovered.<sup>43</sup>

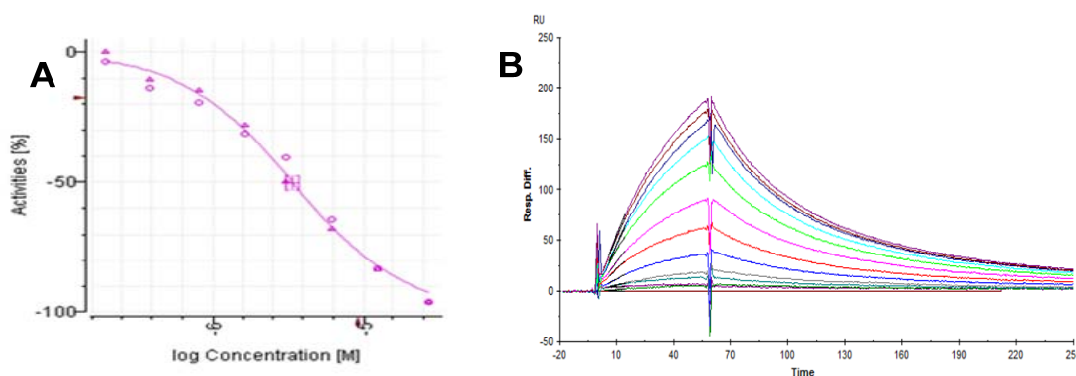


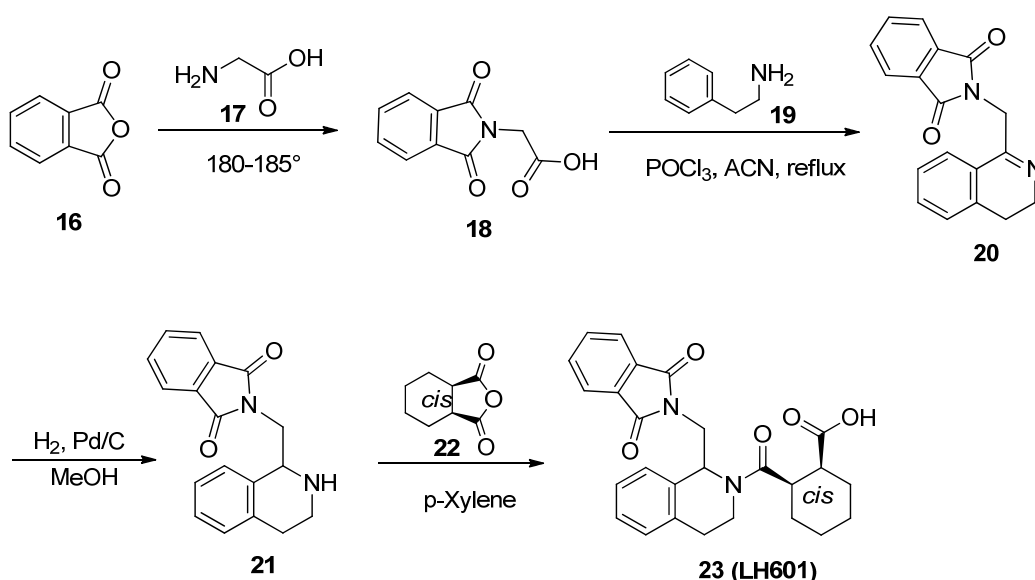
**Figure 16.** Inhibitory Activity Evaluation of Hit 1 for Keap-Nrf2 Protein-Protein Interaction

### **B. Resynthesis of Hit 1 for Activity Confirmation and Stereochemistry Assignment.**

Since there are three chiral centers in hit 1 and the two substituents on the cyclohexyl ring are known to be of *cis* configuration, four stereoisomers were expected to be present and one of the four stereoisomers is likely to be a direct inhibitor of the Keap1-Nrf2 interaction because that ligand-target interactions are often stereospecific. However, the composition of hit 1 sample in the MLPCN library was not defined. Because of the presence of three chiral centers and the undefined stereochemical composition of the hit sample, we synthesized the hit with defined composition for activity confirmation and determination of stereochemical requirement of Keap1 binding.<sup>43</sup>

The resynthesis of Hit 1 was accomplished in four steps starting from phthalic anhydride (**16**) and glycine (**17**) according to scheme 2. Glycine was heated under reflux with phthalic anhydride afforded the target compound **18**.<sup>198-200</sup> Compound **18** was coupled with phenethylamine and then cyclized with elimination of water in the presence of

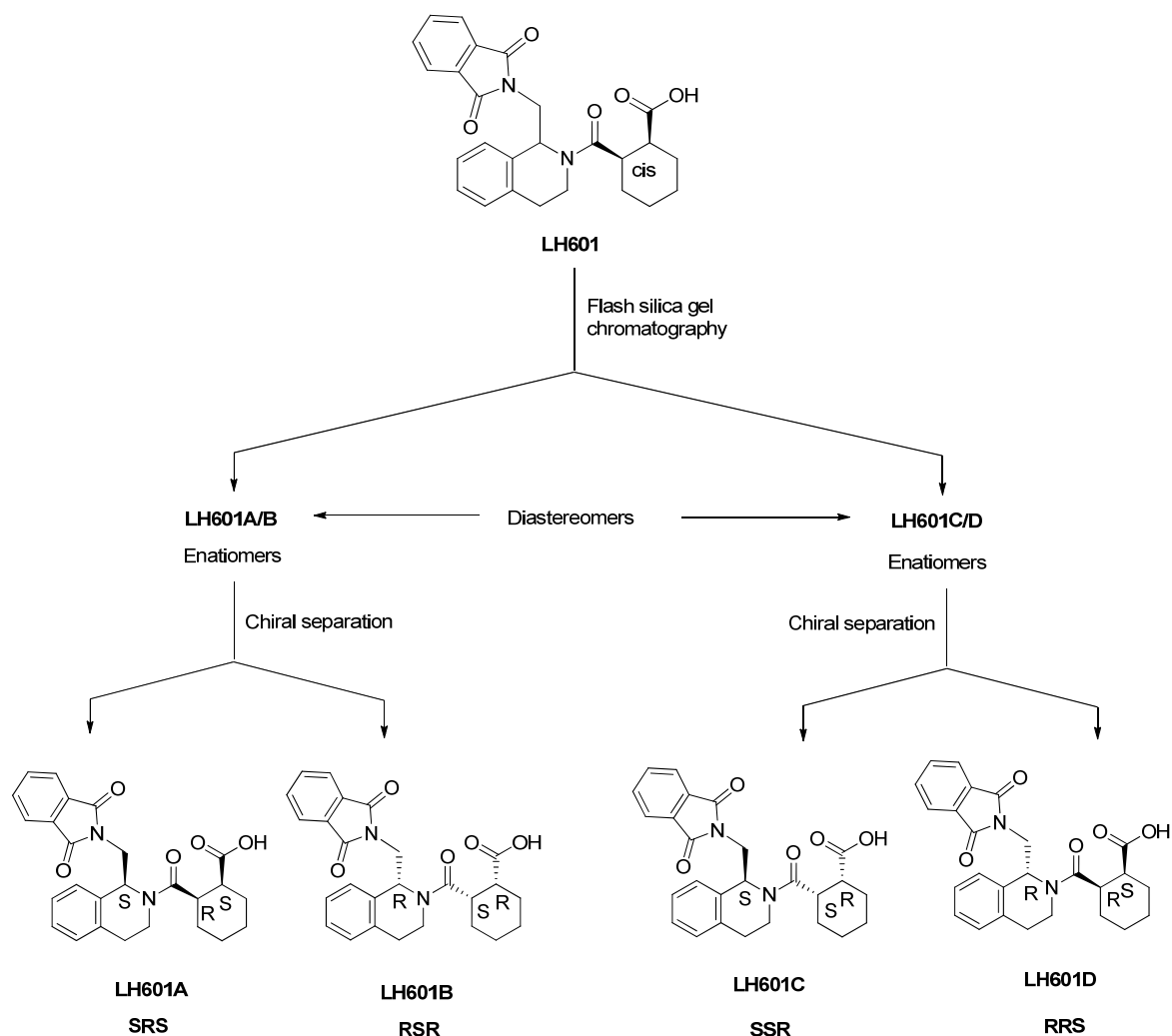
phosphoryl chloride in acetonitrile under reflux to yield the imine compound **20**.<sup>201</sup> Reduction of the imine compound **20** by hydrogenation in the presence of Pd/C in methanol yielded the 1-phthalimidomethyl tetrahydroisoquinoline (**21**).<sup>202</sup> The resynthesized hit 1 (named as LH601) was obtained by reacting 1-phthalimidomethyl tetrahydroisoquinoline (**21**) with *cis*-1,2-cyclohexanedicarboxylic anhydride. As expected, a mixture of four stereoisomers (LH601) was obtained based on our chiral HPLC analysis. The relative configuration of *cis* are defined based on the relative orientation of the two substituents on the cyclohexane ring.



**Scheme 3.** Synthesis of LH601

Then the two diastereomers of LH601 (LH601A/B and LH601C/D) were separated using flash silica gel column chromatography (ISCO) using ethyl acetate (0 to 100% with 1% acetic acid) in hexane. LH601A/B was shown to contain the active isomer in hit 1 and was further separated into the two enantiomers LH601A and LH601B by normal

preparative chiral HPLC (Chiralcel OD) using hexane/10% *i*-PrOH with 0.1% trifluoroacetic acid.



**Scheme 4.** Separation of LH601 Stereoisomers

The HPLC analysis of the four separated isomers of LH601 was performed by chiral HPLC (Chiralcel OD-R) using 85% methanol in water containing 0.1% trifluoroacetic acid. HPLC chromatogram of LH601 is shown in Fig. 17. LH601A is corresponding to

the earliest eluted peak with a retention time of 13.0 min, LH601B is the latest eluted peak with a retention time of 16.2 min, LH601C is the second peak with a retention time of 14.0 min and LH601D is the third peak with a retention time of 14.6 min.

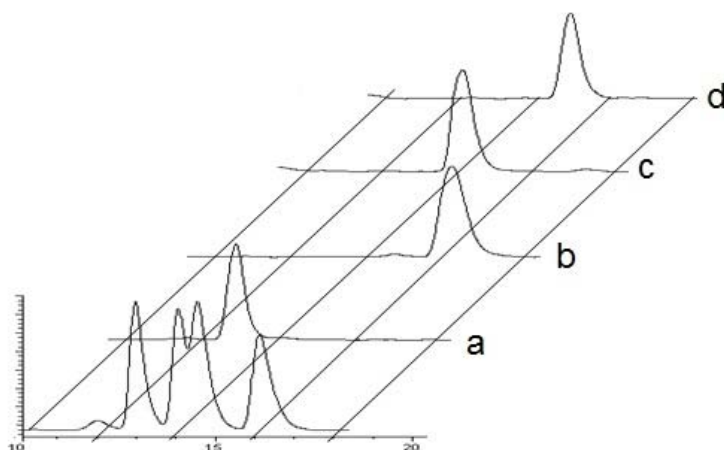


**Figure 17.** HPLC Chromatograms of LH601 (Mixture of Four Isomers) as Compared to Purified Stereoisomers.

a. HPLC Chromatogram of LH601A; b. HPLC Chromatogram of LH601B; c, HPLC Chromatogram of LH601C; d, HPLC Chromatogram of LH601D

The LH601 prepared in our lab was shown to be two fold less active than the hit 1 sample obtained from the NIH MLPCN library in our SPR solution competition assay. After synthesis and determination of Keap1 binding of an equal mixture of all four stereoisomers, we found that the hit 1 sample in the MLPCN library was predominantly composed of one set of enantiomers (~90%) as confirmed by chiral HPLC analysis, probably due to the recrystallization process used for purification in the commercial process. It became clear to us that we needed to determine which of the stereoisomer is

responsible for binding to Keap1 Kelch domain and what is its absolute stereochemistry.<sup>43</sup>

The activity of LH601A, LH601B and LH601C/D were then compared to that of hit 1 in our SPR assay. As shown in the SPR dose-response curves in Fig. 18, we have identified the most active stereoisomer in hit 1 being LH601A with a  $K_d$  of 1  $\mu\text{M}$  while its enantiomer LH601B has a  $K_d$  of only 100  $\mu\text{M}$  and the other diastereomer LH601CD is inactive.<sup>43</sup>

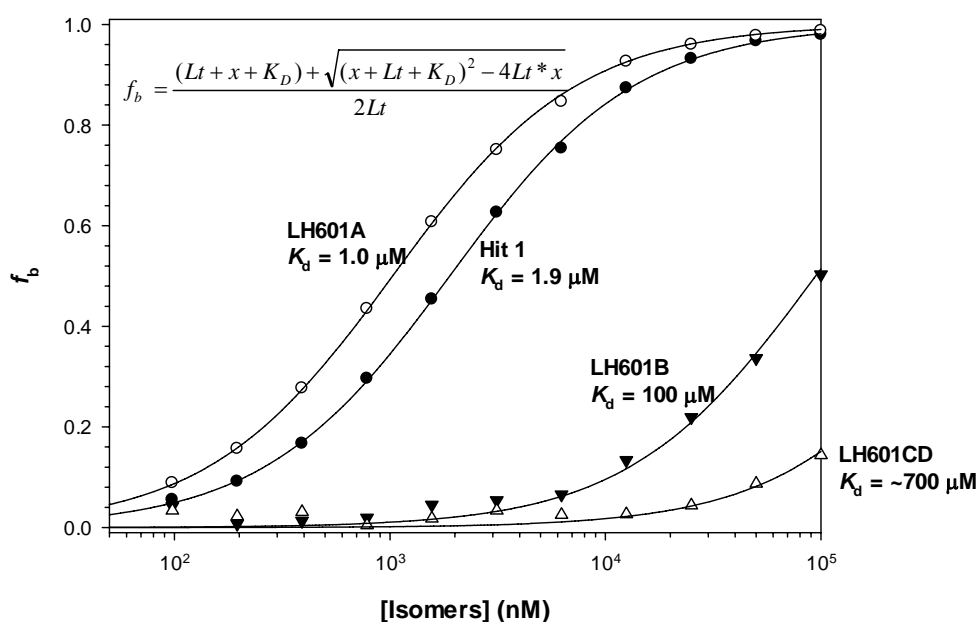


**Figure 18.** Comparison of  $K_d$  of Different Stereoisomers of LH601 to Hit 1

X-ray crystallography performed in the lab of Dr. Marcotrigiano in the department of chemistry at Rutgers was used to assign the stereochemistry of the four isomers. We first

attempted but failed to grow single crystals of LH601A. The LH601A isomer could only be crystallized as a pair with its enantiomer LH601B even when using 96% e.e. of LH601A. Fortunately, LH601D readily crystallized as single crystals of the pure LH601D, which was used to assign the absolute stereochemistry of all four LH601 isomers. The absolute stereochemistry of the hit 1 was further confirmed by taking a stereospecific synthesis of LH601A.<sup>43</sup> The chiral HPLC analysis showed that the stereospecifically synthesized compound corresponds to LH601A, thus the absolute stereochemistry of the active isomer LH601A was unequivocally confirmed.

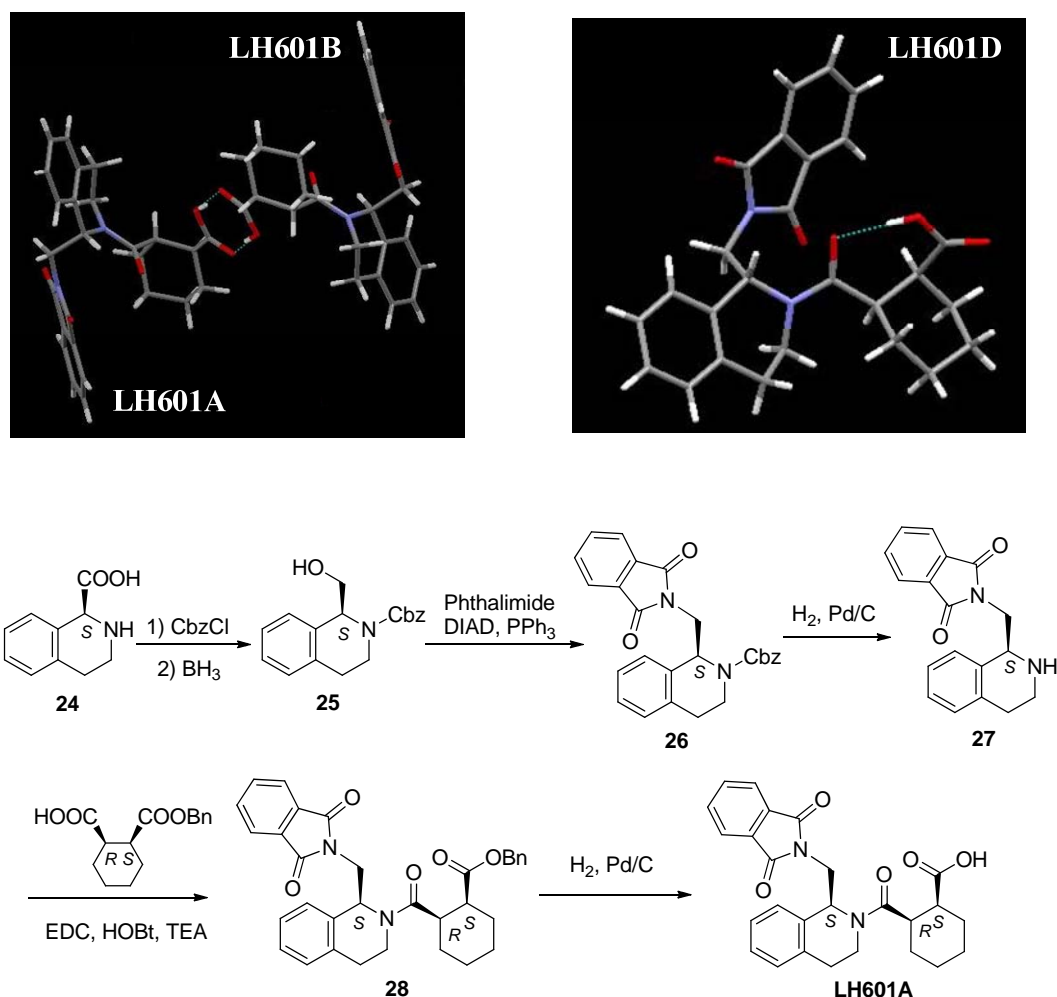


**Figure 19.** X-ray Crystal Structures and Stereospecific Synthesis.

### **III. Design of LH601 Analogs**

#### **A. Design Principle**

Since the structure and activity of the lead compound has been confirmed, our next step is to synthesize various analogs of the lead compound to explore the chemical space in various parts of the lead structure and to optimize the chemical structure of the lead compound to obtain potent Keap1-Nrf2 inhibitors with good physicochemical and pharmaceutical properties.

The drug-receptor interactions can be very specific. Therefore, only a small part of the lead compound may be involved in the appropriate receptor interactions. The pharmacophore may constitute only a small portion of the molecule. It has been found in some cases that what seem to be very complex molecules can be reduced to simpler structures with retention of the desired biological action. One approach in lead modification is to cut away sections of the lead molecule and measure the effects of those modifications on potency. It will not only help evaluate the necessary structure for the required activity but also will simplify the structure and reduce the number of chiral centers which could greatly simplify the synthesis and decrease cost.

We attempted to reduce the leads' molecular size and to improve their other lead-like properties. An example of molecular dissection that could lead to a simpler lead with a smaller molecular weight is shown in Fig. 20. Once we identify the minimal structure

scaffold required for Keap1 binding activity and we will then systemically explore the chemical spaces around the various points of the scaffold to improve the binding affinity and other physicochemical and pharmaceutical properties.

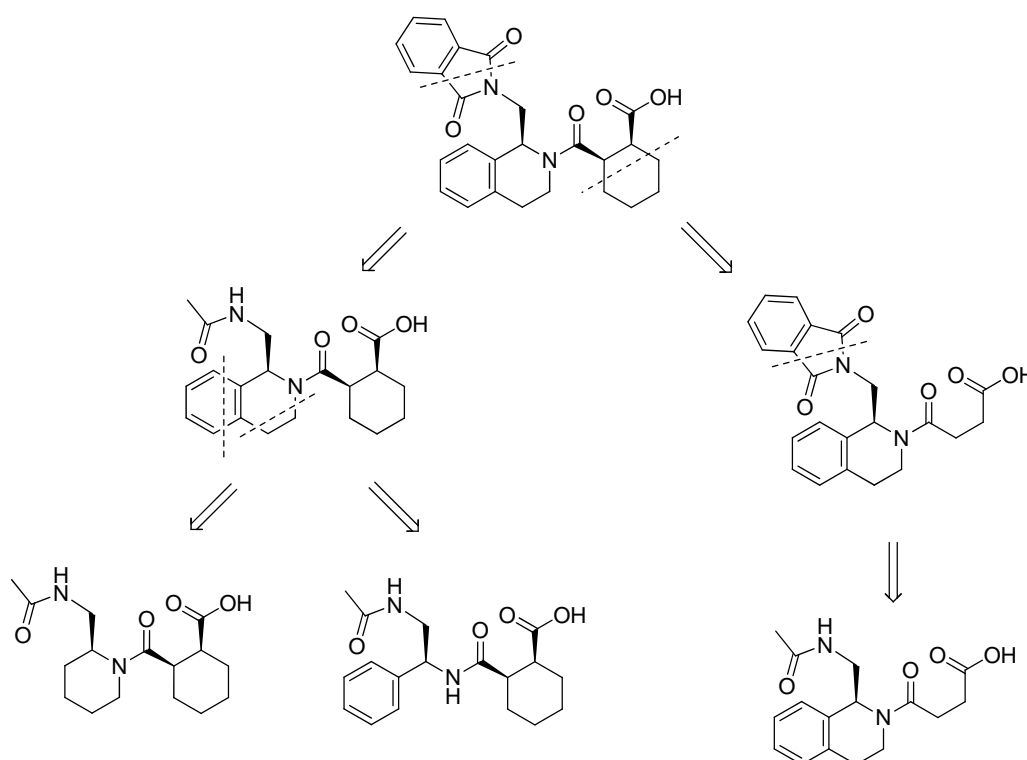


**Figure 20.** Simplification of Lead LH601A

The lead molecule can be mainly divided into three major parts including the cyclohexane carboxylic moiety, the phthalimide moiety and the tetrahydroisoquinoline. We explored the various possible modifications for each part in order to improve the binding affinity. The possible modification sites in the lead molecule are depicted in Fig. 21.

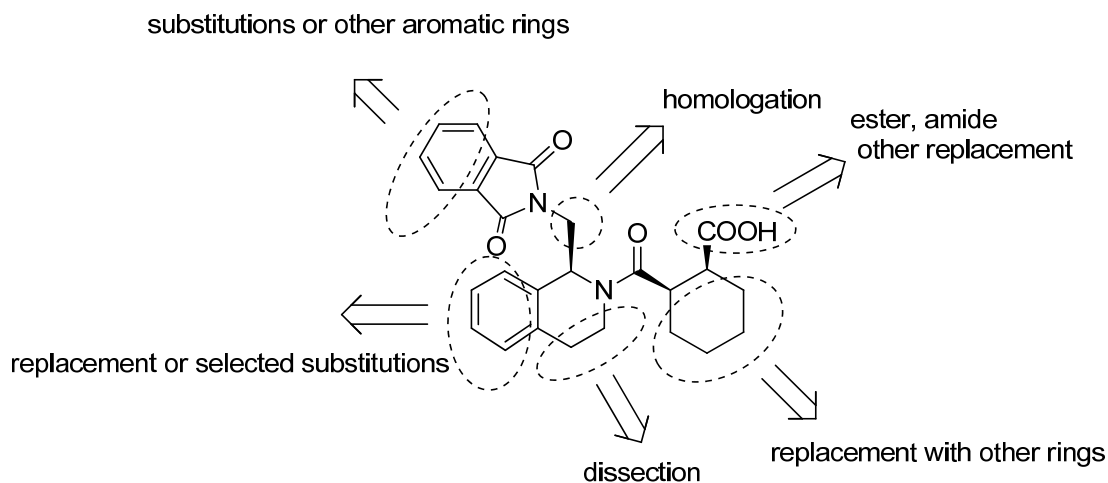


**Figure 21.** The Possible Modification Sites in LH601A.

## B. Modification of the Cyclohexane Carboxylic Acid Moiety

### 1. Replacement of the Carboxylic Acid

Due to the presence of multiple basic residues (Arg380, Arg415, Arg483, His436) in the Nrf2 peptide binding site of Keap1 Kelch domain, the negative carboxylate in LH601A is expected to provide an important interaction with at least one of these basic residues in Keap1 Kelch domain. Thus, we evaluated the importance of this carboxylic acid group in the lead molecule for the binding of Keap1 Kelch domain. The carboxylic acid was transformed to a simple amide analog **30** or a methyl ester analog **29**, the latter can also be used as a prodrug to generate the lead compound in vivo. The carboxylic acid is also replaced with acyl sulfonamide to form the designed analog **31** which can mimic the acidic functionality of carboxylic acid or extended with glycine to form analog **32** while retaining the carboxylic acid group.

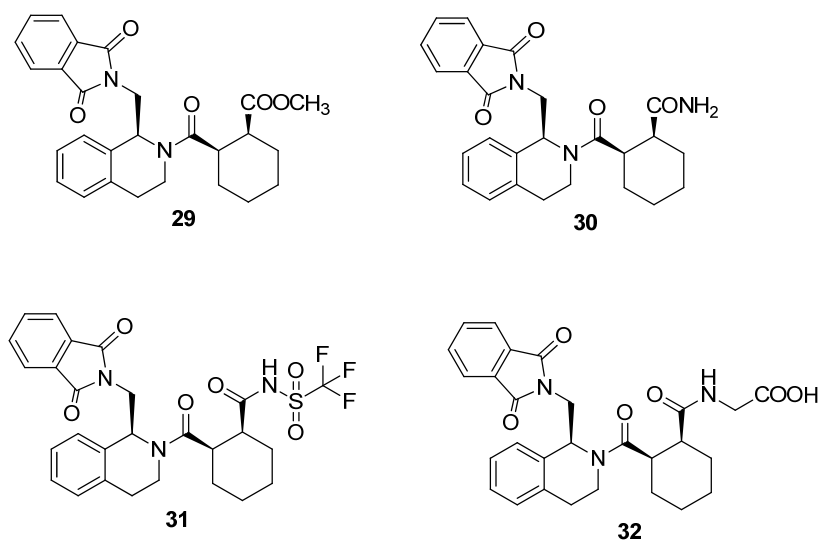


**Figure 22.** Structures of Analogs with Modification of Carboxylic Acid.

## 2. Replacement of the Cyclohexane Ring

To further evaluate the importance of the relative configuration of the two substituents on the cyclohexane for the binding with Keap1 Kelch domain, *trans*-2-carbonyl cyclohexane-1-carboxylic acid was used to replace the *cis*-2-carbonyl cyclohexane-1-carboxylic acid and formed the designed compound **33** with two substituents on the cyclohexyl ring in *trans* configuration. Then two other replacements with different ring structure (**34**) or aromatic ring (**35**) were used to replace *cis*-2-carbonyl cyclohexane-1-carboxylic acid to investigate the importance of cyclohexane for the binding of Keap1 Kelch domain and explore the structure activity relationship.

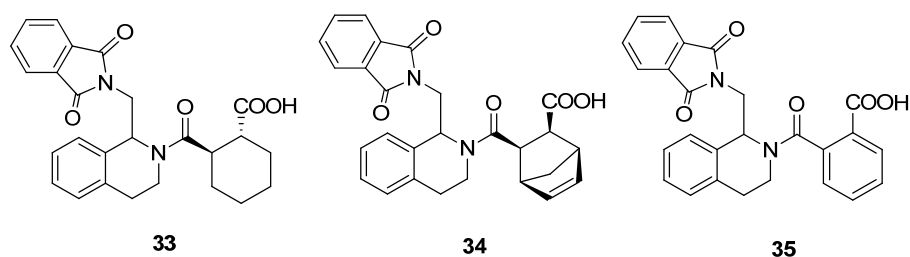


**Figure 23.** Structures of Analogs with Replacement of Cyclohexane Ring.

## C. Modification of Tetrahydroisoquinoline

### 1. Ring-Chain Transformation

One modification that can be made is to dissect tetrahydroisoquinoline and transform the cyclic ring structure into an open ring analog **36**. This is also an important and useful way to simplify the structure of the lead molecule. By converting the cyclic ring into an open system, the constraint of the molecule could be released. This modification could make the molecule into a more flexible conformation, and this modification can help us evaluate the importance of the integrity of tetrahydroisoquinoline and the ethyl in the tetrahydroisoquinoline ring for binding with the Keap1 Kelch domain.

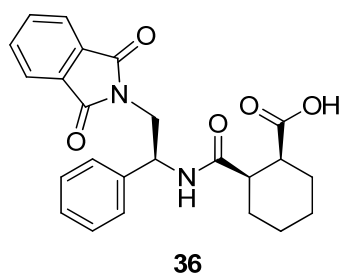


**Figure 24.** Structure of an Analog with Dissected Tetrahydroisoquinoline.

## 2. Replacement of Tetrahydroisoquinoline

To further evaluate the importance of the tetrahydroisoquinoline ring, the analog **37** by replacing the aromatic ring with unsaturated six membered ring while retaining all the other features of the lead molecule was designed and synthesized. The binding affinity of this analog will give us information about the importance of the fused benzene ring in tetrahydroisoquinoline for the binding with Keap1 Kelch domain.

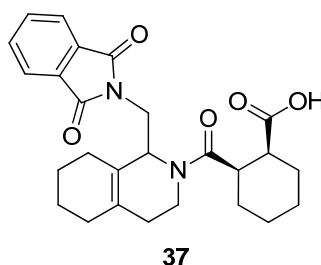


**Figure 25.** Structure of an Analog with Modification of Tetrahydroisoquinoline.

## 3. Substitutions on Tetrahydroisoquinoline

Tetrahydroisoquinoline is a commonly encountered scaffold in pharmaceuticals. It is present in drug molecules from ACE inhibitors to antispasmodics of the anticholinergic class to adrenergic neuron-blocking drugs. Modifications were made on the benzene ring of tetrahydroisoquinoline with additional substituents. Substituents on aromatic rings can alter the electron distribution throughout the ring, which in turn can affect how the molecule interacts with the receptor. Ring substituents also may influence the conformation of a flexible molecule, especially if they are located close to flexible side chains and can participate in steric or electronic intramolecular interactions. Ring substituents also influence the conformations of adjacent substituents via steric

interactions and may significantly affect receptor interactions. We attempted to place electron withdrawing substitutions including fluoro, trifluoromethyl and nitro group and electron donating groups including mono-methoxy, di-methoxy and amino group on the tetrahydroisoquinoline to investigate the electronic effect on the binding affinity with Keap1 Kelch domain. Position isomers of substituents on the aromatic ring also may possess different binding affinity. Therefore, same substituent on different positions of tetrahydroisoquinoline were also designed and synthesized.

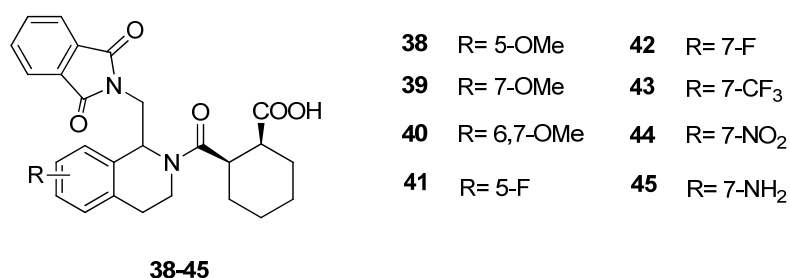


**Figure 26.** Structures of Analogs with Substitutions on Tetrahydroisoquinoline.

#### 4. Substitutions on the Ethyl of Tetrahydroisoquinoline

To further explore the chemical spaces around the various points of the tetrahydroisoquinoline to improve binding affinity, two analogs with substituents on the ethyl of tetrahydroisoquinoline were designed. One analog (**46**) has one methyl substituent while the other one (**47**) has one methyl ester group. As long as space is available in this direction, more modification can be made to enhance the binding affinity.

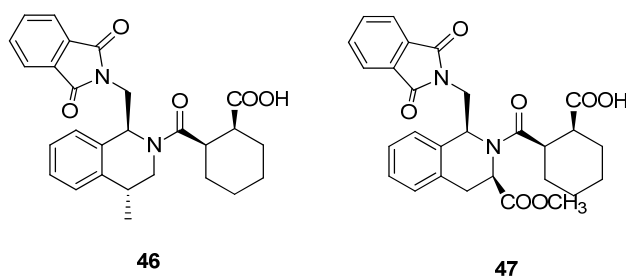


**Figure 27.** Structures of Analogs with Substitution on Ethyl of Tetrahydroisoquinoline.

## D. Modification of Phthalimido Group

### 1. Open Phthalimido Ring

Phthalimido group is not very stable and is prone to hydrolysis. One possibility is to evaluate the binding affinity of some open ring analogs. The phthalimido group can be hydrolyzed into carboxylic acid analog (**48**) and the second carboxylic acid might provide additional interaction with the basic residues in Keap1 Kelch domain and improve the binding affinity. The phthalimido group can also be aminolyzed into various amide analogs (**49-52**) or reduced to analog **53**. In this modification exploration, linear amine, amine with cyclic ring or aromatic group were selected to explore the structure activity relationship.

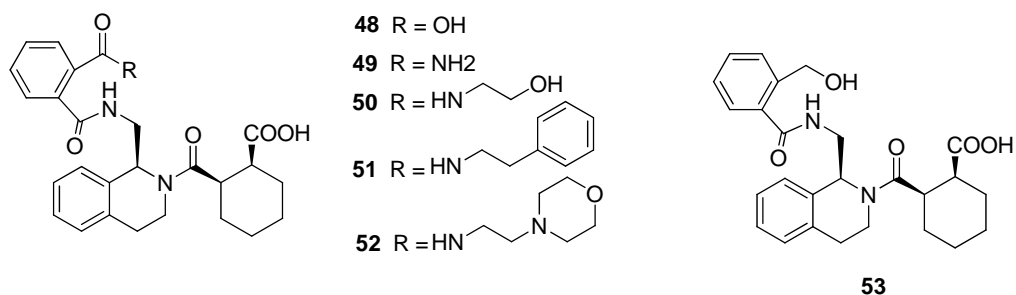


**Figure 28.** Structures of Analogs with Opened Phthalimido Ring.

## 2. Replace the Phthalimido Group with Aryl Sulfonamido or Acyl Amido

Another possibility is to replace the phthalimido group with acyl amido (**54-55**) or aryl sulfonamido groups (**56-58**). Other linker groups will also be evaluated if this modification can maintain or improve the binding affinity. The aryl group can bear different substitutions such as methyl and nitro to explore the structure activity relationship and can also be varied between 5 and 6-membered rings and fused ring systems for further evaluation. In this way, not only the molecule is simplified, but also it will be easier for the synthesis.

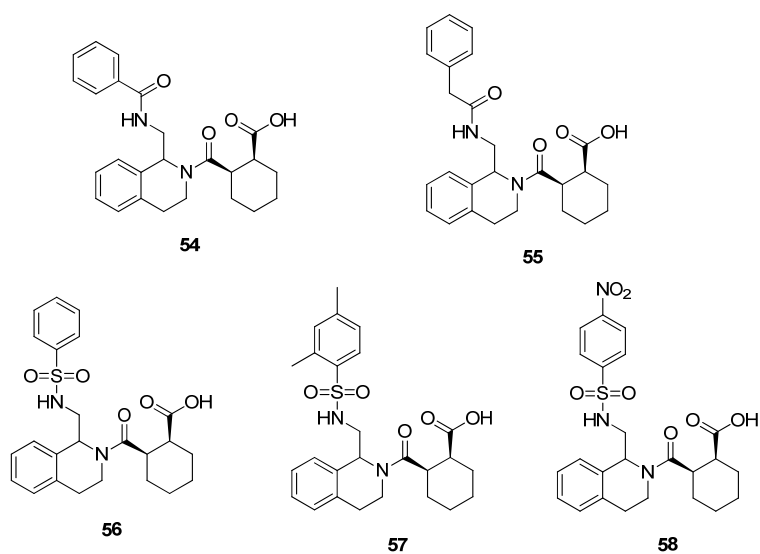


**Figure 29.** Structures of Analogs with Replacement of Phthalimido Group.

### 3. Bioisosteric Replacement of Phthalimido Ring

Bioisosteric replacement is an important research strategy widely used in analog design. Bioisosteres have similar chemical or physical properties, and could produce similar biological properties. One analog (**60**) by replacing the fused benzene ring of phthalimide with pyridine ring was designed. Several potential scaffolds containing heterocyclic ring systems can also be explored as bioisosteric replacements of phthalimido group if this strategy works.

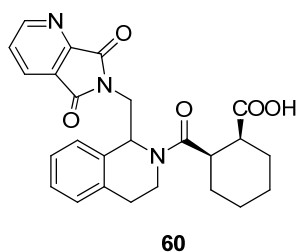


**Figure 30.** Structure of an Analog with Replacement of Phthalimido Group

#### 4. Homologation

Alterations in alkyl chains, such as increasing or decreasing chain length (homologation) can have profound effects on the potency and pharmacologic activity of the molecule. If the alkyl chain is directly involved in the receptor interaction, then chain length can alter the binding characteristics. One analog (**61**) with an extended ethyl linker between phthalimide and tetrahydroisoquinoline was designed. Simply changing the length of an alkyl chain by one  $\text{CH}_2$  unit may seem trivial at first, but in many instances, such small changes are important aspects in the design of analogs. Small changes in conformation will affect the spatial relationship of functional groups in the molecule, thereby influencing receptor binding.

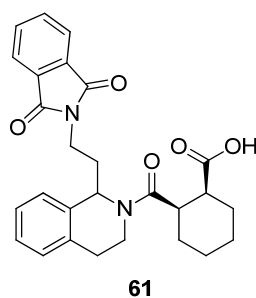


**Figure 31.** Structure of an Analog with Extended Linker between Phthalimide and Tetrahydroisoquinoline

#### E. Modifications on both Phthalimide and Tetrahydroisoquinoline

The preliminary evaluation results showed that methoxy and fluorine substitutions on the tetrahydroisoquinoline are about two fold more active as compared to the lead molecule. Other modifications were also made on the phthalimido group with additional substituents or replacement of the benzene ring of phthalimide with fused aromatic rings.

Analog **62** by replacing phthalimido with 2,3-naphthalimido was shown to be about two fold increase in binding affinity with Keap1 Kelch domain. Based on these preliminary structure activity relationship, two analogs (**63-64**) with either methoxy or fluoro substitution on tetrahydroisoquinoline along with 2,3-naphthalimido replacement of phthalimido were designed and synthesized.

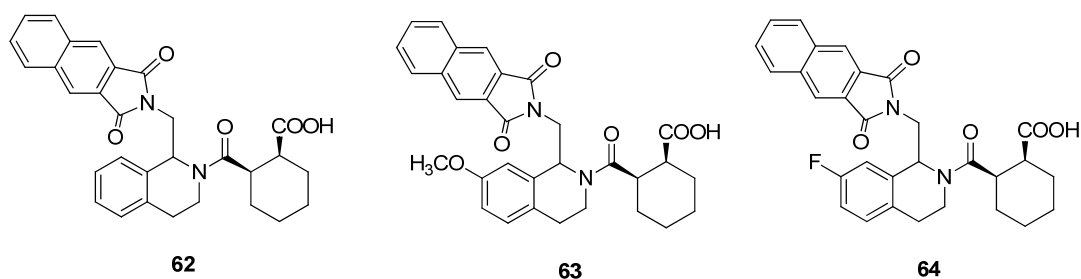


**Figure 32.** Structures of Analogs with Modification on both Phthalimide and Tetrahydroisoquinoline

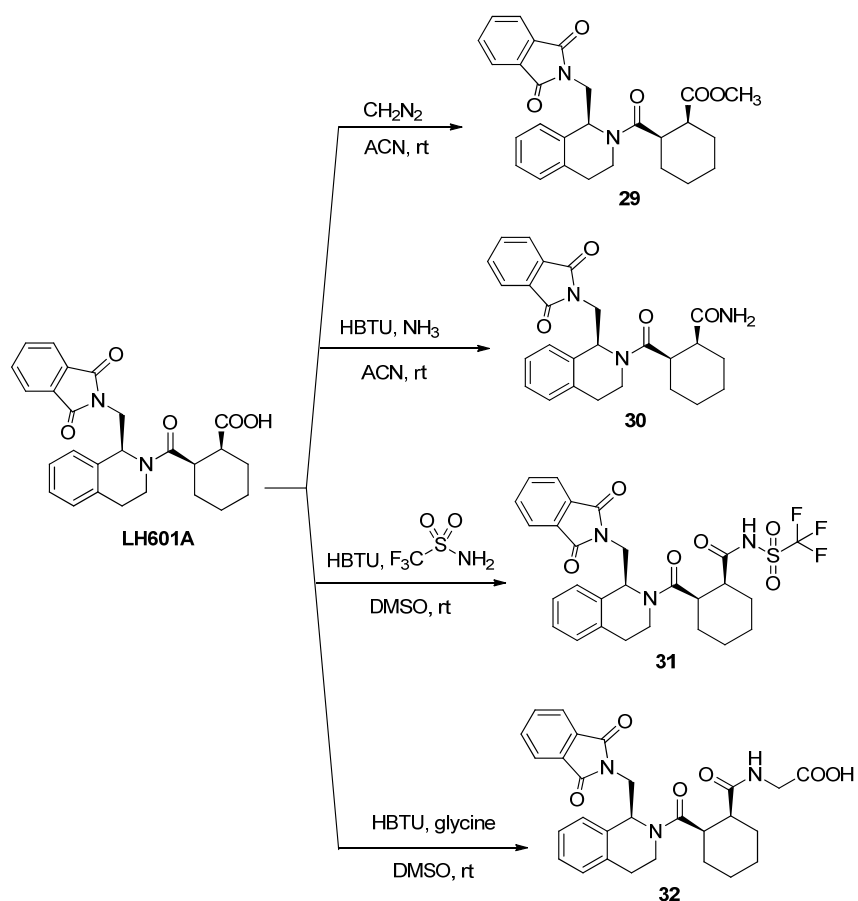
Generally, all the designed compounds were based on the modifications on the three major parts of the lead molecule including the cyclohexane carboxylic acid moiety, the phthalimide moiety and the tetrahydroisoquinoline. We explored the chemical space in various parts of the lead structure and the possible modification for each part in order to improve the binding affinity. All the designed and synthesized analogs of the lead compound were evaluated in fluorescence polarization (FP) assay and surface plasmon resonance (SPR) assay and the obtained preliminary structure activity relationship was used for further structural optimization.

## IV. Results and Discussions

### A. Synthesis of LH601 Analogs

#### *Synthesis of LH601 analogs with replacement of carboxylic acid (29-32)*

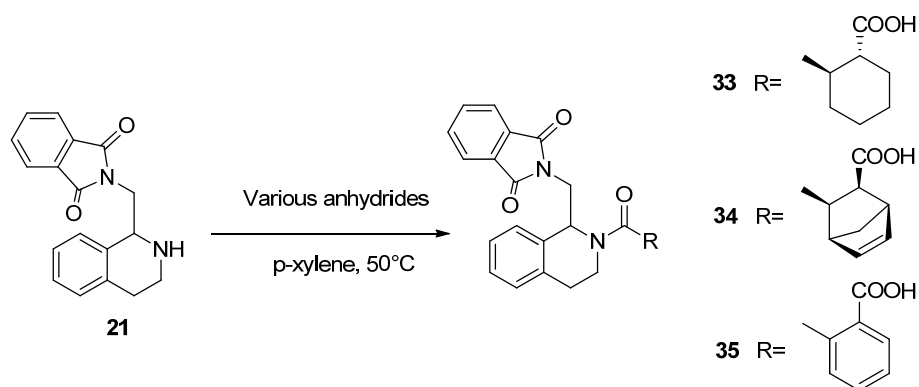
Scheme 5 outlined the synthesis of four analogs of LH601 with replacement of carboxylic acid. LH601A was converted to its methyl ester analog (**29**) with diazomethane quantitatively. Analog **30**, **31** and **32** were obtained respectively in one step by activating the carboxylic acid group in LH601A using HBTU and reacted with anhydrous ammonium, trifluoromethyl sulfonamide and glycine separately.



**Scheme 5.** Synthesis of Analogs with Modification of Carboxylic Acid

*Synthesis of analogs with replacement of cyclohexane ring (33-35)*

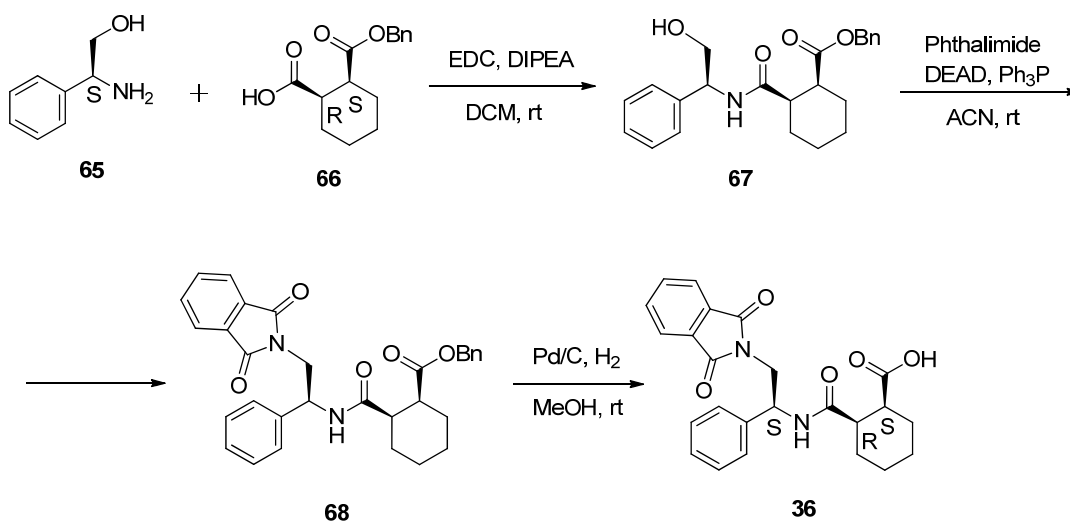
The synthesis of analogs with replacement of cyclohexane (**33-35**) was accomplished in one step according to scheme 6. The desired analogs **33-35** were obtained by reacting 1-phthalimidomethyl tetrahydroisoquinoline (**21**) with their corresponding anhydrides.



**Scheme 6.** Synthesis of Analogs with Replacement of Cyclohexane

*Synthesis of (1S,2R)-2-(((S)-2-(1,3-dioxisoindolin-2-yl)-1-phenylethyl)carbamoyl)cyclohexanecarboxylic acid (36)*

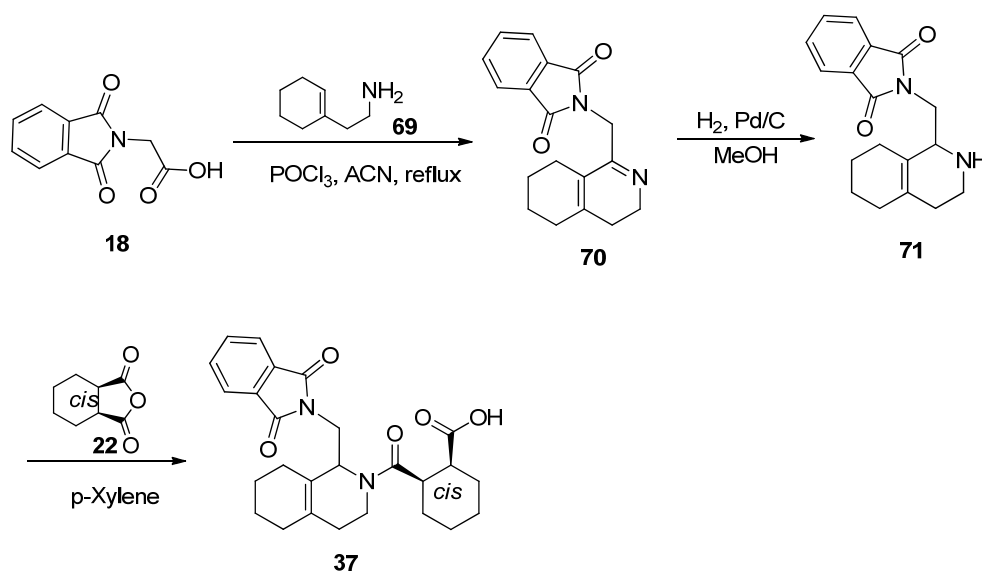
According to scheme 7, (*S*)-2-amino-2-phenylethanol (**65**) was coupled with (*1R,2S*)-2-((benzyloxy)carbonyl)cyclohexanecarboxylic acid (**66**) to yield the targeted compound **67**. Compound **67** was converted to compound **68** using a PPh<sub>3</sub>/DEAD-mediated Mitsunobu reaction. Removing benzyl group by hydrogenation in the presence of a catalytic amount of Pd/C gave the desired analog **36**.



**Scheme 7.** Synthesis of a Dissected Tetrahydroisoquinoline Analog

*Synthesis of cis-2-(1-((1,3-dioxisoindolin-2-yl)methyl)-1,2,3,4,5,6,7,8-octahydroisoquinoline-2-carbonyl)cyclohexanecarboxylic acid (37)*

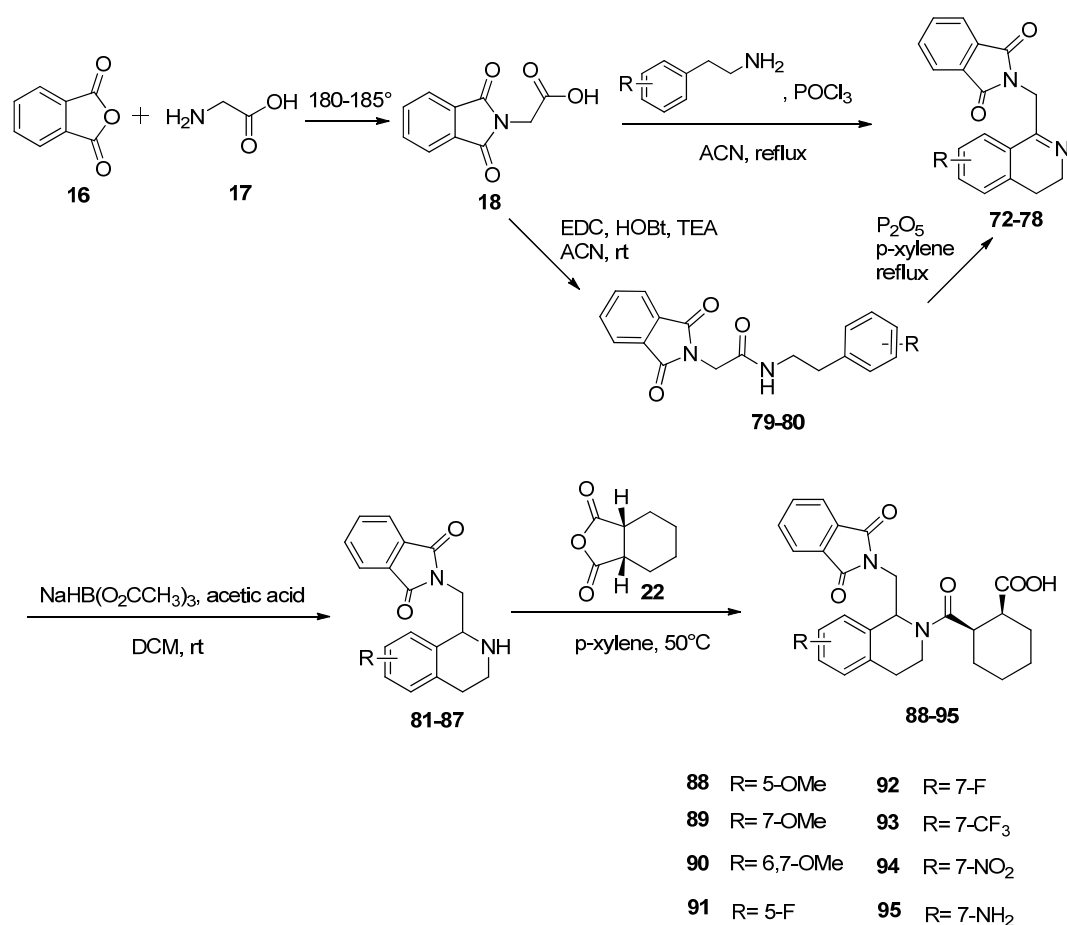
The synthesis of the desired analog **37** was accomplished in three steps starting from intermediate (**18**) according to scheme 8. Compound **18** was coupled with compound **69** and then cyclized in the presence of phosphoryl chloride in acetonitrile under reflux to yield the imine compound **70**. Reduction of the imine compound **70** by hydrogenation in the presence of Pd/C in methanol yielded compound **71**. Reacting amine compound **71** with *cis*-1,2-cyclohexanedicarboxylic anhydride afforded the desired analog **37**.



**Scheme 8.** Synthesis of an Analog with Replacement of Tetrahydroisoquinoline

*Synthesis of analogs with substitutions on tetrahydroisoquinoline (88-95)*

Scheme 9 outlined the synthesis of analogs with substitutions on tetrahydroisoquinoline (88-95). Glycine was heated under reflux with phthalic anhydride to afford compound **18**. Compound **18** was coupled with phenethylamine with different substitutions and then cyclized in the presence of phosphoryl chloride in acetonitrile under reflux to yield the imine compound **72-78**. Reduction of the imine compound **72-78** in the presence of sodium triacetoxyborohydride and acetic acid yielded the amine compound **81-87**. Reacting amine compound **81-87** with *cis*-1,2-cyclohexanedicarboxylic anhydride afforded the desired analogs **88-94** with different substitutions on the tetrahydroisoquinoline.

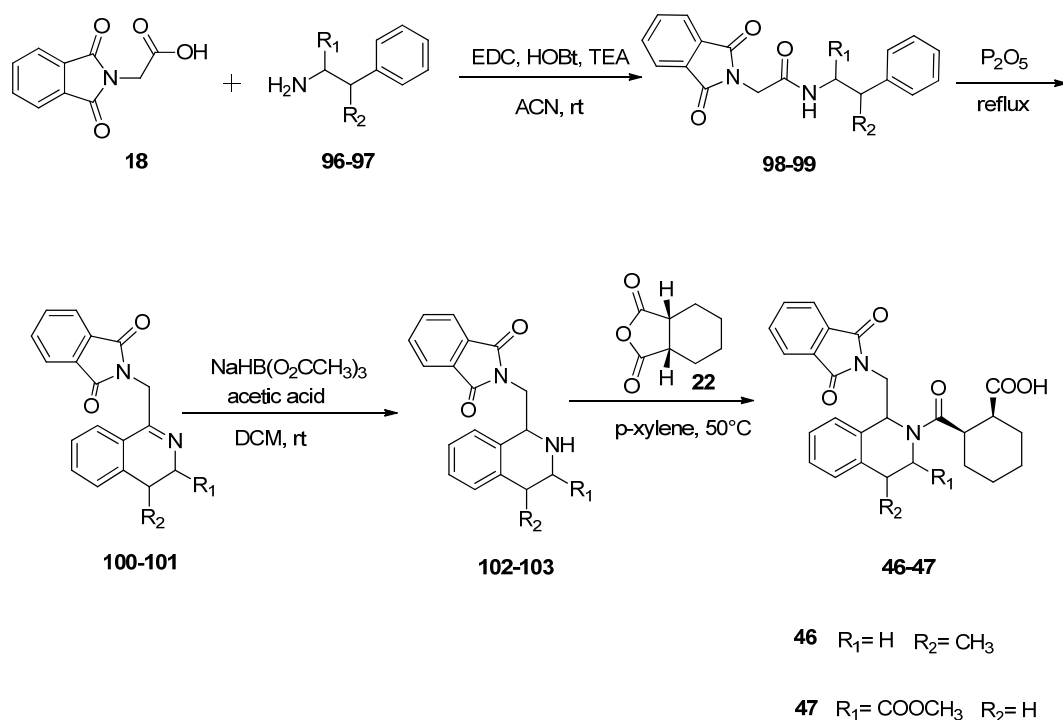


**Scheme 9.** Synthesis of Analogs with Substitutions on Tetrahydroisoquinoline

*Synthesis of analogs with substitutions on ethyl of tetrahydroisoquinoline (46-47)*

According to scheme 10, compound **18** was coupled with compound **96** or **97** in the presence of EDC, HOBT and TEA in acetonitrile at room temperature to yield the compound **98-99**. Cyclization of **98-99** with elimination of water by using P<sub>2</sub>O<sub>5</sub> yielded the imine compound **100-101**. Reduction of the imine compound **100-101** in the presence of sodium triacetoxyborohydride and acetic acid yielded the amine compound **102-103**.

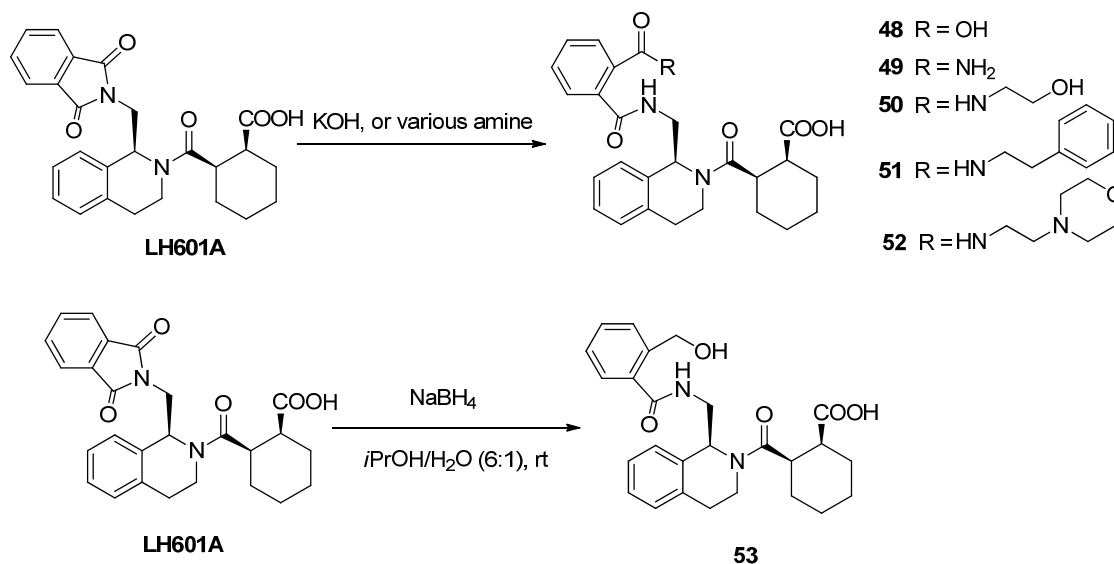
Reacting amine compound **102-103** with *cis*-1,2-cyclohexanedicarboxylic anhydride afforded the desired analogs **46-47** with either methyl or methyl ester substituent on the ethyl of tetrahydroisoquinoline.



**Scheme 10.** Synthesis of Analogs with Substitutions on Ethyl of Tetrahydroisoquinoline

*Synthesis of analogs with opened phthalimido ring (48-53)*

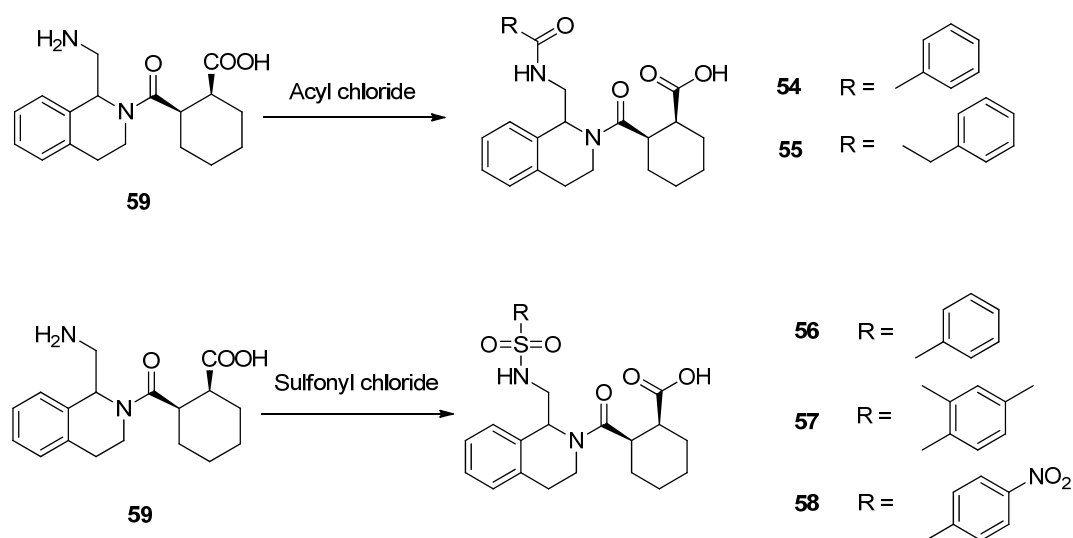
Scheme 10 depicted the synthesis of designed analogs with opened phthalimido ring (**48-53**). LH601A was hydrolyzed in the presence of KOH afforded the desired analog **48**. Analog **49-52** were obtained by reacting LH601A with the selected amines respectively. The desired analog **53** was obtained by reduction of the phthalimide using sodium borohydride in *i*PrOH/H<sub>2</sub>O (6:1) at room temperature.



**Scheme 11.** Synthesis of Analogs with Opened Phthalimido Ring

*Synthesis of analogs with replacement of phthalimido group (54-58)*

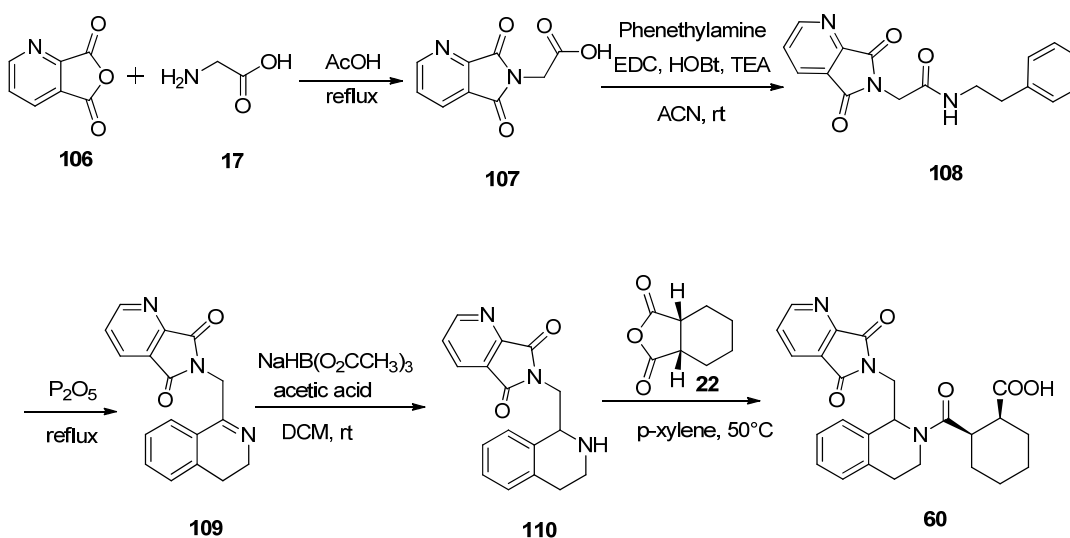
According to scheme 12, compound **59** was obtained by removing the phthalimido group in the presence of hydrazine. Then reacting with various acyl chloride or sulfonyl chloride yielded the desired analogs **54-58** with replacement of the phthalimido group.



**Scheme 12.** Synthesis of Analogs with Replacement of Phthalimido Group

*Synthesis of cis-2-(1-((5,7-dioxo-5H-pyrrolo[3,4-b]pyridin-6(7H)-yl)methyl)-1,2,3,4-tetrahydroisoquinoline-2-carbonyl)cyclohexanecarboxylic acid (60)*

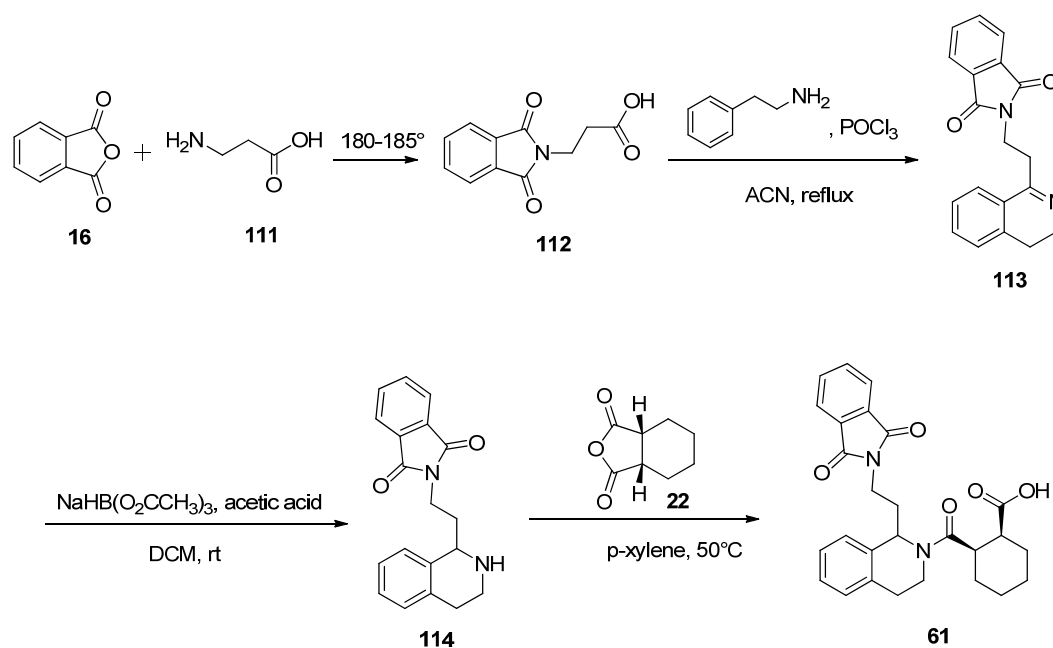
The anhydride compound **106** was heated under reflux with glycine in acetic acid yielded compound **107**. Compound **107** was coupled with phenethylamine in the presence of EDC, HOBt and TEA in acetonitrile at room temperature to yield the compound **108**. Cyclization of **108** with  $P_2O_5$  yielded the imine compound **109**. Reduction of the imine compound **109** in the presence of sodium triacetoxyborohydride and acetic acid yielded the amine compound **110**. Reacting amine compound **110** with *cis*-1,2-cyclohexanedicarboxylic anhydride afforded the desired product **60** with bioisosteric replacement of phthalimido group.



**Scheme 13.** Synthesis of an Analog with Replacement of Phthalimido Group

*Synthesis of cis-2-(1-(2-(1,3-dioxoisoindolin-2-yl)ethyl)-1,2,3,4-tetrahydroisoquinoline-2-carbonyl)cyclohexanecarboxylic acid (61)*

Scheme 14 outlined the synthesis of the analog **61** with extended linker between phthalimide and tetrahydroisoquinoline. 3-aminopropanoic acid (**111**) was heated under reflux with phthalic anhydride yielded compound **112**. Compound **112** was coupled with phenethylamine and then cyclized in the presence of phosphoryl chloride in acetonitrile under reflux to yield the imine compound **113**. Reduction of the imine compound **113** in the presence of sodium triacetoxyborohydride and acetic acid in DCM yielded the amine compound **114**. Reacting amine compound **114** with *cis*-1,2-cyclohexanedicarboxylic anhydride afforded the desired analog **61** with extended linker between phthalimide and tetrahydroisoquinoline.

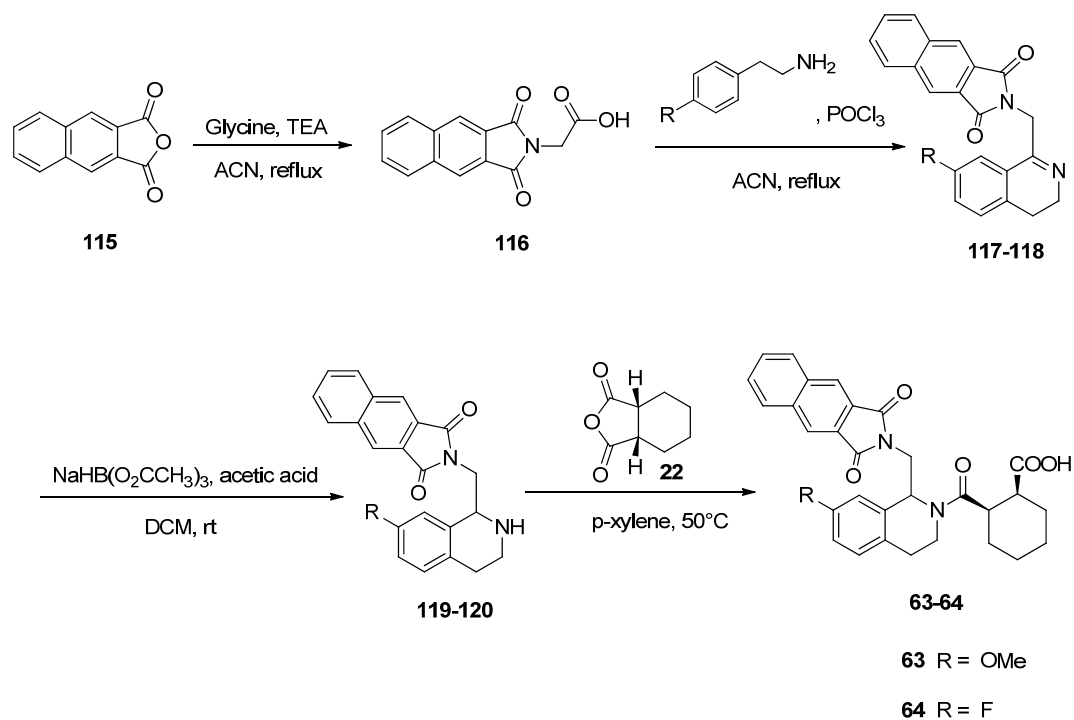


**Scheme 14.** Synthesis of an Analog with Extended Linker between Phthalimide and Tetrahydroisoquinoline

*Synthesis of analogs with modifications on phthalimide and tetrahydroisoquinoline (63-64)*

Scheme 15 outlined the synthesis of analogs with modifications on both phthalimide and tetrahydroisoquinoline (**63-64**). Glycine was heated under reflux with naphthalic anhydride in the presence of TEA in acetonitrile yielded compound **116**.<sup>203, 204</sup> Compound **116** was coupled with 4-methoxyphenethylamine or 4-fluorophenethylamine and then cyclized in the presence of phosphoryl chloride in acetonitrile under reflux to yield the imine compound **117-118**. Reduction of the imine compound **117-118** in the presence of sodium triacetoxylborohydride and acetic acid in DCM yielded the amine compound **119-**

**120.** Reacting amine compound **119-120** with *cis*-1,2-cyclohexanedicarboxylic anhydride afforded the desired analogs **63-64** with modifications on both phthalimide and tetrahydroisoquinoline.



**Scheme 15.** Synthesis of Analogs with Modification on both Phthalimide and Tetrahydroisoquinoline

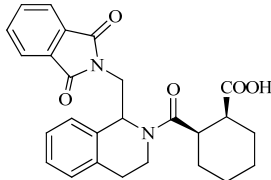
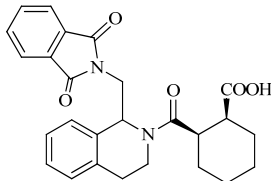
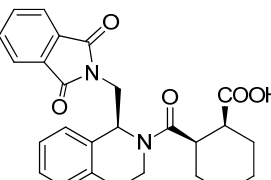
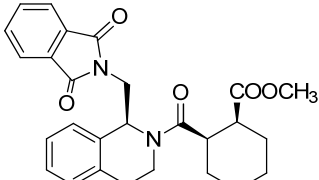
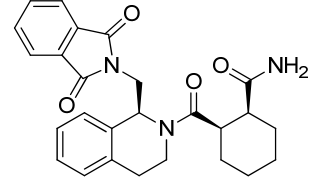
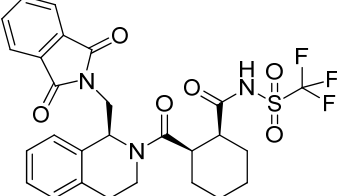
## **B. Inhibitory Activity Evaluation of the Synthesized Small Molecule Inhibitors**

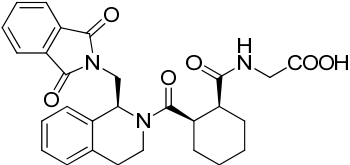
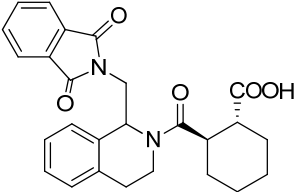
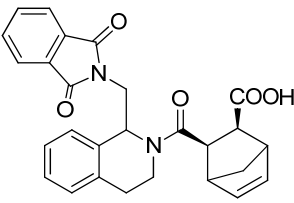
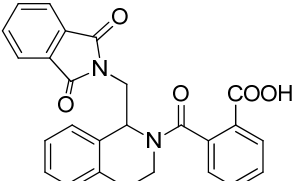
Two competition assays including fluorescence polarization assay (FP) and surface plasmon resonance (SPR) competition binding assay were used for the evaluation of the synthesized small molecule inhibitors of Keap1-Nrf2 protein-protein interaction. Fluorescence polarization (FP) is a general property of fluorescent molecules and is dependent on rotational motions and the molecular size of the species. FP can be considered a competition between the molecular motion and the lifetime of fluorophores in solution. FP is a powerful and homogenous assay for studying ligand-protein interactions in solution and has been used extensively in early drug discovery including the screening of libraries and the determination of competitive binding affinities of ligands to large target molecules.<sup>191, 192</sup> Surface plasmon resonance (SPR) is another biophysical technique which allows the real time measurement of interactions between biomolecules without the application of a specific label. The SPR competition binding assay was carried out on a Biacore 3000 biosensor (GE Healthcare) using the immobilized *N*-biotinylated 16mer Nrf2 peptide as the ligand and Keap1 Kelch domain as the analyte to evaluate the binding affinity of the synthesized analogs with Keap1 Kelch domain.<sup>191, 192</sup>

### **1. Modification on the Cyclohexane Carboxylic Acid Moiety**

The inhibitory activities of analogs with modification on cyclohexane carboxylic acid moiety were evaluated at two concentration 5  $\mu\text{M}$  and 50  $\mu\text{M}$ . The evaluation results were are summarized in Table 2 and Fig. 33.

**Table 2.** Inhibitory Activities of Synthesized Analogs with Modification on Cyclohexane Carboxylic Acid Moiety

Entry	Compound #	Compound Structure	%Inhibition at 50 $\mu$ M	%Inhibition at 5 $\mu$ M	# of isomers
1	LH601 (23)		85.7	26.6	4
2	LH601AB		94.2	70.0	2
3	LH601A		94.1	82.7	1
4	29		1.6	-0.6	1
5	30		36.7	5.6	1
6	31		77.9	33.0	1

7	32		15.5	-5.8	1
8	33		0.4	0.4	4
9	34		42.4	4.9	4
10	35		9.9	1.9	2

---

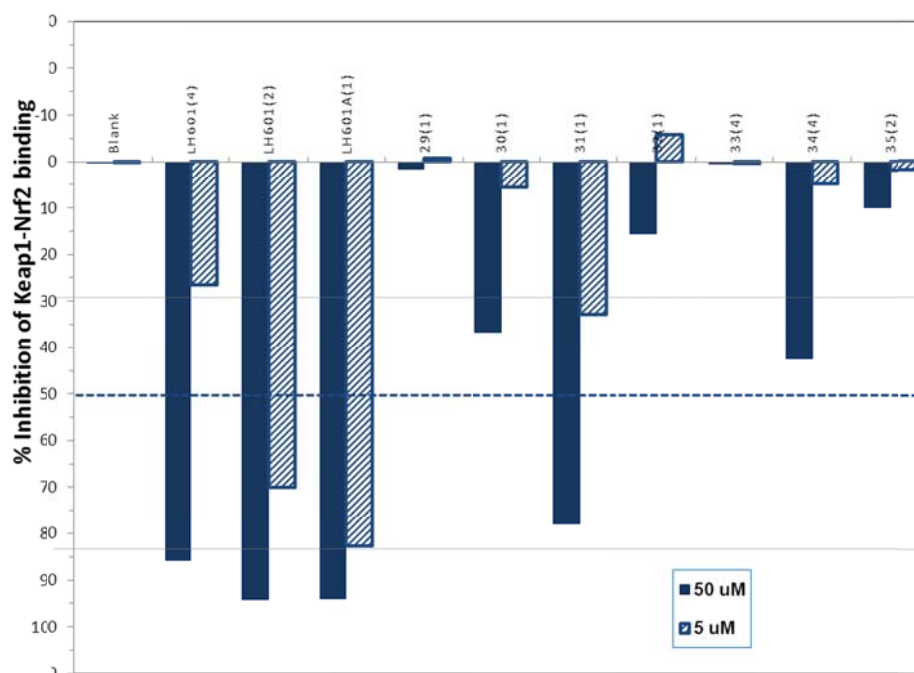


**Figure 33.** Inhibitory Activities of Synthesized Analogs with Modification on Cyclohexane Carboxylic Acid Moiety

From the data shown in Table 2 and Fig. 33, we obtained the following structure-activity relationships:

1) The methyl ester analog **29** of LH601A was completely inactive and the corresponding amide compound **30** was about 20-fold less active than LH601A at 5  $\mu$ M. These data suggested that the acidic functionality is preferred on cycloalkane ring and the free carboxylic acid group in LH601A is required for binding to Keap1 Kelch domain.

2) The glycine conjugate **32** with extended carboxylic acid was completely inactive and the analog **31** with replacement of carboxylic acid with acyl sulfonamide was about 4-fold less active than LH601A at 5  $\mu$ M. These data also suggested that the acidic functionality is preferred for binding to Keap1 Kelch domain and the position of carboxylic acid is also critical for binding to Keap1 Kelch domain.

3) There are three chiral centers in the lead molecule and the two substituents on the cyclohexyl ring are confirmed to be of *cis* configuration. The analog **33** retaining all the chemical features of the lead molecule but with two substituents on the cyclohexyl ring in *trans* configuration was completely inactive. The other two analogs **34** and **35** with cyclohexane ring replaced by (1*R*,4*S*)-bicyclo[2.2.1]hept-2-ene and benzene ring, respectively, were almost not active to bind Keap1 Kelch domain. This information suggests that the *cis* configuration is critical for the molecule to bind Keap1 Kelch domain because ligand-target interactions are often stereospecific. This also suggests that the structure and conformation of the cyclohexane ring is also important for the binding to Keap1 Kelch domain.

## **2. Modification on the Tetrahydroisoquinoline (THIQ)**

The inhibitory activities of analogs with modification on Tetrahydroisoquinoline (THIQ) are summarized in Table 3 and Fig. 34. From the data, we obtained the following structure-activity relationships:

1) One analog **36** was designed with removal of the ethyl linker on the tetrahydroisoquinoline. This molecule was inactive suggesting that the integrity of the tetrahydroisoquinoline is important for the binding with Keap1 Kelch domain.

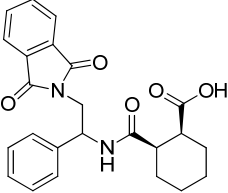
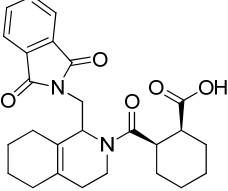
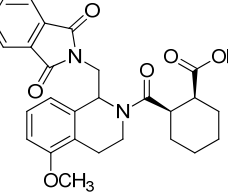
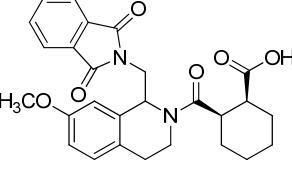
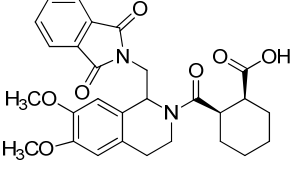
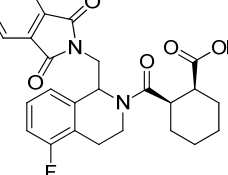
2) One analog **37** was designed with replacement of the tetrahydroisoquinoline with octahydroisoquinoline. This molecule is much less active indicating the integrity of the tetrahydroisoquinoline is important for the binding with Keap1 Kelch domain.

3) Various substitutions including electron donating and electron withdrawing groups on the tetrahydroisoquinoline were evaluated (**38-45**). The results suggested that the molecule can bear both electron donating and electron withdrawing substituents on the tetrahydroisoquinoline. The analogs with methoxy or fluorine substituents on the tetrahydroisoquinoline were more potent and provided about two fold increase in binding affinity with Keap1 Kelch domain.

4) Two analogs with substituents on the ethyl of tetrahydroisoquinoline were designed. The analog **46** has one methyl substituent while the other one **47** has one methyl ester group. The corresponding analog with methyl ester substituent was about 10 fold less active at 5  $\mu$ M and the other one with smaller methyl group was about 5-fold less active than the lead molecule at 5  $\mu$ M, suggesting that the ethyl of the tetrahydroisoquinoline

group in LH601A does not prefer additional substitutions for binding with Keap1 Kelch domain.

**Table 3.** Inhibitory Activities of Synthesized Analogs with Modification on Tetrahydroisoquinoline (THIQ)

Entry	Compound #	Compound Structure	%Inhibition at 50 $\mu$ M	%Inhibition at 5 $\mu$ M	# of isomers
1	36		0.3	0.3	1
2	37		65.0	12.5	2
3	38		95.0	75.3	2
4	39		95.7	81.8	2
5	40		89.0	48.8	2
6	41		66.1	26.6	4

7	42		82.8	36.8	4
8	43		23.4	7.7	4
9	44		49.2	7.4	2
10	45		93.9	57.8	2
11	46		45.9	17.2	2
12	47		9.5	7.4	2

---

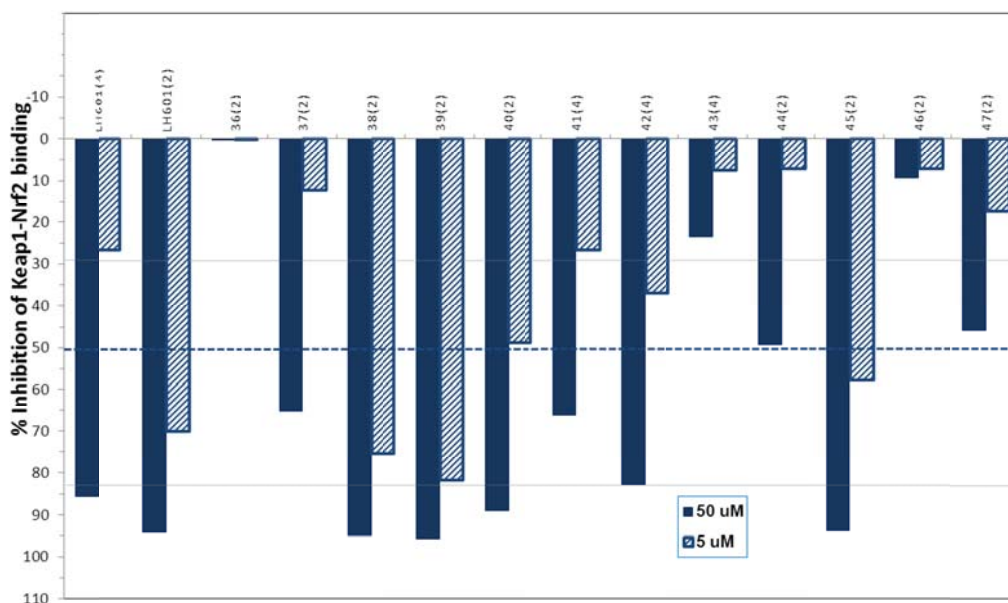


**Figure 34.** Inhibitory Activities of Synthesized Analogs with Modification on Tetrahydroisoquinoline (THIQ)

### 3. Modification on the Phthalimido Group

The inhibitory activities of analogs with modification on phthalimido group are summarized in Table 4 and Fig. 35. From the data, we obtained the following structure-activity relationships:

- 1) One analog **48** with hydrolyzed phthalimido group into carboxylic acid was inactive probably because the additional carboxylic acid interfered the interaction with the Keap1 Kelch domain and decreased the binding affinity.
- 2) Four analogs **49-52** with aminolyzed phthalimido group were also synthesized. The analog **49** with aminolyzed phthalimido group into simple amide was about 2-fold less

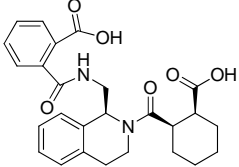
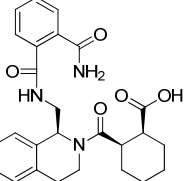
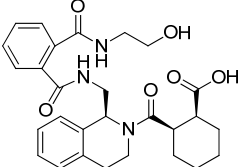
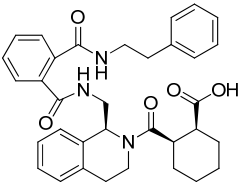
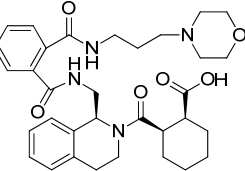
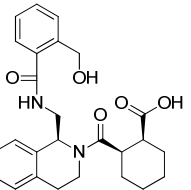
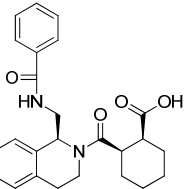
active than the lead molecule at 5  $\mu\text{M}$ . Other analogs with aminolyzed phthalimido group also showed decrease in binding affinity. One analog **53** with one ketone of phthalimido group reduced to hydroxymethyl showed very weak binding affinity with Keap1 Kelch domain. These results indicated that the phthalimido group does not prefer to be opened.

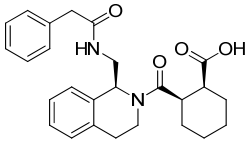
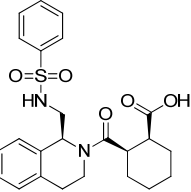
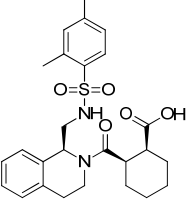
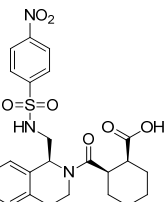
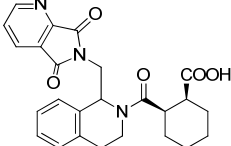
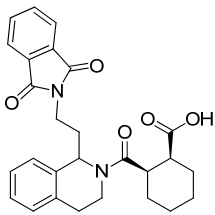
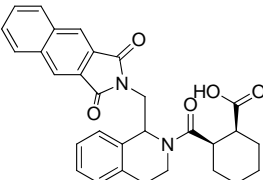
3) In order to simplify the chemical structure of the lead molecule, five analogs with replacement of the phthalimido group with aryl amide **54-55** or aryl sulfonamide **56-58** were synthesized. However, these compounds were almost inactive to bind the Keap1 Kelch domain. These results further indicated that the phthalimido group does not prefer to be opened.

4) The concept of bioisosterism is an important way widely used in the design of analogs. Bioisosteres are substituents or groups that have chemical or physical similarities, and which produce broadly similar biological properties. The analog **60** with replacement of the fused benzene ring of phthalimide with pyridine ring was evaluated but showed no activity. More analogs with replacement of phthalimido with either substitutions or other aromatic rings were designed and synthesized. The analog **62** with naphthalimido replacement of phthalimido was about two fold more active.

5) Homologation is a common way to make analogs. The analog **61** with an ethyl linker instead of methylene between tetrahydroisoquinoline and phthalimido group was inactive. This small change in conformation probably affected the spatial relationship of functional groups in the molecule, thereby influenced the receptor binding. The result indicated that one carbon linker is preferred between tetrahydroisoquinoline and phthalimido group.

**Table 4.** Inhibitory Activities of Synthesized Analogs with Modification on Phthalimido Group

Entry	Compound #	Compound Structure	%Inhibition at 50 $\mu$ M	%Inhibition at 5 $\mu$ M	# of isomers
1	48		9.5	0.9	1
2	49		83.0	38.6	1
3	50		32.1	7.5	1
4	51		47.1	3.3	1
5	52		43.8	6.9	1
6	53		39.3	7.3	1
7	54		-3.5	1.5	1

8	55		36.9	7.0	1
9	56		12.9	3.1	1
10	57		17.1	0.1	1
11	58		26.7	4.0	1
12	60		4.9	-10.2	2
13	61		8.8	-2.2	2
14	62		93.3	74.8	4

---

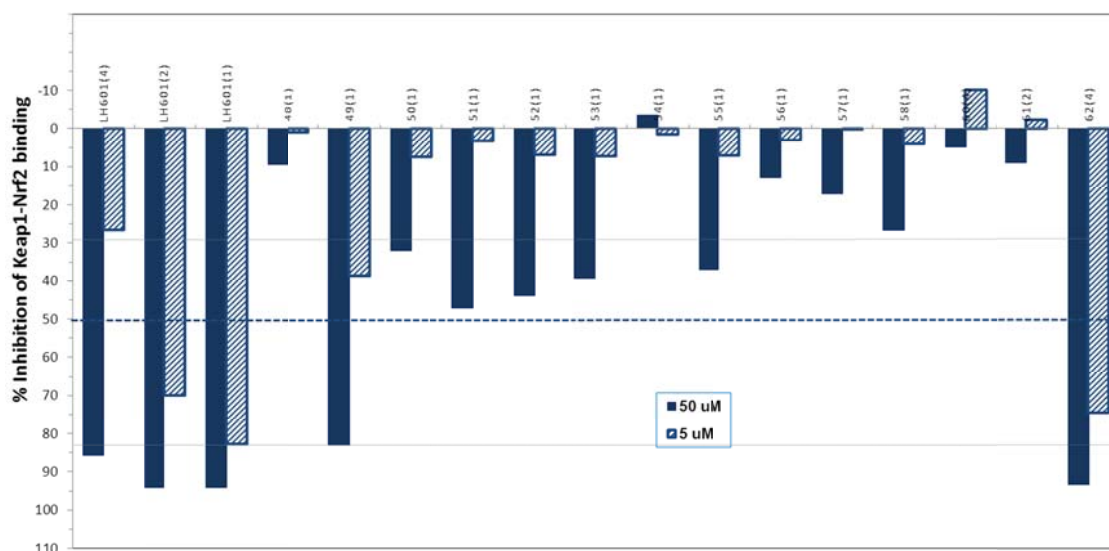


**Figure 35.** Inhibitory Activities of Synthesized Analogs with Modification on Phthalimido Group

#### 4. Analogs with Modifications on both the Phthalimide and Tetrahydroisoquinoline

The inhibitory activities of analogs with modifications on both phthalimide and tetrahydroisoquinoline are summarized in Table 5 and Fig. 36. As expected, the analogs with methoxy (**63**) or fluoro substitution (**64**) on tetrahydroisoquinoline and naphthalimido replacement of phthalimido were more potent and showed about 3-4 fold increase binding affinity with Keap1 Kelch domain at 5  $\mu$ M. These two analogs with modifications on both tetrahydroisoquinoline and phthalimide brought the inhibitory activity of our designed analogs into nanomolar range.

**Table 5.** Inhibitory Activities of Synthesized Analogs with Modification on both Phthalimide and Tetrahydroisoquinoline

Entry	Compound #	Compound structure	%Inhibition at 50 $\mu$ M	%Inhibition at 5 $\mu$ M	# of isomers
1	63		104.4	86.5	4
2	64		104.5	70.5	4

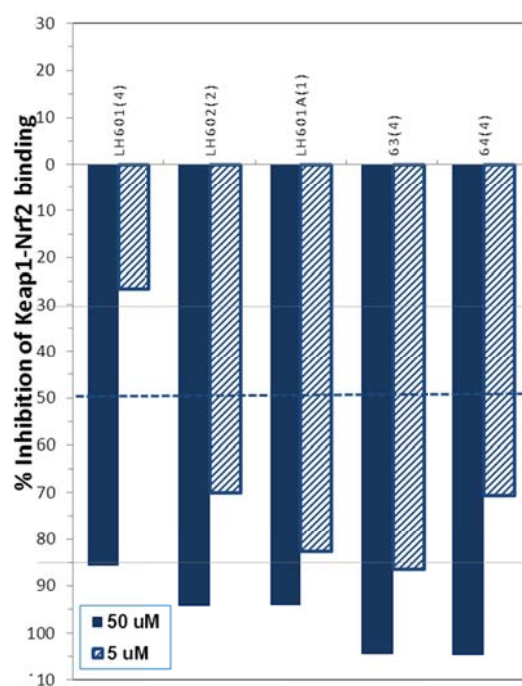


**Figure 36.** Inhibitory Activities of Synthesized Analogs with Modification on both Phthalimide and Tetrahydroisoquinoline

### C. Preliminary Structure Activity Relationship (SAR)

The figure below depicts a summary of the SARs. 1) Acidic functionality preferred on cycloalkane ring. The corresponding methyl ester compound was completely inactive and the corresponding amide compound was about 20-fold less active than LH601A, suggesting that the free carboxylic acid group in LH601A is required for binding to Keap1 Kelch domain. 2) Replacement of the tetrahydroisoquinoline ring was much less active and the integrity of tetrahydroisoquinoline is important for the binding with Keap1 Kelch domain; 3) *Cis* configuration of the two substituents on the cyclohexyl ring is critical for the binding with Keap1 Kelch domain. 4) Tetrahydroisoquinolin ring can bear substituents. Methoxy and fluorine substitutions on the tetrahydroisoquinoline were about two fold more active.

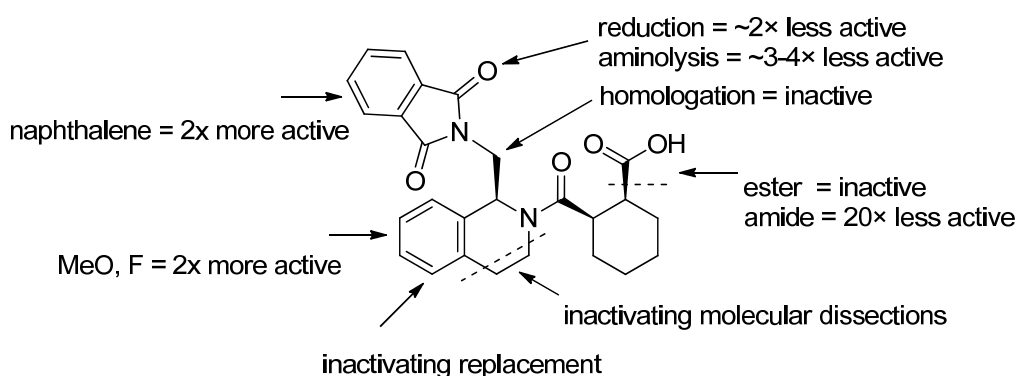


**Figure 37.** Preliminary Structure-Activity Relationships.

5) Phthalimido group prefers not to be opened. Several analogs with opened phthalimide ring were either inactive or showed decreased binding affinity with Keap1 Kelch domain.

6) Phthalimido group can be replaced or substituted. Naphthalimido replacement of phthalimido was about two fold more active. 7) One carbon linker is preferred between tetrahydroisoquinoline (THIQ) and phthalimido group. Analog with an ethyl linker instead of methylene between THIQ and phthalimido group was inactive. 8) The compounds with combined modifications including methoxy or fluoro substitution on tetrahydroisoquinoline and naphthalimido replacement of phthalimide showed about four fold increase binding affinity with Keap1 Kelch domain.<sup>43</sup>

#### **D. ARE Induction and Nrf2 Nuclear Translocation Assays**

The functional activity of LH601A was also determined on ARE gene expression in the CellSensor<sup>®</sup> ARE-bla HepG2 cell line obtained from Invitrogen and on Nrf2 nuclear translocation in the PathHunter<sup>®</sup> U2OS Keap1-Nrf2 Functional Assay obtained from DiscoverX. Fig. 38 illustrates the ARE-inducing activity of LH601A at an EC<sub>50</sub> of 18 μM as compared >100 μM for its enantiomer LH601B and its diastereomers LH601C/D. Fig. 39 demonstrates that LH601A causes Nrf2 nuclear translocation upon inhibition of Keap1-Nrf2 interaction with a similar EC<sub>50</sub> of 12 μM. All these data indicate that LH601A is cell permeable and is capable of inhibiting the Keap1-Nrf2 interaction, leading to the dissociation of Nrf2 from Keap1 in the cytosol, its subsequent translocation to the nucleus, and the upregulation of ARE controlled genes.<sup>43</sup>

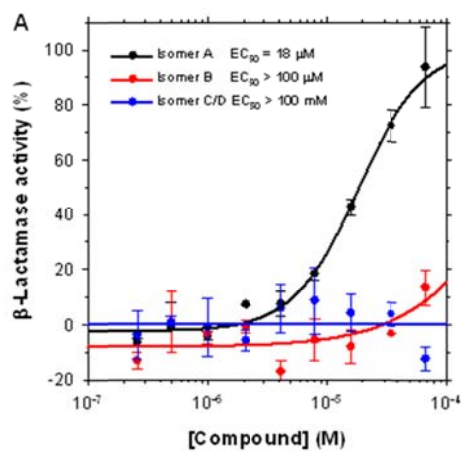


**Figure 38.** ARE-Inducing Activity of LH601A in CellSensor-Lactamase Reporter Assay

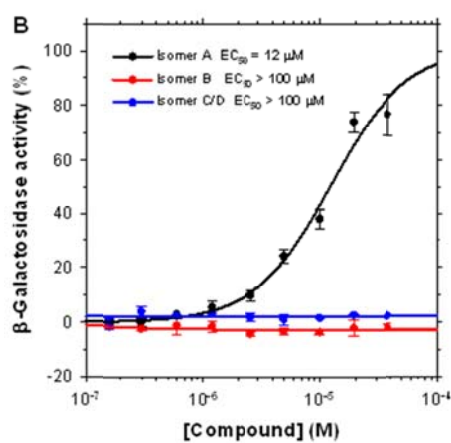


**Figure 39.** Nrf2 Nuclear Translocation Effect of LH601A in the PathHunter U2OS Keap1-Nrf2 Functional Assay.

## V. Summary

Most of the available inhibitors of Keap1-Nrf2-ARE pathway share a common feature of the electrophilicity. Structurally, these compounds are either chemically reactive such as isothiocyanate and Michael acceptors or can be metabolized to chemically reactive species that covalently modify cysteine sulfhydryl groups of Keap1 and activate Nrf2-mediated ARE genes. There are safety concerns about these thiol-reactive compounds over long term use. Risks of off-target toxic effects have also been associated with these ARE inducers due to their potential to react with other cysteine-containing proteins and enzymes. The only direct inhibitors of Keap1-Nrf2 interaction are the peptides based on the Nrf2 Neh domain that are used in the crystallographic studies. Multiple charges are present on these peptides and their poor membrane permeability prevented their use directly in cellular and in vivo assays. However, molecular biological approaches have clearly demonstrated the cytoprotective functions of Nrf2-mediated expression of ARE genes.

A high-throughput screen (HTS) of the MLPCN library using a homogenous fluorescence polarization assay developed in our lab identified a small molecule as a first-in-class inhibitor specifically for the direct inhibition of the Keap1-Nrf2 protein-protein interaction. The HTS hit has three chiral centers. A combination of flash and chiral chromatographic separation demonstrated that Keap1-binding activity resides predominantly in one stereoisomer designated as LH601A, which is at least 100× more potent than the other stereoisomers. The stereochemistry of the four isomers was assigned using X-ray crystallography and confirmed using stereospecific synthesis. LH601A is

functionally active in both an ARE gene reporter assay and an Nrf2 nuclear translocation assay.

Various analogs of LH601A were designed and synthesized to explore the chemical spaces around the various points of the scaffold to improve binding affinity. The preliminary structure-activity relationships (SAR) provided more information and guidance for further structural optimization. All analogs synthesized were evaluated by FP or SPR assay and several compounds were shown to be more potent direct inhibitors of Keap1-Nrf2 protein-protein interaction than LH601A. These direct Keap1-Nrf2 inhibitors can mimic the actions of electrophiles like Michael acceptors and isothiocyanates in the induction of cytoprotective enzymes but are more selective and specific against the Keap-Nrf2 interaction at the protein-protein interface without the associated side effects. Therefore, these direct inhibitors of Keap1-Nrf2 protein-protein interaction have great potential to be developed into innovative therapeutic agents for many diseases and conditions involving oxidative stress.

## CHAPTER 4

### EXPERIMENTAL SECTION

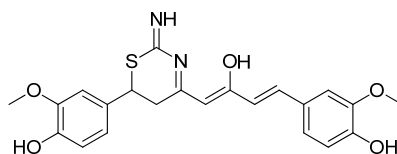
#### General Methods.

Solvents purchased were either ACS reagent grade or HPLC grade. All reagents purchased were ACS grade or better and used without further purification. All reactions were magnetically stirred and monitored by thin-layer chromatography (TLC) using Whatman polymer-backed F254 silica gel plates and/or Shimadzu 2010 LC-MS system, Thermo Finnigan LCQ system, and Thermo Finnigan LTQ system. Flash column chromatography was performed using using a Teledyne ISCO CombiFlash Companion Automated flash chromatographic system with prepacked silica gel columns. Lyophilization was performed on a Savant lyophilizer. Yields were based on the chromatographically pure compounds.  $^1\text{H}$  NMR spectra were recorded on Bruker 400 MHz spectrometers as indicated at ambient temperature and calibrated using residual undeuterated solvents as the internal reference.  $^{13}\text{C}$  NMR spectra were recorded at 100 MHz on a Bruker 400 MHz spectrometer. Chemical shifts are reported in parts per million ( $\delta$ ). Analytical LC-MS spectra were obtained using LC-MS system equipped with a C18 reversed phase column (5  $\mu\text{m}$ , 4.6 x 50 mm). Solvent A was 0.1% HCOOH/ $\text{H}_2\text{O}$ , solvent B was 0.1% HCOOH/ $\text{CH}_3\text{CN}$  or 0.1% HCOOH/MeOH, and the gradient was 5-95% in 5 min, with flow rate 2 mL/min. Stability analysis was performed on HP1090 HPLC system. The reversed phase isolation was performed using Gilson automated preparative HPLC system equipped with a Keystone Hypersil-C18 (5.0  $\mu\text{m}$ , 20 x 150 mm)

at 20 mL/min with a linear gradient of 30-90% of acetonitrile containing 0.1% trifluoroacetic acid. The chiral separation and isolation were performed on Beckman system by normal preparative chiral HPLC (Chiral OD, 20 x 250 mm) using hexane/10% *i*-PrOH with 0.1% trifluoroacetic acid as an isocratic eluent.

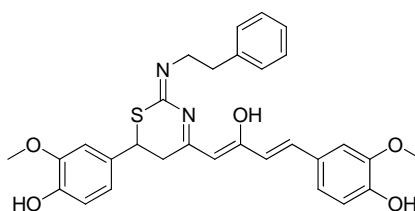
### I. Novel Heterocyclic Curcumin Analogs

#### 4-(4-((1*Z*,3*E*)-2-Hydroxy-4-(4-hydroxy-3-methoxyphenyl)buta-1,3-dien-1-yl)-2-imino-5,6-dihydro-2*H*-1,3-thiazin-6-yl)-2-methoxyphenol (**2**)



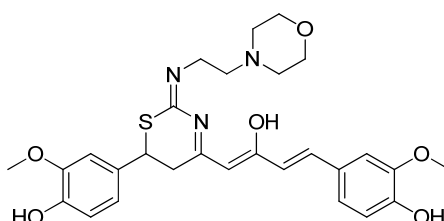
To a mixture of curcumin (10 mg, 0.027 mmol) and thiourea (2.5 mg, 0.032 mmol) was added 6 mL of 4 N HCl in dioxane. The dark reaction mixture was stirred for 12 h at room temperature. The reaction mixture was then concentrated and the residue was purified by flash column chromatography to afford 6 mg of the desired product **2** in 52% yield. <sup>1</sup>H NMR (CD<sub>3</sub>OD-d<sub>4</sub>, 400 MHz): δ 7.75 (d, 1H, *J* = 16.2 Hz), 7.26 (d, 1H, *J* = 4.8 Hz), 7.18 (dd, 1H, *J* = 14.2, 4.8 Hz), 7.03 (d, 1H, *J* = 4.2 Hz), 6.94 (dd, 1H, *J* = 6.8, 8.8 Hz), 6.86 (d, 1H, *J* = 8.2 Hz), 6.84 (d, 1H, *J* = 16.6 Hz), 6.82 (d, 1H, *J* = 4.6 Hz), 6.21 (s, 1H), 3.90 (s, 3H), 3.86 (s, 3H), 3.51 (dd, 1H, *J* = 3.8, 6.2 Hz), 3.47 (t, 1H, *J* = 4.6 Hz), 3.23 (m, 1H). <sup>13</sup>C NMR (CD<sub>3</sub>OD-d<sub>4</sub>, 100 MHz): 190.1, 189.3, 150.3, 150.1, 148.3, 147.5, 147.3, 144.8, 126.3, 125.7, 124.2, 123.2, 120.6, 120.4, 115.5, 111.9, 111.6, 55.7, 55.5, 44.9, 34.6. MS (ESI<sup>+</sup>): *m/z* 427.0 (M+H).

**4-(4-((1*Z*,3*E*)-2-Hydroxy-4-(4-hydroxy-3-methoxyphenyl)buta-1,3-dien-1-yl)-2-(phenethylimino)-5,6-dihydro-2*H*-1,3-thiazin-6-yl)-2-methoxyphenol (3)**



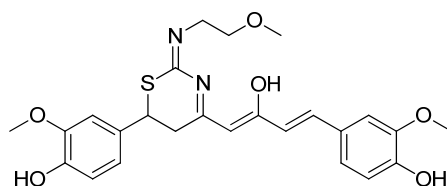
To a mixture of curcumin (100 mg, 0.27 mmol) and 1-phenethylthiourea (58 mg, 0.32 mmol) was added 15 mL 4 N HCl in dioxane. The dark reaction mixture was stirred for 6 h at room temperature. The reaction mixture was then concentrated and the residue was purified by flash column chromatography to afford 91 mg of the desired product **3** in 62% yield. <sup>1</sup>H NMR (CD<sub>3</sub>OD-d<sub>4</sub>, 400 MHz): δ 7.78 (d, 1H, *J* = 16.8 Hz), 7.68 (d, 1H, *J* = 16.2 Hz), 7.35-7.27 (m, 5H), 7.26-7.18 (m, 5H), 7.18 (d, 1H, *J* = 4.4 Hz), 7.12 (dd, 1H, *J* = 12.6, 8.2 Hz), 6.98 (d, 1H, *J* = 12.8 Hz), 6.90-6.70 (m, 7H), 6.20 (s, 1H), 6.08 (s, 1H), 3.89-3.80 (m, 12H), 3.75-3.66 (m, 2H), 3.42-3.38 (m, 2H), 3.21-3.16 (m, 2H), 3.14-3.03 (m, 3H), 3.02-2.96 (m, 2H). <sup>13</sup>C NMR (CD<sub>3</sub>OD-d<sub>4</sub>, 100 MHz): δ 193.4, 192.5, 169.1, 152.3, 150.2, 150.5, 149.6 (x 2), 149.5, 148.5, 147.5, 146.4, 138.6, 138.0, 130.6 (x 2), 130.4 (x 2), 130.2, 130.1 (x 2), 128.3, 128.1, 127.6 (x 2), 127.4 (x 2), 127.3, 125.8, 125.2, 124.8, 124.5, 121.6, 121.3, 117.2, 116.8, 116.6, 116.2, 112.6, 112.2, 108.2, 107.6, 56.6 (x 2), 56.5 (x 2), 47.5, 47.1, 44.9, 44.4, 36.6, 36.1, 35.4, 34.9. MS (ESI<sup>+</sup>): *m/z* 531.0 (M+H).

**4-((1*E*,3*Z*)-3-Hydroxy-4-((*E*)-6-(4-hydroxy-3-methoxyphenyl)-2-((2-morpholinoethyl)imino)-5,6-dihydro-2*H*-1,3-thiazin-4-yl)buta-1,3-dien-1-yl)-2-methoxyphenol (4)**



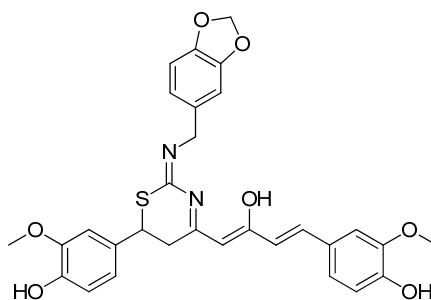
To a mixture of curcumin (37 mg, 0.1 mmol) and 1-(2-morpholinoethyl)thiourea (23 mg, 0.12 mmol) was added 10 mL 4 N HCl in dioxane. The dark reaction mixture was stirred for 12 h at room temperature. The reaction mixture was then concentrated and the residue was purified by flash column chromatography to afford 31 mg of the desired product **4** in 58% yield. <sup>1</sup>H NMR (CD<sub>3</sub>OD-d<sub>4</sub>, 400 MHz): δ 7.66 (d, 1H, *J* = 16.6 Hz), 7.62 (d, 1H, *J* = 8.2 Hz), 7.10 (d, 1H, *J* = 16.2 Hz), 7.05 (d, 1H, *J* = 4.2 Hz), 6.92 (d, 1H, *J* = 5.8 Hz), 6.83 (dd, 1H, *J* = 12.6, 7.8 Hz), 6.81-6.69 (m, 4), 6.20 (s, 1H), 6.03 (s, 1H), 3.84-3.77 (m, 6H), 3.70-3.62 (m, 4H), 3.56 (t, 2H, *J* = 9.2 Hz), 3.31 (s, 2H), 2.56-32.23 (m, 4H). <sup>13</sup>C NMR (CD<sub>3</sub>OD-d<sub>4</sub>, 100 MHz): 191.6, 190.6, 150.1, 150.0, 149.7, 148.3, 148.0, 147.6, 147.5, 147.4, 146.1, 144.0, 126.8, 126.1, 125.6, 124.2, 124.0, 123.8, 123.0, 120.3, 120.0, 115.8, 112.6, 111.3, 111.0, 689.2, 68.7, 68.1, 67.5, 58.2, 58.0, 55.5, 53.8, 44.4, 43.8, 42.8, 41.5, 34.5, 34.1. MS (ESI<sup>+</sup>): *m/z* 540.2 (M+H).

**4-4-((1*Z*,3*E*)-2-Hydroxy-4-(4-hydroxy-3-methoxyphenyl)buta-1,3-dien-1-yl)-2-(2-methoxyethyl)imino)-5,6-dihydro-2*H*-1,3-thiazin-6-yl)-2-methoxyphenol (5)**



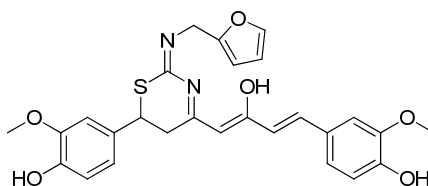
To a mixture of curcumin (37 mg, 0.1 mmol) and 1-(2-methoxyethyl)thiourea (16 mg, 0.12 mmol) was added 5 mL 4 N HCl in dioxane. The dark reaction mixture was stirred for 8 h at room temperature. The reaction mixture was then concentrated and the residue was purified by flash column chromatography to afford 38 mg of the desired product **5** in 79% yield.  $^1\text{H}$  NMR ( $\text{CD}_3\text{OD}-d_4$ , 400 MHz):  $\delta$  7.69 (d, 1H,  $J = 15.6$  Hz), 7.64 (d, 1H,  $J = 9.2$  Hz), 7.18 (d, 1H,  $J = 16.2$  Hz), 7.06 (d, 1H,  $J = 7.8$  Hz), 6.95 (d, 1H,  $J = 3.8$  Hz), 6.84 (d, 1H,  $J = 13.2$  Hz), 6.80-6.70 (m, 4), 6.18 (s, 1H), 6.05 (s, 1H), 3.83-3.77 (m, 6H), 3.74-3.68 (m, 2H), 3.67-3.60 (m, 2H), 3.56 (t, 2H,  $J = 8.8$  Hz), 3.34 (s, 2H), 3.31 (s, 1H).  $^{13}\text{C}$  NMR ( $\text{CD}_3\text{OD}-d_4$ , 100 MHz): 191.1, 190.3, 150.5, 150.2, 150.0, 148.7, 148.0, 147.9, 147.5, 147.4, 146.2, 144.5, 126.4, 126.1, 125.7, 124.4, 124.3, 123.8, 123.0, 120.5, 120.4, 115.8, 111.8, 111.7, 111.4, 68.7, 68.4, 58.2, 58.0, 55.7 (x 2), 44.6, 44.3, 42.3, 41.9, 34.9, 34.4. MS (ESI+):  $m/z$  485.0 (M+H).

**4-(2-((Benzo[d][1,3]dioxol-5-ylmethyl)imino)-4-((1Z,3E)-2-hydroxy-4-(4-hydroxy-3-methoxyphenyl)buta-1,3-dien-1-yl)-5,6-dihydro-2H-1,3-thiazin-6-yl)-2-methoxyphenol (6)**



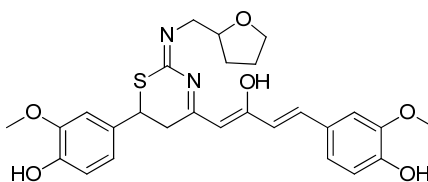
To a mixture of curcumin (37 mg, 0.1 mmol) and 1-benzo[d][1,3]dioxol-4-ylmethylthiourea (25 mg, 0.12 mmol) was added 10 mL 4 N HCl in dioxane. The dark reaction mixture was stirred for 10 h at room temperature. The reaction mixture was then concentrated and the residue was purified by flash column chromatography to afford 29 mg of the desired product **6** in 52% yield. <sup>1</sup>H NMR (DMSO-d<sub>6</sub>, 400 MHz): δ 12.86 (s, 1H), 9.56 (s, 1H), 9.08 (s, 1H), 7.39 (d, 1H, *J* = 14.8 Hz), 7.21 (s, 1H), 7.10-6.95 (m, 3H), 6.90-6.65 (m, 7H), 5.92 (s, 2H), 4.68 (d, 1H, *J* = 12.6 Hz), 3.78 (s, 3H), 3.69 (s, 3H), 2.92 (d, 1H, *J* = 13.8 Hz). <sup>13</sup>C NMR (DMSO-d<sub>6</sub>, 100 MHz): 188.5, 179.9, 154.1, 149.2, 148.7, 148.0, 147.9, 147.7, 146.4, 146.1, 140.9, 139.4, 133.0, 132.7, 131.5, 127.7, 127.2, 126.6, 126.4, 125.2, 123.3, 123.2, 122.7, 121.6, 121.1, 120.8, 120.5, 120.1, 115.7, 116.6, 115.5, 111.3, 111.0, 108.3, 108.2, 108.0, 107.9, 102.3, 100.8, 100.7. MS (ESI<sup>+</sup>): *m/z* 561.3 (M+H).

**4-((*E*)-2-((Furan-2-ylmethyl)imino)-4-((1*Z*,3*E*)-2-hydroxy-4-(4-hydroxy-3-methoxyphenyl)buta-1,3-dien-1-yl)-5,6-dihydro-2*H*-1,3-thiazin-6-yl)-2-methoxyphenol (7)**



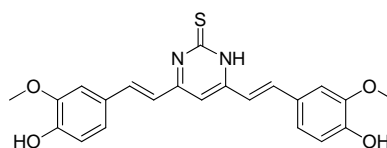
To a mixture of curcumin (37 mg, 0.1 mmol) and 1-(furan-2-ylmethyl)thiourea (19 mg, 0.12 mmol) was added 10 mL 4 N HCl in dioxane. The dark reaction mixture was stirred for 10 h at room temperature. The reaction mixture was then concentrated and the residue was purified by flash column chromatography to get 30 mg of the desired product **7** in 61% yield.  $^1\text{H}$  NMR ( $\text{CD}_3\text{OD}-d_4$ , 400 MHz):  $\delta$  7.82 (d, 1H,  $J = 17.4$  Hz), 7.61 (d, 1H, 8.2 Hz), 7.46 (d, 1H,  $J = 16.6$  Hz), 7.22 (d, 1H  $J = 7.8$  Hz), 7.02 (d, 1H,  $J = 4.6$  Hz), 6.99 (dd, 1H,  $J = 5.6, 13.6$  Hz), 6.88 (d, 1H, 8Hz), 6.86 (d, 1H,  $J = 16.2$  Hz), 6.78 (d, 1H,  $J = 6.6$  Hz), 6.53 (m, 1H), 2.12-1.78 (m, 2H).  $^{13}\text{C}$  NMR ( $\text{CD}_3\text{OD}-d_4$ , 100 MHz):  $\delta$  191.2, 190.4, 163.4, 152.9, 151.8, 151.6, 151.2, 149.8, 149.5, 149.3, 143.8, 129.3, 128.8, 125.6, 124.2, 121.6, 116.9, 115.8, 112.3, 109.9, 108.8, 105.2, 83.9, 63.5, 37.1, 29.2. MS (ESI+):  $m/z$  507.3 (M+H).

**4-(4-(((1Z,3E)-2-Hydroxy-4-(4-hydroxy-3-methoxyphenyl)buta-1,3-dien-1-yl)-2-(((tetrahydrofuran-2-yl)methyl)imino)-5,6-dihydro-2H-1,3-thiazin-6-yl)-2-methoxyphenol (8)**



To a mixture of curcumin (74 mg, 0.2 mmol) and 1-((tetrahydrofuran-2-yl)methyl)thiourea (48 mg, 0.24 mmol) was added 10 mL 4 N HCl in dioxane. The dark reaction mixture was stirred for 12 h at room temperature. The reaction mixture was then concentrated and the residue was purified by flash column chromatography to get 69 mg of the desired product **8** in 67% yield.  $^1\text{H}$  NMR ( $\text{CD}_3\text{OD-d}_4$ , 400 MHz):  $\delta$  7.79 (d, 1H,  $J = 11.8$  Hz), 7.28 (d, 1H,  $J = 16.8$  Hz), 7.20 (d, 1H,  $J = 7.2$  Hz), 7.07 (d, 1H,  $J = 4.4$  Hz), 6.96 (dd, 1H,  $J = 4.8, 12.8$  Hz), 6.88 (d, 1H,  $J = 6.8$  Hz), 6.84 (d, 1H,  $J = 8.0$  Hz), 6.27 (s, 1H), 4.22 (m, 1H), 3.94 (s, 3H), 3.91 (s, 3H), 4.06 (d, 1H,  $J = 7.8$  Hz), 3.82 (t, 1H,  $J = 10.2$  Hz), 3.73-3.60 (m, 2H), 3.59-3.42 (m, 2H), 2.30-1.90 (m, 4H), 1.85-1.60 (m, 2H).  $^{13}\text{C}$  NMR ( $\text{CD}_3\text{OD-d}_4$ , 100 MHz):  $\delta$  192.9, 192.5, 166.7, 151.9, 151.8, 151.6, 151.0, 149.9, 149.5, 149.1, 127.8, 127.8, 125.6, 124.4, 121.8, 116.9 (x 2), 112.3, 109.9, 107.9, 77.9, 69.6, 56.6 (x 2), 50.4, 44.8, 36.6, 30.1, 26.6. MS (ESI+):  $m/z$  510.9 (M+H).

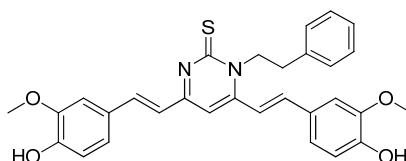
#### 4,6-Bis((*E*)-4-hydroxy-3-methoxystyryl)-1-phenethylpyrimidine-2(1*H*)-thione (**9**)



To a solution of **2** (43 mg, 0.1 mmol) in 2 mL DMF was added  $\text{K}_2\text{CO}_3$  (100 mg, 0.72 mmol). The suspension was stirred for 24 h at room temperature. The reaction mixture was then evaporated to dryness and the obtained dark material was dissolved in DCM, and washed with 0.1 N HCl and water. The organic layer was dried over anhydrous  $\text{Na}_2\text{SO}_4$  and concentrated. The obtained residue was purified by preparative RP-HPLC to get 23 mg of the desired product in 56% yield.  $^1\text{H}$  NMR ( $\text{CD}_3\text{OD-d}_4$ , 400 MHz):  $\delta$  7.92

(d, 1H,  $J = 18.2$  Hz), 7.86 (d, 1H,  $J = 6.8$  Hz), 7.78 (d, 1H,  $J = 12.4$  Hz), 7.68 (d, 1H,  $J = 8.6$  Hz), 7.53 (d, 1H,  $J = 16.6$  Hz), 7.39 (d, 1H,  $J = 9.8$  Hz), 6.89 (d, 1H,  $J = 6.8$  Hz), 6.77 (m, 1H), 6.72 (s, 1H), 6.63 (m, 1H), 6.56 (m, 1H), 3.73 (s, 3H), 3.68 (s, 3H).  $^{13}\text{C}$  NMR ( $\text{CD}_3\text{OD-d}_4$ , 100 MHz):  $\delta$  178.8, 162.2, 153.5, 152.5, 150.1, 149.8, 139.1, 132.6, 130.8, 130.1, 128.4, 128.3, 128.0, 126.5, 124.9, 117.8, 116.2, 113.6, 112.4, 102.5, 56.9, 56.8. MS (ESI+):  $m/z$  409.3 (M+H).

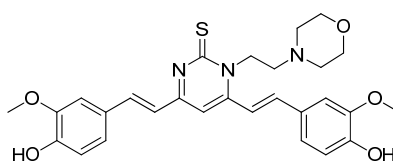
**4,6-Bis((*E*)-4-hydroxy-3-methoxystyryl)-1-phenethylpyrimidine-2(1*H*)-thione (10)**



To a solution of **3** (53 mg, 0.1 mmol) in 2 mL DMF was added  $\text{K}_2\text{CO}_3$  (100 mg, 0.72 mmol). The suspension was stirred for 18 h at room temperature. The reaction mixture was then evaporated to dryness and the obtained dark material was dissolved in DCM, and washed with 0.1 N HCl and water. The organic layer was dried over anhydrous  $\text{Na}_2\text{SO}_4$  and concentrated. The obtained residue was purified by preparative RP-HPLC to get 25 mg of the desired product in 50% yield.  $^1\text{H}$  NMR ( $\text{CD}_3\text{OD-d}_4$ , 400 MHz):  $\delta$  8.12 (d, 1H,  $J = 13.6$  Hz), 7.78 (d, 1H,  $J = 8.8$  Hz), 7.61 (s, 1H), 7.15 (m, 9H), 6.83 (m, 4H), 4.91 (s, 2H), 3.92 (s, 3H), 3.79 (s, 3H), 3.20 (m, 2H).  $^{13}\text{C}$  NMR ( $\text{CD}_3\text{OD-d}_4$ , 100 MHz):  $\delta$  177.8, 162.3, 159.5, 153.4, 152.5, 150.3, 149.8, 149.5, 148.2, 138.7, 132.8, 130.1 (x 2),

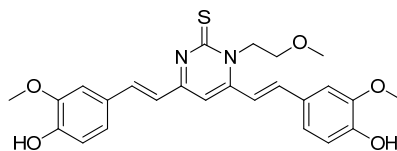
130.0, 128.3, 128.2, 126.5, 126.3, 125.7, 117.2, 117.0, 115.0, 113.8, 112.6, 112.4, 102.6, 56.7, 56.6, 54.0, 33.3. MS (ESI+):  $m/z$  513.1 (M+H).

**(E)-6-(4-Hydroxy-3-methoxyphenethyl)-4-(4-hydroxystyryl)-1-((tetrahydrofuran-2-yl)methyl)pyrimidine-2(1H)-thione (11)**



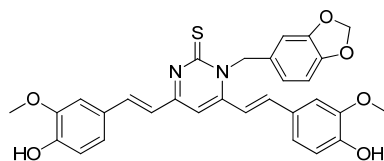
To a solution of **4** (20 mg, 0.037 mmol) in 2 mL DMF was added  $K_2CO_3$  (100 mg, 0.72 mmol). The suspension was stirred for 24 h at room temperature. The reaction mixture was then evaporated to dryness and the obtained dark material was dissolved in DCM, and washed with 0.1 N HCl and water. The organic layer was dried over anhydrous  $Na_2SO_4$  and concentrated. The obtained residue was purified by preparative RP-HPLC to get 10 mg of the desired product in 52% yield.  $^1H$  NMR ( $CD_3OD-d_4$ , 400 MHz):  $\delta$  8.23 (d, 1H,  $J = 16.2$  Hz), 7.89 (d, 1H,  $J = 9.2$  Hz), 7.51 (s, 1H), 7.28 (d, 1H,  $J = 10.6$  Hz), 7.25-6.92 (m, 4H), 6.90-6.56 (m, 3H), 3.88 (s, 3H), 3.78 (s, 3H), 3.68-3.46 (m, 4H), 3.20 (d, 2H,  $J = 4.8$  Hz), 2.89-1.90 (m, 6H).  $^{13}C$  NMR ( $CD_3OD-d_4$ , 100 MHz):  $\delta$  177.2, 161.6, 158.6, 153.2, 152.1, 149.3, 149.1, 148.8, 148.4, 132.6, 128.2, 128.0, 125.8, 125.3, 119.2, 118.3, 117.2, 113.1, 112.5, 102.8, 60.8, 58.9 (x 2), 56.3 (x 2), 48.9, 48.6, 43.8. MS (ESI+):  $m/z$  522.1 (M+H).

**4,6-Bis(*E*)-4-hydroxy-3-methoxystyryl)-1-(2-methoxyethyl)pyrimidine-2(1*H*)-thione (12)**



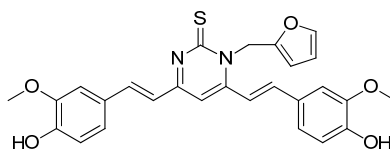
To a solution of **5** (30 mg, 0.1 mmol) in 2 mL DMF was added  $K_2CO_3$  (100 mg, 0.72 mmol). The suspension was stirred for 24 h at room temperature. The reaction mixture was then evaporated to dryness and the obtained dark material was dissolved in DCM, and washed with 0.1 N HCl and water. The organic layer was dried over anhydrous  $Na_2SO_4$  and concentrated. The obtained residue was purified by preparative RP-HPLC to get 14 mg of the desired product in 50% yield.  $^1H$  NMR ( $CD_3OD-d_4$ , 400 MHz):  $\delta$  7.83 (d, 1H,  $J = 13.6$  Hz), 7.56 (s, 1H), 7.54 (d, 1H,  $J = 16.8$  Hz), 7.52 (d, 1H,  $J = 14.4$  Hz), 7.36 (s, 1H), 7.22 (d, 1H,  $J = 12.2$  Hz), 7.15 (s, 1H), 7.12 (d, 1H,  $J = 8.8$  Hz), 7.04 (d, 1H,  $J = 8.2$  Hz), 6.84 (d, 1H,  $J = 16.8$  Hz), 6.84 (s, 1H), 3.85 (s, 3H), 3.76 (t, 2H,  $J = 6.2$  Hz), 3.30 (s, 3H), 2.86 (t, 2H,  $J = 6.8$  Hz).  $^{13}C$  NMR ( $CD_3OD-d_4$ , 100 MHz):  $\delta$  177.5, 162.8, 159.1, 153.0, 152.5, 149.8, 149.7, 149.4, 148.4, 132.8, 128.6, 128.1, 126.1, 125.7, 117.5, 117.1, 116.8, 112.6, 112.5, 103.4, 70.5, 59.6, 56.6 (x 2), 53.6. MS (ESI+):  $m/z$  467.1 (M+H).

**1-(Benzo[d][1,3]dioxol-5-ylmethyl)-4,6-bis(*E*)-4-hydroxy-3-methoxystyryl)pyrimidine-2(1*H*)-thione (13)**



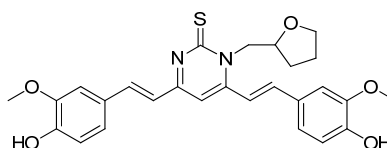
To a solution of **6** (20 mg, 0.036 mmol) in 2 mL DMF was added  $K_2CO_3$  (100 mg, 0.72 mmol). The suspension was stirred for 24 h at room temperature. The reaction mixture was then evaporated to dryness and the obtained dark material was dissolved in DCM, and washed with 0.1 N HCl and water. The organic layer was dried over anhydrous  $Na_2SO_4$  and concentrated. The obtained residue was purified by preparative RP-HPLC to get 13 mg of the desired product in 67% yield.  $^1H$  NMR ( $CD_3OD-d_4$ , 400 MHz):  $\delta$  9.72 (s, 1H), 9.61 (s, 1H), 7.83 (d, 1H,  $J=14.8$  Hz), 7.52 (d, 1H,  $J=16.2$  Hz), 7.41 (s, 1H), 7.31 (d, 1H,  $J=8.2$  Hz), 7.36 (s, 1H), 7.12 (d, 1H,  $J=6.4$  Hz), 7.06 (d, 1H,  $J=16.2$  Hz), 7.02 (s, 1H), 6.93 (dd, 1H,  $J=10.6, 6.6$  Hz), 6.92 (s, 1H), 6.88 (s, 1H), 6.80 (s, 1H), 6.79 (m, 1H), 5.96 (s, 2H), 4.76 (d, 1H,  $J=5.6$  Hz), 3.85 (s, 3H), 3.81 (s, 3H).  $^{13}C$  NMR ( $CD_3OD-d_4$ , 100 MHz):  $\delta$  177.2, 162.5, 159.3, 153.3, 152.7, 149.8, 149.7, 148.9, 148.2, 137.6, 135.6, 132.8, 129.8, 128.3, 126.3, 126.3, 125.9, 123.2, 121.1, 119.8, 117.0, 116.9, 115.8, 112.5, 111.8, 102.8, 100.8, 56.5 (x 2), 53.8. MS (ESI+):  $m/z$  543.2 (M+H).

**1-(Furan-2-ylmethyl)-4,6-bis((E)-4-hydroxy-3-methoxystyryl)pyrimidine-2(1H)-thione (14)**



To a solution of **7** (47 mg, 0.09 mmol) in 2 mL DMF was added  $K_2CO_3$  (100 mg, 0.72 mmol). The suspension was stirred for 24 h at room temperature. The reaction mixture was then evaporated to dryness and the obtained dark material was dissolved in DCM, and washed with 0.1 N HCl and water. The organic layer was dried over anhydrous  $Na_2SO_4$  and concentrated. The obtained residue was purified by preparative RP-HPLC to get 21 mg of the desired product in 44% yield.  $^1H$  NMR ( $CD_3OD-d_4$ , 400 MHz):  $\delta$  8.17 (d, 1H,  $J = 13.6$  Hz), 8.02 (d, 1H,  $J = 16.2$  Hz), 7.73 (s, 1H), 7.42 (d, 1H,  $J = 6.8$  Hz), 7.40 (d, 1H,  $J = 10.2$  Hz), 7.30 (d, 1H,  $J = 7.8$  Hz), 7.24 (m, 3H), 6.81 (m, 3H), 6.56 (d, 1H,  $J = 10.6$  Hz), 6.34 (q, 1H), 6.06 (s, 2H), 3.90 (s, 3H), 3.76 (s, 3H).  $^{13}C$  NMR ( $CD_3OD-d_4$ , 100 MHz):  $\delta$  177.2, 163.1, 159.3, 153.8, 152.5, 149.9, 149.7, 149.4, 148.3, 141.6, 140.3, 132.6, 128.6, 128.5, 126.1, 125.7, 117.6, 117.1, 116.3, 112.6, 112.3, 108.9, 108.3, 102.4, 56.5 (x 2), 55.9. MS (ESI+):  $m/z$  489.03 (M+H).

**(E)-6-(4-Hydroxy-3-methoxyphenethyl)-4-(4-hydroxystyryl)-1-((tetrahydrofuran-2-yl)methyl)pyrimidine-2(1H)-thione (15)**

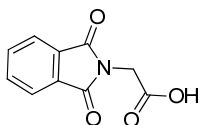


To a solution of **8** (35 mg, 0.068 mmol) in 2 mL DMF was added  $K_2CO_3$  (100 mg, 0.72 mmol). The suspension was stirred for 24 h at room temperature. The reaction mixture was then evaporated to dryness and the obtained dark material was dissolved in DCM, and washed with 0.1 N HCl and water. The organic layer was dried over anhydrous

Na<sub>2</sub>SO<sub>4</sub> and concentrated. The obtained residue was purified by preparative RP-HPLC to get 24 mg of the desired product in 71% yield. <sup>1</sup>H NMR (CD<sub>3</sub>OD-d<sub>4</sub>, 400 MHz): δ 8.05 (d, 1H, *J* = 16.4 Hz), 7.79 (d, 1H, *J* = 12.6 Hz), 7.56 (s, 1H), 7.39 (d, 1H, *J* = 13.2 Hz), 7.21-7.07 (m, 3H), 6.81-6.69 (m, 4H), 4.45 (m, 2H), 3.87 (s, 3H), 3.78 (s, 3H), 3.68 (m, 2H), 2.11 (m, 1H), 2.00-1.74 (m, 2H), 1.68 (m, 2H). <sup>13</sup>C NMR (CD<sub>3</sub>OD-d<sub>4</sub>, 100 MHz): δ 177.9, 162.5, 158.6, 152.9, 152.4, 149.7, 149.1, 147.9, 128.6, 128.2, 126.0, 125.8, 117.4, 117.1, 116.9, 116.8, 115.8, 112.5, 112.1, 103.8, 77.8, 69.7, 57.5, 56.5 (x 2), 30.4, 26.6. MS (ESI<sup>+</sup>): *m/z* 493.0 (M+H).

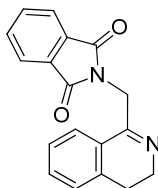
## II. Direct Small Molecule Inhibitors of Keap1-Nrf2 Protein-Protein Interaction

### *N*-Phthaloyl glycine (**18**).



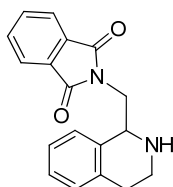
Glycine (**17**, 3.09 g; 40 mmol) and phthalic anhydride (**16**, 8.88 g; 60 mmol) were taken together and fused at 180-185 °C with stirring for 30 min and cooled to room temperature. The obtained white solid was washed with 50% aq. ethanol and dried to get 7.9 g of product, yield 96%. <sup>1</sup>H NMR (DMSO-*d*<sub>6</sub>, 400 MHz): δ 13.24 (s, 1H), 7.91 (m, 4H), 4.33 (s, 2H). <sup>13</sup>C NMR (DMSO-*d*<sub>6</sub>, 100 MHz) δ 169.6, 169.0, 158.3, 133.6, 132.1, 128.8, 41.9. MS (ESI<sup>+</sup>): *m/z* 206.2 (M+H).

### 3,4-Dihydro-1-phthalimidomethylisoquinoline (**20**).



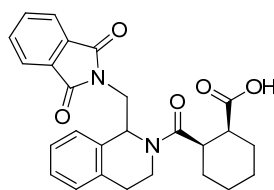
To a suspension of *N*-phthaloyl glycine (**18**, 2.4 g, 19.5 mmol) and phenethylamine (**19**, 2.65 mL, 21.5 mmol) in acetonitrile (100 mL) was added POCl<sub>3</sub> (7.25 mL, 78 mmol). The resulting solution was heated at 85 °C for 24 h, then cooled to room temperature and concentrated under reduced pressure. The obtained dark residue was diluted with DCM (100 mL) and washed with aq. NaHCO<sub>3</sub> (100 mL) and water (100 mL), then followed by brine (100 mL). The organic layer was concentrated and the crude was precipitated with ethyl acetate, washed with ethyl acetate and dried to get 5.2 g of light yellow solid, yield 73%. <sup>1</sup>H NMR (DMSO-*d*<sub>6</sub>, 400 MHz): δ 7.90 (m, 4H), 7.78 (d, 1H, 8.8), 7.48 (td, 1H, *J* = 12.6, 6.8 Hz), 7.41 (d, 1H, *J* = 7.8 Hz), 7.32 (d, 1H, *J* = 10.2 Hz), 4.90 (t, 2H, *J* = 5.6 Hz), 3.47 (t, 2H, *J* = 6.8 Hz), 2.62 (t, 2H, *J* = 4.8 Hz). <sup>13</sup>C NMR (DMSO-*d*<sub>6</sub>, 100 MHz) δ 174.2, 158.3, 133.9, 132.3, 129.8, 128.5, 128.3, 123.3, 123.1, 116.5, 109.2, 47.6, 41.5, 25.8. MS (*ESI*<sup>+</sup>): *m/z* 291.1 (M+H).

**(±)-1-Phthalimidomethyl-1,2,3,4-tetrahydroisoquinoline (21).**



To a solution of 3,4-dihydro-1-phthalimidomethyl-isoquinoline (**20**, 580 mg, 2 mmol) in DCM (10 mL) was added acetic acid (120  $\mu$ L) and  $\text{NaBH}(\text{OAc})_3$  (636 mg, 3 mmol). The obtained suspension was stirred at room temperature for 1 h and reaction mixture was diluted with DCM (50 mL) and washed with water (2 x 25 mL) and brine (25 mL). The organic layer was concentrated and the crude was purified via column chromatography (ISCO) using acetonitrile (0 to 100%) in DCM as eluent and fractions were concentrated to give 420 mg of light colored solid, yield 72%.  $^1\text{H}$  NMR ( $\text{CDCl}_3$ , 400 MHz):  $\delta$  7.81 (m, 4H), 7.22 (m, 4H), 4.36 (d, 1H,  $J = 6.6$  Hz), 4.08 (d, 1H,  $J = 8.2$  Hz), 3.89 (dd, 1H,  $J = 4.4, 12.2$  Hz), 3.27 (m, 1H), 2.96 (m, 1H), 2.77 (m, 2H), 1.72 (s, 1H).  $^{13}\text{C}$  NMR ( $\text{CDCl}_3$ , 100 MHz):  $\delta$  168.3, 136.5, 134.1, 130.3, 128.6, 127.6, 126.6, 123.2, 113.8, 110.9, 53.6, 42.9, 39.8, 29.5. MS ( $\text{ESI}^+$ ):  $m/z$  293.2 (M+H).

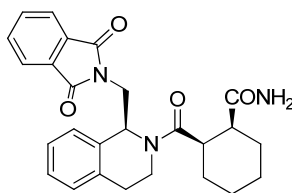
**(1S,2R)-2-((S)-1-((1,3-Dioxoisindolin-2-yl)methyl)-1,2,3,4-tetrahydroisoquinoline-2-carbonyl)cyclohexanecarboxylic acid (LH601A).**



To a solution of ( $\pm$ )-1-phthalimidomethyl-1,2,3,4-tetrahydroisoquinoline (**21**, 29 mg, 0.1 mmol) in 1 mL *p*-xylene was added *cis*-cyclohexyldicarboxylic anhydride (**22**, 17 mg, 0.11 mmol) and stirred at 50  $^\circ\text{C}$  for 24 h. The obtained precipitate was filtered and washed with diethyl ether and dried. Impure final products were purified via column chromatography (ISCO) using ethyl acetate (0 to 100%) in hexane as eluent. An equal

mixture of all four isomers of LH601 (**23**) was obtained as a white powder, yield 74%. Diastereomers were separated using flash silica gel column chromatography (ISCO) using ethyl acetate (0 to 100% with 1% acetic acid) in hexane and the enantiomeric pairs were separated by normal preparative chiral HPLC (Chiralcel OD) using hexane/10% *i*-PrOH with 0.1% trifluoroacetic acid as an isocratic eluent. <sup>1</sup>H NMR (CD<sub>3</sub>OD-*d*<sub>4</sub>, 400 MHz): δ 7.99-7.80 (m, 4H), 7.38-7.19 (m, 4H), 5.99 (dd, *J* = 4.2, 8.4 Hz, 1H), 4.29-4.21 (m, 1H), 4.13 (dd, *J* = 8.4, 12.6 Hz, 1H), 4.01-3.96 (m, 1H), 3.93 (dd, *J* = 4.6, 16.2 Hz, 1H), 3.80-3.71 (m, 1H), 3.70-3.62 (m, 1H), 3.15-2.98 (m, 1H), 2.95-2.80 (m, 1H), 2.48-2.36 (m, 1H), 2.01-1.90 (m, 2H), 1.75-1.57 (m, 2H), 1.48-1.43 (m, 1H), 1.12-0.98 (m, 1H), 0.88-0.68 (m, 1H). <sup>13</sup>C NMR (CD<sub>3</sub>OD-*d*<sub>4</sub>, 100 MHz): δ 177.8, 176.4, 169.8, 136.2, 135.4, 134.9, 133.5, 130.3, 128.5, 128.4, 127.3, 124.3, 51.8, 44.3, 42.1, 40.9, 38.5, 29.9, 28.8, 28.5, 25.6, 24.6. MS(ESI<sup>+</sup>): *m/z* 447.2 (M+H).

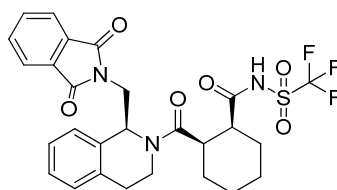
**(1*S*,2*R*)-2-((*S*)-1-((1,3-Dioxoisindolin-2-yl)methyl)-1,2,3,4-tetrahydroisoquinoline-2-carbonyl)cyclohexanecarboxamide (30).**



To a solution of LH601A (2 mg, 0.0045 mmol) in 400  $\mu$ L acetonitrile was added HBTU (2 mg, 0.0054 mmol) and stirred for 30 min at room temperature. Then anhydrous ammonium was bubble into the reaction mixture for 1 min. The reaction mixture was concentrated and the residue was purified by column chromatography using acetonitrile (0 to 20%) in DCM as eluent to give 1.6 mg designed product, yield 80.2%. <sup>1</sup>H NMR

(CD<sub>3</sub>OD-*d*<sub>4</sub>, 400 MHz):  $\delta$  7.89-7.81 (m, 4H), 7.51-7.22 (m, 4H), 5.99 (dd, *J* = 4.2, 6.8 Hz, 1H), 4.12 (dd, *J* = 8.2, 12.2 Hz, 1H), 4.12-3.98 (m, 1H), 3.86 (dd, *J* = 4.4, 16.2 Hz, 1H), 3.81-3.73 (m, 2H), 3.23-3.12 (m, 1H), 2.91-2.86 (m, 1H), 2.35-2.29 (m, 1H), 2.21-1.97 (m, 1H), 1.82-1.67 (m, 2H), 1.55-1.41 (m, 2H), 1.32-0.98 (m, 2H), 1.01-0.58 (m, 1H). <sup>13</sup>C NMR (CD<sub>3</sub>OD-*d*<sub>4</sub>, 100 MHz):  $\delta$  177.6, 176.2, 169.3, 136.2, 135.2, 134.8, 133.2, 129.8, 128.6, 128.1, 126.9, 124.9, 52.3, 44.9, 41.8, 40.3, 38.9, 29.8, 28.6, 28.1, 25.9. MS(ESI<sup>+</sup>): *m/z* 446.2 (M+H).

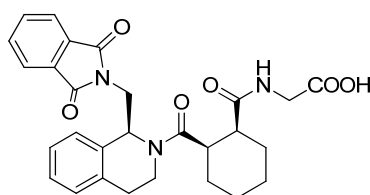
**2-((1*S*,2*R*)-2-((*S*)-1-((1,3-Dioxoisindolin-2-yl)methyl)-1,2,3,4-tetrahydroisoquinoline-2-carbonyl)cyclohexanecarboxamido)acetic acid (31).**



To a solution of LH601A (10 mg, 0.02 mmol) in 3 mL acetonitrile was added trifluoromethanesulfonamide (0.6 mg, 0.04 mmol), HBTU (11.4 mg, 0.03 mmol) and DIPEA (34.7  $\mu$ L, 0.2 mmol) and the resulted suspension was stirred for 24 h at room temperature. The reaction mixture was concentrated and the residue was purified by column chromatography (ISCO) using acetonitrile (0 to 100%) in DCM as eluent to afford 4.8 mg designed product as a white powder, yield 37.2%. <sup>1</sup>H NMR (CD<sub>3</sub>OD-*d*<sub>4</sub>, 400 MHz):  $\delta$  7.86-7.79 (m, 4H), 7.18 (d, *J* = 8.8 Hz, 1H), 6.96 (s, 1H), 6.83 (d, *J* = 4.6 Hz, 1H), 5.96 (dd, *J* = 4.2, 8.8 Hz, 1H), 4.16 (dd, *J* = 7.6, 11.8 Hz, 1H), 4.02-3.95 (m, 1H), 3.91 (dd, *J* = 3.6, 14.8 Hz, 1H), 3.79 (s, 3H), 3.76-3.71 (m, 2H), 3.22-3.03 (m, 1H), 2.89-2.80 (m, 1H), 2.42-2.31 (m, 1H), 2.21-1.90 (m, 2H), 1.75-1.60 (m, 2H), 1.56-1.45 (m,

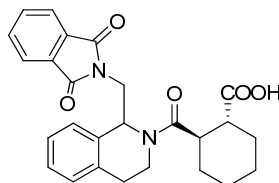
2H), 1.32-0.68 (m, 2H).  $^{13}\text{C}$  NMR ( $\text{CD}_3\text{OD}-d_4$ , 100 MHz):  $\delta$  177.8, 176.5, 168.9, 166.6, 158.9, 137.2, 134.6, 134.2, 133.8, 131.2, 129.9, 127.5, 127.1, 125.3, 51.6, 45.3, 42.8, 41.3, 36.8, 30.2, 28.9, 28.3, 26.5, 25.2. MS(ESI+):  $m/z$  578.1 (M+H).

**2-((1S,2R)-2-((S)-1-((1,3-Dioxoisindolin-2-yl)methyl)-1,2,3,4-tetrahydroisoquinoline-2-carbonyl)cyclohexanecarboxamido)acetic acid (32).**



To a solution of LH601A (10 mg, 0.02 mmol) in 600  $\mu\text{L}$  DMSO was added glycine (1.8 mg, 0.02 mmol), HBTU (8.7 mg, 0.02 mmol) and DIPEA (10.4  $\mu\text{L}$ , 0.06 mmol) and the resulted suspension was stirred for 30 min at room temperature. The reaction mixture was concentrated and the residue was purified by column chromatography (ISCO) using acetonitrile (0 to 100%) in DCM as eluent to afford 5.2 mg desired product as a white powder while 4.6 mg starting material was recovered, yield 88%.  $^1\text{H}$  NMR ( $\text{CD}_3\text{OD}-d_4$ , 400 MHz):  $\delta$  7.89-7.81 (m, 4H), 7.12 (d,  $J$  = 8.4 Hz, 1H), 6.93 (s, 1H), 6.83 (d,  $J$  = 4.6 Hz, 1H), 5.98 (dd,  $J$  = 4.4, 7.6 Hz, 1H), 4.12 (dd,  $J$  = 8.0, 12.4 Hz, 1H), 4.02-3.97 (m, 1H), 3.94 (dd,  $J$  = 4.6, 16.2 Hz, 1H), 3.83 (s, 3H), 3.80-3.73 (m, 2H), 3.10-2.98 (m, 1H), 2.85-2.80 (m, 1H), 2.40-2.36 (m, 1H), 2.01-1.97 (m, 2H), 1.75-1.67 (m, 2H), 1.48-1.43 (m, 2H), 1.12-0.42 (m, 2H).  $^{13}\text{C}$  NMR ( $\text{CD}_3\text{OD}-d_4$ , 100 MHz):  $\delta$  177.3, 176.5, 169.8, 166.3, 136.8, 135.4, 134.2, 134.1, 131.2, 129.5, 127.4, 127.1, 124.2, 51.9, 50.3, 44.6, 42.8, 40.9, 38.6, 29.5, 28.8, 28.3, 25.9. MS(ESI+):  $m/z$  504.1 (M+H).

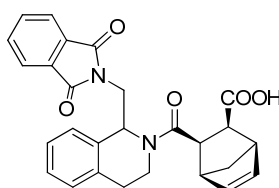
**(±)-*trans*-2-(1-((1,3-Dioxoisindolin-2-yl)methyl)-1,2,3,4-tetrahydroisoquinoline-2-carbonyl)cyclohexanecarboxylic acid (33).**



To a solution of (±)-1-phthalimidomethyl-1,2,3,4-tetrahydroisoquinoline (**21**, 10 mg, 0.03 mmol) in 1 mL *p*-xylene was added *trans*-cyclohexyldicarboxylic anhydride (6.3 mg, 0.04 mmol) and stirred at 50 °C for 24 h. The reaction mixture was concentrated and the resulted residue was purified via column chromatography (ISCO) using ethyl acetate (0 to 100%) in hexane as eluent to afford 11.8 mg product as a white powder, yield 78.6%.

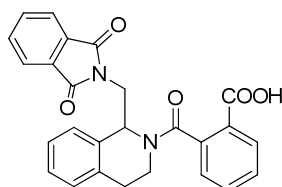
<sup>1</sup>H NMR (CD<sub>3</sub>OD-*d*<sub>4</sub>, 400MHz): δ 12.9 (s, 1H), 7.69 (m, 4H), 7.31 (m, 1H), 7.12 (m, 3H), 5.96 (d, 1H, *J* = 5.2 Hz), 4.02 (m, 2H), 3.86 (dd, 1H, *J* = 4.4, 11.8 Hz), 3.74 (m, 2H), 2.63 (m, 3H), 1.51 (m, 2H), 1.30 (m, 6H). <sup>13</sup>C NMR (CD<sub>3</sub>OD-*d*<sub>4</sub>, 100 MHz): δ 178.1, 176.8, 169.3, 136.3, 135.4, 134.9, 133.8, 131.1, 128.4, 128.2, 127.8, 124.3, 51.9, 44.6, 42.2, 40.5, 38.2, 30.3, 28.5, 27.6, 25.2, 24.9. MS(*ESI*<sup>+</sup>): *m/z* 447.2 (M+H).

**(±)-(1*R*,2*S*,3*R*,4*S*)-3-(1-((1,3-Dioxoisindolin-2-yl)methyl)-1,2,3,4-tetrahydroisoquinoline-2-carbonyl)bicyclo[2.2.1]hept-5-ene-2-carboxylic acid (34).**



To a solution of ( $\pm$ )-1-phthalimidomethyl-1,2,3,4-tetrahydroisoquinoline (**21**, 10 mg, 0.03 mmol) in 1 mL p-xylene was added anhydride (6.7 mg, 0.04 mmol) and stirred at 50 °C for 24 h. The reaction mixture was concentrated and the resulted residue was purified via column chromatography (ISCO) using ethyl acetate (0 to 100%) in hexane as eluent to afford 11.7 mg white powder, yield 75%.  $^1\text{H}$  NMR ( $\text{CDCl}_3$ , 400MHz):  $\delta$  12.9 (s, 1H), 7.75 (m, 4H), 7.32 (d, 1H,  $J = 8.8$  Hz), 7.19 (m, 3H), 5.96 (d, 1H,  $J = 12.2$  Hz), 4.03 (t, 1H), 3.82 (dd, 1H,  $J = 4.2, 16.2$  Hz), 3.76 (m, 1H), 2.90-2.82 (m, 3H), 2.48 (m, 1H), 2.18-2.09 (m, 2H), 1.32-1.23 (m, 5H).  $^{13}\text{C}$  NMR ( $\text{CD}_3\text{OD}-d_4$ , 100 MHz):  $\delta$  177.5, 176.8, 169.9, 136.3, 135.5, 134.9, 133.6, 132.3, 131.3, 129.8, 128.5, 128.1, 127.3, 125.2, 51.9, 44.1, 43.2, 41.2, 39.9, 28.8, 28.3, 26.8, 25.6. MS(ESI+):  $m/z$  457.1 (M+H).

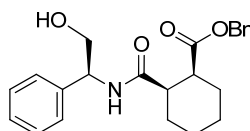
**( $\pm$ )-2-(1-((1,3-Dioxoisindolin-2-yl)methyl)-1,2,3,4-tetrahydroisoquinoline-2-carbonyl) benzoic acid (**35**).**



To a solution of ( $\pm$ )-1-phthalimidomethyl-1,2,3,4-tetrahydroisoquinoline (**21**, 20 mg, 0.07 mmol) in 1 mL p-xylene was added phthalic anhydride anhydride (15 mg, 0.1 mmol) and stirred at 50 °C for 24 h. The reaction mixture was concentrated and the resulted residue was purified via column chromatography (ISCO) using ethyl acetate (0 to 100%) in hexane as eluent to afford 12.4 mg white powder, yield 72%.  $^1\text{H}$  NMR ( $\text{CD}_3\text{OD}-d_4$ , 400MHz):  $\delta$  12.9 (s, 1H), 7.9 (d, 1H,  $J = 12.6$  Hz), 7.83 (m, 3H), 7.70 (m, 2H), 7.49 (d, 1H,  $J = 16.6$  Hz), 7.39 (d, 1H,  $J = 11.2$  Hz), 7.10 (m, 4H), 6.0 (dd, 1H,  $J = 4.2, 10.6$  Hz),

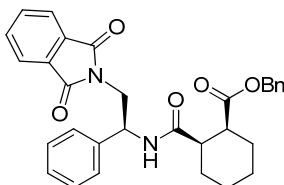
4.1 (d, 1H,  $J = 8.8$  Hz), 3.91 (d, 1H,  $J = 10.2$  Hz), 3.59 (m, 1H), 3.31 (m, 1H), 2.83 (m, 1H), 2.68 (m, 2H).  $^{13}\text{C}$  NMR ( $\text{CD}_3\text{OD}-d_4$ , 100 MHz):  $\delta$  178.3, 176.8, 168.9, 137.3, 136.1, 135.4, 134.9, 133.9, 133.5, 131.1, 130.6, 128.5, 128.3, 127.6, 127.1, 124.3, 122.3, 121.9, 52.1, 42.3, 40.4, 38.3. MS(*ESI*<sup>+</sup>):  $m/z$  441.3 (M+H).

**(1*S*,2*R*)-Benzyl 2-(((*S*)-2-hydroxy-1-phenylethyl)carbamoyl)cyclohexanecarboxylate (67).**



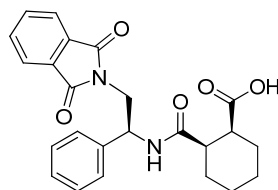
To a solution of (1*R*,2*S*)-2-((benzyloxy)carbonyl)cyclohexanecarboxylic acid (**66**, 382 mg, 1.46 mmol) and (*S*)-2-phenylglycinol (**65**, 200 mg, 1.46 mmol) in 10 mL DCM was added EDC (308 mg, 1.6 mmol) and DIPEA (761  $\mu\text{L}$ , 4.38 mmol). The reaction mixture was stirred at room temperature for 2 h. The reaction mixture was then diluted with DCM (100 mL) and washed with 0.5 N HCl solution, aq.  $\text{NaHCO}_3$  (100 mL) and water (100 mL), then followed by brine (100 mL). The organic layer was concentrated and the crude was purified via column chromatography (ISCO) using acetonitrile (0 to 30%) in DCM as eluent and fractions were concentrated to give 152 mg solid, yield 54.6%.  $^1\text{H}$  NMR ( $\text{CDCl}_3$ , 400MHz):  $\delta$  7.52-7.33 (m, 10H), 6.45(dd, 1H,  $J = 6.6, 13.2$  Hz), 5.21-5.00 (m, 2H), 4.01-3.73 (m, 2H), 3.21 (m, 1H), 2.98 (m, 2H), 2.70-2.61 (m, 1H), 2.32-2.20 (m, 2H), 1.73-1.52 (m, 2H), 1.19-1.33 (m, 2H).  $^{13}\text{C}$  NMR ( $\text{CDCl}_3$ , 100MHz):  $\delta$  174.3, 174.1, 139.3, 136.1, 128.8, 128.7, 128.5, 128.1, 128.0, 127.7, 127.6, 126.7, 66.3, 55.6, 43.3, 42.8, 27.3, 26.9, 24.2, 23.3, 23.2. MS(*ESI*<sup>+</sup>):  $m/z$  382.1 (M+H).

**(1*S*,2*R*)-Benzyl-2-(((*S*)-2-(1,3-dioxoisindolin-2-yl)-1-phenylethyl)carbamoyl)cyclohexanecarboxylate (68).**



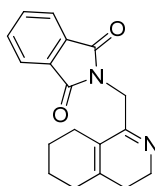
To a solution of **67** (40 mg, 0.13 mmol), phthalimide (21 mg, 0.14 mmol) and Ph<sub>3</sub>P (36.7 mg, 0.14 mmol) in THF (6 mL) was added DEAD (65  $\mu$ L, 0.14 mmol). The reaction mixture was stirred at room temperature for 3 h. The reaction mixture was then concentrated under reduced pressure and the resulted residue was purified via column chromatography (ISCO) using DCM (0 to 100%) in hexane as eluent and fractions were concentrated to give 36 mg solid, yield 69.2%. <sup>1</sup>H NMR (CDCl<sub>3</sub>, 400MHz):  $\delta$  7.72 (m, 2H), 7.61 (m, 2H), 7.36-7.01 (m, 10H), 5.36 (dd, 1H,  $J = 3.8, 13.6$  Hz), 4.21-4.12 (m, 2H), 4.12-4.10 (m, 2H), 2.82-2.68 (m, 1H), 2.52-2.41(m, 1H), 2.18-1.82 (m, 2H), 1.70-1.53 (m, 2H), 1.38-1.12 (m, 4H). <sup>13</sup>C NMR (CDCl<sub>3</sub>, 100MHz):  $\delta$  174.2, 172.6, 169.8, 139.3, 136.6, 133.2, 128.9, 128.6, 128.5, 127.7, 127.6, 125.8, 66.8, 55.3, 42.6, 36.6, 28.1, 26.5, 24.8, 23.6, 22.8. MS(ESI<sup>+</sup>):  $m/z$  511.1 (M+H).

**(1*S*,2*R*)-2-(((*S*)-2-(1,3-Dioxoisindolin-2-yl)-1-phenylethyl)carbamoyl)cyclohexanecarboxylic acid (36).**



To a solution of **68** (16 mg, 0.03 mmol) in methanol (3 mL) was added a catalytic amount (2 mg) of 5% Pd/C. The reaction mixture was stirred at room temperature for 2 h under H<sub>2</sub>. The Pd/C was filtered off and the filtration was concentrated over vacuum. The resulted residue was purified via column chromatography (ISCO) using acetonitrile (0 to 100%) in DCM as eluent and fractions were concentrated to give 11.2 mg solid, yield 86%. <sup>1</sup>H NMR (CDCl<sub>3</sub>, 400MHz): δ 8.00-7.71 (m, 4H), 7.52-7.20 (m, 5H), 5.46 (dd, 1H, *J* = 5.6, 13.6 Hz), 4.21-3.80 (m, 2H), 2.82-2.68 (m, 1H), 2.62-2.51(m, 1H), 2.18-1.82 (m, 2H), 1.76-1.12 (m, 6H). <sup>13</sup>C NMR (CDCl<sub>3</sub>, 100MHz): δ 174.6, 171.3, 169.3, 136.2, 133.3, 128.9, 128.1, 128.0, 127.6, 126.8, 125.8, 55.5, 42.3, 36.9, 28.3, 26.6, 25.2, 23.6, 23.1. MS(*ESI*<sup>+</sup>): *m/z* 421.2 (M+H).

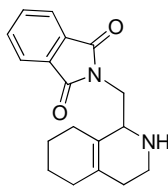
### 3,4-Dihydro-1-phthalimidomethylisoquinoline (**70**).



To a suspension of *N*-phthaloyl glycine (**18**, 300 mg, 1.46 mmol) and 2-(cyclohex-1-en-1-yl)ethanamine (**69**, 244 uL, 1.76 mmol) in *p*-xylene (20 mL) was added POCl<sub>3</sub> (1.33 mL, 14.6 mmol). The resulting solution was heated at 85 °C for 24 h, then cooled to room temperature and concentrated under reduced pressure. The obtained dark residue was

diluted with DCM (100 mL) and washed with aq. NaHCO<sub>3</sub> (100 mL) and water (100 mL), then followed by brine (100 mL). The organic layer was concentrated and the crude was precipitated with ethyl acetate, washed with ethyl acetate and dried to get 263 mg of light yellow solid, yield 61%. <sup>1</sup>H NMR (DMSO-*d*<sub>6</sub>, 400 MHz): δ 7.90 (m, 4H), 7.78 (d, 1H, *J* = 13.6 Hz), 7.48 (d, 1H, *J* = 10.8 Hz), 7.41 (dd, 1H, *J* = 8.6, 12.8 Hz), 7.32 (d, 1H, *J* = 11.4 Hz), 4.90 (t, 2H, *J* = 8.2 Hz), 3.47 (t, 2H, *J* = 6.6 Hz), 2.62 (t, 2H, *J* = 5.2 Hz). <sup>13</sup>C NMR (DMSO-*d*<sub>6</sub>, 100 MHz) δ 174.2, 158.3, 133.9, 132.3, 129.8, 128.5, 128.3, 123.3, 123.1, 116.5, 109.2, 47.6, 41.5, 25.8. MS (ESI<sup>+</sup>): *m/z* 295.3 (M+H).

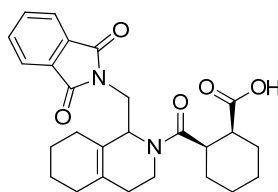
**(±)-1-Phthalimidomethyl-1,2,3,4-tetrahydroisoquinoline (71).**



To a solution of 3,4-dihydro-1-phthalimidomethyl-isoquinoline (**70**, 50 mg, 0.17 mmol) in DCM (3 mL) was added acetic acid (24 μL) and NaBH(OAc)<sub>3</sub> (108 mg, 0.51 mmol). The obtained suspension was stirred at room temperature for 1 h and reaction mixture was diluted with DCM (50 mL) and washed with water (2 x 25 mL) and brine (25 mL). The organic layer was concentrated and the crude was purified via column chromatography (ISCO) using acetonitrile (0 to 40%) in DCM as eluent and fractions were concentrated to give 32 mg desired product, yield 64%. <sup>1</sup>H NMR (CDCl<sub>3</sub>, 400 MHz): δ 7.81 (m, 4H), 7.22 (m, 4H), 4.36 (d, 1H, *J* = 10.2 Hz), 4.08 (d, 1H, *J* = 4.6 Hz), 3.89 (dd, 1H, *J* = 3.8, 9.8 Hz), 3.27 (m, 1H), 2.96 (m, 1H), 2.77 (m, 2H), 1.72 (s, 1H). <sup>13</sup>C

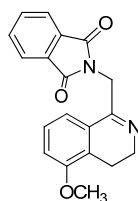
NMR (CDCl<sub>3</sub>, 100 MHz):  $\delta$  168.3, 136.5, 134.1, 130.3, 128.6, 127.6, 126.6, 123.2, 113.8, 110.9, 53.6, 42.9, 39.8, 29.5. MS (ESI<sup>+</sup>):  $m/z$  297.1 (M+H).

***Cis*-2-(( $\pm$ )-1-((1,3-dioxisoindolin-2-yl)methyl)-1,2,3,4-tetrahydroisoquinoline-2-carbonyl)cyclohexanecarboxylic acid (**37**).**



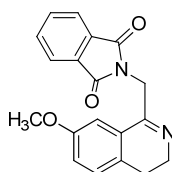
To a solution of **71** (32 mg, 0.11 mmol) in 8 mL *p*-xylene was added *cis*-cyclohexyldicarboxylic anhydride (**22**, 25 mg, 0.16 mmol) and stirred at 50 °C for 24 h. The reaction mixture was concentrated and the residue was purified by column chromatography (ISCO) using ethyl acetate (0 to 100% with 1% acetic acid) in hexane as eluent to afford 21 mg desired product as a white powder, yield 43.8%.. <sup>1</sup>H NMR (CD<sub>3</sub>OD-*d*<sub>4</sub>, 400 MHz):  $\delta$  7.99-7.80 (m, 4H), 7.38-7.19 (m, 4H), 5.99 (dd,  $J$  = 4.8, 7.6 Hz, 1H), 4.29-4.21 (m, 1H), 4.13 (dd,  $J$  = 6.6, 12.6 Hz, 1H), 4.01-3.96 (m, 1H), 3.93 (dd,  $J$  = 4.0, 16.2 Hz, 1H), 3.80-3.71 (m, 1H), 3.70-3.62 (m, 1H), 3.15-2.98 (m, 1H), 2.95-2.80 (m, 1H), 2.48-2.36 (m, 1H), 2.01-1.90 (m, 2H), 1.75-1.57 (m, 2H), 1.48-1.43 (m, 1H), 1.12-0.98 (m, 1H), 0.88-0.68 (m, 1H). <sup>13</sup>C NMR (CD<sub>3</sub>OD-*d*<sub>4</sub>, 100 MHz):  $\delta$  177.8, 176.4, 169.8, 136.2, 135.4, 134.9, 133.5, 130.3, 128.5, 128.4, 127.3, 124.3, 51.8, 44.3, 42.1, 40.9, 38.5, 29.9, 28.8, 28.5, 25.6. MS(ESI<sup>+</sup>):  $m/z$  451.2 (M+H).

**2-((5-Methoxy-3,4-dihydroisoquinolin-1-yl)methyl)isoindoline-1,3-dione (**72**).**



To a solution of *N*-phthaloylglycine (**18**, 200 mg, 0.97 mmol) in 20 mL acetonitrile was added 2-methoxyphenylethylamine (219  $\mu$ L, 1.46 mmol) and POCl<sub>3</sub> (886  $\mu$ L, 9.7 mmol). The resulting solution was heated at 85 °C for 24 h, then cooled to room temperature and concentrated under reduced pressure. The obtained dark residue was diluted with 100 mL DCM and washed with sat NaHCO<sub>3</sub> solution, water and brine, then dried over anhydrous Na<sub>2</sub>SO<sub>4</sub>. Filtered and the filtration was concentrated and the residue was purified by column chromatography using acetonitrile (0 to 100%) in DCM as eluent to afford 112 mg product, yield 59.2%. <sup>1</sup>H NMR (CDCl<sub>3</sub>, 400 MHz)  $\delta$  7.98 (m, 2H), 7.76 (m, 2H), 7.21 (dd, 1H, *J* = 5.6, 12.2 Hz), 7.15 (d, 1H, *J* = 14.6 Hz), 6.99 (d, 1H, *J* = 12.8 Hz), 4.95 (s, 2H), 3.88 (s, 3H), 3.65 (t, 2H, *J* = 6.8 Hz), 2.72 (t, 2H, *J* = 9.2 Hz). <sup>13</sup>C NMR (CDCl<sub>3</sub>, 100 MHz)  $\delta$  168.3, 156.0, 134.5, 132.6, 128.2, 127.1, 126.2, 123.9, 123.2, 116.3, 110.6, 55.6, 46.4, 40.8, 21.0. MS (*ESI*<sup>+</sup>): *m/z* 321.3 (M+H)

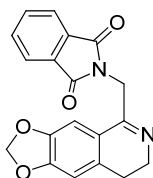
**2-((7-Methoxy-3,4-dihydroisoquinolin-1-yl)methyl)isoindoline-1,3-dione (73).**



To a solution of *N*-phthaloylglycine (**18**, 1.0 g, 4.9 mmol) in 100 mL acetonitrile was added 4-methoxyphenylethylamine (786  $\mu$ L, 5.4 mmol) and POCl<sub>3</sub> (4.5 mL, 49 mmol).

The resulting solution was heated at 85 °C for 24 h, then cooled to room temperature and concentrated under reduced pressure. The obtained dark residue was diluted with 100 mL DCM and washed with sat NaHCO<sub>3</sub> solution, water and brine, then dried over anhydrous Na<sub>2</sub>SO<sub>4</sub>. Filtered and the filtration was concentrated and the residue was purified by column chromatography using acetonitrile (0 to 100%) in DCM as eluent to afford 560 mg product, yield 56.2%. <sup>1</sup>H NMR (CDCl<sub>3</sub>, 400 MHz): δ 7.96 (m, 2H), 7.79 (m, 2H), 7.23 (d, 1H, *J* = 10.6 Hz), 7.15 (s, 1H), 6.96 (d, 1H, *J* = 12.2 Hz), 4.93 (s, 2H), 3.88 (s, 3H), 3.63 (t, 2H, *J* = 7.6 Hz), 2.62 (t, 2H, *J* = 10.2 Hz). <sup>13</sup>C NMR (CDCl<sub>3</sub>, 100 MHz) δ 169.3, 158.6, 133.8, 132.5, 129.8, 128.5, 128.2, 123.6, 123.1, 116.3, 109.8, 55.6, 47.3, 41.3, 25.1. MS (*ESI*<sup>+</sup>): *m/z* 321.3 (M+H)

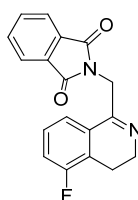
**2-((6,7-Dimethoxy-3,4-dihydroisoquinolin-1-yl)methyl)isoindoline-1,3-dione (74).**



To a suspension of *N*-phthaloylglycine (**18**, 500 mg, 2.44 mmol) and 3,4-dimethoxyphenylethylamine (662 uL, 3.66 mmol) in 30 mL acetonitrile was added POCl<sub>3</sub> (900 uL, 9.8 mmol). The suspension was stirred for 6 h under reflux. Acetonitrile and phosphoryl chloride was removed by vacuum. The reaction mixture was then diluted with 30 mL DCM and washed with sat NaHCO<sub>3</sub> solution, water and brine, then dried over anhydrous Na<sub>2</sub>SO<sub>4</sub>. The filtration was concentrated and the residue was purified by column chromatography using acetonitrile (0 to 100%) in DCM as eluent to afford 213 mg, yield 38.8%. <sup>1</sup>H NMR (CDCl<sub>3</sub>, 400 MHz): δ 7.71 (m, 2H), 7.62 (m, 2H), 7.08 (s, 1H), 6.89 (s,

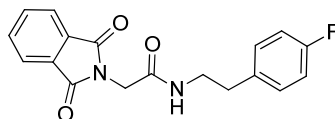
1H), 4.76 (s, 2H), 3.82 (s, 3H), 3.78 (s, 3H), 3.35 (t, 2H,  $J = 5.6$  Hz), 2.51 (t, 2H,  $J = 6.2$  Hz).  $^{13}\text{C}$  NMR ( $\text{CDCl}_3$ , 100 MHz)  $\delta$  169.8, 158.8, 134.2, 133.6, 132.3, 129.8, 128.8, 128.2, 123.5, 123.2, 116.3, 108.6, 55.8, 55.3, 47.6, 41.5, 25.8. MS (*ESI+*):  $m/z$  351.3 (M+H)

**2-((5-Fluoro-3,4-dihydroisoquinolin-1-yl)methyl)isoindoline-1,3-dione (75).**



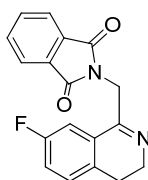
To a suspension of *N*-phthaloylglycine (**18**, 200 mg, 0.98 mmol) and 2-fluorophenylethylamine (146  $\mu\text{L}$ , 0.98 mmol) in 10 mL acetonitrile was added  $\text{POCl}_3$  (900  $\mu\text{L}$ , 9.8 mmol). The suspension was stirred for 6 h under reflux. Acetonitrile and phosphoryl chloride was removed by vacuum. The reaction mixture was then diluted with 30 mL DCM and washed with sat  $\text{NaHCO}_3$  solution, water and brine, then dried over anhydrous  $\text{Na}_2\text{SO}_4$ . The filtration was concentrated and the residue was purified by column chromatography using acetonitrile (0 to 100%) in DCM as eluent to afford 133mg imine compound, yield 66.5%.  $^1\text{H}$  NMR ( $\text{CDCl}_3$ , 400 MHz):  $\delta$  7.92 (d, 2H,  $J = 13.4$  Hz), 7.81 (d, 2H,  $J = 12.2$  Hz), 7.36 (m, 1H), 7.26 (m, 1H), 7.18 (d, 1H,  $J = 9.8$  Hz), 4.92 (s, 2H), 3.79 (t, 2H,  $J = 4.4$  Hz), 2.76 (t, 2H,  $J = 6.8$  Hz).  $^{13}\text{C}$  NMR ( $\text{CDCl}_3$ , 100 MHz)  $\delta$  168.5, 163.2, 160.9, 158.1, 134.3, 133.7, 132.1, 128.6, 123.4, 117.8, 110.6, 47.8, 41.8, 25.6. MS (*ESI+*)  $m/z$  309.3 (M+H)

**2-(1,3-Dioxoisindolin-2-yl)-N-(4-fluorophenethyl)acetamide (79).**



To a solution of *N*-phthaloylglycine (**18**, 300 mg, 1.46 mmol) in 15 mL acetonitrile was added 4-fluoro-phenylethylamine (191  $\mu$ L, 1.46 mmol), EDC (280 mg, 1.46 mmol) and DIPEA (508  $\mu$ L, 2.92 mmol). The reaction mixture was stirred for 6 h at room temperature. Acetonitrile was removed by vacuum. The reaction mixture was then diluted with 50 mL DCM and washed with 0.5 N HCl solution, sat  $\text{NaHCO}_3$  solution, water and brine, then dried over anhydrous  $\text{Na}_2\text{SO}_4$ . The filtration was concentrated and the residue was purified by column chromatography using acetonitrile (0 to 100%) in DCM as eluent to afford 412 mg product, yield 86.4%.  $^1\text{H}$  NMR ( $\text{CDCl}_3$ , 400 MHz):  $\delta$  7.92 (d, 2H,  $J = 11.8$  Hz), 7.81 (d, 2H,  $J = 8.6$  Hz), 7.36 (m, 2H), 7.26 (m, 2H), 7.18 (d, 1H,  $J = 11.2$  Hz), 4.92 (s, 2H), 3.49 (t, 2H,  $J = 3.8$  Hz), 2.76 (t, 2H,  $J = 7.6$  Hz).  $^{13}\text{C}$  NMR ( $\text{CDCl}_3$ , 100 MHz)  $\delta$  169.2, 164.8, 161.8, 136.6, 136.3, 135.8, 133.5, 131.2, 124.3, 116.2, 42.3, 41.1, 35.6. MS (*ESI*<sup>+</sup>):  $m/z$  327.1 (M+H)

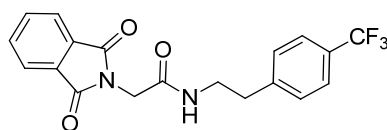
**2-((7-Fluoro-3,4-dihydroisoquinolin-1-yl)methyl)isoindoline-1,3-dione (76).**



To a solution of **79** (300 mg, 0.92 mmol) in 40 mL *p*-xylene was added  $\text{P}_2\text{O}_5$  (783 mg, 5.5 mmol). The suspension was stirred for 20 h under reflux. The reaction mixture was

cooled to room temperature and p-xylene was removed. 30 mL sat NaHCO<sub>3</sub> solution was added, then extracted with DCM (30 mL, 3x). The combined DCM extract was washed with water and brine, then dried over anhydrous Na<sub>2</sub>SO<sub>4</sub>. Filtered and the filtration was concentrated and dried over vacuum to afford the 203 mg desired product, yield 71.5%. <sup>1</sup>H NMR (CDCl<sub>3</sub>, 400 MHz): δ 7.81 (d, 2H, *J* = 14.2 Hz), 7.69 (d, 2H, *J* = 10.6 Hz), 7.23 (m, 1H), 7.16 (m, 1H), 7.10 (m, 1H), 4.82 (s, 2H), 3.57 (t, 2H, *J* = 5.6 Hz), 2.53 (t, 2H, *J* = 12.4 Hz). <sup>13</sup>C NMR (CDCl<sub>3</sub>, 100 MHz) δ 168.2, 162.8, 160.3, 157.8, 133.9, 133.2, 132.4, 129.1, 123.4, 117.7, 110.9, 47.0, 41.1, 25.1. MS (ESI<sup>+</sup>): *m/z* 309.3 (M+H)

**2-(1,3-Dioxoisindolin-2-yl)-N-(4-(trifluoromethyl)phenethyl)acetamide (80).**



To a solution of *N*-phthaloylglycine (**18**, 100 mg, 0.49 mmol) in 10 mL acetonitrile was added 4-trifluoro-phenylethylamine (76 uL, 0.49 mmol), EDC (103 mg, 0.54 mmol) and DIPEA (256 uL, 1.47 mmol). The reaction mixture was stirred for 3 h at room temperature. Acetonitrile was removed by vacuum. The reaction mixture was then diluted with 50 mL DCM and washed with 0.5 N HCl solution, sat NaHCO<sub>3</sub> solution, water and brine, then dried over anhydrous Na<sub>2</sub>SO<sub>4</sub>. The filtration was concentrated and the residue was purified by column chromatography using acetonitrile (0 to 100%) in DCM as eluent to afford 109 mg product, yield 85.8%. <sup>1</sup>H NMR (CDCl<sub>3</sub>, 400 MHz): δ 7.82 (d, 2H, *J* = 13.2 Hz), 7.76 (d, 2H, *J* = 8.8 Hz), 7.46 (d, 2H, *J* = 11.2 Hz), 7.23 (d, 2H, *J* = 14.2 Hz), 4.31 (s, 2H), 3.49 (t, 2H, *J* = 4.6 Hz), 2.86 (t, 2H, *J* = 7.6 Hz). <sup>13</sup>C NMR (CDCl<sub>3</sub>, 100

MHz)  $\delta$  167.6, 166.2, 142.6, 134.3, 131.9, 129.1, 128.8, 125.5, 125.3, 123.6, 40.9, 40.6, 35.3. MS (*ESI+*):  $m/z$  377.1 (M+H)

**2-((7-(Trifluoromethyl)-3,4-dihydroisoquinolin-1-yl)methyl)isoindoline-1,3-dione (77).**



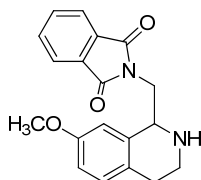
To a solution of **80** (40 mg, 0.11 mmol) in 5 mL p-xylene was added  $P_2O_5$  (76 mg, 0.53 mmol). The suspension was stirred for 20 h under reflux. The reaction mixture was cooled to room temperature and p-xylene was removed. 30 mL sat  $NaHCO_3$  solution was added, then extracted with DCM (30 mL, 3x). The combined DCM extract was washed with water and brine, then dried over anhydrous  $Na_2SO_4$ . Filtered and the filtration was concentrated and dried over vacuum to afford the 36 mg desired product, yield 89.8%.  $^1H$  NMR ( $CDCl_3$ , 400 MHz):  $\delta$  7.83 (m, 2H), 7.65 (m, 2H), 7.23 (d, 1H,  $J = 12.8$  Hz), 7.11 (s, 1H), 7.02 (d, 1H,  $J = 11.2$  Hz), 4.92 (s, 2H), 3.60 (t, 2H,  $J = 4.6$  Hz), 2.73 (t, 2H,  $J = 6.6$  Hz).  $^{13}C$  NMR ( $CDCl_3$ , 100 MHz)  $\delta$  168.1, 141.2, 134.3, 133.9, 132.4, 132.3, 130.1, 129.8, 129.0, 128.5, 123.5, 121.1, 45.9, 38.9, 25.8. MS (*ESI+*):  $m/z$  359.1 (M+H)

**(±)-2-((5-Methoxy-1,2,3,4-tetrahydroisoquinolin-1-yl)methyl)isoindoline-1,3-dione (81).**



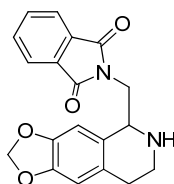
To a solution of **72** (50 mg, 0.16 mmol) in DCM (6 mL) was added acetic acid (11  $\mu$ L, 0.19 mmol) and  $\text{NaBH}(\text{OAc})_3$  (50 mg, 0.23 mmol). The obtained suspension was stirred at room temperature for 2 h and reaction mixture was diluted with DCM (30 mL), washed with water (2 x 20 mL) and brine (20 mL), then dried over anhydrous  $\text{Na}_2\text{SO}_4$ . Filtered and the organic layer was concentrated and the crude was purified by column chromatography (ISCO) using acetonitrile (0 to 100%) in DCM as eluent and fractions were concentrated to give 46 mg of white solid, yield 91.8%.  $^1\text{H}$  NMR ( $\text{CDCl}_3$ , 400 MHz):  $\delta$  7.79 (d, H,  $J = 12.2$  Hz), 7.66 (d, 2H,  $J = 10.8$  Hz), 7.21 (m, 1H), 6.82 (m, 1H), 6.68 (m, 1H), 4.36 (d, 1H,  $J = 5.6$  Hz), 3.99 (d, 1H,  $J = 8.4$  Hz), 3.72 (s, 3H), 3.47-3.38 (m, 1H), 3.32-3.18 (m, 1H), 2.96-2.80 (m, 1H), 2.77-2.50 (m, 2H).  $^{13}\text{C}$  NMR ( $\text{CDCl}_3$ , 100 MHz):  $\delta$  168.6, 157.3, 136.7, 133.9, 132.2, 127.9, 125.6, 123.6, 119.0, 108.0, 55.3, 54.0, 42.2, 38.3, 23.2. MS ( $\text{ESI}^+$ ):  $m/z$  323.2 ( $\text{M}+\text{H}$ ).

**( $\pm$ )-2-((7-Methoxy-1,2,3,4-tetrahydroisoquinolin-1-yl)methyl)isoindoline-1,3-dione (82).**



To a solution of **73** (30 mg, 0.09 mmol) in DCM (6 mL) was added acetic acid (7  $\mu$ L, 0.11 mmol) and NaBH(OAc)<sub>3</sub> (29 mg, 0.14 mmol). The obtained suspension was stirred at room temperature for 2 h and reaction mixture was diluted with DCM (30 mL), washed with water (2 x 20 mL) and brine (20 mL), then dried over anhydrous Na<sub>2</sub>SO<sub>4</sub>. Filtered and the organic layer was concentrated and the crude was purified by column chromatography (ISCO) using acetonitrile (0 to 100%) in DCM as eluent and fractions were concentrated to give 29 mg of white solid, yield 95.4%. <sup>1</sup>H NMR (CDCl<sub>3</sub>, 400 MHz):  $\delta$  7.83 (d, 2H, *J* = 11.2 Hz), 7.68 (d, 2H, *J* = 12.6 Hz), 7.11 (m, 1H), 6.71 (s, 1H), 6.60 (m, 1H), 4.32 (d, 1H, *J* = 4.2 Hz), 3.98 (d, 1H, *J* = 6.8 Hz), 3.82 (m, 1H), 3.79 (s, 3H), 3.32-3.28 (m, 1H), 2.99-2.90 (m, 1H), 2.72-2.60 (m, 2H). <sup>13</sup>C NMR (CDCl<sub>3</sub>, 100 MHz):  $\delta$  168.6, 157.8, 136.9, 134.1, 132.2, 130.4, 127.6, 123.6, 113.6, 111.5, 55.3, 53.3, 42.5, 39.1, 29.6. MS (*ESI*<sup>+</sup>): *m/z* 323.3 (M+H).

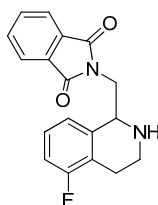
**(±)-2-((6,7-Dimethoxy-1,2,3,4-tetrahydroisoquinolin-1-yl)methyl)isoindoline-1,3-dione (83).**



To a solution of **74** (20 mg, 0.06 mmol) in DCM (2 mL) was added acetic acid (4  $\mu$ L, 0.07 mmol) and NaBH(OAc)<sub>3</sub> (18 mg, 0.09 mmol). The obtained suspension was stirred at room temperature for 2 h and reaction mixture was diluted with DCM (30 mL), washed with water (2 x 20 mL) and brine (20 mL), then dried over anhydrous Na<sub>2</sub>SO<sub>4</sub>. Filtered and the organic layer was concentrated and the crude was purified by column

chromatography (ISCO) using acetonitrile (0 to 100%) in DCM as eluent and fractions were concentrated to give 16 mg of white solid, yield 79.6%.  $^1\text{H}$  NMR ( $\text{CDCl}_3$ , 400 MHz):  $\delta$  7.82 (m, 2H), 7.63 (m, 2H), 7.03 (s, 1H), 6.83 (s, 1H), 4.36 (s, 2H), 3.98 (s, 3H), 3.91 (s, 3H), 3.79 (m, 1H), 3.36-3.25 (m, 2H), 2.82-2.66 (m, 2H).  $^{13}\text{C}$  NMR ( $\text{CDCl}_3$ , 100 MHz):  $\delta$  168.6, 157.8, 136.9, 134.1, 132.2, 130.4, 126.6, 123.6, 113.6, 111.5, 55.3, 53.3, 42.5, 39.1, 29.6. MS (ESI+):  $m/z$  353.1 (M+H).

**(±)-2-((5-Fluoro-1,2,3,4-tetrahydroisoquinolin-1-yl)methyl)isoindolin-1,3-dione (84).**



To a solution of **75** (30 mg, 0.1 mmol) in DCM (6 mL) was added acetic acid (7  $\mu\text{L}$ , 0.12 mmol) and  $\text{NaBH}(\text{OAc})_3$  (31 mg, 0.15 mmol). The obtained suspension was stirred at room temperature for 2 h and reaction mixture was diluted with DCM (30 mL), washed with water (2 x 20 mL) and brine (20 mL), then dried over anhydrous  $\text{Na}_2\text{SO}_4$ . Filtered and the organic layer was concentrated and the crude was purified by column chromatography (ISCO) using acetonitrile (0 to 100%) in DCM as eluent and fractions were concentrated to give 17 mg of white solid, yield 84.6%.  $^1\text{H}$  NMR ( $\text{CDCl}_3$ , 400 MHz):  $\delta$  7.78 (d, H,  $J = 9.8$  Hz), 7.56 (d, 2H,  $J = 12.2$  Hz), 7.00 (d, 1H,  $J = 16.4$  Hz), 6.92 (d, 1H,  $J = 14.2$  Hz), 6.72 (m, 1H), 4.26 (m, 1H), 3.92 (m, 1H), 3.79 (d, 1H,  $J = 7.8$  Hz), 3.27 (m, 1H), 2.96 (m, 1H), 2.77-2.48 (m, 2H).  $^{13}\text{C}$  NMR ( $\text{CDCl}_3$ , 100 MHz):  $\delta$

166.8, 160.2, 157.8, 136.0, 132.0, 130.3, 124.8, 121.6, 120.5, 111.4, 51.9, 40.3, 36.0, 20.3.

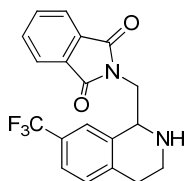
MS (*ESI+*): *m/z* 311.2 (M+H).

**(±)-2-((7-Fluoro-1,2,3,4-tetrahydroisoquinolin-1-yl)methyl)isoindoline-1,3-dione (85).**



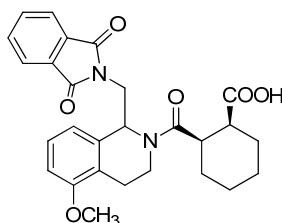
To a solution of **76** (100 mg, 0.32 mmol) in DCM (10 mL) was added acetic acid (23  $\mu$ L, 0.38 mmol) and NaBH(OAc)<sub>3</sub> (103 mg, 0.48 mmol). The obtained suspension was stirred at room temperature for 2 h and reaction mixture was diluted with DCM (30 mL), washed with water (2 x 20 mL) and brine (20 mL), then dried over anhydrous Na<sub>2</sub>SO<sub>4</sub>. Filtered and the organic layer was concentrated and the crude was purified by column chromatography (ISCO) using acetonitrile (0 to 100%) in DCM as eluent and fractions were concentrated to give 89 mg of white solid, yield 88.5%. <sup>1</sup>H NMR (CDCl<sub>3</sub>, 400 MHz):  $\delta$  7.86 (m, 2H), 7.71 (m, 2H), 7.18 (m, 1H), 7.01 (m, 1H), 6.88 (m, 1H), 4.36 (d, 1H, *J* = 6.8 Hz), 4.09 (m, 1H), 3.80 (d, 1H, *J* = 9.2 Hz), 3.26 (m, 1H), 2.96 (m, 1H), 2.70 (m, 2H). <sup>13</sup>C NMR (CDCl<sub>3</sub>, 100 MHz):  $\delta$  168.6, 162.2, 136.6, 134.0, 131.1, 130.9, 123.6, 114.0, 113.2, 54.2, 42.3, 38.9, 28.8. MS (*ESI+*): *m/z* 311.2 (M+H).

**(±)-2-((7-(Trifluoromethyl)-1,2,3,4-tetrahydroisoquinolin-1-yl)methyl)isoindoline-1,3-dione (86).**



To a solution of **77** (24 mg, 0.07 mmol) in DCM (4 mL) was added acetic acid (4.8  $\mu$ L, 0.08 mmol) and  $\text{NaBH}(\text{OAc})_3$  (21 mg, 0.1 mmol). The obtained suspension was stirred at room temperature for 2 h and reaction mixture was diluted with DCM (30 mL), washed with water (2 x 20 mL) and brine (20 mL), then dried over anhydrous  $\text{Na}_2\text{SO}_4$ . Filtered and the organic layer was concentrated and the crude was purified by column chromatography (ISCO) using acetonitrile (0 to 100%) in DCM as eluent and fractions were concentrated to give 18 mg of white solid, yield 74.7%.  $^1\text{H}$  NMR ( $\text{CDCl}_3$ , 400 MHz):  $\delta$  7.81 (m, 2H), 7.69 (m, 2H), 7.28 (d, 1H,  $J = 10.4$  Hz), 7.01 (s, 1H), 6.88 (d, 1H,  $J = 14.2$  Hz), 4.46 (d, 1H,  $J = 4.6$  Hz), 4.01 (m, 1H), 3.82 (d, 1H,  $J = 8.8$  Hz), 3.36 (m, 1H), 2.96 (m, 1H), 2.72 (m, 2H).  $^{13}\text{C}$  NMR ( $\text{CDCl}_3$ , 100 MHz):  $\delta$  168.6, 139.8, 134.0, 133.8, 132.1, 130.1, 129.5, 129.0, 128.6, 123.6, 123.2, 54.1, 42.1, 38.4, 29.2. MS ( $\text{ESI}^+$ ):  $m/z$  361.1 ( $\text{M}+\text{H}$ ).

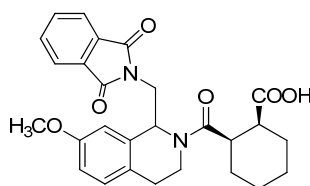
**(1S,2R)-2-(( $\pm$ )-1-((1,3-Dioxoisindolin-2-yl)methyl)-5-methoxy-1,2,3,4-tetrahydroisoquinoline-2-carbonyl)cyclohexanecarboxylic acid (**88**).**



To a solution of **81** (8 mg, 0.025 mmol) in 2 mL *p*-xylene was added *cis*-cyclohexyldicarboxylic anhydride (7.7 mg, 0.05 mmol) and stirred at 50  $^\circ\text{C}$  for 24 h. The

reaction mixture was concentrated and the residue was purified by column chromatography (ISCO) using ethyl acetate (0 to 100%) in hexane as eluent to afford 4.8 mg desired product as a white powder, yield 38.4%. Diastereomers were separated by HPLC using acetonitrile with 0.1% trifluoroacetic acid (30 to 90%) in water with 0.1% trifluoroacetic acid.  $^1\text{H}$  NMR ( $\text{CD}_3\text{OD}-d_4$ , 400 MHz):  $\delta$  7.77-7.68 (m, 4H), 7.15 (dd,  $J = 8.2, 8.8$  Hz, 1H), 6.88 (d,  $J = 8.6$  Hz, 1H), 6.74 (d,  $J = 7.2$  Hz, 1H), 5.88 (dd,  $J = 4.6, 8.6$  Hz, 1H), 4.03 (dd,  $J = 8.2, 12.2$  Hz, 1H), 3.95 (dd,  $J = 5.2, 16.4$  Hz, 1H), 3.83 (dd,  $J = 4.4, 15.2$  Hz, 1H), 3.76 (s, 3H), 3.70-3.58 (m, 2H), 2.86-2.78 (m, 1H), 2.75-2.62 (m, 1H), 2.32-2.25 (m, 1H), 1.93-1.82 (m, 1H), 1.70-1.57 (m, 2H), 1.46-1.33 (m, 2H), 1.12-0.78 (m, 2H), 0.42-0.29 (m, 1H).  $^{13}\text{C}$  NMR ( $\text{CD}_3\text{OD}-d_4$ , 100 MHz):  $\delta$  177.7, 176.3, 169.9, 158.6, 135.9, 135.8, 133.5, 128.3, 124.9, 124.2, 120.6, 109.6, 55.8, 52.3, 49.7, 43.2, 42.7, 41.8, 38.5, 28.5, 27.5, 25.9, 22.9. MS (*ESI+*):  $m/z$  477.2 (M+H).

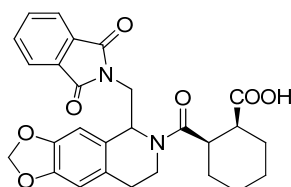
**(1*S*,2*R*)-2-(( $\pm$ )-1-((1,3-Dioxoisindolin-2-yl)methyl)-7-methoxy-1,2,3,4-tetrahydroisoquinoline-2-carbonyl)cyclohexanecarboxylic acid (89).**



To a solution of **82** (20 mg, 0.06 mmol) in 8 mL *p*-xylene was added *cis*-cyclohexyldicarboxylic anhydride (15 mg, 0.10 mmol) and stirred at 50 °C for 24 h. The reaction mixture was concentrated and the residue was purified by column chromatography (ISCO) using ethyl acetate (0 to 100% with 1% acetic acid) in hexane as

eluent to afford 27.5 mg desired product as a white powder, yield 92.3%. Diastereomers were separated by HPLC using acetonitrile with 0.1% trifluoroacetic acid (30 to 90%) in water with 0.1% trifluoroacetic acid.  $^1\text{H}$  NMR ( $\text{CD}_3\text{OD}-d_4$ , 400 MHz):  $\delta$  7.89-7.81 (m, 4H), 7.12 (d,  $J = 7.6$  Hz, 1H), 6.93 (s, 1H), 6.83 (d,  $J = 4.6$  Hz, 1H), 5.98 (dd,  $J = 4.2, 8.4$  Hz, 1H), 4.12 (dd,  $J = 8.2, 11.8$  Hz, 1H), 4.02-3.97 (m, 1H), 3.94 (dd,  $J = 4.8, 16.2$  Hz, 1H), 3.83 (s, 3H), 3.80-3.73 (m, 2H), 3.10-2.98 (m, 1H), 2.85-2.80 (m, 1H), 2.40-2.36 (m, 1H), 2.01-1.97 (m, 1H), 1.75-1.67 (m, 2H), 1.48-1.43 (m, 2H), 1.12-0.98 (m, 2H), 0.51-0.42 (m, 1H).  $^{13}\text{C}$  NMR ( $\text{CD}_3\text{OD}-d_4$ , 100 MHz):  $\delta$  176.9, 176.3, 168.5, 146.2, 136.2, 134.5, 133.7, 130.3, 128.9, 127.5, 126.6, 124.1, 55.6, 51.2, 44.7, 42.0, 41.2, 38.8, 32.6, 29.3, 28.8, 28.3, 25.9. MS (*ESI+*):  $m/z$  477.2 (M+H).

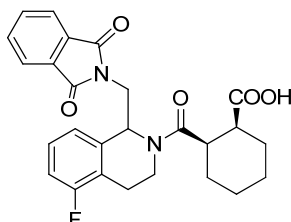
**(1*S*,2*R*)-2-(( $\pm$ )-1-((1,3-Dioxoisindolin-2-yl)methyl)-6,7-dimethoxy-1,2,3,4-tetrahydroisoquinoline-2-carbonyl)cyclohexanecarboxylic acid (90).**



To a solution of **83** (20 mg, 0.06 mmol) in 5 mL *p*-xylene was added *cis*-cyclohexyldicarboxylic anhydride (17 mg, 0.11 mmol) and stirred at 50 °C for 24 h. The reaction mixture was concentrated and the residue was purified by column chromatography (ISCO) using ethyl acetate (0 to 100% with 1% acetic acid) in hexane as eluent to afford 23 mg as a white powder, yield 79.9%. Diastereomers were separated by HPLC using acetonitrile with 0.1% trifluoroacetic acid (30 to 90%) in water with 0.1%

trifluoroacetic acid.  $^1\text{H-NMR}$  ( $\text{CD}_3\text{OD-}d_4$ , 400 MHz):  $\delta$  7.77-7.69 (m, 4H), 6.83 (s, 1H), 6.66 (s, 1H), 5.80 (dd,  $J = 5.2, 8.8$  Hz, 1H), 4.00 (dd,  $J = 8.2, 12.6$  Hz, 1H), 3.88 (dd,  $J = 4.2, 15.6$  Hz, 1H), 3.82 (dd,  $J = 4.4, 16.2$  Hz, 1H), 3.77 (s, 3H), 3.72 (s, 3H), 3.70-3.58 (m, 2H), 2.98-2.87 (m, 1H), 2.75-2.60 (m, 1H), 2.32-2.22 (m, 1H), 1.98-1.81 (m, 1H), 1.68-1.51 (m, 2H), 1.41-1.33 (m, 2H), 1.11-0.75 (m, 2H), 0.42-0.28 (m, 1H).  $^{13}\text{C-NMR}$  ( $\text{CD}_3\text{OD-}d_4$ , 100 MHz):  $\delta$  176.3, 169.8, 168.2, 149.8, 149.3, 135.4, 133.4, 128.6, 127.0, 124.3, 113.5, 111.9, 56.7, 56.5, 51.5, 44.3, 42.0, 40.9, 29.5, 28.5, 25.9, 22.6 MS (*ESI+*):  $m/z$  507.2 (M+H).

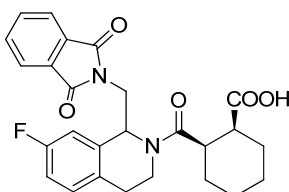
**( $\pm$ )-*cis*-2-(1-((1,3-Dioxoisindolin-2-yl)methyl)-5-fluoro-1,2,3,4-tetrahydroisoquinoline-2-carbonyl)cyclohexanecarboxylic acid (91).**



To a solution of **84** (12 mg, 0.04 mmol) in 3 mL *p*-xylene was added *cis*-cyclohexyldicarboxylic anhydride (9 mg, 0.06 mmol) and stirred at 50 °C for 24 h. The reaction mixture was concentrated and the residue was purified by column chromatography (ISCO) using ethyl acetate (0 to 100% with 1% acetic acid) in hexane as eluent to afford 14.2 mg desired product as a white powder, yield 78.9%.  $^1\text{H-NMR}$  ( $\text{CD}_3\text{OD-}d_4$ , 400 MHz):  $\delta$  7.78-7.50 (m, 4H), 7.21-6.82 (m, 3H), 6.02 (dd,  $J = 4.2, 9.2$  Hz, 1H), 4.10-3.50 (m, 4H), 3.11-2.41 (m, 3H), 2.33-1.71 (m, 4H), 1.29-.082 (m, 5H).  $^{13}\text{C}$  NMR ( $\text{CD}_3\text{OD-}d_4$ , 100 MHz):  $\delta$  177.8, 175.8, 168.2, 156.6, 145.8, 135.6, 134.9, 132.5,

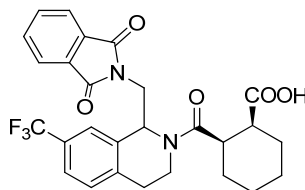
131.5, 128.5, 126.3, 124.8, 51.8, 44.8, 42.3, 40.9, 38.5, 32.4, 29.2, 28.8, 28.1, 25.2. MS (*ESI+*):  $m/z$  465.2 (M+H).

**(±)-*cis*-2-(1-((1,3-Dioxoisindolin-2-yl)methyl)-7-fluoro-1,2,3,4-tetrahydroisoquinoline-2-carbonyl)cyclohexanecarboxylic acid (92).**



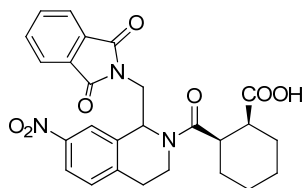
To a solution of **85** (20 mg, 0.06 mmol) in 8 mL *p*-xylene was added *cis*-cyclohexyldicarboxylic anhydride (15 mg, 0.10 mmol) and stirred at 50 °C for 24 h. The reaction mixture was concentrated and the residue was purified by column chromatography (ISCO) using ethyl acetate (0 to 100% with 1% acetic acid) in hexane as eluent to afford 27.5 mg desired product as a white powder, yield 92.3%. <sup>1</sup>H NMR (CD<sub>3</sub>OD-*d*<sub>4</sub>, 400 MHz): δ 7.78 (d, 2H, *J* = 11.2 Hz), 7.70 (d, 2H, *J* = 9.2 Hz), 7.13 (d, *J* = 8.4 Hz, 1H), 6.93 (d, 1H, *J* = 13.2 Hz), 6.83 (d, *J* = 8.6 Hz, 1H), 5.92 (dd, *J* = 4.6, 9.8 Hz, 1H), 4.02 (d, *J* = 7.2 Hz, 1H), 3.92 (d, *J* = 4.6, 12.2 Hz, 1H), 3.80 (dd, *J* = 4.2, 16.6 Hz, 1H), 3.66-3.60 (m, 2H), 3.10-2.90 (m, 1H), 2.85-2.80 (m, 1H), 2.30-2.26 (m, 1H), 2.01-1.97 (m, 2H), 1.70-1.50 (m, 2H), 1.48-1.43 (m, 2H), 1.12-0.79 (m, 2H). <sup>13</sup>C NMR (CD<sub>3</sub>OD-*d*<sub>4</sub>, 100 MHz): δ 177.6, 176.2, 169.8, 152.3, 143.2, 136.8, 134.2, 134.9, 130.3, 128.4, 127.6, 125.8, 51.6, 44.3, 42.0, 40.6, 38.5, 33.1, 30.3, 28.8, 28.2, 24.8. MS (*ESI+*):  $m/z$  465.2 (M+H).

**(±)-cis-2-(1-((1,3-Dioxisoindolin-2-yl)methyl)-7-(trifluoromethyl)-1,2,3,4-tetrahydroisoquinoline-2-carbonyl)cyclohexanecarboxylic acid (93).**



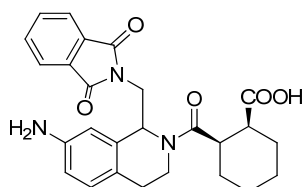
To a solution of **86** (15 mg, 0.04 mmol) in 8 mL p-xylene was added *cis*-cyclohexyldicarboxylic anhydride (9 mg, 0.06 mmol) and stirred at 50 °C for 24 h. The reaction mixture was concentrated and the residue was purified by column chromatography (ISCO) using ethyl acetate (0 to 100% with 1% acetic acid) in hexane as eluent to afford 17.8 mg desired product as a white powder, yield 84.7%. <sup>1</sup>H NMR (CD<sub>3</sub>OD-*d*<sub>4</sub>, 400 MHz): δ 8.01-7.78 (m, 4H), 7.53 (s, 1H), 7.48 (d, 1H, *J* = 10.4 Hz), 7.33 (d, 1H, *J* = 11.2 Hz), 5.99 (d, 1H, *J* = 10.6 Hz), 4.02 (m, 1H), 3.96 (m, 1H), 3.85 (m, 1H), 3.60-3.50 (m, 2H), 3.18-2.92 (m, 1H), 2.83-2.78 (m, 1H), 2.36-2.26 (m, 1H), 2.11-1.99 (m, 2H), 1.70-1.50 (m, 2H), 1.49-1.42 (m, 2H), 1.22-0.62 (m, 2H). <sup>13</sup>C NMR (CD<sub>3</sub>OD-*d*<sub>4</sub>, 100 MHz): δ 177.3, 175.9, 167.9, 152.1, 140.0, 136.2, 133.2, 134.9, 132.5, 131.2, 128.4, 124.8, 52.3, 45.1, 41.6, 40.9, 38.9, 32.3, 29.6, 28.9, 28.6, 25.9. MS (*ESI*<sup>+</sup>): *m/z* 515.1 (M+H).

**(1*S*,2*R*)-2-((*S*)-1-((1,3-Dioxisoindolin-2-yl)methyl)-nitro-1,2,3,4-tetrahydroisoquinoline-2-carbonyl)cyclohexanecarboxylic acid (94).**



LH601A (10 mg) was dissolved in 600  $\mu\text{L}$  70%  $\text{HNO}_3$  and stirred for 18 h at room temperature. Water was added to the solution and the resulted precipitated was collected by filtration and washed with water. The collected solid was dried over vacuum to give 9.6 mg product, yield 87.3%.  $^1\text{H}$  NMR ( $\text{CD}_3\text{OD}-d_4$ , 400 MHz):  $\delta$  8.15 (d,  $J = 10.6$  Hz, 1H), 8.01 (dd,  $J = 4.8, 11.6$  Hz, 1H), 7.80-7.69 (m, 4H), 6.01 (dd,  $J = 4.2, 8.4$  Hz, 1H), 4.12-4.03 (m, 1H), 4.01 (dd,  $J = 8.0, 11.6$  Hz, 1H), 4.01-3.92 (m, 1H), 3.81-3.73 (m, 2H), 3.13-2.88 (m, 1H), 2.85-2.73 (m, 1H), 2.30-2.26 (m, 1H), 1.91-1.87 (m, 1H), 1.72-1.55 (m, 2H), 1.48-1.31 (m, 2H), 1.02-0.80 (m, 2H), 0.50-0.32 (m, 1H).  $^{13}\text{C}$  NMR ( $\text{CD}_3\text{OD}-d_4$ , 100 MHz):  $\delta$  177.7, 176.5, 169.6, 147.9, 144.4, 142.2, 137.9, 135.5, 133.4, 131.2, 125.6, 123.0, 122.3, 51.8, 44.3, 41.7, 41.5, 40.2, 38.2, 30.2, 28.4, 27.5, 25.6. MS ( $\text{ESI}^+$ ):  $m/z$  491.2 (M+H).

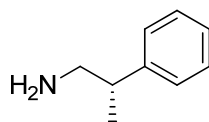
**(1S,2R)-2-((S)-Amino-1-((1,3-dioxoisindolin-2-yl)methyl)-1,2,3,4-tetrahydroisoquinoline-2-carbonyl)cyclohexanecarboxylic acid (95).**



To a solution of **94** (6 mg) in 2 mL methanol was added a catalytical amount of 5% Pd/C and stirred for 4 h under  $\text{H}_2$ . The Pd/C was filtered off and the filtration was concentrated.

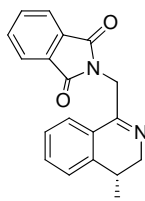
The residue was purified by column chromatography using acetonitrile (0 to 100%) in DCM as eluent to give 5 mg designed product, yield 89%. <sup>1</sup>H-NMR (CD<sub>3</sub>OD-*d*<sub>4</sub>, 400 MHz): δ 7.79-7.69 (m, 4H), 7.13 (d, *J* = 9.2 Hz, 1H), 7.11 (s, 1H), 6.93 (d, *J* = 8.0 Hz, 1H), 5.96 (dd, *J* = 3.8, 7.6 Hz, 1H), 4.02 (dd, *J* = 8.2, 13.2 Hz, 1H), 4.02-3.92 (m, 1H), 3.86 (dd, *J* = 4.4, 14.2 Hz, 1H), 3.81-3.73 (m, 2H), 3.13-2.98 (m, 1H), 2.81-2.76 (m, 1H), 2.30-2.26 (m, 1H), 2.01-1.87 (m, 1H), 1.72-1.57 (m, 2H), 1.48-1.41 (m, 2H), 1.12-0.98 (m, 2H), 1.11-0.82 (m, 1H). <sup>13</sup>C NMR (CD<sub>3</sub>OD-*d*<sub>4</sub>, 100 MHz): δ 177.3, 176.4, 169.9, 144.6, 141.2, 136.5, 135.1, 133.5, 132.1, 128.5, 128.7, 125.1, 52.1, 46.2, 43.1, 41.8, 38.5, 33.6, 29.2, 28.9, 28.5, 26.2. MS (*ESI*<sup>+</sup>): *m/z* 462.2 (M+H).

**(*R*)-Methyl 2-amino-3-phenylpropanoate (96).**



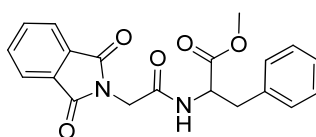
To a solution of D-phenylalanine (600 mg, 3.6 mmol) in 8 mL methanol was added sulfonyl chloride (405 μL, 5.4 mmol). The reaction mixture was stirred for 12 h at room temperature. Ether was added and the precipitate was collected by filtration and washed with ether to afford 566 mg product, yield 86.9%. <sup>1</sup>H NMR (CDCl<sub>3</sub>, 400 MHz): δ 7.51-7.03 (m, 5H), 4.33 (t, 1H, *J* = 7.8 Hz), 3.42-3.00 (m, 5H). <sup>13</sup>C NMR (CDCl<sub>3</sub>, 100 MHz) δ 170.4, 135.3, 130.5, 130.3, 130.2, 128.9, 55.3, 53.7, 37.5. MS (*ESI*<sup>+</sup>): *m/z* 180.1 (M+H)

**(*R*)-2-((4-Methyl-3,4-dihydroisoquinolin-1-yl)methyl)isoindoline-1,3-dione (100).**



To a solution of *N*-phthaloylglycine (**18**, 84 mg, 0.49 mmol) in 20 mL acetonitrile was added *R*-beta-methylphenethylamine (84 mg, 0.49 mmol) and POCl<sub>3</sub> (224 uL, 2.45 mmol). The resulting solution was heated at 85 °C for 24 h, then cooled to room temperature and concentrated under reduced pressure. The obtained dark residue was diluted with 100 mL DCM and washed with sat NaHCO<sub>3</sub> solution, water and brine, then dried over anhydrous Na<sub>2</sub>SO<sub>4</sub>. The filtration was concentrated and the residue was purified by column chromatography using acetonitrile (0 to 100%) in DCM as eluent to afford 62 mg product, yield 41.9%. <sup>1</sup>H NMR (CDCl<sub>3</sub>, 400 MHz) δ 7.98 (m, 2H), 7.86-7.72 (m, 4H), 7.51 (m, 2H), 5.35 (s, 2H), 4.02 (m, 1H), 3.85 (m, 1H), 3.32 (m, 1H), 1.48 (m, 3H). <sup>13</sup>C NMR (CDCl<sub>3</sub>, 100 MHz) δ 172.6, 167.3, 143.5, 138.0, 134.6, 131.9, 129.1, 128.6, 127.7, 127.3, 124.0, 123.2, 47.6, 39.0, 29.8, 19.1. MS (*ESI*<sup>+</sup>): *m/z* 305.1 (M+H)

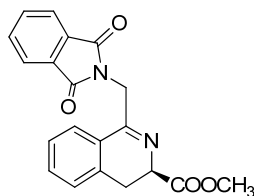
**(*R*)-Methyl 2-(2-(1,3-dioxoisindolin-2-yl)acetamido)-3-phenylpropanoate (99).**



To a solution of *N*-phthaloylglycine (**18**, 115 mg, 0.56 mmol) in 10 mL acetonitrile was added (*R*)-methyl 2-amino-3-phenylpropanoate (100 mg, 0.56 mmol), EDC (128 mg, 0.67 mmol) and DIPEA (292 uL, 1.68 mmol). The reaction mixture was stirred for 4 h at room temperature. Acetonitrile was removed by vacuum. The reaction mixture was then

diluted with 50 mL DCM and washed with 0.5 N HCl solution, sat NaHCO<sub>3</sub> solution, water and brine, then dried over anhydrous Na<sub>2</sub>SO<sub>4</sub>. The filtration was concentrated and the residue was purified by column chromatography using acetonitrile (0 to 50%) in DCM as eluent to afford 169 mg product, yield 66.9%. <sup>1</sup>H NMR (CDCl<sub>3</sub>, 400 MHz): δ 7.72 (m, 2H), 7.51 (m, 2H), 7.16-6.86 (m, 5H), 6.18 (d, 1H, *J* = 11.8 Hz), 4.72 (d, 1H, *J* = 4.8 Hz), 4.12 (m, 1H), 3.50 (s, 3H), 2.96 (m, 2H). <sup>13</sup>C NMR (CDCl<sub>3</sub>, 100 MHz) δ 171.4, 167.5, 165.5, 135.4, 134.2, 132.0, 129.3, 128.5, 127.1, 123.6, 53.3, 52.4, 40.7, 37.6. MS (*ESI*<sup>+</sup>): *m/z* 367.1 (M+H)

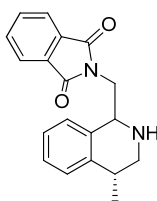
**(*R*)-Methyl 1-((1,3-dioxoisindolin-2-yl)methyl)-3,4-dihydroisoquinoline-3-carboxylate (101).**



To a solution of **99** (30 mg, 0.08 mmol) in 5 mL *p*-xylene was added P<sub>2</sub>O<sub>5</sub> (58 mg, 0.41 mmol). The suspension was stirred for 3 h under reflux. The reaction mixture was cooled to room temperature and *p*-xylene was removed. 30 mL sat NaHCO<sub>3</sub> solution was added, then extracted with DCM (30 mL, 3x). The combined DCM extract was washed with water and brine, then dried over anhydrous Na<sub>2</sub>SO<sub>4</sub>. The filtration was concentrated and the residue was purified by column chromatography using acetonitrile (0 to 100%) in DCM as eluent to afford 6 mg, 21%. <sup>1</sup>H NMR (CDCl<sub>3</sub>, 400 MHz): δ 7.96-7.72 (m, 2H), 7.71-7.68 (m, 2H), 7.32-7.12 (m, 4H), 4.89 (s, 2H), 4.68 (t, 1H, *J* = 11.6 Hz), 3.79 (s, 3H),

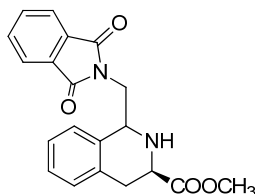
3.63 (d, 2H,  $J = 7.6$  Hz).  $^{13}\text{C}$  NMR ( $\text{CDCl}_3$ , 100 MHz)  $\delta$  174.6, 169.3, 158.1, 133.4, 132.3, 129.9, 128.5, 128.3, 123.6, 123.0, 116.5, 108.9, 60.3, 52.3, 47.6, 41.5. MS ( $\text{ESI}^+$ ):  $m/z$  349.1 (M+H)

**2-(((4*R*)-4-Methyl-1,2,3,4-tetrahydroisoquinolin-1-yl)methyl)isoindoline-1,3-dione (102).**



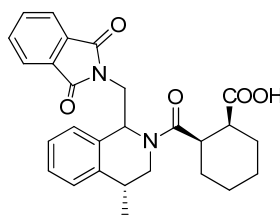
To a solution of **100** (32 mg, 0.1 mmol) in DCM (6 mL) was added acetic acid (7.6  $\mu\text{L}$ , 0.13 mmol) and  $\text{NaBH}(\text{OAc})_3$  (33 mg, 0.16 mmol). The obtained suspension was stirred at room temperature for 2 h and reaction mixture was diluted with DCM (30 mL), washed with water (2 x 20 mL) and brine (20 mL), then dried over anhydrous  $\text{Na}_2\text{SO}_4$ . Filtered and the organic layer was concentrated and the crude was purified by column chromatography (ISCO) using acetonitrile (0 to 100%) in DCM as eluent and fractions were concentrated to give 26 mg white solid, yield 81.2%.  $^1\text{H}$  NMR ( $\text{CDCl}_3$ , 400 MHz)  $\delta$  7.92 (m, 2H), 7.86-7.71 (m, 4H), 7.53 (m, 2H), 5.68 (t, 1H,  $J = 6.6$  Hz), 4.89 (s, 2H), 4.12 (m, 1H), 3.95 (m, 1H), 3.31 (m, 1H), 1.53 (m, 3H).  $^{13}\text{C}$  NMR ( $\text{CDCl}_3$ , 100 MHz):  $\delta$  168.6, 136.5, 134.6, 131.2, 128.6, 127.3, 126.8, 123.2, 113.2, 109.8, 53.2, 43.3, 39.2, 29.6, 25.6. MS ( $\text{ESI}^+$ ):  $m/z$  307.1 (M+H).

**(3*R*)-Methyl 1-((1,3-dioxisoindolin-2-yl)methyl)-1,2,3,4-tetrahydroisoquinoline-3-carboxylate (103).**



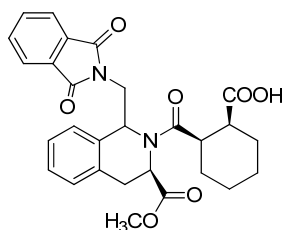
To a solution of **101** (133 mg, 0.38 mmol) in DCM (10 mL) was added acetic acid (23  $\mu$ L, 0.38 mmol) and  $\text{NaBH}(\text{OAc})_3$  (103 mg, 0.48 mmol). The obtained suspension was stirred at room temperature for 2 h and reaction mixture was diluted with DCM (30 mL), washed with water (2 x 20 mL) and brine (20 mL), then dried over anhydrous  $\text{Na}_2\text{SO}_4$ . Filtered and the organic layer was concentrated and the crude was purified by column chromatography (ISCO) using acetonitrile (0 to 100%) in DCM as eluent and fractions were concentrated to give 103 mg white solid, yield 77.6%.  $^1\text{H}$  NMR ( $\text{CDCl}_3$ , 400 MHz):  $\delta$  7.85-7.69 (m, 4H), 7.765-7.56 (m, 4H), 4.66 (d, 1H,  $J = 11.6$  Hz), 4.01 (m, 1H), 3.82 (d, 1H,  $J = 7.2$  Hz), 3.56 (s, 3H), 3.21 (m, 1H), 2.95 (m, 1H), 2.71 (m, 1H).  $^{13}\text{C}$  NMR ( $\text{CDCl}_3$ , 100 MHz):  $\delta$  168.3, 136.5, 134.1, 130.3, 128.6, 127.6, 126.6, 123.2, 113.8, 110.9, 53.6, 42.9, 39.8, 29.5. MS ( $\text{ESI}^+$ ):  $m/z$  351.2 (M+H).

**((1*S*,2*R*)-2-((4*R*)-1-((1,3-Dioxisoindolin-2-yl)methyl)-4-methyl-1,2,3,4-tetrahydroisoquinoline-2-carbonyl)cyclohexanecarboxylic acid (46).**



To a solution of (**102**, 10 mg, 0.03 mmol) in 2 mL p-xylene was added *cis*-cyclohexyldicarboxylic anhydride (7.5 mg, 0.05 mmol) and stirred at 50 °C for 24 h. The reaction mixture was concentrated and the residue was purified by column chromatography (ISCO) using ethyl acetate (0 to 100%) in hexane as eluent to afford 13.2 mg as a white powder, yield 88%. Diastereomers were separated by HPLC using acetonitrile with 0.1% trifluoroacetic acid (30 to 90%) in water with 0.1% trifluoroacetic acid. <sup>1</sup>H NMR (CD<sub>3</sub>OD-*d*<sub>4</sub>, 400 MHz): δ 7.89-7.76 (m, 2H), 7.71-7.62 (m, 2H), 7.50-7.12 (m, 4H), 5.98 (dd, 1H), 4.22-4.20 (m, 1H), 4.17 (dd, 1H), 4.01-3.96 (m, 1H), 3.98 (dd, 1H), 3.80-3.75 (m, 1H), 3.70-3.63 (m, 1H), 3.15-2.98 (m, 1H), 2.95-2.81 (m, 1H), 2.45-2.33 (m, 1H), 2.01-1.92 (m, 1H), 1.75-1.57 (m, 2H), 1.48-1.43 (m, 1H), 1.35 (d, 3H), 1.12-0.59 (m, 2H). <sup>13</sup>C NMR (CD<sub>3</sub>OD-*d*<sub>4</sub>, 400 MHz): δ 177.3, 176.7, 169.2, 136.9, 134.8, 132.9, 131.2, 130.3, 129.3, 128.4, 126.6, 124.8, 51.2, 44.1, 42.7, 40.2, 39.2, 32.8, 29.6, 28.8, 28.1, 26.1, 25.3. MS (*ESI*<sup>+</sup>): *m/z* 461.1 (M+H).

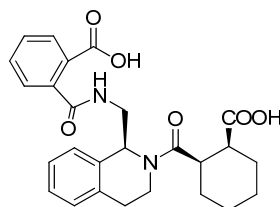
**(1*S*,2*R*)-2-((3*R*)-1-((1,3-Dioxisoindolin-2-yl)methyl)-3-(methoxycarbonyl)-1,2,3,4-tetrahydroisoquinoline-2-carbonyl)cyclohexanecarboxylic acid (47).**



To a solution of **103** (4.3 mg, 0.085 mmol) in 600 uL p-xylene was added *cis*-cyclohexyldicarboxylic anhydride (3.8 mg, 0.013 mmol) and stirred at 50 °C for 24 h. The reaction mixture was concentrated and the residue was purified by column

chromatography (ISCO) using ethyl acetate (0 to 100% with 1% acetic acid) in hexane as eluent to afford 3.0 mg as a white powder, yield 48.4%. Diastereomers were separated by HPLC using acetonitrile with 0.1% trifluoroacetic acid (30 to 90%) in water with 0.1% trifluoroacetic acid.  $^1\text{H}$  NMR ( $\text{CD}_3\text{OD}-d_4$ , 400 MHz):  $\delta$  7.79-7.69 (m, 4H), 7.46-7.21 (m, 2H), 7.11-6.93 (m, 1H), 5.82 (d, 1H,  $J = 6.6$  Hz), 4.23 (t, 1H,  $J = 7.8$  Hz), 4.09 (d, 1H,  $J = 16.2$  Hz), 3.99 (m, 1H), 3.76 (s, 3H), 3.60-3.58 (m, 2H), 2.86-2.58 (m, 2H), 2.71-2.65 (m, 1H), 2.38-2.23 (m, 1H), 1.98-1.80 (m, 2H), 1.72-1.39 (m, 4H).  $^{13}\text{C}$  NMR ( $\text{CD}_3\text{OD}-d_4$ , 100 MHz):  $\delta$  177.6, 176.4, 169.8, 166.5, 136.2, 135.2, 135.1, 134.5, 132.2, 129.3, 128.4, 127.1, 126.1, 56.2, 53.6, 51.8, 44.4, 42.6, 40.6, 32.3, 29.5, 28.8, 28.1, 25.8. MS (ESI+):  $m/z$  505.1(M+H).

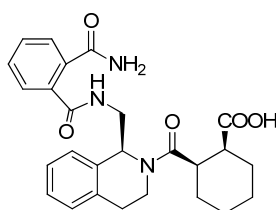
**2-(((S)-2-(((1R,2S)-2-Carboxycyclohexanecarbonyl)-1,2,3,4-tetrahydroisoquinolin-1-yl)methyl)carbamoyl)benzoic acid (48).**



To a solution of LH601A (8 mg, 0.02 mmol) in 2 mL 50% ACN/H<sub>2</sub>O was added KOH (1.5 mg, 0.03 mmol) and stirred for 30 min at room temperature. The acetonitrile was removed and pH was adjusted to acidic and then ether was added. The resulted precipitate was collected by filtration and dried over vacuum to give 7.6 mg product, yield 91.6%.  $^1\text{H}$  NMR ( $\text{CD}_3\text{OD}-d_4$ , 400 MHz):  $\delta$  7.73-7.60 (m, 4H), 7.31-7.09 (m, 4H), 5.96 (dd,  $J = 4.8, 9.2$  Hz, 1H), 4.01 (dd,  $J = 8.2, 12.6$  Hz, 1H), 3.81-3.52 (m, 2H), 3.46-3.41 (m, 1H), 3.22-3.09 (m, 1H), 3.05-2.87 (m, 1H), 2.69-2.43 (m, 2H), 2.38-2.26 (m,

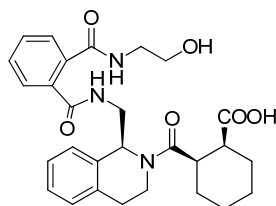
2H), 2.17-2.06 (m, 2H), 2.03-1.50 (m, 2H), 1.49-0.86 (m, 2H). MS (*ESI+*):  $m/z$  465.2 (M+H).

**(1*S*,2*S*)-2-((*S*)-1-((2-Carbamoylbenzamido)methyl)-1,2,3,4-tetrahydroisoquinoline-2-carbonyl)cyclohexanecarboxylic acid (49).**



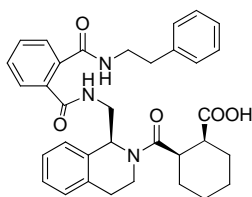
To a solution of LH601A (10 mg) in 1 mL methanol was bubbled through anhydrous ammonium for 5 min and stirred for 1 h at room temperature. The reaction mixture was concentrated and the residue was purified by column chromatography using acetonitrile (0 to 100%) in DCM as eluent to give the 4.3 mg designed product while 5.2 mg starting material was recovered, yield 86.1%. <sup>1</sup>H NMR (CD<sub>3</sub>OD-*d*<sub>4</sub>, 400 MHz):  $\delta$  7.79-7.61 (m, 4H), 7.33-7.12 (m, 4H), 5.99 (dd,  $J = 4.8, 7.6$  Hz, 1H), 4.02 (dd,  $J = 8.0, 13.2$  Hz, 1H), 3.88-3.52 (m, 2H), 3.51-3.42 (m, 1H), 3.12-3.03 (m, 1H), 3.00-2.82 (m, 2H), 2.69-2.48 (m, 2H), 2.33-2.22 (m, 2H), 2.13-2.06 (m, 1H), 2.00-1.51 (m, 2H), 1.48-0.89 (m, 2H). MS (*ESI+*):  $m/z$  464.2 (M+H).

**(1*S*,2*R*)-2-((*S*)-1-((2-((2-Hydroxyethyl)carbamoyl)benzamido)methyl)-1,2,3,4-tetrahydroisoquinoline-2-carbonyl)cyclohexanecarboxylic acid (50).**



To a solution of LH601A (4 mg, 0.01 mmol) in 400 uL acetonitrile and 400 uL DCM was added ethanolamine (5.5 uL, 0.09 mmol) and stirred for 2 h at room temperature. The reaction mixture was concentrated and the residue was purified by HPLC using acetonitrile with 0.1% trifluoroacetic acid (10 to 90%) in water with 0.1% trifluoroacetic acid to give the 1.6 mg designed product, yield 35%.  $^1\text{H}$  NMR ( $\text{CD}_3\text{OD}-d_4$ , 400 MHz):  $\delta$  7.79-7.61 (m, 4H), 7.33-7.12 (m, 4H), 5.92 (d, 1H,  $J = 5.8$  Hz), 4.01 (m, 1H), 3.81-3.50 (m, 2H), 3.65-3.42 (m, 1H), 3.40 (t, 2H,  $J = 8.6$  Hz), 3.11-3.03 (m, 1H), 3.00-2.92 (m, 2H), 2.86 (t, 2H,  $J = 4.2$  Hz), 2.69-2.45 (m, 2H), 2.33-2.20 (m, 2H), 2.13-2.00 (m, 1H), 2.00-1.51 (m, 2H), 1.49-1.23 (m, 2H). MS ( $\text{ESI}^+$ ):  $m/z$  508.1 (M+H).

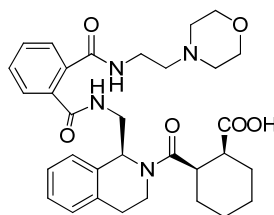
**(1*S*,2*R*)-2-((*S*)-1-((2-(Phenethylcarbamoyl)benzamido)methyl)-1,2,3,4-tetrahydroisoquinoline-2-carbonyl)cyclohexanecarboxylic acid (51).**



To a solution of LH601A (4 mg, 0.01 mmol) in 400 uL acetonitrile was added phenethylamine (11.3 uL, 0.09 mmol) and stirred for 2 h at room temperature. The reaction mixture was concentrated and the residue was purified by HPLC using acetonitrile with 0.1% trifluoroacetic acid (10 to 90%) in water with 0.1% trifluoroacetic

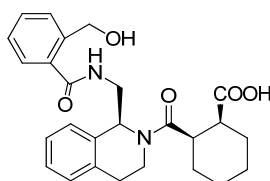
acid to give the 2.2 mg designed product, yield 43%.  $^1\text{H NMR}$  ( $\text{CD}_3\text{OD}-d_4$ , 400 MHz):  $\delta$  7.75-7.61 (m, 4H), 7.45-7.26 (m, 9H), 5.89 (d, 1H,  $J = 10.6$  Hz), 4.05 (m, 1H), 3.88-3.72 (m, 2H), 3.66 (t, 2H,  $J = 12.6$  Hz), 3.51-3.41 (m, 1H), 3.21-3.13 (m, 1H), 3.00-2.82 (m, 2H), 2.76 (t, 2H,  $J = 5.2$  Hz), 2.69-2.48 (m, 2H), 2.33-2.21 (m, 2H), 2.13-2.02 (m, 1H), 2.03-1.81 (m, 2H), 1.66-1.46 (m, 2H). MS ( $\text{ESI}^+$ ):  $m/z$  568.1 (M+H).

**(1*S*,2*R*)-2-((*S*)-1-((2-(2-Morpholinoethyl)carbamoyl)benzamido)methyl)-1,2,3,4-tetrahydroisoquinoline-2-carbonyl)cyclohexanecarboxylic acid (52).**



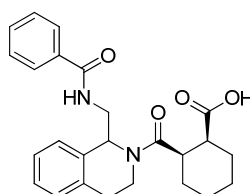
To a solution of LH601A (4 mg, 0.01 mmol) in 400  $\mu\text{L}$  acetonitrile was added N-3-(aminopropyl)morpholine (13  $\mu\text{L}$ , 0.09 mmol) and stirred for 2 h at room temperature. The reaction mixture was concentrated and the residue was purified by HPLC using acetonitrile with 0.1% trifluoroacetic acid (10 to 90%) in water with 0.1% trifluoroacetic acid to give the 1.6 mg designed product, yield 31%.  $^1\text{H NMR}$  ( $\text{CD}_3\text{OD}-d_4$ , 400 MHz):  $\delta$  7.68-7.62 (m, 4H), 7.33-7.12 (m, 4H), 5.91 (d, 1H,  $J = 10.2$  Hz), 4.09 (m, 1H), 3.88-3.71 (m, 2H), 3.66 (t, 2H,  $J = 9.2$  Hz), 3.51-3.42 (m, 1H), 3.28 (m, 4H), 3.19 (m, 4H), 3.12-3.03 (m, 1H), 3.00-2.92 (m, 2H), 2.79 (t, 2H,  $J = 4.8$  Hz), 2.69-2.43 (m, 2H), 2.36-2.20 (m, 2H), 2.19-2.05 (m, 1H), 2.03-1.82 (m, 2H), 1.78-1.58 (m, 2H). MS ( $\text{ESI}^+$ ):  $m/z$  577.1 (M+H).

**(1*S*,2*R*)-2-((*S*)-1-((2-(Hydroxymethyl)benzamido)methyl)-1,2,3,4-tetrahydroisoquinoline-2-carbonyl)cyclohexanecarboxylic acid (53).**



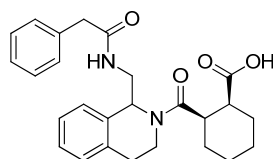
To a solution of LH601A (2.6 mg, 0.006 mmol) in iPrOH/water (1 mL) was added NaBH<sub>4</sub> (2 mg, 0.06) and the reaction mixture was stirred at room temperature for 4 h. The reaction mixture was concentrated and the residue was purified by HPLC using acetonitrile with 0.1% trifluoroacetic acid (10 to 90%) in water with 0.1% trifluoroacetic acid to give 1.9 mg white solid, yield 73%. <sup>1</sup>H NMR (DMSO-d<sub>6</sub>, 400 MHz) δ 7.79-7.69 (m, 4H), 7.40-7.12 (m, 4H), 5.88 (d, 1H, *J* = 11.6 Hz), 4.68 (s, 2H), 4.01 (m, 1H), 3.89-3.93 (m, 1H), 3.81 (d, 1H, *J* = 14.2 Hz), 3.56-3.66 (m, 1H), 2.73-2.97 (m, 2H), 2.23 (dt, 1H), 1.83 (dq, 1H), 1.67-1.58 (m, 2H), 1.25-1.32 (m, 3H), 1.81-0.96 (m, 3H). MS (*ESI*<sup>+</sup>): *m/z* 382.1 (M+H)

**(1*S*,2*R*)-2-((*S*)-1-(Benzamidomethyl)-1,2,3,4-tetrahydroisoquinoline-2-carbonyl)cyclohexanecarboxylic acid (54).**



To a solution of LH601A (2.8 mg, 0.006 mmol) in 800  $\mu$ L DCM was added hydrazine (1.2  $\mu$ L, 0.009 mmol) and stirred for 1 h at room temperature. The precipitate was filtered off and the filtration was concentrated and dried over vacuum. Then benzoyl chloride (5.6  $\mu$ L, 0.048 mmol) and DIPEA (6  $\mu$ L, 0.06 mmol) were added to a solution of the dried residue in acetonitrile and stirred for 2 h at room temperature. The reaction mixture was concentrated and the residue was purified by HPLC using acetonitrile with 0.1% trifluoroacetic acid (10 to 90%) in water with 0.1% trifluoroacetic acid to afford 1.2 mg of the designed product, yield 46.2%.  $^1\text{H NMR}$  ( $\text{CD}_3\text{OD}-d_4$ , 400 MHz):  $\delta$  7.58-7.51 (m, 4H), 7.30-7.21 (m, 5H), 5.90 (dd,  $J = 4.4, 8.2$  Hz, 1H), 4.06-3.88 (m, 2H), 3.72-3.68 (m, 1H), 3.65 (dd,  $J = 4.8, 13.6$  Hz, 1H), 3.00-2.69 (m, 4H), 2.35-2.23 (m, 1H), 2.10-2.02 (m, 2H), 1.88-1.71 (m, 2H), 1.69-1.56 (m, 2H), 1.46-1.08 (m, 1H). MS ( $\text{ESI}^+$ ):  $m/z$  421.1 (M+H).

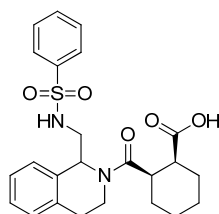
**(1*S*,2*R*)-2-((*S*)-1-((2-Phenylacetamido)methyl)-1,2,3,4-tetrahydroisoquinoline-2-carbonyl)cyclohexanecarboxylic acid (55).**



To a solution of LH601A (3 mg, 0.006 mmol) in 1 mL DCM was added hydrazine (1.5  $\mu$ L, 0.048 mmol) and stirred for 1 h at room temperature. The precipitate was filtered off and the filtration was concentrated and dried over vacuum. Then phenylacetyl chloride (1.2  $\mu$ L, 0.09 mmol) and DIPEA (1.8  $\mu$ L, 0.018 mmol) were added to a solution of the

dried residue in acetonitrile and stirred for 2 h at room temperature. The reaction mixture was concentrated and the residue was purified by HPLC using acetonitrile with 0.1% trifluoroacetic acid (10 to 90%) in water with 0.1% trifluoroacetic acid to afford 1.8 mg of the designed product, yield 62.1%. <sup>1</sup>H NMR (CD<sub>3</sub>OD-*d*<sub>4</sub>, 400 MHz): δ 7.57-7.50 (m, 4H), 7.35-7.19 (m, 5H), 5.90 (dd, *J* = 5.2, 8.4 Hz, 1H), 4.72 (s, 2H), 4.00-3.81 (m, 2H), 3.72-3.68 (m, 1H), 3.61 (dd, *J* = 4.0, 15.8 Hz, 1H), 3.03-2.66 (m, 4H), 2.23-2.12 (m, 1H), 2.11-2.02 (m, 2H), 1.90-1.73 (m, 2H), 1.68-1.48 (m, 2H), 1.33-1.05 (m, 1H). MS (*ESI*<sup>+</sup>): *m/z* 435.2 (M+H).

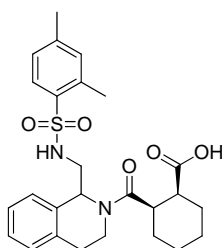
**(1*S*,2*R*)-2-((*S*)-1-(Phenylsulfonamidomethyl)-1,2,3,4-tetrahydroisoquinoline-2-carbonyl)cyclohexanecarboxylic acid (56).**



To a solution of LH601A (2 mg, 0.005 mmol) in 500 uL DCM was added hydrazine (1 uL, 0.007 mmol) and stirred for 1 h at room temperature. The precipitate was filtered off and the filtration was concentrated and dried over vacuum. Then benzene sulfonyl chloride (6 uL, 0.05 mmol) and DIPEA (1.5 uL, 0.05 mmol) were added to a solution of the dried residue in acetonitrile and stirred for 1 h at room temperature. The reaction mixture was concentrated and the residue was purified by HPLC using acetonitrile with 0.1% trifluoroacetic acid (10 to 90%) in water with 0.1% trifluoroacetic acid to afford 0.8 mg of the designed product, yield 42.3%. <sup>1</sup>H NMR (CD<sub>3</sub>OD-*d*<sub>4</sub>, 400 MHz): δ 7.58-7.51 (m, 4H), 7.30-7.21 (m, 5H), 5.76 (d, 1H, *J* = 14.2 Hz), 4.03-3.86 (m, 2H), 3.72-3.68 (m,

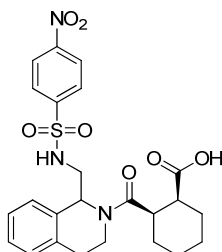
1H), 3.68 (d, 1H,  $J = 8.2$  Hz), 3.12-2.86 (m, 4H), 2.35-2.23 (m, 1H), 2.15-2.02 (m, 2H), 1.98-1.73 (m, 2H), 1.71-1.62 (m, 2H), 1.56-0.69 (m, 1H). MS (*ESI+*):  $m/z$  457.1 (M+H).

**(1*S*,2*R*)-2-((*S*)-1-((2,4-Dimethylphenylsulfonamido)methyl)-1,2,3,4-tetrahydroisoquinoline-2-carbonyl)cyclohexanecarboxylic acid (57).**



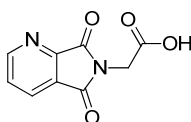
To a solution of LH601A (2 mg, 0.005 mmol) in 500  $\mu$ L DCM was added hydrazine (1  $\mu$ L, 0.007 mmol) and stirred for 30 min at room temperature. The precipitate was filtered off and the filtration was concentrated and dried over vacuum. Then 2,4-dimethylbenzene sulfonyl chloride (3.3 mg, 0.016 mmol) and DIPEA (1.2  $\mu$ L, 0.016 mmol) were added to a solution of the dried residue in acetonitrile and stirred for 1 h at room temperature. The reaction mixture was concentrated and the residue was purified by HPLC using acetonitrile with 0.1% trifluoroacetic acid (10 to 90%) in water with 0.1% trifluoroacetic acid to afford 0.8 mg of the designed product, yield 41.1%.  $^1\text{H}$  NMR ( $\text{CD}_3\text{OD}-d_4$ , 400 MHz):  $\delta$  7.62-7.50 (m, 4H), 7.42-7.20 (m, 3H), 5.72 (d, 1H,  $J = 8.8$  Hz), 4.13-3.92 (m, 2H), 3.72-3.63 (m, 1H), 3.58 (d, 1H,  $J = 11.2$  Hz), 3.23-2.85 (m, 4H), 2.56 (s, 3H), 2.50 (s, 3H), 2.35-2.22 (m, 1H), 2.15-2.02 (m, 2H), 1.98-1.73 (m, 2H), 1.72-0.78 (m, 3H). MS (*ESI+*):  $m/z$  485.2 (M+H).

**((1*S*,2*R*)-2-((*S*)-1-((4-Nitrophenylsulfonamido)methyl)-1,2,3,4-tetrahydroisoquinoline-2-carbonyl)cyclohexanecarboxylic acid (58).**



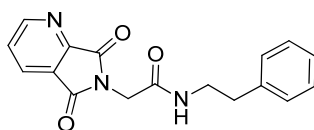
To a solution of LH601A (2 mg, 0.005 mmol) in 500  $\mu$ L DCM was added hydrazine (1  $\mu$ L, 0.007 mmol) and stirred for 1 h at room temperature. The precipitate was filtered off and the filtration was concentrated and dried over vacuum. Then 4-nitrobenzene sulfonyl chloride (2 mg, 0.09 mmol) and DIPEA (1.8  $\mu$ L, 0.07 mmol) were added to a solution of the dried residue in acetonitrile and stirred for 1 h at room temperature. The reaction mixture was concentrated and the residue was purified by HPLC using acetonitrile with 0.1% trifluoroacetic acid (10 to 90%) in water with 0.1% trifluoroacetic acid to afford 0.9 mg of the designed product, yield 40.9%.  $^1\text{H NMR}$  ( $\text{CD}_3\text{OD}-d_4$ , 400 MHz):  $\delta$  8.15 (d, 2H,  $J = 16.2$  Hz), 7.96 (d, 2H,  $J = 10.2$  Hz), 7.62-7.49 (m, 4H), 5.75 (dd, 1H,  $J = 10.6, 15.2$  Hz), 4.08-3.82 (m, 2H), 3.73-3.63 (m, 1H), 3.55 (d, 1H,  $J = 7.8$  Hz), 3.34-2.93 (m, 4H), 2.35-2.23 (m, 1H), 2.15-2.01 (m, 2H), 1.98-1.62 (m, 3H), 1.61-0.88 (m, 2H). MS ( $\text{ESI}^+$ ):  $m/z$  502.1 (M+H).

**2-(5,7-Dioxo-5*H*-pyrrolo[3,4-*b*]pyridin-6(7*H*)-yl)acetic acid (107).**



Glycine (**17**, 251 mg; 3.3 mmol) and anhydride (**106**, 500 mg; 3.3 mmol) were added to 6 mL acetic acid and heated to reflux with stirring for 3 h and cooled to room temperature. The acetic acid was removed by reduced pressure and the residue was suspended in 50% aq. Ethanol. The obtained white solid was washed with 50% aq. ethanol and dried to get 412 mg of product, yield 59.6%.  $^1\text{H}$  NMR (DMSO- $d_6$ , 400 MHz):  $\delta$  8.88 (d, 1H,  $J = 11.4$  Hz), 8.31 (d, 1H,  $J = 12.6$  Hz), 7.82 (dd, 1H,  $J = 11.4, 13.2$  Hz), 4.39 (s, 2H).  $^{13}\text{C}$  NMR (DMSO- $d_6$ , 100 MHz)  $\delta$  173.6, 169.0, 158.3, 133.8, 132.1, 128.8, 127.9, 42.3. MS (ESI $^+$ ):  $m/z$  207.1 (M+H).

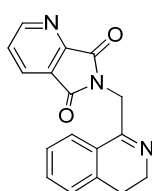
**2-(5,7-Dioxo-5H-pyrrolo[3,4-b]pyridin-6(7H)-yl)-N-phenethylacetamide (108).**



To a solution of **107** (100 mg, 0.48 mmol) in 15 mL acetonitrile was added phenylethylamine (60  $\mu\text{L}$ , 0.48 mmol), HBTU (182 mg, 0.48 mmol) and DIPEA (254  $\mu\text{L}$ , 1.46 mmol). The reaction mixture was stirred for 3 h at room temperature. Acetonitrile was removed by vacuum. The reaction mixture was then diluted with 50 mL DCM and washed with 0.5 N HCl solution, sat  $\text{NaHCO}_3$  solution, water and brine, then dried over anhydrous  $\text{Na}_2\text{SO}_4$ . The filtration was concentrated and the residue was purified by column chromatography using acetonitrile (0 to 100%) in DCM as eluent to afford 92 mg product, yield 61.3%.  $^1\text{H}$  NMR ( $\text{CDCl}_3$ , 400 MHz):  $\delta$  8.92 (d, 1H,  $J = 10.2$  Hz), 8.32 (d, 1H,  $J = 7.8$  Hz), 7.76 (dd, 1H), 7.46-7.18 (m, 5H), 4.42 (s, 2H,  $J = 6.8$  Hz), 3.49 (t, 2H,  $J = 5.8$  Hz), 3.23 (t, 2H,  $J = 4.6$  Hz).  $^{13}\text{C}$  NMR ( $\text{CDCl}_3$ , 100 MHz)  $\delta$  172.8, 167.6, 159.3,

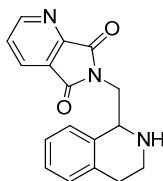
146.3, 143.8, 138.0, 131.9, 129.1, 127.8, 124.0, 123.2, 47.5, 39.6, 28.9. MS (*ESI+*): *m/z* 310.1 (M+H)

**6-((3,4-Dihydroisoquinolin-1-yl)methyl)-5H-pyrrolo[3,4-b]pyridine-5,7(6H)-dione (109).**



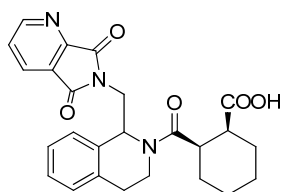
To a solution of **108** (30 mg, 0.1 mmol) in 10 mL p-xylene was added P<sub>2</sub>O<sub>5</sub> (41 mg, 0.29 mmol). The suspension was stirred for 4 h under reflux. The reaction mixture was cooled to room temperature and p-xylene was removed. 30 mL sat NaHCO<sub>3</sub> solution was added, then extracted with DCM (30 mL, 3x). The combined DCM extract was washed with water and brine, then dried over anhydrous Na<sub>2</sub>SO<sub>4</sub>. Filtered and the filtration was concentrated and dried over vacuum to afford the 16 mg desired product, yield 57.1%. <sup>1</sup>H NMR (CD<sub>3</sub>OD-*d*<sub>4</sub>, 400 MHz): δ 8.76 (d, 1H, *J* = 11.6 Hz), 8.16 (d, 1H, *J* = 7.4 Hz), 7.76 (dd, 1H, *J* = 6.8, 11.2 Hz), 7.52-7.01 (m, 4H), 4.01 (m, 1H), 3.69 (m, 2H), 3.58 (m, 2H), 3.23 (m, 1H). <sup>13</sup>C NMR (CD<sub>3</sub>OD-*d*<sub>4</sub>, 100 MHz): δ 176.3, 156.3, 147.2, 141.2, 136.9, 134.3, 129.3, 128.6, 127.5, 126.6, 125.3, 124.3, 123.8, 53.8, 41.5, 33.6. MS (*ESI+*): *m/z* 292.1 (M+H).

**6-((1,2,3,4-Tetrahydroisoquinolin-1-yl)methyl)-5H-pyrrolo[3,4-b]pyridine-5,7(6H)-dione (110).**



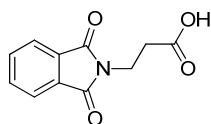
To a solution of **109** (16 mg, 0.05 mmol) in DCM (2 mL) was added acetic acid (4  $\mu$ L, 0.06 mmol) and  $\text{NaBH}(\text{OAc})_3$  (17.4 mg, 0.08 mmol). The obtained suspension was stirred at room temperature for 2 h and reaction mixture was diluted with DCM (30 mL), washed with water (2 x 20 mL) and brine (20 mL), then dried over anhydrous  $\text{Na}_2\text{SO}_4$ . Filtered and the organic layer was concentrated and the crude was purified by column chromatography (ISCO) using acetonitrile (0 to 100%) in DCM as eluent and fractions were concentrated to give 8.3 mg white solid, yield 52.6%.  $^1\text{H}$  NMR ( $\text{CD}_3\text{OD}-d_4$ , 400 MHz):  $\delta$  8.79 (d, 1H,  $J = 12.6$  Hz), 8.16 (d, 1H,  $J = 9.8$  Hz), 7.76 (dd, 1H,  $J = 7.8, 13.6$  Hz), 7.45-7.08 (m, 4H), 5.77 (d, 1H,  $J = 13.2$  Hz), 4.06 (m, 1H), 3.69 (m, 2H), 3.55 (m, 2H), 3.28 (m, 1H).  $^{13}\text{C}$  NMR ( $\text{CD}_3\text{OD}-d_4$ , 100 MHz):  $\delta$  176.8, 155.7, 147.3, 142.5, 136.9, 134.8, 129.3, 128.6, 127.9, 125.3, 124.9, 123.3, 51.9, 43.2, 41.5, 33.3. MS ( $\text{ESI}^+$ ):  $m/z$  294.1 (M+H).

**( $\pm$ )-cis-2-(1-((5,7-Dioxo-5H-pyrrolo[3,4-b]pyridin-6(7H)-yl)methyl)-1,2,3,4-tetrahydroisoquinoline-2-carbonyl)cyclohexanecarboxylic acid (60).**



To a solution of **110** (8.3 mg, 0.03 mmol) in 1.5 mL p-xylene was added *cis*-cyclohexyldicarboxylic anhydride (6.5 mg, 0.04 mmol) and stirred at 50 °C for 24 h. The reaction mixture was concentrated and the residue was purified by column chromatography (ISCO) using ethyl acetate (0 to 100%) in hexane as eluent to afford 10.6 mg desired product as a white powder, yield 84.1%. <sup>1</sup>H-NMR (CD<sub>3</sub>OD-*d*<sub>4</sub>, 400 MHz): δ 8.72 (d, 1H, *J* = 11.6 Hz), 8.23 (d, 1H, *J* = 13.6 Hz), 7.78 (dd, 1H, *J* = 11.2, 14.6 Hz), 7.45-7.03 (m, 4H), 5.89 (d, 1H, *J* = 9.8 Hz), 4.02 (m, 1H), 3.98 (m, 1H), 3.68 (m, 2H), 3.03 (d, 1H, *J* = 6.4 Hz), 2.78 (d, 1H, *J* = 4.8 Hz), 2.36 (m, 2H), 1.78-1.68 (m, 2H), 1.62-1.56 (m, 2H), 1.50-1.38 (m, 2H), 1.23-1.02 (m, 2H), <sup>13</sup>C NMR (CD<sub>3</sub>OD-*d*<sub>4</sub>, 100 MHz): δ 176.9, 175.2, 168.3, 156.8, 146.8, 141.2, 136.6, 134.9, 129.3, 128.5, 127.8, 126.8, 124.8, 123.9, 52.6, 46.5, 42.8, 41.3, 38.6, 32.1, 28.6, 26.6, 26.2, 25.6. MS (*ESI*<sup>+</sup>): *m/z* 448.1 (M+H).

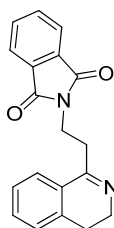
### 3-(1,3-Dioxoisindolin-2-yl)propanoic acid (**112**).



A mixture of phthalic anhydride (**16**, 1 g, 6.8 mmol) and beta-alanine (**111**, 570 mg, 6.8 mmol) were heated to 190-200°C in a sealed tube. Stirred for additional 30min at 190-200°C after the solids totally melted. The reaction mixture was cooled to room

temperature and 50% acetonitrile/water was added. The resulted suspension was filtered and the white precipitate was further washed with 50% acetonitrile/water, then dried under vacuum overnight to 1.3 g N-phthaloyl-beta-alanine, yield 76%.  $^1\text{H}$  NMR (DMSO- $d_6$ , 400 MHz):  $\delta$  13.36 (s, 1H), 7.93-7.82 (m, 4H), 4.12 (t, 2H,  $J = 7.6$  Hz), 2.89 (t, 2H,  $J = 4.8$  Hz).  $^{13}\text{C}$  NMR (DMSO- $d_6$ , 100 MHz)  $\delta$  170.3, 169.3, 158.9, 133.2, 132.8, 128.1, 36.8, 31.2. MS (*ESI+*):  $m/z$  220.1 (M+H).

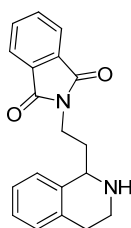
**2-(2-(3,4-Dihydroisoquinolin-1-yl)ethyl)isoindoline-1,3-dione (113).**



To a suspension of N-phthaloyl-beta-alanine (**112**, 200 mg, 0.9 mmol) and phenethylamine (132  $\mu\text{L}$ , 1.1 mmol) in  $\text{CH}_3\text{CN}$  (20 mL) was added  $\text{POCl}_3$  (831  $\mu\text{L}$ , 9 mmol). The resulting solution was heated at 85  $^\circ\text{C}$  for 24 h, then cooled to room temperature and concentrated under reduced pressure. The obtained dark residue was diluted with DCM (100 mL) and washed with aq.  $\text{NaHCO}_3$  (100 mL) and water (100 mL), then followed by brine (100 mL). The filtration was concentrated and the residue was purified by column chromatography using acetonitrile (0 to 100%) in DCM as eluent to afford the 120 mg desired product, yield 73%.  $^1\text{H}$  NMR (DMSO- $d_6$ , 400 MHz):  $\delta$  7.90 (m, 4H), 7.78 (d, 1H,  $J = 15.2$  Hz), 7.48 (m, 1H), 7.41 (d, 1H,  $J = 10.2$  Hz), 7.32 (d, 1H,  $J = 12.6$  Hz), 4.90 (t, 2H,  $J = 8.8$  Hz), 3.47 (t, 2H,  $J = 5.6$  Hz), 2.62 (t, 2H,  $J = 5.2$  Hz).  $^{13}\text{C}$

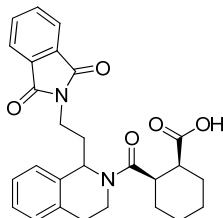
NMR (DMSO-*d*<sub>6</sub>, 100 MHz)  $\delta$  173.1, 159.8, 133.3, 132.1, 128.3, 127.9, 127.3, 123.9, 122.5, 118.2, 109.6, 41.6, 38.9, 32.3, 26.6. MS (*ESI*<sup>+</sup>): *m/z* 305.1 (M+H).

**2-(2-(1,2,3,4-Tetrahydroisoquinolin-1-yl)ethyl)isoindolin-1,3-dione (114).**



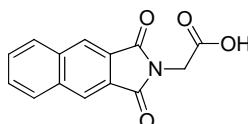
To a solution of **113** (150 mg, 0.5 mmol) in DCM (10 mL) was added acetic acid (36  $\mu$ L) and NaBH(OAc)<sub>3</sub> (159 mg, 0.75 mmol). The obtained suspension was stirred at room temperature for 1 h and reaction mixture was diluted with DCM (50 mL) and washed with sat NaHCO<sub>3</sub> solution (25 mL), water (2 x 25 mL) and brine (25 mL). The organic layer was concentrated and the crude was purified via column chromatography (ISCO) using acetonitrile (0 to 100%) in DCM as eluent and fractions were concentrated to give 160 mg of light colored product, yield 72%. <sup>1</sup>H NMR (CDCl<sub>3</sub>, 400 MHz):  $\delta$  7.81 (m, 4H), 7.22 (m, 4H), 4.36 (dd, 1H, *J* = 5.8 Hz), 4.08 (m, 1H), 3.89 (dd, 1H, *J* = 4.2, 7.8 Hz), 3.27 (m, 1H), 2.96 (m, 1H), 2.77 (m, 2H), 1.72 (s, 1H). <sup>13</sup>C NMR (CDCl<sub>3</sub>, 100 MHz):  $\delta$  168.9, 136.3, 134.6, 131.3, 128.9, 125.3, 126.6, 123.9, 114.2, 112.3, 53.3, 38.3, 36.8, 29.5, 25.6. MS (*ESI*<sup>+</sup>): *m/z* 293.2 (M+H).

**(1*S*,2*R*)-2-((±)-1-(2-(1,3-Dioxoisindolin-2-yl)ethyl)-1,2,3,4-tetrahydroisoquinoline-2-carbonyl)cyclohexanecarboxylic acid (61).**



To a solution of **114** (13 mg, 0.04 mmol) in 1 mL *p*-xylene was added *cis*-cyclohexyldicarboxylic anhydride (9.8 mg, 0.06 mmol) and stirred at 50 °C for 24 h. The reaction mixture was concentrated and the residue was purified via column chromatography (ISCO) using ethyl acetate (0 to 100%) in hexane as eluent to afford 15 mg product, yield 76.5%. Diastereomers were separated by HPLC using acetonitrile with 0.1% trifluoroacetic acid (30 to 90%) in water with 0.1% trifluoroacetic acid. <sup>1</sup>H NMR (CD<sub>3</sub>OD-*d*<sub>4</sub>, 400 MHz): δ 7.89-7.79 (m, 4H), 7.26-7.10 (m, 4H), 5.68 (dd, *J* = 4.2, 8.8 Hz, 1H), 4.12-3.50 (m, 4H), 3.49-3.38 (m, 2H), 3.20-3.03 (m, 2H), 2.68-2.50 (m, 1H), 2.40-2.00 (m, 4H), 1.92-1.51 (m, 3H), 1.50-1.32 (m, 2H). <sup>13</sup>C NMR (CD<sub>3</sub>OD-*d*<sub>4</sub>, 100 MHz): δ 176.9, 175.2, 168.3, 136.9, 135.4, 135.1, 132.5, 131.6, 128.9, 128.4, 126.6, 124.1, 51.9, 42.0, 41.1, 38.5, 33.6, 30.9, 29.3, 27.8, 28.5, 25.6, 24.9. MS (*ESI*<sup>+</sup>): *m/z* 461.2 (M+H).

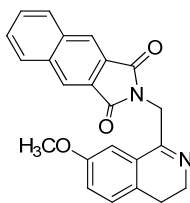
**2-(1,3-Dioxo-1*H*-benzo[*f*]isoindol-2(3*H*)-yl)acetic acid (116).**



To a suspension of 2,3-naphthalic anhydride (**115**, 2.0 g; 10 mmol) was added glycine (**17**, 752 mg; 10 mmol) and TEA (250 μL, 1 mmol). The mixture was heated to reflux for

24 h, then cooled to room temperature. The precipitate was collected and washed with DCM, then dried over vacuum to afford 2.12 g designed product, yield 82.5%.  $^1\text{H}$  NMR (DMSO- $d_6$ , 400 MHz):  $\delta$  7.83 (m, 2H), 7.36 (m, 4H), 4.28 (s, 2H).  $^{13}\text{C}$  NMR (DMSO- $d_6$ , 100 MHz)  $\delta$  169.3, 168.6, 136.6, 133.3, 128.9, 127.2, 125.3, 41.9. MS (ESI+):  $m/z$  256.1 (M+H).

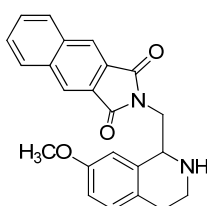
**2-((7-Methoxy-3,4-dihydroisoquinolin-1-yl)methyl)-1H-benzo[f]isoindole-1,3(2H)-dione (117).**



To a suspension of **116** (600 mg, 2.35 mmol) and 4-methoxyphenethylamine (327  $\mu\text{L}$ , 2.35 mmol) in acetonitrile (100 mL) was added  $\text{POCl}_3$  (644  $\mu\text{L}$ , 7.05 mmol). The resulting solution was heated at 85  $^\circ\text{C}$  for 24 h, then cooled to room temperature and concentrated under reduced pressure. The obtained dark residue was diluted with DCM (100 mL) and washed with aq.  $\text{NaHCO}_3$  (100 mL) and water (100 mL), then followed by brine (100 mL). The organic layer was concentrated and the crude was purified by column chromatography using acetonitrile (0 to 100%) in DCM as eluent to get 426 mg of light yellow solid product, yield 48.9%.  $^1\text{H}$  NMR ( $\text{CDCl}_3$ , 400 MHz):  $\delta$  8.23-8.15 (m, 2H), 8.02 (m, 2H), 7.56 (m, 2H), 7.25-6.78 (m, 3H), 4.96 (s, 2H), 3.85 (s, 3H), 3.66 (t, 2H,  $J = 7.8$  Hz), 2.69 (t, 2H,  $J = 4.4$  Hz).  $^{13}\text{C}$  NMR ( $\text{CDCl}_3$ , 100 MHz)  $\delta$  169.9, 156.3,

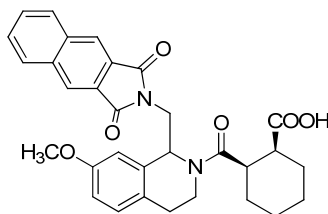
133.8, 133.2, 129.8, 128.3, 128.0, 126.6, 125.8, 123.6, 123.3, 116.9, 109.5, 55.5, 47.2, 41.9, 25.8. MS (*ESI+*):  $m/z$  371.1 (M+H).

**2-((7-Methoxy-1,2,3,4-tetrahydroisoquinolin-1-yl)methyl)-1*H*-benzo[*f*]isoindole-1,3(2*H*)-dione (119).**



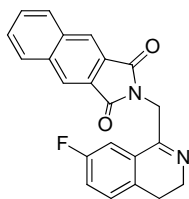
To a solution of **117** (400 mg, 1.1 mmol) in DCM (50 mL) was added acetic acid (78  $\mu$ L, 1.3 mmol) and  $\text{NaBH}(\text{OAc})_3$  (343 mg, 1.6 mmol). The obtained suspension was stirred at room temperature for 2 h and reaction mixture was diluted with DCM (100 mL) and washed with water (2 x 50 mL) and brine (50 mL). The organic layer was concentrated and the crude was purified by column chromatography using acetonitrile (0 to 100%) in DCM as eluent to give 312 mg product, yield 78%.  $^1\text{H}$  NMR ( $\text{CDCl}_3$ , 400 MHz):  $\delta$  8.26-8.09 (m, 2H), 8.01 (m, 2H), 7.62 (m, 2H), 7.33-6.83 (m, 3H), 4.35 (d, 1H,  $J = 6.6$  Hz), 4.08 (m, 1H), 3.89 (d, 1H,  $J = 10.4$  Hz), 3.85 (s, 3H), 3.29 (m, 1H), 2.93 (m, 1H), 2.73 (m, 2H).  $^{13}\text{C}$  NMR ( $\text{CDCl}_3$ , 100 MHz):  $\delta$  168.3, 155.3, 136.6, 134.3, 132.2, 131.5, 130.4, 127.9, 125.6, 123.6, 112.8, 110.9, 55.8, 53.2, 42.1, 39.6, 28.5. MS (*ESI+*):  $m/z$  373.2 (M+H).

(±)-*cis*-2-(1-((1,3-Dioxo-1*H*-benzo[*f*]isoindol-2(3*H*)-yl)methyl)-7-methoxy-1,2,3,4-tetrahydroisoquinoline-2-carbonyl)cyclohexanecarboxylic acid (**63**).



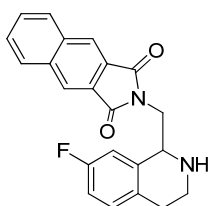
To a solution of **119** (260 mg, 0.7 mmol) in 50 mL *p*-xylene was added *cis*-cyclohexyldicarboxylic anhydride (216 mg, 1.4 mmol) and stirred at 50 °C for 24 h. The reaction mixture was concentrated and the crude was purified via column chromatography (ISCO) using acetonitrile (0 to 20%) in DCM as eluent to afford 296 mg white powder, yield 80.6%. <sup>1</sup>H NMR (CD<sub>3</sub>OD-*d*<sub>4</sub>, 400 MHz): δ 8.22-8.03 (m, 2H), 7.93 (m, 2H), 7.65 (m, 2H), 7.36-6.80 (m, 3H), 5.92 (dd, 1H, *J* = 6.8, 8.6 Hz), 5.23 (d, 1H, *J* = 11.2 Hz), 4.43-4.23 (m, 1H), 4.21-4.00 (m, 2H), 3.83 (s, 3H), 3.80-3.52 (m, 2H), 3.12-2.53 (m, 2H), 2.45-2.28 (m, 2H), 2.20-1.89 (m, 2H), 1.85-1.56 (m, 2H), 1.50-0.89 (m, 2H). <sup>13</sup>C NMR (CD<sub>3</sub>OD-*d*<sub>4</sub>, 100 MHz): δ 177.2, 169.8, 168.5, 146.5, 136.2, 134.5, 133.1, 131.2, 128.9, 128.3, 127.5, 126.5, 125.3, 124.8, 55.3, 51.1, 44.6, 42.2, 41.2, 38.9, 32.6, 29.1, 28.9, 28.1, 25.2. MS (*ESI*<sup>+</sup>): *m/z* 527.1 (M+H).

2-((7-Fluoro-3,4-dihydroisoquinolin-1-yl)methyl)-1*H*-benzo[*f*]isoindole-1,3(2*H*)-dione (**118**).



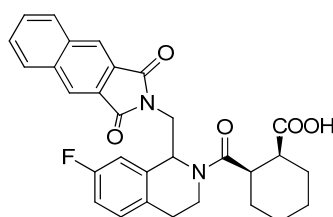
To a suspension of **116** (600 mg, 2.35 mmol) and 4-fluorophenethylamine (327  $\mu$ L, 2.35 mmol) in acetonitrile (100 mL) was added POCl<sub>3</sub> (644  $\mu$ L, 7.05 mmol). The resulting solution was heated at 85 °C for 24 h, then cooled to room temperature and concentrated under reduced pressure. The obtained dark residue was diluted with DCM (100 mL) and washed with aq. NaHCO<sub>3</sub> (100 mL) and water (100 mL), then followed by brine (100 mL). The organic layer was concentrated and the crude was purified by column chromatography using acetonitrile (0 to 100%) in DCM as eluent to get 460 mg of light yellow solid product, yield 54.5%. <sup>1</sup>H NMR (CDCl<sub>3</sub>, 400 MHz):  $\delta$  8.28-8.10 (m, 2H), 8.01 (m, 2H), 7.62 (m, 2H), 7.33-6.79 (m, 3H), 4.92 (s, 2H), 3.78 (s, 3H), 3.58 (t, 2H,  $J = 7.8$  Hz), 2.78 (t, 2H,  $J = 8.4$  Hz). <sup>13</sup>C NMR (CDCl<sub>3</sub>, 100 MHz)  $\delta$  169.8, 155.2, 133.5, 133.2, 129.5, 127.3, 126.9, 126.6, 125.3, 123.6, 123.6, 115.3, 109.9, 55.2, 47.1, 43.2, 26.8. MS (ESI<sup>+</sup>):  $m/z$  359.2 (M+H).

**2-((7-Fluoro-1,2,3,4-tetrahydroisoquinolin-1-yl)methyl)-1H-benzo[f]isindole-1,3(2H)-dione (120).**



To a solution of **118** (460 mg, 1.3 mmol) in DCM (20 mL) was added acetic acid (169  $\mu$ L, 2.82 mmol) and NaBH(OAc)<sub>3</sub> (747 mg, 3.5 mmol). The obtained suspension was stirred at room temperature for 1 h and reaction mixture was diluted with DCM (50 mL) and washed with water (2 x 25 mL) and brine (25 mL). The organic layer was concentrated and the crude was purified by column chromatography using acetonitrile (0 to 100%) in DCM as eluent to give 322 mg of light colored product, yield 70%. <sup>1</sup>H NMR (CDCl<sub>3</sub>, 400 MHz):  $\delta$  8.26-8.03 (m, 2H), 7.95 (m, 2H), 7.66 (m, 2H), 7.31-6.80 (m, 3H), 4.45 (d, 1H, *J* = 7.2 Hz), 4.12 (m, 1H), 3.83 (d, 1H, *J* = 8.6 Hz), 3.83 (s, 3H), 3.29 (m, 1H), 2.95 (m, 1H), 2.76 (m, 2H). <sup>13</sup>C NMR (CDCl<sub>3</sub>, 100 MHz):  $\delta$  169.5, 156.2, 136.6, 134.6, 132.1, 131.2, 130.4, 128.3, 125.6, 123.3, 112.5, 111.3, 55.5, 53.1, 42.8, 39.8, 26.9. MS (*ESI*<sup>+</sup>): *m/z* 361.1 (M+H).

**(±)-cis-2-(1-((1,3-Dioxo-1H-benzo[f]isoindol-2(3H)-yl)methyl)-7-fluoro-1,2,3,4-tetrahydroisoquinoline-2-carbonyl)cyclohexanecarboxylic acid (64).**



To a solution of **118** (300 mg, 0.83 mmol) in 50 mL *p*-xylene was added *cis*-cyclohexyldicarboxylic anhydride (256 mg, 1.66 mmol) and stirred at 50 °C for 24 h. The reaction mixture was concentrated and the crude was purified via column chromatography (ISCO) using acetonitrile (0 to 20%) in DCM as eluent to afford 353 mg white powder, yield 82.6%. <sup>1</sup>H-NMR (CD<sub>3</sub>OD-*d*<sub>4</sub>, 400 MHz):  $\delta$  8.31-8.12 (m, 2H), 7.96

(m, 2H), 7.69 (m, 2H), 7.45-6.92 (m, 3H), 5.95 (dd, 1H,  $J = 6.8, 9.4$  Hz), 5.26 (d, 1H,  $J = 9.2$  Hz), 4.43-4.21 (m, 1H), 4.18-4.01 (m, 2H), 3.90-3.61 (m, 2H), 3.06-2.55 (m, 2H), 2.50-2.19 (m, 2H), 1.98-1.76 (m, 2H), 1.73-1.56 (m, 2H), 1.51-0.88 (m, 2H).  $^{13}\text{C}$  NMR ( $\text{CD}_3\text{OD}-d_4$ , 100 MHz):  $\delta$  177.9, 169.8, 168.8, 146.2, 138.1, 135.2, 133.1, 131.6, 128.3, 128.1, 127.5, 126.1, 125.6, 122.9, 55.8, 51.8, 44.5, 42.1, 41.5, 38.0, 32.5, 29.0, 28.5, 27.6, 25.8. MS (*ESI+*):  $m/z$  515.1 (M+H).

#### **Stability Study of Selected Heterocyclic Curcumin Analogs.**

To 990  $\mu\text{L}$  Dulbecco's Modified Eagle's Medium (pH 7.4) with 5% methanol in the absence or presence of 1% FBS was added 10  $\mu\text{L}$  of 10 mM tested compound in DMSO and incubated at 37  $^\circ\text{C}$ . At different time intervals, aliquots (50  $\mu\text{L}$ ) were withdrawn and subjected to HPLC analysis (YMC-ODS-A column, 5  $\mu\text{m}$ , 4.6 x 50 mm, gradient elution from 10-90% acetonitrile containing 0.1% TFA at a flow rate at 1 mL/min, detection wavelength at 220 nm and 254 nm). The half-life was determined based on the disappearance of the test compound.

#### **ARE-induction in an ARE-luciferase reporter assay in SW480 cell line.**

Human colon cancer cell line SW480 (from ATCC) was routinely maintained in RPMI medium supplemented with 10% FBS, 2 mM L-glutamine, 100 U/ml of penicillin, and 100  $\mu\text{g}/\text{ml}$  of streptomycin at 37  $^\circ\text{C}$  in 5%  $\text{CO}_2$ . To establish the ARE-luciferase reporter cells, SW480 cells were infected with the lentivirus carrying ARE-luciferase reporter and a puromycin selection marker (Superarray/Qiagen), and stable cells were selected using

puromycin (5 g/ml). To determine the effects of novel heterocyclic curcumin analogs, SW480 cells stably carrying ARE-luciferase reporter were seeded onto 96-well culture plate at the density of 10,000 cells/well in 5% FBS RPMI medium. After overnight culture, cells were treated with curcumin analogs at two doses, 1 and 10  $\mu$ M. Every treatment was performed in triplicates. SFN and curcumin were used as the positive controls. After 6-h treatment, culture medium was removed from culture wells, and cells were lysed in passive lysis buffer (Promega) (100  $\mu$ L/well). A 10  $\mu$ L of lysate of each well was transferred to 96-well luciferase assay plate. Luciferase activities were determined by GloMax®-96 Microplate Luminometer (Promega) using the luciferase assay substrate (Promega) loaded into 96-well assay plate automatically.

#### **Fluorescence Polarization Assay (FP Assay)**

A fluorescence polarization competition assay was established and miniaturized to a 384-well plate format to determine the potency of inhibitors of the Keap1-Nrf2 interaction. FITC labeled Nrf2 9mer peptide amide containing the ETGE motif were designed and synthesized as tracers to detect the direct inhibitors of Keap1-Nrf2 interaction. Each well had a final volume of 40  $\mu$ L that consisted of 10  $\mu$ L of 40 nM FITC-9mer Nrf2 peptide amide and 10  $\mu$ L of 400 nM Keap1 Kelch domain protein, 10  $\mu$ L of HEPES buffer, and 10  $\mu$ L of an inhibitor sample of varying concentrations. The binding experiments were performed in triplicates, with initial concentration of the inhibitor typically set between 5  $\mu$ M and 50  $\mu$ M depending on the inhibitor potency. The plate was centrifuged at 370 g for 2 min to get rid of any air bubbles in the assay solution and to ensure thorough

mixing. The plate was covered and allowed to equilibrate for 30 min at room temperature. The plate was centrifuged again prior to FP measurements.<sup>191</sup>

### **Surface Plasmon Resonance (SPR) Competition Assay**

The SPR competition binding assay was carried out on a Biacore 3000 biosensor (GE Healthcare) using the immobilized N-biotinylated 16mer Nrf2 peptide as the ligand and Keap1 Kelch domain as the analyte to evaluate the binding affinity of the analogs with Keap1 as described previously.<sup>192</sup> Briefly, the streptavidin surface on a CM5 chip was slowly saturated by the biotin-labeled Nrf2 peptide, and the maximum immobilization level of 300 RU was finally achieved. Fc1 of the chip without the Nrf2 peptide was used as the blank surface. All interactions between the Keap1 Kelch domain and the immobilized biotin-16mer Nrf2 peptide were carried out with a 1 min association time and a 3 min dissociation time at a flow rate of 30  $\mu\text{L}/\text{min}$ . The sensor chip surfaces were regenerated with a 0.5 min injection of 1 M NaCl at a flow rate of 30  $\mu\text{L}/\text{min}$ . The regeneration step was followed by two buffer washes of IFC and the needle. The data analysis was performed using BIA evaluation software v4.1 by measuring the slope of the initial association phase from the SPR sensograms after double subtraction of responses from the reference surface and the zero blank in the absence of the Keap1 Kelch domain. To calculate the concentrations of free (i.e., unbound) Keap1 Kelch domain, a standard curve was constructed using serially diluted solutions of Keap1 Kelch domain with concentrations covering the observed Keap1 Kelch domain concentrations in the competition assay. For the competition binding assay, a solution of Keap1 Kelch domain

at a fixed concentration of 20 nM or 40 nM and two concentrations of synthesized inhibitors at 5  $\mu$ M and 50  $\mu$ M was introduced over each surface (Fc1 and Fc2)

## REFERENCES

- (1) Frenkel, K. Carcinogen-mediated oxidant formation and oxidative DNA damage. *Pharmacol. Ther.* **1992**, *53*, 127-66.
- (2) Nath, R. G.; Ocando, J. E.; Chung, F. L. Detection of 1, N<sup>2</sup>-propanodeoxyguanosine adducts as potential endogenous DNA lesions in rodent and human tissues. *Cancer Res.* **1996**, *56*, 452-6.
- (3) Wiseman, H.; Halliwell, B. Damage to DNA by reactive oxygen and nitrogen species: role in inflammatory disease and progression to cancer. *Biochem. J.* **1996**, *313* ( Pt 1), 17-29.
- (4) Klaunig, J. E.; Kamendulis, L. M. The role of oxidative stress in carcinogenesis. *Annu. Rev. Pharmacol. Toxicol.* **2004**, *44*, 239-67.
- (5) Finkel, T.; Holbrook, N. J. Oxidants, oxidative stress and the biology of ageing. *Nature* **2000**, *408*, 239-47.
- (6) Leeuwenburgh, C.; Heinecke, J. W. Oxidative stress and antioxidants in exercise. *Curr. Med. Chem.* **2001**, *8*, 829-38.
- (7) Wojcik, M.; Burzynska-Pedziwiatr, I.; Wozniak, L. A. A review of natural and synthetic antioxidants important for health and longevity. *Curr. Med. Chem.* **2010**, *17*, 3262-88.
- (8) Giudice, A.; Montella, M. Activation of the Nrf2-ARE signaling pathway: a promising strategy in cancer prevention. *Bioessays* **2006**, *28*, 169-81.
- (9) Morgan, P. E.; Dean, R. T.; Davies, M. J. Inactivation of cellular enzymes by carbonyls and protein-bound glycation/glycooxidation products. *Arch. Biochem. Biophys.* **2002**, *403*, 259-69.
- (10) Lee, C.; Yim, M. B.; Chock, P. B.; Yim, H. S.; Kang, S. O. Oxidation-reduction properties of methylglyoxal-modified protein in relation to free radical generation. *J. Biol. Chem.* **1998**, *273*, 25272-8.
- (11) Barnham, K. J.; Masters, C. L.; Bush, A. I. Neurodegenerative diseases and oxidative stress. *Nat. Rev. Drug Discov.* **2004**, *3*, 205-14.
- (12) Benz, C. C.; Yau, C. Ageing, oxidative stress and cancer: paradigms in parallax. *Nat. Rev. Cancer* **2008**, *8*, 875-9.

- (13) Khansari, N.; Shakiba, Y.; Mahmoudi, M. Chronic inflammation and oxidative stress as a major cause of age-related diseases and cancer. *Recent Pat. Inflamm. Allergy Drug Discov.* **2009**, *3*, 73-80.
- (14) Federico, A.; Morgillo, F.; Tuccillo, C.; Ciardiello, F.; Loguercio, C. Chronic inflammation and oxidative stress in human carcinogenesis. *Int. J. Cancer* **2007**, *121*, 2381-6.
- (15) Sayre, L. M.; Perry, G.; Smith, M. A. Oxidative stress and neurotoxicity. *Chem. Res. Toxicol.* **2008**, *21*, 172-88.
- (16) Magesh, S.; Chen, Y.; Hu, L. Small molecule modulators of Keap1-Nrf2-ARE pathway as potential preventive and therapeutic agents. *Med. Res. Rev.* **2012**, *32*, 687-726.
- (17) Balkwill, F.; Charles, K. A.; Mantovani, A. Smoldering and polarized inflammation in the initiation and promotion of malignant disease. *Cancer Cell* **2005**, *7*, 211-7.
- (18) Sporn, M. B.; Liby, K. T. Cancer chemoprevention: scientific promise, clinical uncertainty. *Nat. Clin. Pract. Oncol.* **2005**, *2*, 518-25.
- (19) Hayes, J. D.; McMahon, M. NRF2 and KEAP1 mutations: permanent activation of an adaptive response in cancer. *Trends Biochem. Sci.* **2009**, *34*, 176-88.
- (20) Kensler, T. W.; Wakabayashi, N.; Biswal, S. Cell survival responses to environmental stresses via the Keap1-Nrf2-ARE pathway. *Annu. Rev. Pharmacol. Toxicol.* **2007**, *47*, 89-116.
- (21) Lee, J. M.; Johnson, J. A. An important role of Nrf2-ARE pathway in the cellular defense mechanism. *J. Biochem. Mol. Biol.* **2004**, *37*, 139-43.
- (22) Taguchi, K.; Motohashi, H.; Yamamoto, M. Molecular mechanisms of the Keap1-Nrf2 pathway in stress response and cancer evolution. *Genes Cells* **2011**, *16*, 123-40.
- (23) Hu, R.; Saw, C. L.; Yu, R.; Kong, A. N. Regulation of NF-E2-related factor 2 signaling for cancer chemoprevention: antioxidant coupled with antiinflammatory. *Antioxid. Redox Signal* **2010**, *13*, 1679-98.
- (24) Singh, S.; Vrishni, S.; Singh, B. K.; Rahman, I.; Kakkar, P. Nrf2-ARE stress response mechanism: a control point in oxidative stress-mediated dysfunctions and chronic inflammatory diseases. *Free Radic. Res.* **2010**, *44*, 1267-88.
- (25) Talalay, P. Chemoprotection against cancer by induction of phase 2 enzymes. *Biofactors* **2000**, *12*, 5-11.

- (26) Nguyen, T.; Sherratt, P. J.; Pickett, C. B. Regulatory mechanisms controlling gene expression mediated by the antioxidant response element. *Annu. Rev. Pharmacol. Toxicol.* **2003**, *43*, 233-60.
- (27) Dinkova-Kostova, A. T.; Talalay, P. Direct and indirect antioxidant properties of inducers of cytoprotective proteins. *Mol. Nutr. Food Res.* **2008**, *52 Suppl 1*, S128-38.
- (28) Holtzclaw, W. D.; Dinkova-Kostova, A. T.; Talalay, P. Protection against electrophile and oxidative stress by induction of phase 2 genes: the quest for the elusive sensor that responds to inducers. *Adv. Enzyme Regul.* **2004**, *44*, 335-67.
- (29) Kansanen, E.; Kuosmanen, S. M.; Leinonen, H.; Levonen, A. L. The Keap1-Nrf2 pathway: Mechanisms of activation and dysregulation in cancer. *Redox Biol.* **2013**, *1*, 45-49.
- (30) Kansanen, E.; Jyrkkanen, H. K.; Levonen, A. L. Activation of stress signaling pathways by electrophilic oxidized and nitrated lipids. *Free Radic. Biol. Med.* **2012**, *52*, 973-82.
- (31) Nguyen, T.; Yang, C. S.; Pickett, C. B. The pathways and molecular mechanisms regulating Nrf2 activation in response to chemical stress. *Free Radic. Biol. Med.* **2004**, *37*, 433-41.
- (32) Stewart, J. D.; Hengstler, J. G.; Bolt, H. M. Control of oxidative stress by the Keap1-Nrf2 pathway. *Arch. Toxicol.* **2011**, *85*, 239.
- (33) Baird, L.; Dinkova-Kostova, A. T. The cytoprotective role of the Keap1-Nrf2 pathway. *Arch. Toxicol.* **2011**, *85*, 241-72.
- (34) Zhang, Y.; Gordon, G. B. A strategy for cancer prevention: stimulation of the Nrf2-ARE signaling pathway. *Mol. Cancer Ther.* **2004**, *3*, 885-93.
- (35) Prestera, T.; Zhang, Y.; Spencer, S. R.; Wilczak, C. A.; Talalay, P. The electrophile counterattack response: protection against neoplasia and toxicity. *Adv. Enzyme Regul.* **1993**, *33*, 281-96.
- (36) Lyakhovich, V. V.; Vavilin, V. A.; Zenkov, N. K.; Menshchikova, E. B. Active defense under oxidative stress. The antioxidant responsive element. *Biochemistry (Mosc)* **2006**, *71*, 962-74.
- (37) Calkins, M. J.; Johnson, D. A.; Townsend, J. A.; Vargas, M. R.; Dowell, J. A.; Williamson, T. P.; Kraft, A. D.; Lee, J. M.; Li, J.; Johnson, J. A. The Nrf2/ARE pathway as a potential therapeutic target in neurodegenerative disease. *Antioxid. Redox Signal* **2009**, *11*, 497-508.

- (38) Jeong, W. S.; Jun, M.; Kong, A. N. Nrf2: a potential molecular target for cancer chemoprevention by natural compounds. *Antioxid. Redox Signal* **2006**, *8*, 99-106.
- (39) Lau, A.; Villeneuve, N. F.; Sun, Z.; Wong, P. K.; Zhang, D. D. Dual roles of Nrf2 in cancer. *Pharmacol. Res.* **2008**, *58*, 262-70.
- (40) Yates, M. S.; Kensler, T. W. Chemopreventive promise of targeting the Nrf2 pathway. *Drug News Perspect* **2007**, *20*, 109-17.
- (41) Li, J.; Ichikawa, T.; Janicki, J. S.; Cui, T. Targeting the Nrf2 pathway against cardiovascular disease. *Expert Opin. Ther. Targets* **2009**, *13*, 785-94.
- (42) Yu, X.; Kensler, T. Nrf2 as a target for cancer chemoprevention. *Mutat. Res.* **2005**, *591*, 93-102.
- (43) Hu, L.; Magesh, S.; Chen, L.; Wang, L.; Lewis, T. A.; Chen, Y.; Khodier, C.; Inoyama, D.; Beamer, L. J.; Emge, T. J.; Shen, J.; Kerrigan, J. E.; Kong, A. N.; Dandapani, S.; Palmer, M.; Schreiber, S. L.; Munoz, B. Discovery of a small-molecule inhibitor and cellular probe of Keap1-Nrf2 protein-protein interaction. *Bioorg. Med. Chem. Lett.* **2013**, *23*, 3039-43.
- (44) Kansanen, E.; Kivela, A. M.; Levonen, A. L. Regulation of Nrf2-dependent gene expression by 15-deoxy-Delta12,14-prostaglandin J2. *Free Radic. Biol. Med.* **2009**, *47*, 1310-7.
- (45) Uruno, A.; Motohashi, H. The Keap1-Nrf2 system as an in vivo sensor for electrophiles. *Nitric Oxide* **2011**, *25*, 153-60.
- (46) Zhang, D. D. Mechanistic studies of the Nrf2-Keap1 signaling pathway. *Drug Metab. Rev.* **2006**, *38*, 769-89.
- (47) Wakabayashi, N.; Dinkova-Kostova, A. T.; Holtzclaw, W. D.; Kang, M. I.; Kobayashi, A.; Yamamoto, M.; Kensler, T. W.; Talalay, P. Protection against electrophile and oxidant stress by induction of the phase 2 response: fate of cysteines of the Keap1 sensor modified by inducers. *Proc. Natl. Acad. Sci. U S A* **2004**, *101*, 2040-5.
- (48) Kang, M. I.; Kobayashi, A.; Wakabayashi, N.; Kim, S. G.; Yamamoto, M. Scaffolding of Keap1 to the actin cytoskeleton controls the function of Nrf2 as key regulator of cytoprotective phase 2 genes. *Proc. Natl. Acad. Sci. U S A* **2004**, *101*, 2046-51.
- (49) Kobayashi, A.; Kang, M. I.; Okawa, H.; Ohtsuji, M.; Zenke, Y.; Chiba, T.; Igarashi, K.; Yamamoto, M. Oxidative stress sensor Keap1 functions as an adaptor for Cul3-based E3 ligase to regulate proteasomal degradation of Nrf2. *Mol. Cell Biol.* **2004**, *24*, 7130-9.

- (50) Zipper, L. M.; Mulcahy, R. T. The Keap1 BTB/POZ dimerization function is required to sequester Nrf2 in cytoplasm. *J. Biol. Chem.* **2002**, *277*, 36544-52.
- (51) Dinkova-Kostova, A. T.; Holtzclaw, W. D.; Cole, R. N.; Itoh, K.; Wakabayashi, N.; Katoh, Y.; Yamamoto, M.; Talalay, P. Direct evidence that sulfhydryl groups of Keap1 are the sensors regulating induction of phase 2 enzymes that protect against carcinogens and oxidants. *Proc. Natl. Acad. Sci. U S A* **2002**, *99*, 11908-13.
- (52) Luo, Y.; Egger, A. L.; Liu, D.; Liu, G.; Mesecar, A. D.; van Breemen, R. B. Sites of alkylation of human Keap1 by natural chemoprevention agents. *J. Am. Soc. Mass Spectrom.* **2007**, *18*, 2226-32.
- (53) Itoh, K.; Chiba, T.; Takahashi, S.; Ishii, T.; Igarashi, K.; Katoh, Y.; Oyake, T.; Hayashi, N.; Satoh, K.; Hatayama, I.; Yamamoto, M.; Nabeshima, Y. An Nrf2/small Maf heterodimer mediates the induction of phase II detoxifying enzyme genes through antioxidant response elements. *Biochem. Biophys. Res. Commun.* **1997**, *236*, 313-22.
- (54) Itoh, K.; Wakabayashi, N.; Katoh, Y.; Ishii, T.; Igarashi, K.; Engel, J. D.; Yamamoto, M. Keap1 represses nuclear activation of antioxidant responsive elements by Nrf2 through binding to the amino-terminal Neh2 domain. *Genes Dev.* **1999**, *13*, 76-86.
- (55) Katoh, Y.; Itoh, K.; Yoshida, E.; Miyagishi, M.; Fukamizu, A.; Yamamoto, M. Two domains of Nrf2 cooperatively bind CBP, a CREB binding protein, and synergistically activate transcription. *Genes Cells* **2001**, *6*, 857-68.
- (56) McMahon, M.; Thomas, N.; Itoh, K.; Yamamoto, M.; Hayes, J. D. Redox-regulated turnover of Nrf2 is determined by at least two separate protein domains, the redox-sensitive Neh2 degron and the redox-insensitive Neh6 degron. *J. Biol. Chem.* **2004**, *279*, 31556-67.
- (57) Zhang, Y.; Crouch, D. H.; Yamamoto, M.; Hayes, J. D. Negative regulation of the Nrf1 transcription factor by its N-terminal domain is independent of Keap1: Nrf1, but not Nrf2, is targeted to the endoplasmic reticulum. *Biochem. J.* **2006**, *399*, 373-85.
- (58) Nioi, P.; Nguyen, T.; Sherratt, P. J.; Pickett, C. B. The carboxy-terminal Neh3 domain of Nrf2 is required for transcriptional activation. *Mol. Cell Biol.* **2005**, *25*, 10895-906.
- (59) Jain, A. K.; Bloom, D. A.; Jaiswal, A. K. Nuclear import and export signals in control of Nrf2. *J. Biol. Chem.* **2005**, *280*, 29158-68.

- (60) Kobayashi, M.; Itoh, K.; Suzuki, T.; Osanai, H.; Nishikawa, K.; Katoh, Y.; Takagi, Y.; Yamamoto, M. Identification of the interactive interface and phylogenetic conservation of the Nrf2-Keap1 system. *Genes Cells* **2002**, *7*, 807-20.
- (61) Katsuoka, F.; Motohashi, H.; Ishii, T.; Aburatani, H.; Engel, J. D.; Yamamoto, M. Genetic evidence that small maf proteins are essential for the activation of antioxidant response element-dependent genes. *Mol. Cell Biol.* **2005**, *25*, 8044-51.
- (62) Li, W.; Kong, A. N. Molecular mechanisms of Nrf2-mediated antioxidant response. *Mol. Carcinog.* **2009**, *48*, 91-104.
- (63) Zhang, D. D.; Hannink, M. Distinct cysteine residues in Keap1 are required for Keap1-dependent ubiquitination of Nrf2 and for stabilization of Nrf2 by chemopreventive agents and oxidative stress. *Mol. Cell Biol.* **2003**, *23*, 8137-51.
- (64) Rachakonda, G.; Xiong, Y.; Sekhar, K. R.; Stamer, S. L.; Liebler, D. C.; Freeman, M. L. Covalent modification at Cys151 dissociates the electrophile sensor Keap1 from the ubiquitin ligase CUL3. *Chem. Res. Toxicol.* **2008**, *21*, 705-10.
- (65) Wasserman, W. W.; Fahl, W. E. Functional antioxidant responsive elements. *Proc. Natl. Acad. Sci. U S A* **1997**, *94*, 5361-6.
- (66) Sykiotis, G. P.; Bohmann, D. Stress-activated cap'n'collar transcription factors in aging and human disease. *Sci. Signal* **2010**, *3*, re3.
- (67) Dhakshinamoorthy, S.; Jain, A. K.; Bloom, D. A.; Jaiswal, A. K. Bach1 competes with Nrf2 leading to negative regulation of the antioxidant response element (ARE)-mediated NAD(P)H:quinone oxidoreductase 1 gene expression and induction in response to antioxidants. *J. Biol. Chem.* **2005**, *280*, 16891-900.
- (68) Rushmore, T. H.; Morton, M. R.; Pickett, C. B. The antioxidant responsive element. Activation by oxidative stress and identification of the DNA consensus sequence required for functional activity. *J. Biol. Chem.* **1991**, *266*, 11632-9.
- (69) McMahon, M.; Itoh, K.; Yamamoto, M.; Hayes, J. D. Keap1-dependent proteasomal degradation of transcription factor Nrf2 contributes to the negative regulation of antioxidant response element-driven gene expression. *J. Biol. Chem.* **2003**, *278*, 21592-600.
- (70) Nguyen, T.; Sherratt, P. J.; Huang, H. C.; Yang, C. S.; Pickett, C. B. Increased protein stability as a mechanism that enhances Nrf2-mediated transcriptional activation of the antioxidant response element. Degradation of Nrf2 by the 26 S proteasome. *J. Biol. Chem.* **2003**, *278*, 4536-41.

- (71) Cullinan, S. B.; Gordan, J. D.; Jin, J.; Harper, J. W.; Diehl, J. A. The Keap1-BTB protein is an adaptor that bridges Nrf2 to a Cul3-based E3 ligase: oxidative stress sensing by a Cul3-Keap1 ligase. *Mol. Cell Biol.* **2004**, *24*, 8477-86.
- (72) Malhotra, D.; Portales-Casamar, E.; Singh, A.; Srivastava, S.; Arenillas, D.; Happel, C.; Shyr, C.; Wakabayashi, N.; Kensler, T. W.; Wasserman, W. W.; Biswal, S. Global mapping of binding sites for Nrf2 identifies novel targets in cell survival response through ChIP-Seq profiling and network analysis. *Nucleic Acids Res.* **2010**, *38*, 5718-34.
- (73) Giudice, A.; Arra, C.; Turco, M. C. Review of molecular mechanisms involved in the activation of the Nrf2-ARE signaling pathway by chemopreventive agents. *Methods Mol. Biol.* **2010**, *647*, 37-74.
- (74) Zhang, D. D.; Lo, S. C.; Sun, Z.; Habib, G. M.; Lieberman, M. W.; Hannink, M. Ubiquitination of Keap1, a BTB-Kelch substrate adaptor protein for Cul3, targets Keap1 for degradation by a proteasome-independent pathway. *J. Biol. Chem.* **2005**, *280*, 30091-9.
- (75) Li, W.; Yu, S. W.; Kong, A. N. Nrf2 possesses a redox-sensitive nuclear exporting signal in the Neh5 transactivation domain. *J. Biol. Chem.* **2006**, *281*, 27251-63.
- (76) Suzuki, H.; Tashiro, S.; Sun, J.; Doi, H.; Satomi, S.; Igarashi, K. Cadmium induces nuclear export of Bach1, a transcriptional repressor of heme oxygenase-1 gene. *J. Biol. Chem.* **2003**, *278*, 49246-53.
- (77) Eggler, A. L.; Gay, K. A.; Mesecar, A. D. Molecular mechanisms of natural products in chemoprevention: induction of cytoprotective enzymes by Nrf2. *Mol. Nutr. Food Res.* **2008**, *52 Suppl 1*, S84-94.
- (78) Wu, K. C.; McDonald, P. R.; Liu, J. J.; Chaguturu, R.; Klaassen, C. D. Implementation of a high-throughput screen for identifying small molecules to activate the Keap1-Nrf2-ARE pathway. *PLoS One* **2012**, *7*, e44686.
- (79) Zhang, D. D. The Nrf2-Keap1-ARE signaling pathway: The regulation and dual function of Nrf2 in cancer. *Antioxid. Redox Signal* **2010**, *13*, 1623-6.
- (80) Hong, F.; Sekhar, K. R.; Freeman, M. L.; Liebler, D. C. Specific patterns of electrophile adduction trigger Keap1 ubiquitination and Nrf2 activation. *J. Biol. Chem.* **2005**, *280*, 31768-75.
- (81) McMahon, M.; Thomas, N.; Itoh, K.; Yamamoto, M.; Hayes, J. D. Dimerization of substrate adaptors can facilitate cullin-mediated ubiquitylation of proteins by a "tethering" mechanism: a two-site interaction model for the Nrf2-Keap1 complex. *J. Biol. Chem.* **2006**, *281*, 24756-68.

- (82) Zhang, Q.; Pi, J.; Woods, C. G.; Andersen, M. E. A systems biology perspective on Nrf2-mediated antioxidant response. *Toxicol. Appl. Pharmacol.* **2010**, *244*, 84-97.
- (83) Tong, K. I.; Kobayashi, A.; Katsuoka, F.; Yamamoto, M. Two-site substrate recognition model for the Keap1-Nrf2 system: a hinge and latch mechanism. *Biol. Chem.* **2006**, *387*, 1311-20.
- (84) Tong, K. I.; Padmanabhan, B.; Kobayashi, A.; Shang, C.; Hirotsu, Y.; Yokoyama, S.; Yamamoto, M. Different electrostatic potentials define ETGE and DLG motifs as hinge and latch in oxidative stress response. *Mol. Cell Biol.* **2007**, *27*, 7511-21.
- (85) Tong, K. I.; Katoh, Y.; Kusunoki, H.; Itoh, K.; Tanaka, T.; Yamamoto, M. Keap1 recruits Neh2 through binding to ETGE and DLG motifs: characterization of the two-site molecular recognition model. *Mol. Cell Biol.* **2006**, *26*, 2887-900.
- (86) Kobayashi, A.; Kang, M. I.; Watai, Y.; Tong, K. I.; Shibata, T.; Uchida, K.; Yamamoto, M. Oxidative and electrophilic stresses activate Nrf2 through inhibition of ubiquitination activity of Keap1. *Mol. Cell Biol.* **2006**, *26*, 221-9.
- (87) Egger, A. L.; Small, E.; Hannink, M.; Mesecar, A. D. Cul3-mediated Nrf2 ubiquitination and antioxidant response element (ARE) activation are dependent on the partial molar volume at position 151 of Keap1. *Biochem. J.* **2009**, *422*, 171-80.
- (88) Tkachev, V. O.; Menshchikova, E. B.; Zenkov, N. K. Mechanism of the Nrf2/Keap1/ARE signaling system. *Biochemistry (Mosc)* **2011**, *76*, 407-22.
- (89) Kaspar, J. W.; Jaiswal, A. K. An autoregulatory loop between Nrf2 and Cul3-Rbx1 controls their cellular abundance. *J. Biol. Chem.* **2010**, *285*, 21349-58.
- (90) Lukosz, M.; Jakob, S.; Buchner, N.; Zschauer, T. C.; Altschmied, J.; Haendeler, J. Nuclear redox signaling. *Antioxid. Redox Signal* **2010**, *12*, 713-42.
- (91) Stepkowski, T. M.; Kruszewski, M. K. Molecular cross-talk between the NRF2/KEAP1 signaling pathway, autophagy, and apoptosis. *Free Radic. Biol. Med.* **2011**, *50*, 1186-95.
- (92) Wakabayashi, N.; Slocum, S. L.; Skoko, J. J.; Shin, S.; Kensler, T. W. When NRF2 talks, who's listening? *Antioxid. Redox Signal* **2010**, *13*, 1649-63.
- (93) Wakabayashi, N.; Shin, S.; Slocum, S. L.; Agoston, E. S.; Wakabayashi, J.; Kwak, M. K.; Misra, V.; Biswal, S.; Yamamoto, M.; Kensler, T. W. Regulation of notch1 signaling by nrf2: implications for tissue regeneration. *Sci. Signal* **2010**, *3*, ra52.

- (94) Huang, H. C.; Nguyen, T.; Pickett, C. B. Regulation of the antioxidant response element by protein kinase C-mediated phosphorylation of NF-E2-related factor 2. *Proc. Natl. Acad. Sci. U S A* **2000**, *97*, 12475-80.
- (95) Clerk, A.; Sugden, P. H. Untangling the Web: specific signaling from PKC isoforms to MAPK cascades. *Circ. Res.* **2001**, *89*, 847-9.
- (96) Huang, H. C.; Nguyen, T.; Pickett, C. B. Phosphorylation of Nrf2 at Ser-40 by protein kinase C regulates antioxidant response element-mediated transcription. *J. Biol. Chem.* **2002**, *277*, 42769-74.
- (97) Chen, C. Y.; Jang, J. H.; Li, M. H.; Surh, Y. J. Resveratrol upregulates heme oxygenase-1 expression via activation of NF-E2-related factor 2 in PC12 cells. *Biochem. Biophys. Res. Commun.* **2005**, *331*, 993-1000.
- (98) Reuter, S.; Gupta, S. C.; Chaturvedi, M. M.; Aggarwal, B. B. Oxidative stress, inflammation, and cancer: how are they linked? *Free Radic. Biol. Med.* **2010**, *49*, 1603-16.
- (99) Kern, J. T.; Hannink, M.; Hess, J. F. Disruption of the Keap1-containing ubiquitination complex as an antioxidant therapy. *Curr. Top. Med. Chem.* **2007**, *7*, 972-8.
- (100) Lee, J. M.; Li, J.; Johnson, D. A.; Stein, T. D.; Kraft, A. D.; Calkins, M. J.; Jakel, R. J.; Johnson, J. A. Nrf2, a multi-organ protector? *FASEB J.* **2005**, *19*, 1061-6.
- (101) Lewis, K. N.; Mele, J.; Hayes, J. D.; Buffenstein, R. Nrf2, a guardian of healthspan and gatekeeper of species longevity. *Integr. Comp. Biol.* **2010**, *50*, 829-43.
- (102) Boyle, P.; Levin, B. World Cancer Report. *WHO Press: Geneva, Switzerland* **2008**, 512.
- (103) Slocum, S. L.; Kensler, T. W. Nrf2: control of sensitivity to carcinogens. *Arch. Toxicol.* **2011**, *85*, 273-84.
- (104) Shapiro, T. A.; Fahey, J. W.; Dinkova-Kostova, A. T.; Holtzclaw, W. D.; Stephenson, K. K.; Wade, K. L.; Ye, L.; Talalay, P. Safety, tolerance, and metabolism of broccoli sprout glucosinolates and isothiocyanates: a clinical phase I study. *Nutr. Cancer* **2006**, *55*, 53-62.
- (105) Cornblatt, B. S.; Ye, L.; Dinkova-Kostova, A. T.; Erb, M.; Fahey, J. W.; Singh, N. K.; Chen, M. S.; Stierer, T.; Garrett-Mayer, E.; Argani, P.; Davidson, N. E.; Talalay, P.; Kensler, T. W.; Visvanathan, K. Preclinical and clinical evaluation of sulforaphane for chemoprevention in the breast. *Carcinogenesis* **2007**, *28*, 1485-90.

- (106) Hatcher, H.; Planalp, R.; Cho, J.; Torti, F. M.; Torti, S. V. Curcumin: from ancient medicine to current clinical trials. *Cell Mol. Life Sci.* **2008**, *65*, 1631-52.
- (107) Zhang, Y.; Munday, R. Dithiolethiones for cancer chemoprevention: where do we stand? *Mol. Cancer Ther.* **2008**, *7*, 3470-9.
- (108) de Vries, H. E.; Witte, M.; Hondius, D.; Rozemuller, A. J.; Drukarch, B.; Hoozemans, J.; van Horsen, J. Nrf2-induced antioxidant protection: a promising target to counteract ROS-mediated damage in neurodegenerative disease? *Free Radic. Biol. Med.* **2008**, *45*, 1375-83.
- (109) Du, Y.; Wooten, M. C.; Gearing, M.; Wooten, M. W. Age-associated oxidative damage to the p62 promoter: implications for Alzheimer disease. *Free Radic. Biol. Med.* **2009**, *46*, 492-501.
- (110) Tufekci, K. U.; Civi Bayin, E.; Genc, S.; Genc, K. The Nrf2/ARE Pathway: A Promising Target to Counteract Mitochondrial Dysfunction in Parkinson's Disease. *Parkinsons Dis.* **2011**, *2011*, 314082.
- (111) Calabrese, V.; Cornelius, C.; Mancuso, C.; Pennisi, G.; Calafato, S.; Bellia, F.; Bates, T. E.; Giuffrida Stella, A. M.; Schapira, T.; Dinkova Kostova, A. T.; Rizzarelli, E. Cellular stress response: a novel target for chemoprevention and nutritional neuroprotection in aging, neurodegenerative disorders and longevity. *Neurochem. Res.* **2008**, *33*, 2444-71.
- (112) van Muiswinkel, F. L.; Kuiperij, H. B. The Nrf2-ARE Signalling pathway: promising drug target to combat oxidative stress in neurodegenerative disorders. *Curr. Drug Targets CNS Neurol Disord.* **2005**, *4*, 267-81.
- (113) Cho, H. Y.; Kleeberger, S. R. Nrf2 protects against airway disorders. *Toxicol. Appl. Pharmacol.* **2010**, *244*, 43-56.
- (114) Suzuki, M.; Betsuyaku, T.; Ito, Y.; Nagai, K.; Nasuhara, Y.; Kaga, K.; Kondo, S.; Nishimura, M. Down-regulated NF-E2-related factor 2 in pulmonary macrophages of aged smokers and patients with chronic obstructive pulmonary disease. *Am. J. Respir. Cell Mol. Biol.* **2008**, *39*, 673-82.
- (115) Boutten, A.; Goven, D.; Artaud-Macari, E.; Boczkowski, J.; Bonay, M. NRF2 targeting: a promising therapeutic strategy in chronic obstructive pulmonary disease. *Trends Mol. Med.* **2011**, *17*, 363-71.
- (116) Reddy, S. P. The antioxidant response element and oxidative stress modifiers in airway diseases. *Curr. Mol. Med.* **2008**, *8*, 376-83.

- (117) He, X.; Kan, H.; Cai, L.; Ma, Q. Nrf2 is critical in defense against high glucose-induced oxidative damage in cardiomyocytes. *J. Mol. Cell Cardiol.* **2009**, *46*, 47-58.
- (118) Wang, X.; Hai, C. X. ROS acts as a double-edged sword in the pathogenesis of type 2 diabetes mellitus: is Nrf2 a potential target for the treatment? *Mini Rev. Med. Chem.* **2011**, *11*, 1082-92.
- (119) Jiang, T.; Huang, Z.; Lin, Y.; Zhang, Z.; Fang, D.; Zhang, D. D. The protective role of Nrf2 in streptozotocin-induced diabetic nephropathy. *Diabetes* **2010**, *59*, 850-60.
- (120) Negi, G.; Kumar, A.; Joshi, R. P.; Sharma, S. S. Oxidative stress and Nrf2 in the pathophysiology of diabetic neuropathy: old perspective with a new angle. *Biochem. Biophys. Res. Commun.* **2011**, *408*, 1-5.
- (121) Pergola, P. E.; Krauth, M.; Huff, J. W.; Ferguson, D. A.; Ruiz, S.; Meyer, C. J.; Warnock, D. G. Effect of bardoxolone methyl on kidney function in patients with T2D and Stage 3b-4 CKD. *Am. J. Nephrol.* **2011**, *33*, 469-76.
- (122) Koenitzer, J. R.; Freeman, B. A. Redox signaling in inflammation: interactions of endogenous electrophiles and mitochondria in cardiovascular disease. *Ann. N Y Acad. Sci.* **2010**, *1203*, 45-52.
- (123) Ichikawa, T.; Li, J.; Meyer, C. J.; Janicki, J. S.; Hannink, M.; Cui, T. Dihydro-CDDO-trifluoroethyl amide (dh404), a novel Nrf2 activator, suppresses oxidative stress in cardiomyocytes. *PLoS One* **2009**, *4*, e8391.
- (124) Collins, A. R.; Lyon, C. J.; Xia, X.; Liu, J. Z.; Tangirala, R. K.; Yin, F.; Boyadjian, R.; Bikineyeva, A.; Pratico, D.; Harrison, D. G.; Hsueh, W. A. Age-accelerated atherosclerosis correlates with failure to upregulate antioxidant genes. *Circ. Res.* **2009**, *104*, e42-54.
- (125) Sussan, T. E.; Jun, J.; Thimmulappa, R.; Bedja, D.; Antero, M.; Gabrielson, K. L.; Polotsky, V. Y.; Biswal, S. Disruption of Nrf2, a key inducer of antioxidant defenses, attenuates ApoE-mediated atherosclerosis in mice. *PLoS One* **2008**, *3*, e3791.
- (126) Freigang, S.; Ampenberger, F.; Spohn, G.; Heer, S.; Shamshiev, A. T.; Kisielow, J.; Hersberger, M.; Yamamoto, M.; Bachmann, M. F.; Kopf, M. Nrf2 is essential for cholesterol crystal-induced inflammasome activation and exacerbation of atherosclerosis. *Eur. J. Immunol.* **2011**, *41*, 2040-51.
- (127) Theiss, A. L.; Vijay-Kumar, M.; Obertone, T. S.; Jones, D. P.; Hansen, J. M.; Gewirtz, A. T.; Merlin, D.; Sitaraman, S. V. Prohibitin is a novel regulator of

- antioxidant response that attenuates colonic inflammation in mice. *Gastroenterology* **2009**, *137*, 199-208, 208 e1-6.
- (128) Khor, T. O.; Huang, M. T.; Kwon, K. H.; Chan, J. Y.; Reddy, B. S.; Kong, A. N. Nrf2-deficient mice have an increased susceptibility to dextran sulfate sodium-induced colitis. *Cancer Res.* **2006**, *66*, 11580-4.
- (129) Aleksunes, L. M.; Manautou, J. E. Emerging role of Nrf2 in protecting against hepatic and gastrointestinal disease. *Toxicol. Pathol.* **2007**, *35*, 459-73.
- (130) Nagai, N.; Thimmulappa, R. K.; Cano, M.; Fujihara, M.; Izumi-Nagai, K.; Kong, X.; Sporn, M. B.; Kensler, T. W.; Biswal, S.; Handa, J. T. Nrf2 is a critical modulator of the innate immune response in a model of uveitis. *Free Radic. Biol. Med.* **2009**, *47*, 300-6.
- (131) Wruck, C. J.; Fragoulis, A.; Gurzynski, A.; Brandenburg, L. O.; Kan, Y. W.; Chan, K.; Hassenpflug, J.; Freitag-Wolf, S.; Varoga, D.; Lippross, S.; Pufe, T. Role of oxidative stress in rheumatoid arthritis: insights from the Nrf2-knockout mice. *Ann. Rheum. Dis.* **2011**, *70*, 844-50.
- (132) Maicas, N.; Ferrandiz, M. L.; Brines, R.; Ibanez, L.; Cuadrado, A.; Koenders, M. I.; van den Berg, W. B.; Alcaraz, M. J. Deficiency of Nrf2 accelerates the effector phase of arthritis and aggravates joint disease. *Antioxid. Redox Signal* **2011**, *15*, 889-901.
- (133) Chen, L.; Magesh, S.; Wang, H.; Yang, C. S.; Kong, AN.; Hu, L. Design and synthesis of novel iminothiazinylbutadienols and divinylpyrimidinethiones as potential anti-inflammatory agents. *Bioorg. Med. Chem. Lett.* **2014**, *in press*.
- (134) Govindarajan, V. S. Turmeric--chemistry, technology, and quality. *Crit. Rev. Food Sci. Nutr.* **1980**, *12*, 199-301.
- (135) Scapagnini, G.; Colombrita, C.; Amadio, M.; D'Agata, V.; Arcelli, E.; Sapienza, M.; Quattrone, A.; Calabrese, V. Curcumin activates defensive genes and protects neurons against oxidative stress. *Antioxid. Redox Signal* **2006**, *8*, 395-403.
- (136) Balogun, E.; Hoque, M.; Gong, P.; Killeen, E.; Green, C. J.; Foresti, R.; Alam, J.; Motterlini, R. Curcumin activates the haem oxygenase-1 gene via regulation of Nrf2 and the antioxidant-responsive element. *Biochem. J.* **2003**, *371*, 887-95.
- (137) McNally, S. J.; Harrison, E. M.; Ross, J. A.; Garden, O. J.; Wigmore, S. J. Curcumin induces heme oxygenase 1 through generation of reactive oxygen species, p38 activation and phosphatase inhibition. *Int. J. Mol. Med.* **2007**, *19*, 165-72.

- (138) Thangapazham, R. L.; Sharma, A.; Maheshwari, R. K. Multiple molecular targets in cancer chemoprevention by curcumin. *AAPS. J.* **2006**, *8*, E443-9.
- (139) Ak, T.; Gulcin, I. Antioxidant and radical scavenging properties of curcumin. *Chem. Biol. Interact.* **2008**, *174*, 27-37.
- (140) Goel, A.; Kunnumakkara, A. B.; Aggarwal, B. B. Curcumin as "Curecumin": from kitchen to clinic. *Biochem. Pharmacol.* **2008**, *75*, 787-809.
- (141) Leyon, P. V.; Kuttan, G. Studies on the role of some synthetic curcuminoid derivatives in the inhibition of tumour specific angiogenesis. *J. Exp. Clin. Cancer Res.* **2003**, *22*, 77-83.
- (142) Menon, V. P.; Sudheer, A. R. Antioxidant and anti-inflammatory properties of curcumin. *Adv. Exp. Med. Biol.* **2007**, *595*, 105-25.
- (143) Ruby, A. J.; Kuttan, G.; Babu, K. D.; Rajasekharan, K. N.; Kuttan, R. Anti-tumour and antioxidant activity of natural curcuminoids. *Cancer Lett.* **1995**, *94*, 79-83.
- (144) Shishodia, S.; Chaturvedi, M. M.; Aggarwal, B. B. Role of curcumin in cancer therapy. *Curr. Probl. Cancer* **2007**, *31*, 243-305.
- (145) Duvoix, A.; Blasius, R.; Delhalle, S.; Schnekenburger, M.; Morceau, F.; Henry, E.; Dicato, M.; Diederich, M. Chemopreventive and therapeutic effects of curcumin. *Cancer Lett.* **2005**, *223*, 181-90.
- (146) Zhao, R.; Yang, B.; Wang, L.; Xue, P.; Deng, B.; Zhang, G.; Jiang, S.; Zhang, M.; Liu, M.; Pi, J.; Guan, D. Curcumin protects human keratinocytes against inorganic arsenite-induced acute cytotoxicity through an NRF2-dependent mechanism. *Oxid. Med. Cell Longev.* **2013**, *2013*, 412576.
- (147) Jiang, H.; Tian, X.; Guo, Y.; Duan, W.; Bu, H.; Li, C. Activation of nuclear factor erythroid 2-related factor 2 cytoprotective signaling by curcumin protect primary spinal cord astrocytes against oxidative toxicity. *Biol. Pharm. Bull.* **2011**, *34*, 1194-7.
- (148) Soetikno, V.; Sari, F. R.; Lakshmanan, A. P.; Arumugam, S.; Harima, M.; Suzuki, K.; Kawachi, H.; Watanabe, K. Curcumin alleviates oxidative stress, inflammation, and renal fibrosis in remnant kidney through the Nrf2-keap1 pathway. *Mol. Nutr. Food Res.* **2013**, *57*, 1649-59.
- (149) Jurenka, J. S. Anti-inflammatory properties of curcumin, a major constituent of *Curcuma longa*: a review of preclinical and clinical research. *Altern. Med. Rev.* **2009**, *14*, 141-53.

- (150) Bayet-Robert, M.; Kwiatkowski, F.; Leheurteur, M.; Gachon, F.; Planchat, E.; Abrial, C.; Mouret-Reynier, M. A.; Durando, X.; Barhomeuf, C.; Chollet, P. Phase I dose escalation trial of docetaxel plus curcumin in patients with advanced and metastatic breast cancer. *Cancer Biol. Ther.* **2010**, *9*, 8-14.
- (151) Radhakrishna Pillai, G.; Srivastava, A. S.; Hassanein, T. I.; Chauhan, D. P.; Carrier, E. Induction of apoptosis in human lung cancer cells by curcumin. *Cancer Lett.* **2004**, *208*, 163-70.
- (152) Ohtsu, H.; Xiao, Z.; Ishida, J.; Nagai, M.; Wang, H. K.; Itokawa, H.; Su, C. Y.; Shih, C.; Chiang, T.; Chang, E.; Lee, Y.; Tsai, M. Y.; Chang, C.; Lee, K. H. Antitumor agents. 217. Curcumin analogues as novel androgen receptor antagonists with potential as anti-prostate cancer agents. *J. Med. Chem.* **2002**, *45*, 5037-42.
- (153) Aggarwal, B. B.; Kumar, A.; Bharti, A. C. Anticancer potential of curcumin: preclinical and clinical studies. *Anticancer Res.* **2003**, *23*, 363-98.
- (154) Gururaj, A. E.; Belakavadi, M.; Venkatesh, D. A.; Marme, D.; Salimath, B. P. Molecular mechanisms of anti-angiogenic effect of curcumin. *Biochem. Biophys. Res. Commun.* **2002**, *297*, 934-42.
- (155) Hsu, C. H.; Cheng, A. L. Clinical studies with curcumin. *Adv. Exp. Med. Biol.* **2007**, *595*, 471-80.
- (156) Anand, P.; Kunnumakkara, A. B.; Newman, R. A.; Aggarwal, B. B. Bioavailability of curcumin: problems and promises. *Mol. Pharm.* **2007**, *4*, 807-18.
- (157) Sharma, R. A.; Steward, W. P.; Gescher, A. J. Pharmacokinetics and pharmacodynamics of curcumin. *Adv. Exp. Med. Biol.* **2007**, *595*, 453-70.
- (158) Garcea, G.; Jones, D. J.; Singh, R.; Dennison, A. R.; Farmer, P. B.; Sharma, R. A.; Steward, W. P.; Gescher, A. J.; Berry, D. P. Detection of curcumin and its metabolites in hepatic tissue and portal blood of patients following oral administration. *Br. J. Cancer* **2004**, *90*, 1011-5.
- (159) Wang, Y. J.; Pan, M. H.; Cheng, A. L.; Lin, L. I.; Ho, Y. S.; Hsieh, C. Y.; Lin, J. K. Stability of curcumin in buffer solutions and characterization of its degradation products. *J. Pharm. Biomed. Anal.* **1997**, *15*, 1867-76.
- (160) Tomren, M. A.; Masson, M.; Loftsson, T.; Tonnesen, H. H. Studies on curcumin and curcuminoids XXXI. Symmetric and asymmetric curcuminoids: stability, activity and complexation with cyclodextrin. *Int. J. Pharm.* **2007**, *338*, 27-34.
- (161) Rosemond, M. J.; St John-Williams, L.; Yamaguchi, T.; Fujishita, T.; Walsh, J. S. Enzymology of a carbonyl reduction clearance pathway for the HIV integrase

- inhibitor, S-1360: role of human liver cytosolic aldo-keto reductases. *Chem. Biol. Interact.* **2004**, *147*, 129-39.
- (162) Straganz, G. D.; Glieder, A.; Brecker, L.; Ribbons, D. W.; Steiner, W. Acetylacetone-cleaving enzyme Dke1: a novel C-C-bond-cleaving enzyme from *Acinetobacter johnsonii*. *Biochem. J.* **2003**, *369*, 573-81.
- (163) Grogan, G. Emergent mechanistic diversity of enzyme-catalysed beta-diketone cleavage. *Biochem. J.* **2005**, *388*, 721-30.
- (164) Katsori, A. M.; Chatzopoulou, M.; Dimas, K.; Kontogiorgis, C.; Patsilnakos, A.; Trangas, T.; Hadjipavlou-Litina, D. Curcumin analogues as possible anti-proliferative & anti-inflammatory agents. *Eur. J. Med. Chem.* **2011**, *46*, 2722-35.
- (165) Qiu, Y.; Yanase, T.; Hu, H.; Tanaka, T.; Nishi, Y.; Liu, M.; Sueishi, K.; Sawamura, T.; Nawata, H. Dihydrotestosterone suppresses foam cell formation and attenuates atherosclerosis development. *Endocrinology* **2010**, *151*, 3307-16.
- (166) Du, Z. Y.; Liu, R. R.; Shao, W. Y.; Mao, X. P.; Ma, L.; Gu, L. Q.; Huang, Z. S.; Chan, A. S. Alpha-glucosidase inhibition of natural curcuminoids and curcumin analogs. *Eur. J. Med. Chem.* **2006**, *41*, 213-8.
- (167) Robinson, T. P.; Ehlers, T.; Hubbard, I. R.; Bai, X.; Arbiser, J. L.; Goldsmith, D. J.; Bowen, J. P. Design, synthesis, and biological evaluation of angiogenesis inhibitors: aromatic enone and dienone analogues of curcumin. *Bioorg. Med. Chem. Lett.* **2003**, *13*, 115-7.
- (168) Liang, G.; Shao, L.; Wang, Y.; Zhao, C.; Chu, Y.; Xiao, J.; Zhao, Y.; Li, X.; Yang, S. Exploration and synthesis of curcumin analogues with improved structural stability both in vitro and in vivo as cytotoxic agents. *Bioorg. Med. Chem.* **2009**, *17*, 2623-31.
- (169) Zhao, C.; Cai, Y.; He, X.; Li, J.; Zhang, L.; Wu, J.; Zhao, Y.; Yang, S.; Li, X.; Li, W.; Liang, G. Synthesis and anti-inflammatory evaluation of novel mono-carbonyl analogues of curcumin in LPS-stimulated RAW 264.7 macrophages. *Eur. J. Med. Chem.* **2010**, *45*, 5773-80.
- (170) Zhang, Q.; Zhong, Y.; Yan, L. N.; Sun, X.; Gong, T.; Zhang, Z. R. Synthesis and preliminary evaluation of curcumin analogues as cytotoxic agents. *Bioorg. Med. Chem. Lett.* **2011**, *21*, 1010-4.
- (171) Yadav, B.; Taurin, S.; Rosengren, R. J.; Schumacher, M.; Diederich, M.; Somers-Edgar, T. J.; Larsen, L. Synthesis and cytotoxic potential of heterocyclic cyclohexanone analogues of curcumin. *Bioorg. Med. Chem.* **2010**, *18*, 6701-7.

- (172) Amolins, M. W.; Peterson, L. B.; Blagg, B. S. Synthesis and evaluation of electron-rich curcumin analogues. *Bioorg. Med. Chem.* **2009**, *17*, 360-7.
- (173) Pitt, W. R.; Parry, D. M.; Perry, B. G.; Groom, C. R. Heteroaromatic rings of the future. *J. Med. Chem.* **2009**, *52*, 2952-63.
- (174) Sun, A.; Lu, Y. J.; Hu, H.; Shoji, M.; Liotta, D. C.; Snyder, J. P. Curcumin analog cytotoxicity against breast cancer cells: exploitation of a redox-dependent mechanism. *Bioorg. Med. Chem. Lett.* **2009**, *19*, 6627-31.
- (175) Cornago, P. C., R. M.; Bouissane, L.; Alkorta, I.; Elguero, J. A study of the tautomerism of  $\beta$ -dicarbonyl compounds with special emphasis on curcuminoids. *Tetrahedron* **2008**, *64*, 8089.
- (176) Fuchs, J. R.; Pandit, B.; Bhasin, D.; Etter, J. P.; Regan, N.; Abdelhamid, D.; Li, C.; Lin, J.; Li, P. K. Structure-activity relationship studies of curcumin analogues. *Bioorg. Med. Chem. Lett.* **2009**, *19*, 2065-9.
- (177) Awasthi, S.; Pandya, U.; Singhal, S. S.; Lin, J. T.; Thiviyathan, V.; Seifert, W. E., Jr.; Awasthi, Y. C.; Ansari, G. A. Curcumin-glutathione interactions and the role of human glutathione S-transferase P1-1. *Chem. Biol. Interact.* **2000**, *128*, 19-38.
- (178) Shoemaker, R. H. The NCI60 human tumour cell line anticancer drug screen. *Nat. Rev. Cancer* **2006**, *6*, 813-23.
- (179) Pergola, P. E.; Raskin, P.; Toto, R. D.; Meyer, C. J.; Huff, J. W.; Grossman, E. B.; Krauth, M.; Ruiz, S.; Audhya, P.; Christ-Schmidt, H.; Wittes, J.; Warnock, D. G.; Investigators, B. S. Bardoxolone methyl and kidney function in CKD with type 2 diabetes. *N. Engl. J. Med.* **2011**, *365*, 327-36.
- (180) Nagaraj, S.; Youn, J. I.; Weber, H.; Iclozan, C.; Lu, L.; Cotter, M. J.; Meyer, C.; Becerra, C. R.; Fishman, M.; Antonia, S.; Sporn, M. B.; Liby, K. T.; Rawal, B.; Lee, J. H.; Gabrilovich, D. I. Anti-inflammatory triterpenoid blocks immune suppressive function of MDSCs and improves immune response in cancer. *Clin. Cancer Res.* **2010**, *16*, 1812-23.
- (181) Egner, P. A.; Chen, J. G.; Wang, J. B.; Wu, Y.; Sun, Y.; Lu, J. H.; Zhu, J.; Zhang, Y. H.; Chen, Y. S.; Friesen, M. D.; Jacobson, L. P.; Munoz, A.; Ng, D.; Qian, G. S.; Zhu, Y. R.; Chen, T. Y.; Botting, N. P.; Zhang, Q.; Fahey, J. W.; Talalay, P.; Groopman, J. D.; Kensler, T. W. Bioavailability of Sulforaphane from two broccoli sprout beverages: results of a short-term, cross-over clinical trial in Qidong, China. *Cancer Prev. Res. (Phila)* **2011**, *4*, 384-95.
- (182) Kim, S. G.; Kim, Y. M.; Choi, J. Y.; Han, J. Y.; Jang, J. W.; Cho, S. H.; Um, S. H.; Chon, C. Y.; Lee, D. H.; Jang, J. J.; Yu, E.; Lee, Y. S. Oltipraz therapy in patients

with liver fibrosis or cirrhosis: a randomized, double-blind, placebo-controlled phase II trial. *J. Pharm. Pharmacol.* **2011**, *63*, 627-35.

- (183) Presterla, T.; Holtzclaw, W. D.; Zhang, Y.; Talalay, P. Chemical and molecular regulation of enzymes that detoxify carcinogens. *Proc. Natl. Acad. Sci. U S A* **1993**, *90*, 2965-9.
- (184) Talalay, P.; De Long, M. J.; Prochaska, H. J. Identification of a common chemical signal regulating the induction of enzymes that protect against chemical carcinogenesis. *Proc. Natl. Acad. Sci. U S A* **1988**, *85*, 8261-5.
- (185) Prochaska, H. J.; De Long, M. J.; Talalay, P. On the mechanisms of induction of cancer-protective enzymes: a unifying proposal. *Proc. Natl. Acad. Sci. U S A* **1985**, *82*, 8232-6.
- (186) Spencer, S. R.; Xue, L. A.; Klenz, E. M.; Talalay, P. The potency of inducers of NAD(P)H:(quinone-acceptor) oxidoreductase parallels their efficiency as substrates for glutathione transferases. Structural and electronic correlations. *Biochem. J.* **1991**, *273* ( Pt 3), 711-7.
- (187) Keum, Y. S.; Chang, P. P.; Kwon, K. H.; Yuan, X.; Li, W.; Hu, L.; Kong, A. N. 3-Morpholinopropyl isothiocyanate is a novel synthetic isothiocyanate that strongly induces the antioxidant response element-dependent Nrf2-mediated detoxifying/antioxidant enzymes in vitro and in vivo. *Carcinogenesis* **2008**, *29*, 594-9.
- (188) Prawan, A.; Keum, Y. S.; Khor, T. O.; Yu, S.; Nair, S.; Li, W.; Hu, L.; Kong, A. N. Structural influence of isothiocyanates on the antioxidant response element (ARE)-mediated heme oxygenase-1 (HO-1) expression. *Pharm. Res.* **2008**, *25*, 836-44.
- (189) Place, A. E.; Suh, N.; Williams, C. R.; Risingsong, R.; Honda, T.; Honda, Y.; Gribble, G. W.; Leesnitzer, L. M.; Stimmel, J. B.; Willson, T. M.; Rosen, E.; Sporn, M. B. The novel synthetic triterpenoid, CDDO-imidazolide, inhibits inflammatory response and tumor growth in vivo. *Clin. Cancer Res.* **2003**, *9*, 2798-806.
- (190) Han, S. S.; Peng, L.; Chung, S. T.; DuBois, W.; Maeng, S. H.; Shaffer, A. L.; Sporn, M. B.; Janz, S. CDDO-Imidazolide inhibits growth and survival of c-Myc-induced mouse B cell and plasma cell neoplasms. *Mol. Cancer* **2006**, *5*, 22.
- (191) Inoyama, D.; Chen, Y.; Huang, X.; Beamer, L. J.; Kong, A. N.; Hu, L. Optimization of fluorescently labeled Nrf2 peptide probes and the development of a fluorescence polarization assay for the discovery of inhibitors of Keap1-Nrf2 interaction. *J. Biomol. Screen* **2012**, *17*, 435-47.

- (192) Chen, Y.; Inoyama, D.; Kong, A. N.; Beamer, L. J.; Hu, L. Kinetic analyses of Keap1-Nrf2 interaction and determination of the minimal Nrf2 peptide sequence required for Keap1 binding using surface plasmon resonance. *Chem. Biol. Drug Des.* **2011**, *78*, 1014-21.
- (193) Padmanabhan, B.; Tong, K. I.; Ohta, T.; Nakamura, Y.; Scharlock, M.; Ohtsuji, M.; Kang, M. I.; Kobayashi, A.; Yokoyama, S.; Yamamoto, M. Structural basis for defects of Keap1 activity provoked by its point mutations in lung cancer. *Mol. Cell* **2006**, *21*, 689-700.
- (194) Li, X.; Zhang, D.; Hannink, M.; Beamer, L. J. Crystal structure of the Kelch domain of human Keap1. *J. Biol. Chem.* **2004**, *279*, 54750-8.
- (195) Li, X.; Zhang, D.; Hannink, M.; Beamer, L. J. Crystallization and initial crystallographic analysis of the Kelch domain from human Keap1. *Acta. Crystallogr. D. Biol. Crystallogr.* **2004**, *60*, 2346-8.
- (196) Beamer, L. J.; Li, X.; Bottoms, C. A.; Hannink, M. Conserved solvent and side-chain interactions in the 1.35 Angstrom structure of the Kelch domain of Keap1. *Acta. Crystallogr. D. Biol. Crystallogr.* **2005**, *61*, 1335-42.
- (197) Lo, S. C.; Li, X.; Henzl, M. T.; Beamer, L. J.; Hannink, M. Structure of the Keap1:Nrf2 interface provides mechanistic insight into Nrf2 signaling. *EMBO. J.* **2006**, *25*, 3605-17.
- (198) Bansode, T. N.; Shelke, J. V.; Dongre, V. G. Synthesis and antimicrobial activity of some new N-acyl substituted phenothiazines. *Eur. J. Med. Chem.* **2009**, *44*, 5094-8.
- (199) Wang, B.; Gao, Y.; Li, H. W.; Hu, Z. P.; Wu, Y. The switch-on luminescence sensing of histidine-rich proteins in solution: a further application of a Cu<sup>2+</sup> ligand. *Org. Biomol. Chem.* **2011**, *9*, 4032-4.
- (200) Wang, B.; Li, H. W.; Gao, Y.; Zhang, H.; Wu, Y. A multifunctional fluorescence probe for the detection of cations in aqueous solution: the versatility of probes based on peptides. *J. Fluoresc.* **2011**, *21*, 1921-31.
- (201) Roszkowski, R.; Maurin, J. K.; Czarnocki, Z. Enantioselective synthesis of (R)-(-)-praziquantel (PZQ). *Tetrahedron: Asymmetry* **2006**, *17*, 1415-19.
- (202) Grunewald, G. L.; Sall, D. J.; Monn, J. A. Conformational and steric aspects of the inhibition of phenylethanolamine N-methyltransferase by benzylamines. *J. Med. Chem.* **1988**, *31*, 433-44.

- (203) Katritzky, A. R.; Ozcan, S.; Todadze, E. Synthesis and fluorescence of the new environment-sensitive fluorophore 6-chloro-2,3-naphthalimide derivative. *Org. Biomol. Chem.* **2010**, *8*, 1296-300.
- (204) Pinter, A.; Haberhauer, G. Oxazole Cyclopeptides for Chirality Transfer in C<sub>3</sub>-Symmetric Octahedral Metal Complexes. *Eur. J. Org. Chem.* **2008**, *14*, 2375-87.